SOCIETÀ NAZIONALE DI SCIENZE LETTERE E ARTI IN NAPOLI

RENDICONTO
DELL'ACCADEMIA DELLE SCIENZE
FISICHE E MATEMATICHE

SERIE IV - VOL. LXXXVI - ANNO CLVIII

(2019)

GIANNINI EDITORE

La pubblicazione è stata resa possibile grazie ai contributi
- della Regione Campania
- della Fondazione Banco di Napoli
- del Ministero per i Beni Culturali
- dell'Associazione "Amici della Società Nazionale di Scienze Lettere e Arti in Napoli"
- del Dipartimento di Matematica e Applicazioni "Renato Caccioppoli"

N. 86 - Dicembre 2019

ISSN 0370-3568

Nessuna parte di questa pubblicazione può essere tradotta, riprodotta, copiata o trasmessa senza l'autorizzazione scritta dell'Editore.

Fotocopie per uso personale del lettore possono essere effettuate nei limiti del 15% di ciascuna pubblicazione. Le riproduzioni ad uso differente da quello personale potranno avvenire, per un numero di pagine non superiore al 15% per pubblicazione, solo a seguito di specifica autorizzazione rilasciata da AIDRO, via delle Erbe, n. 2, 20121 Milano, telefax 02 809506, e-mail segreteria@aidro.org

Direttore responsabile: Carlo Sbordone
Volume a cura di Carmine Colella

© 2020 by Accademia delle Scienze Fisiche e Matematiche
Tutti i diritti sono riservati

Prima edizione italiana

Finito di stampare in Italia nel mese di giugno 2020
da Officine Grafiche Francesco Giannini & figli S.p.A. - Napoli

Autorizzazione del Tribunale di Napoli n. 780 del 14/08/1954
ISBN 978-88-6906-124-0

Indice

Parte A – Scienze Naturali

Parte B – Scienze Matematiche

Appendice

Parte A
Scienze Naturali

Rend. Acc. Sc. fis. mat. Napoli
Vol. LXXXVI, (2019) pp. 7-23

DOI 10.32092/1015

YB-1 protein is secreted as consequence of oxidative stress and induces G2/M phase block in receiving cells

Nota di Andrea Maria Guarino[1]
(Adunanza del 15 marzo 2019)

Keywords: YB-1, Stress Granules, Cell proliferation, Secretion

Abstract - Cell signalling is the complex network of connections between cells and inside the single cell. Protein trafficking is deeply involved in cell signalling. Different proteins are ordered in clusters of receptors of extracellular signals, transducers, sensors and biological response effectors. Together, they are arranged in molecular pathways that are required for the maintenance of cell homeostasis. Protein secretion is a relevant component of eukaryotic cell signalling. The prototype cold-shock Y-box binding protein 1 (YB-1) is a multifunctional protein which regulates a variety of fundamental biological processes. Among them, cellular stress response and cell proliferation. Recently YB-1 has been found in human extracellular fluids and shown to be secreted by different cell types. My recent research activity was focused on YB-1 protein secretion to investigate on its role as a potential paracrine signal to elicit changes or responses in nearby cells, altering their behaviour. Low amounts of extracellular YB-1 are released by HEK293T cells in physiological condition. Interestingly, YB-1 secretion was enhanced following oxidative insults. In parallel, the assembly of YB-1 in stress granules (SGs), cytoplasmic foci where untranslated mRNAs are sorted or processed for re-initiation, degradation, or packaging into mRNPs was verified. Purified recombinant human YB-1 (rYB-1) and enriched fractions of YB-1 from HEK293T cell culture medium (CCM-YB-1) were produced. Both forms of YB-1 protein have anti-proliferative activity on different recipient cell lines, including HaCaT cells. In particular, inhibition of human keratinocytes proliferation by extracellular YB-1 was associated to a G2/M cell cycle arrest, induction of p21WAF and reduction of ΔNp63α protein level. The obtained results suggest that sustained release of full length YB-1 protein, by stress stimuli acts as paracrine/autocrine signal stimulating cell cycle arrest.

[1] Vincitore del Premio "Lisa De Conciliis" per il 2018. Dipartimento di Biologia, Università Federico II di Napoli, Complesso Universitario di Monte S. Angelo, via Cinthia, 80126 Napoli

Riassunto - I meccanismi ed i processi che regolano la vita ed il comportamento di una cellula sono profondamente interconnessi ed interdipendenti. Tale interconnessione richiede un continuo scambio di *informazioni* nella forma di molecole solubili, lipidi e proteine. La proteina YB-1, ampiamente studiata nel panorama scientifico, svolge diversi ruoli all'interno della cellula. Recentemente è stato proposto un duplice ruolo per la proteina, in condizioni di stress cellulare: la proteina risponde allo stress ossidativo con la formazione di Granuli da Stress venendo al contempo secreta. La forma secreta induce, in cellule riceventi, blocco della proliferazione cellulare.

1 – INTRODUCTION

1.1 - Cell Signalling

Cell signalling is at the basis of cellular homeostasis and has to be intended as a complex network of connections between cells and inside the single cell. Simplifying, signalling machineries act as highly dynamic two-components system, composed by a sensor, which senses the internal or external change, and an effector, which execute the best response to the variation experienced.

All cells communicate with each other and with the surroundings (Uings and Farrow 2000).

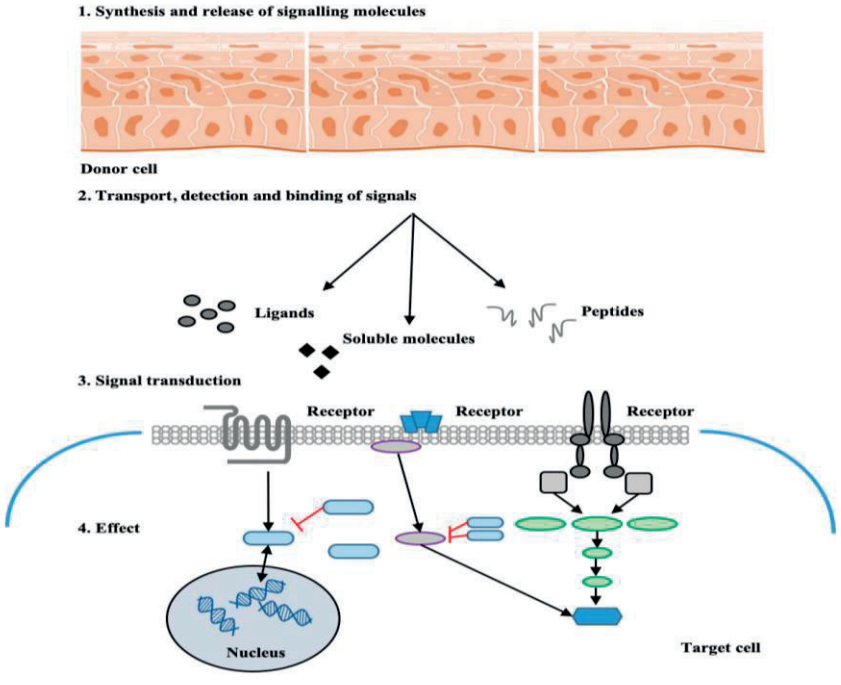

Fig. 1 – General representation of cellular signalling pathway.

Eukaryotic cell communication takes places basically thanks to the trafficking and exchange of soluble molecules, proteins, lipids and also through mechanical contacts (Fig. 1).

Signalling can adopt different mechanisms, protein secretion among them plays a major role. Accordingly, the analysis of protein secretory pathways has been the focus of many research fields throughout the years.

This trafficking route is a linear movement of cargoes, which traverse distinct organelles in a membrane-bound way (Szul and Sztul 2011); starting from the rough endoplasmic reticulum (RER), where newly synthetized proteins are concentrated in transport vesicles which travel along the cell to the Golgi Apparatus (GA), then to the trans-Golgi network (TGN) and then fuse with the plasma membrane (Tartakoff, Vassalli, and Détraz 1978).

A first definition of the collection of proteins secreted through Conventional Protein Secretion (CPS) was *secretome*; nowadays the definition encompasses proteins shed from the cell surface and intracellular proteins released through non-classical (or unconventional) secretion pathway or exosomes.

Less, indeed, is known about Unconventional Protein Secretion, also known as ER/Golgi-independent protein secretion although it was discovered more than 20 years ago (Cleves 1997) (Fig. 2).

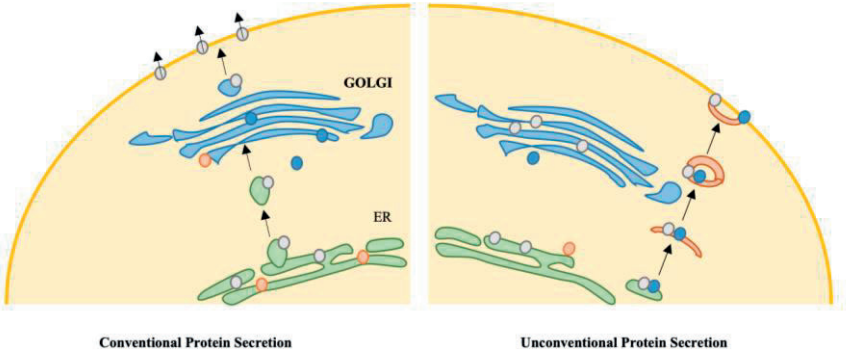

Fig. 2 – Schematic representation of the two major secretory pathways.

Beyond solving a fundamental problem in current cell biology, the molecular analysis of these processes is of major importance as these export routes are taken by viral proteins, angiogenic growth factors, inflammatory cytokines and components of the extracellular matrix.

1.2 - The Y-box binding protein 1

YB-1 is a member of the evolutionarily conserved cold shock domain (CSD) proteins and was first identified as a DNA/RNA binding protein (Kohno *et al*.

2003) involved in the control of gene expression both at transcriptional and translational level (Eliseeva *et al.*, 2011; Matsumoto *et al.*, 2012).

Human YB-1 is made up of three domains: A/P rich N- terminal domain, a highly conserved CSD domain and a large C-terminus (Fig. 3).The Cold Shock Domain is composed by five β-barrel strands connected by a long flexible loop; it contains the RNA binding motifs *RNP1* and *RNP2*, which mediate the interaction with nucleic acids, both specific and unspecific (Eliseeva *et al*. 2011). The Alanine/Proline domain is involved in protein-protein interaction and, according to the literature, enhances and stabilizes the CTD specific binding with RNAs. The CTD domain includes alternating basic and acid clusters and is implicated in DNA/RNA binding and protein-protein interaction. Except the CSD, which owns a precise secondary structure, the protein shows no ordered three-dimensional structure (Fig. 3); this gives YB-1 the possibility to modulate its structure gaining different fixed organizations through the interaction with several distinct partners (Lyabin *et al.*, 2014).

YB-1 subcellular localization is finely regulated. Specific nuclear localization (NLS) and cytoplasmic retention signals (CRS), all localized in the CTD domain, contribute and direct the multifunctional tasking of YB-1 (Di Costanzo *et al*. 2012).

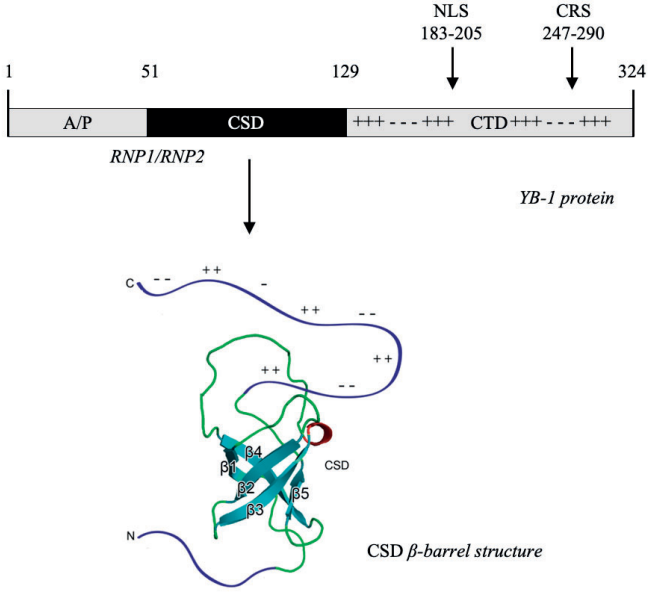

Fig. 3 – Schematic representation of human YB-1 protein.

Combining its structural flexibility and the possibility to move from a cellular district to another, derives that YB-1 is involved in the control of several biological processes including cell proliferation, migration, DNA damage, RNA sorting and many others. In normal resting cells, YB-1 localizes to cytoplasm where it is a major component of P-body and messenger ribonucleoproteins (mRNPs) acting, predominantly, as a RNA binding protein (Guarino *et al*. 2018; Yang *et al*. 2011). Furthermore, YB-1 activates translation of specific transcripts via its ability to bind UTRs of target mRNAs (low YB-1/mRNA ratio); at high YB-1/mRNA ratio, instead, it functions as a component of translationally inactive mRNPs, and directly blocks the initiation of translation inhibiting mRNA degradation (Evdokimova *et al*. 2001).

Mitogens and stress stimuli can trigger YB-1 nuclear translocation where it acts as a transcription factor, at the G1-S transition of the cell cycle, for instance (Kim *et al*. 2013; Ohga *et al*. 1998).

Recent studies link YB-1 to the cellular response to oxidative stress and DNA repair mechanisms, leading to the concept of YB-1 as a stress sensor. Indeed, following acute oxidative stress, YB-1 localizes to cytoplasmic Stress Granules (SGs), organelle-like structures devoid of membranes, engaged in mRNA sorting and pro-survival translational reprogramming (Anderson and Kedersha, 2008; Somasekharan *et al.*, 2015).

In particular, YB-1 is recruited in TIA-containing Stress Granules (SGs) where it functions as a component of translationally inactive mRNPs to directly block translational initiation of highly expressed transcripts (Lyons *et al.* 2016).

1.3 - Stress Granules

Eukaryotes respond to detrimental conditions by activating a set of conserved processes that aim to re-establish cellular homeostasis. This multifaceted response is critical for cell survival (Mahboubi and Stochaj 2017). It is characterized by stress-dependent changes in the transcriptome and down-regulation of global translation (Morimoto 2011; Thomas *et al.* 2011). At the same time, the production of molecular chaperones is enhanced to promote the refolding or degradation of damaged proteins (Morimoto 2011).

After exposure to distinct environmental insults, such as oxidative stress, hypothermia or extreme heat, eukaryotic cells relocate proteins and messenger RNA into transient, dynamic structures known as Stress Granules (SGs).

Stress granules are dynamic cytosolic aggregates composed by ribonucleoproteins, induced during cellular stress when protein synthesis is inhibited (Khong and Jan 2011).

In response to environmental stress such as oxidative stress or heat shock, cells respond by shutting down overall protein synthesis. This results in the disassembly of polyribosomes, leading to stalled initiation complexes that are dy-

namically recruited to cytoplasmic foci called, hence, stress granules. Stress granules biology is very complex; they somehow evolve from Processing Bodies (PBs) which are linked to exosomes, by sharing proteins and RNAs *(Kedersha et al*. 2005; Khong and Jan 2011). YB-1 performs a role in SGs formation, in particular in sodium arsenite response, by activating translation of HSP70 and G3BP1 protein, which is a well characterized SGs nucleator and recruiting tRNAs generated by angiogenin cleavage (Lyons *et al*. 2016).

1.4 - YB-1 secretion

A newly identified YB-1 feature is its ability to be secreted in cell culture media and human body fluids (Hanssen *et al*. 2013). YB-1 secretion is particularly active in association with malignancies, bacterial infections and inflammatory diseases (Kang *et al*. 2014).

The precise molecular mechanisms through which YB-1 is secreted is still under investigation, but it is generally accepted that YB-1 is secreted through non canonical pathways (Frye *et al*. 2009) and there are evidences about different proteins and molecular machineries involved. One of the most recently proposed mechanism, indicates that YB-1 is secreted via exosome vesicles following a specific ubiquitination process (Palicharla and Maddika 2015); this seems to be in contrast with other mechanisms proposed so far, for instance acetylation-dependent secretion (Brandt *et al*. 2012). In exosomes YB-1 is believed to sort RNA by type and quantity in a cell specific manner (Shurtleff *et al*. 2017).

Moreover, it is still not clear if YB-1 protein is secreted as a sum of multiple fragments and what are the effects of secreted YB-1 on distinct target cells. As a matter of fact, bioinformatic analysis of YB-1 aminoacidic sequence predict that it may represent a precursor for bioactive paracrine molecules; interactions between secreted YB-1 and some extracellular receptor domains, for instance Notch 3, have been proposed (Rauen *et al*. 2009). Due to its simultaneous presence in P-bodies, Stress Granules (SGs) and exosomes YB-1 is thought to function as a regulator of peptides/RNAs trafficking in and outside the cell.

My recent research activity was aimed to investigate on this phenomenon.

2 - YB-1 IS INVOLVED IN CELLULAR STRESS RESPONSE

Human embryonic kidney 293T (HEK293T) cell line is a popular, heterologous expression system for producing recombinant proteins in mammalian cells (Thomas *et al*. 2011) and it is also widely used for production of secreted proteins (Aydin *et al*. 2012). For these reasons it has been chosen as a good cell model system to analyse YB-1 response to stress.

First, I analysed YB-1 subcellular distribution in normal conditions: immunofluorescence and confocal microscopy revealed that YB- 1 was abundant and

almost exclusively cytoplasmic. Interestingly, observed small cytoplasmic aggregates that appeared to be randomly distributed throughout the cell (Fig. 4, white arrows).

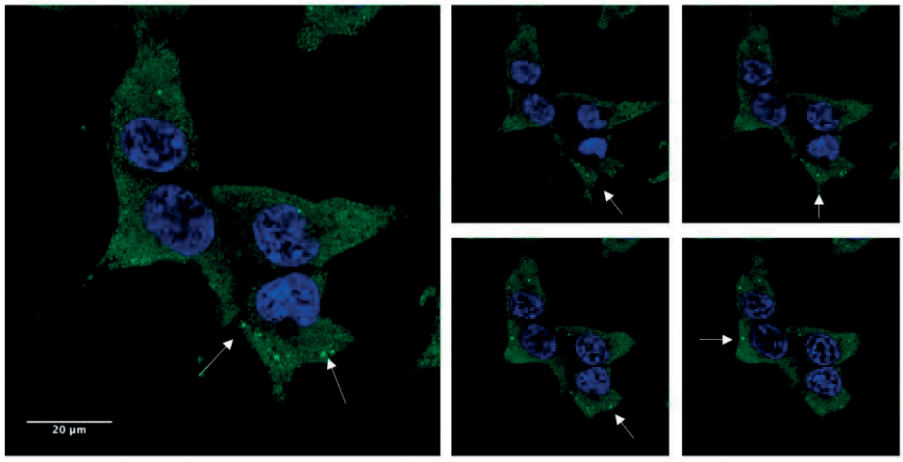

Fig. 4 – Confocal immunofluorescence of HEK293T stained with α-YB-1 (green), nuclei are stained with DAPI (blue); arrows indicate YB-1 aggregates.

Knowing that YB-1 has been found in P-bodies in many mammalian cell lines, for example in Hep-2 and Hela cells (Anderson, Kedersha, and Ivanov 2015; Yang *et al*. 2011), I evaluated the possibility that also HEK293T have YB-1 positive P-bodies.

Therefore, I performed double immunofluorescence with antibodies against YB-1 (abcam) and GW182 (Santa Cruz Biotechnology), and as shown in Fig. 5, YB-1 and GW182 co-localize in cytoplasmic aggregates, confirming that they are P-bodies.

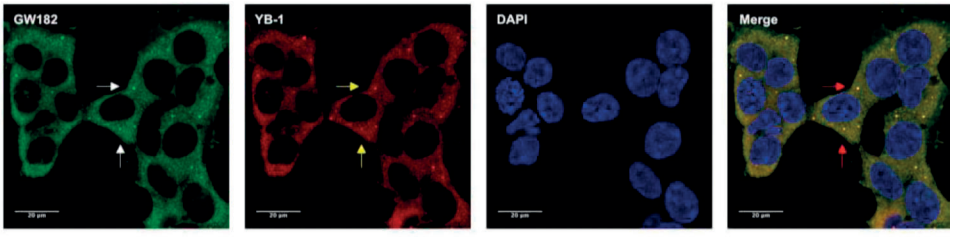

Fig. 5 – Confocal immunofluorescence of HEK293T stained with α-GW182 (green) and α-YB-1 (red), nuclei are stained with DAPI (blue); white, yellow and red arrows indicate respectively, YB-1, GW182 and YB-1/GW182 aggregates.

Once defined the subcellular distribution of YB-1 protein in normal conditions I treated cells with different stressors. Following heat shock or treatment with 250 μM sodium arsenite (Na Ars) or 500 μM hydrogen peroxide (H_2O_2), YB-1 was found to co-localize with PABP1, a canonical SGs marker (Kedersha and Anderson 2007), in cytoplasmic stress granules (Fig. 6). Interestingly, SGs size and overall number per cell were different depending on the type of stimulus applied confirming previous finding indicating stress-specific differences in composition and assembly of stress granules (Aulas *et al*. 2017).

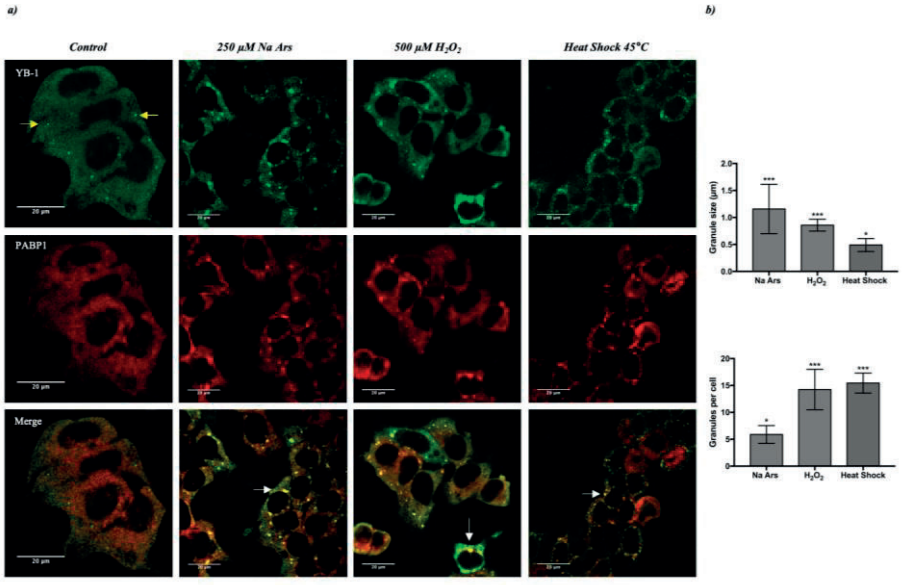

Fig. 6 – (a) confocal immunofluorescence of un-treated (control) HEK293T and treated with different stressors, stained with α-YB-1 (green) and α-PABP1 (red), nuclei are stained with DAPI (blue); yellow arrows indicate YB-1 positive P-bodies; withe arrows indicate YB-1 and PABP1 positive stress granules; (b) *(upper panel)* size of granules and *(lower panel)* number of granules after treatments compared to control; statistical analysis was performed using 1-way ANOVA followed by Dunnett's multiple comparisons test. Levels of significance are indicated (***$p<0.001$, *$p = 0.001$).

YB-1 protein was immunoprecipitated from extracts of untreated or sodium arsenite treated HEK293T cells. As show in Fig. 7a PABP1 was detectable in YB-1 immunocomplexes exclusively from cells treated with arsenite thereby indicating that YB-1 and PABP1 association occurs predominantly in SGs. To assess the relevance of YB-1 in SGs assembly, I depleted HEK293T cells of YB-1 using a specific siRNA pool against endogenous YB-1 mRNA (siYB1). By immunoblot and densitometric analysis I found that the expression level of YB-1 protein was reduced to 55% of control (Fig. 7b). YB-1 knock-down consistently

impaired the assembly of arsenite-induced PABP1-positive stress granules by reducing their size and number (Figs. 7c and d). Interestingly, in YB-1 depleted cells, PABP1 showed a more nuclear localization both in resting condition and under stress stimuli (Fig. 7c) suggesting that YB-1 can influence PABP1 subcellular distribution.

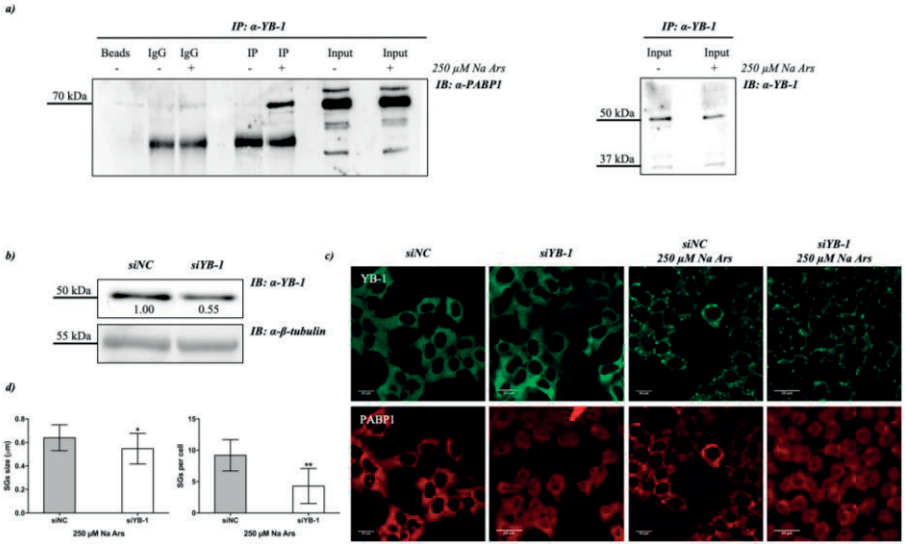

Fig. 7 – (a) co-immunoprecipitation of HEK293T total protein extracts treated (+) or not (-) with 250 μM Na Ars for 30'. Input samples immunorevealed with α-PABP1 and α-YB-1 are shown; (b) western blot of total extract from control (siNC) or 100 nM YB-1 silenced (siYB-1) HEK293T; the degree of reduction of YB-1 protein siRNA-treated cells compared with control is indicated beneath each band in the western blot (where the relative unit 1.0 represents YB-1 levels in cells transfected with the control siRNA). β-tubulin was used as loading control; (c) confocal immunofluorescence of control (siNC) and silenced (siYB-1) HEK293T cells, treated or not with 250 μM Na Ars for 30', stained with α-YB-1 (green) and α-PABP1 (red); (d) *(left panel)* size of granules and *(right panel)* number of granules in YB-1 silenced cells treated with Na Ars compared to siNC (control) cells; statistical analysis was performed using unpaired t-test with Welch's correction (**p = 0.010 and *p = 0.02).

3 - YB-1 IS SECRETED AFTER STRESS

Despite the apparent enrichment of YB-1 in SGs, I observed a significant reduction of intracellular YB-1 protein level in total extracts of Na Ars and H_2O_2-treated HEK293T (Figs. 8a and b). The observed decrease of YB-1 was not caused by cell death and subsequent leakage of cell contents as the level of GAPDH and actinin proteins, used as control, remained unaffected (Figs. 8a and

b). By immunoblot analysis of nuclear and cytoplasmic subcellular fractions I found that the reduction of YB-1 protein level induced by sodium arsenite was exclusively at the expense of the cytoplasmic pool, while nuclear YB-1 was totally unaffected (Fig. 8c).

Moreover, after 30' and 60' treatment with 250 μM sodium arsenite or 500 μM hydrogen peroxide, cell viability was only slightly reduced (90% and 94%, respectively) compared to control cells (Fig. 8d), further indicating that extracellular accumulation of YB-1 was not due to cell injury.

Thus, I hypothesized that oxidative stress would enhance YB-1 protein secretion.

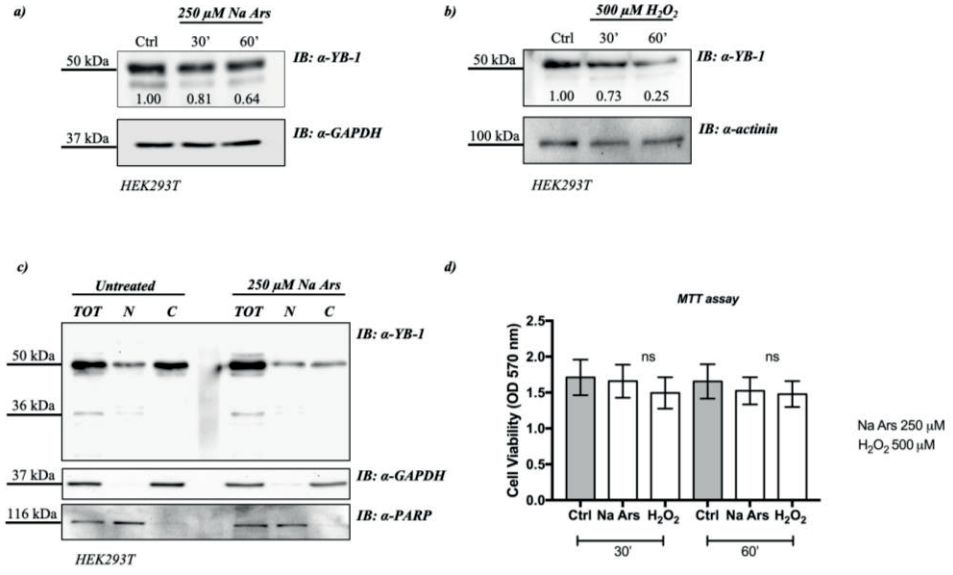

Fig. 8 – Western blot of total protein extracts from HEK293T treated with 250 μM Na Ars (a) or 500 μM H_2O_2 (b) for 30' and 60'; GAPDH and actinin were used as loading control. The degree of reduction of YB-1 protein levels in treated cells compared with controls is indicated beneath each band in the western blot (where the relative unit 1.0 represents YB-1 levels in control cells); c) western blot of total extract and nuclear/cytoplasmic fractionation of Na Ars treated and untreated HEK293T. GAPDH and PARP were used as loading control for cytoplasm and nucleus respectively; d) *c*ell viability assay of HEK293T cells treated with 250 μM Na Ars and 500 μM H_2O_2 for 30' and 60', ns indicate no statistically significance (ordinary 1-way ANOVA and Dunnett's multiple comparison; ns means no statistical significance).

4 - SECRETED YB-1 AFFECTS CELL PROLIFERATION

To analyse the effects of extracellular YB-1 on receiving cells, an enriched YB-1 fraction from HEK293T conditioned cell culture medium (CCM-YB-1) by ammonium sulphate precipitation followed by HPLC purification was prepared. Furthermore, a recombinant YB-1 from *E. coli*, was produced (data not shown). We have previously demonstrated that intracellular YB-1 is implicated in keratinocyte proliferation and survival to oxidative stress (Ciani *et al*. 2018; di Martino *et al*. 2016). To get an insight into the function of secreted YB-1, the proliferative response of HaCaT cells, human immortalized keratinocytes, to the addition of recombinant YB-1 and purified YB-1 from HEK293T cell culture medium (CCM-YB-1) was evaluated.

HaCaT cells were incubated for the indicated time with increasing amounts (5.0, 7.5 and 10 µg/ml) of rYB-1 protein, CCM-YB-1 or Bovine Serum Albumin (BSA) as control in serum supplemented culture medium. As shown in Fig. 9, treatments with CCM-YB-1 or rYB-1 reduced the rate of proliferation of HaCaT cells while equivalent amounts of BSA were ineffective (data not shown).

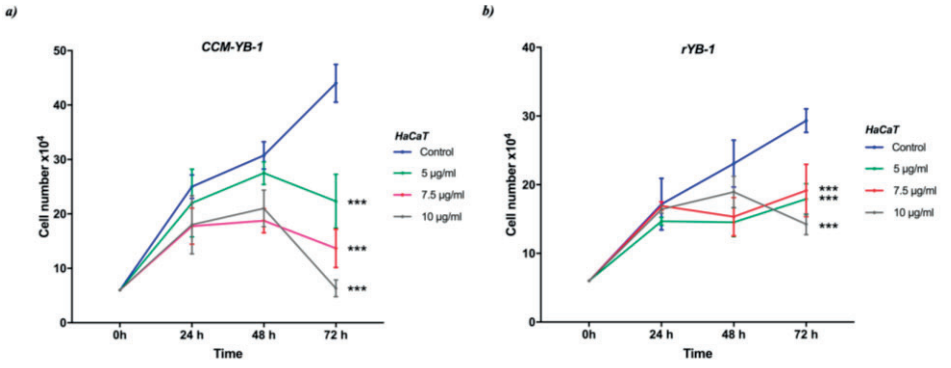

Fig. 9 - Cell proliferation profile of HaCaT cells incubated with indicated concentrations of CCM-YB-1 (a), rYB- 1 (b); statistical analysis was performed using 2-way ANOVA followed by Dunnett's multiple comparisons test. Levels of significance are indicated (***$p<0.001$).

YB-1 is normally released in the culture medium by HEK293T cells but not by HaCaT or CaCo2 (human colon adenocarcinoma) cells even though all these cell lines express high level of endogenous YB- 1. This may depend on a particular pathway constitutively activated in HEK293T cells or may rely on specific post-translational modifications occurring in HEK293T and possibly other cell contexts facilitating YB-1 extracellular release.

This effect was not cell type specific since it was also observed using HEK293T and CaCo2 as receiving cells (Fig. 10).

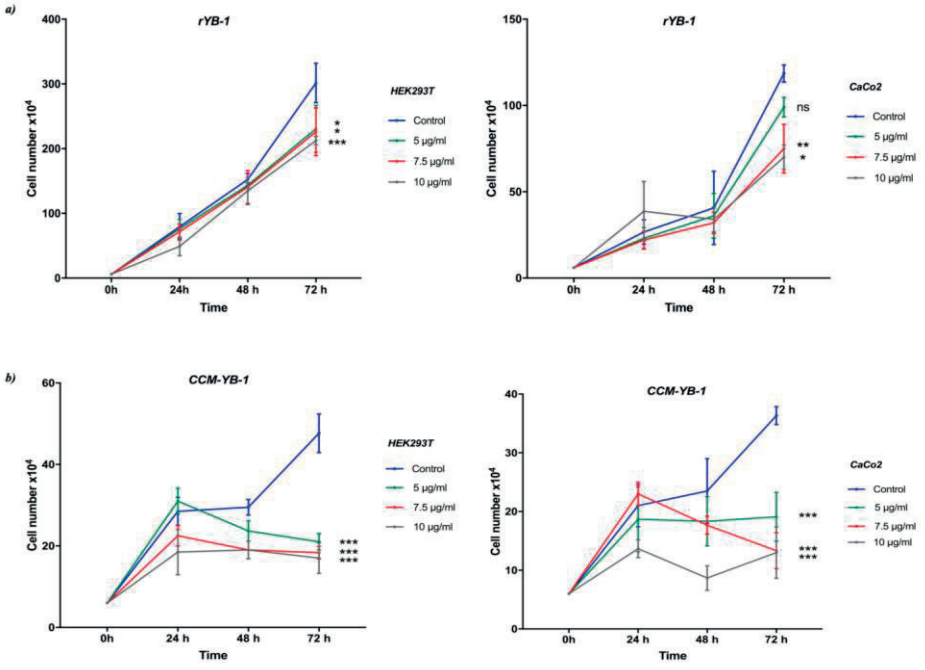

Fig. 10 – Cell proliferation profile of HEK293T (a) and CaCo2 (b) incubated with indicated concentrations of CCM-YB1 (*upper panels*) and rYB-1 (*lower panels*). Statistical analysis was performed using 2-way ANOVA followed by Dunnett's multiple comparisons test (***p<0.001, **p = 0.003, *p = 0.03, ns indicates no statistical significance).

Remarkably, compared to rYB-1, CCM-YB-1 exerted a stronger inhibitory effect on all cell lines tested (Figs. 9, 10a and b).

Flow cytometry analysis of HaCaT cells treated with extracellular YB-1 revealed that cell proliferation slowdown was due to a G2/M cell cycle arrest (Fig. 11a). Finally, to explore the molecular mechanism underlying inhibition of cell proliferation by extracellular YB-1, I analysed by quantitative PCR the mRNA level of *p21waf* and Δ*np63*α in rYB-1 or CCM-YB-1 treated HaCaT cells. p21WAF is a relevant cell cycle marker that induces G1 and G2/M cell cycle arrest by inhibiting the kinase activity of CDK-cyclin complexes (Abbas and Dutta 2009) while Δ*np63*α maintains the proliferative capacity of keratinocytes (McDade *et al.*, 2011).

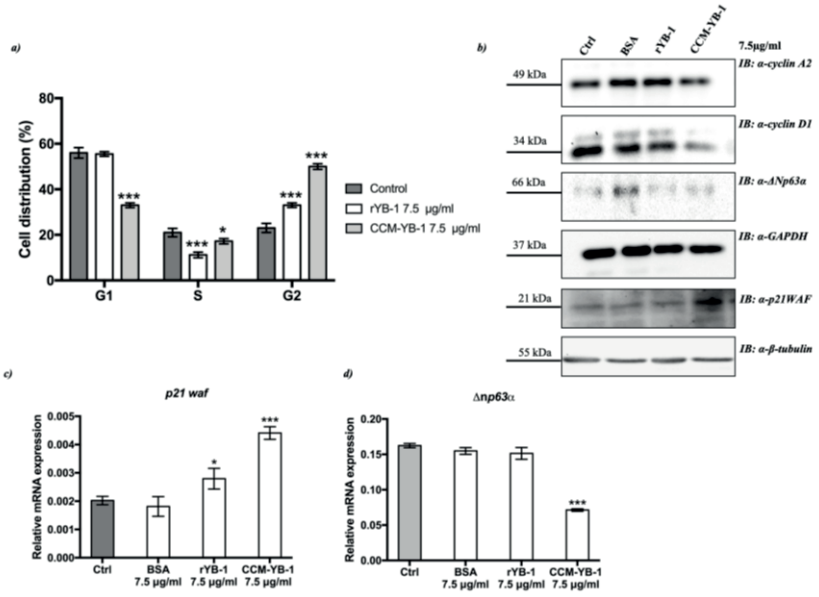

Fig. 11 – (a) cell cycle profile of HaCaT cells treated with 7.5 µg/ml of CCM-YB-1, rYB-1, BSA or left untreated for 48 hours. Statistical analysis was performed using 2-way ANOVA followed by Dunnett's multiple comparisons test. Levels of significance are indicated (***p<0.001, *p = 0.01); (b) western blot of total extracts of HaCaT cell treated with rYB-1 and CCM-YB1 and revealed with the indicated antibodies. GAPDH and β-tubulin were used as loading control; c-d) RT-qPCR analysis of *p21waf* and Δ*np63*α in HaCaT cells treated with 7.5 µg/ml of CCM- YB-1, rYB-1, BSA or left untreated (Ctrl) for 48 hours. Statistical analysis was performed using 1-way ANOVA followed by Dunnett's multiple comparisons test. Levels of significance are indicated (***p<0.001, *p = 0.01).

p21waf was strongly induced by both rYB-1 and CCM-YB-1 while Δ*np63*α was significantly downregulated only by treatment with CCM-YB-1 (Fig. 11 c and d). By western blot analysis we also confirmed reduction of Δ*np63*α and induction of p21WAF at protein level (Fig. 11b). Moreover, according to the observed cell cycle arrest the level of cyclin A2 and cyclin D1 were also reduced (Fig. 11b).

5 - CONCLUSION

In my recent activity I have reported evidences that the extracellular release of YB-1 by HEK293T is not the result of a passive mechanism, but follows a rationale. In other cell types, such as CaCo2 and HaCaT cells, even if the general YB-1 behaviour is conserved and the protein is abundant as in HEK293T cells

(Ciani *et al*. 2018; Di Costanzo *et al.* 2012; di Martino *et al.* 2016), no YB-1 secretion occurs.

Based on all these observations I can reasonably conclude that secretion of YB-1 upon oxidative and inflammatory stimuli is cell-type dependent and that enhanced level of YB-1 in the extracellular environment is a clear sign of cellular stress. The production of a recombinant form of the protein and the purification of a fraction from conditioned culture medium, allowed me to have two *tools* to perform functional studies on receiving cells. Referring to the major molecular pathway in which YB-1 is involved (Lyabin *et al.*, 2014) I decided to verify possible effects on cell proliferation and inflammation. As receiving cells, after different preliminary tests, I choose HaCaT cells which offer a well-studied and simplified model of the skin (di Martino *et al*. 2016). Treatments were performed mostly with a fixed concentration of exYB-1 (7.5 μg/ml) as indicated in the text, because, among all concentration tested, was the one which gave reproducible and consistent results.

Both extracellular YB-1 forms seem to negatively control cell proliferation inducing a G2/M phase arrest. The effect of CCM-YB-1 is stronger compared to that of rYB-1, perhaps as a consequence of the post-post-translational modifications as discussed above.

To summarize, it can be said that treatment with exYB-1 produce effect on cell proliferation in immortalized keratinocyte. The same effect on cell proliferation was observed also in HEK293T cells, which have a complex karyotype, with two or more copies of each chromosome, including three copies of the X chromosome, and in CaCo2, cells of human adenocarcinoma. Those findings could represent a starting point to verify if secreted YB-1 could work not only as signal, but also as effector molecule. Further investigations should be extended to untransformed cell lines, to verify the potential role of YB-1 as anti-proliferative agent for cancer cells.

6 - REFERENCES

Abbas T. and Dutta A. (2009) P21 in Cancer: Intricate Networks and Multiple Activities. *Nature Revision*, **9**(6): 400-414.

Anderson P. and Kedersha N. (2008) Stress Granules: The Tao of RNA Triage. *Trends in Biochemical Sciences,* **33**(3):141-150.

Anderson P., Kedersha N., and Ivanov P. (2015) Stress Granules, P-Bodies and Cancer. *Biochimica et Biophysica Acta - Gene Regulatory Mechanisms,* **1849**(7):861–870.

Aulas A., Fay M.M., Lyons S.M., Achorn C.A., Kedersha N., Anderson P., and Ivanov P. (2017) Stress-Specific Differences in Assembly and Composition of Stress Granules and Related Foci. *Journal of Cell Science*, **130**(5):927-937.

Aydin Halil, Farshad C. Azimi, Jonathan D. Cook, and Jeffrey E. Lee. (2012) A Convenient and General Expression Platform for the Production of Secreted Proteins from Human Cells. *Journal of Visualized Experiments,* **65** e4045.

Brandt Sabine, Ute Raffetseder, Sonja Djudjaj, Anja Schreiter, Bert Kadereit, Melanie Michele, Melanie Pabst, Cheng Zhu, and Peter R. Mertens. (2011) Cold Shock Y-Box Protein-1 Participates in Signaling Circuits with Auto-Regulatory Activities. European *Journal of Cell Biology*, **91**(6-7):464-71.

Ciani Francesca, Simona Tafuri, Annaelena Troiano, Alessio Cimmino, Bianca S. Fioretto, Andrea M. Guarino, Alessandra Pollice, Maria Vivo, Antonio Evidente, Domenico Carotenuto, and Viola Calabrò. (2018) Anti-Proliferative and pro-Apoptotic Effects of Uncaria Tomentosa Aqueous Extract in Squamous Carcinoma Cells. *Journal of Ethnopharmacology,* **211**:285-294.

Cleves Ann E. (1997) Protein Transport: The Nonclassical Ins and Outs. *Current Biology*, **7**(5):318-320.

Di Costanzo A., Troiano A., Di Martino O., Cacace A., Natale C.F., Ventre M., Netti P., Caserta S., Pollice A., La Mantia G., and Calabrò V. (2012) The P63 Protein Isoform ΔNp63α Modulates Y-Box Binding Protein 1 in Its Subcellular Distribution and Regulation of Cell Survival and Motility Genes. *Journal of Biological Chemistry,* **287**(36):30170-30180.

di Martino O., Troiano A., Guarino A.M., Pollice A., Vivo M., La Mantia G., and Calabrò V. (2016) ΔNp63α Controls YB-1 Protein Stability: Evidence on YB-1 as a New Player in Keratinocyte Differentiation. *Genes to Cells,* **21**(6):648-660.

Eliseeva I.A., Kim E.R., Guryanov S.G., Ovchinnikov L.P., and Lyabin D.N. (2011) Y-Box-Binding Protein 1 (YB-1) and Its Functions. *Biochemistry (Moscow),* **76**(13):1402-33.

Evdokimova V., Ruzanov P., Imataka H., Raught B., Svitkin Y., Ovchinnikov L.P, and Sonenberg N. (2001) The Major MRNA-Associated Protein YB-1 Is a Potent 5′ Cap-Dependent MRNA Stabilizer. *EMBO Journal*, **20**(19):5491-5502.

Frye B.C., Halfter S., Djudjaj S., Muehlenberg P., Weber S., Raffetseder U., En-Nia A-, Knott H., Baron J.M., Dooley S., Bernhagen J., and Mertens P.R. (2009) Y-Box Protein-1 Is Actively Secreted through a Non-Classical Pathway and Acts as an Extracellular Mitogen. *EMBO Reports*, **10**(7):783–789.

Guarino A.M., Troiano A., Pizzo E., Bosso A., Vivo M., Pinto G., Amoresano A., Pollice A., La Mantia G., and Calabrò V. (2018) Oxidative Stress Causes Enhanced Secretion of YB-1 Protein That Restrains Proliferation of Receiving Cells. *Genes,* **9**(10), 513.

Hanssen L., Alidousty C., Djudjaj S., Frye B.C, Rauen T., Boor P., Mertens P.R., van Roeyen C.R, Tacke F., Heymann F., Tittel A.P., Koch A., Floege J., Ostendorf T., and Raffetseder U. (2013) YB-1 Is an Early and Central Mediator of Bacterial and Sterile Inflammation In Vivo. *The Journal of Immunology*, **191**(5).

Kang S., Taeyun A.L., Eun A.R., Eunhye L., Hyun J.C., Sungwook L., and Boyoun P. (2014) Differential Control of Interleukin-6 MRNA Levels by Cellular Distribution of YB-1. *PLoS ONE,* **9**(11):e112754.

Kedersha N. and Anderson P. (2007) Mammalian Stress Granules and Processing Bodies. *Methods in Enzymology*, **431**:61-81.

Kedersha N., Stoecklin G., Ayodele M., Yacono P., Lykke-Andersen J., Fitzler M.J., Scheuner D., Kaufman R.J., Golan D.E., and Anderson P. (2005) Stress Granules and Processing Bodies Are Dynamically Linked Sites of MRNP Remodeling. *Journal of Cell Biology,* **169**(6):871-884.

Khong A. and Jan E. (2011) Modulation of Stress Granules and P Bodies during Dicistrovirus Infection. *Journal of Virology*, **85**(4):1439-1451.

Kim E.R., Selyutina A.A,. Buldakov I.A., Evdokimova V., Ovchinnikov L.P., and Sorokin A.V. (2013) The Proteolytic YB-1 Fragment Interacts with DNA Repair Machinery and Enhances Survival during DNA Damaging Stress. *Cell Cycle*, **12**(24):3791-3803.

Kohno K., Izumi H., Uchiumi T., Ashizuka M., and Kuwano M. (2003) The Pleiotropic Functions of the Y-Box-Binding Protein, YB-1. *BioEssays*, **25**(7): 91-698.

Lyabin D.N., Eliseeva I.A., and Ovchinnikov L.P. (2014) YB-1 Protein: Functions and Regulation. *Wiley Interdisciplinary Reviews: RNA,* **5**(1):95-110.

Lyons S.M., Achorn C., Kedersha N.L., Anderson P.J., and Ivanov P. (2016) YB-1 Regulates TiRNA-Induced Stress Granule Formation but Not Translational Repression. *Nucleic Acids Research,* **44**(14):6949-6960.

Mahboubi H. and Ursula S. (2017) Cytoplasmic Stress Granules: Dynamic Modulators of Cell Signaling and Disease. *Biochimica et Biophysica Acta - Molecular Basis of Disease*, **1863**(4):884-895.

Matsumoto S., Uchiumi T., Tanamachi H., Saito T., Yagi M., Takazaki S., Kanki T., and Kang D. (2012) Ribonucleoprotein Y-Box-Binding Protein-1 Regulates Mitochondrial Oxidative Phosphorylation (OXPHOS) Protein Expression after Serum Stimulation through Binding to OXPHOS MRNA. *Biochemical Journal,* **443**(2):573-584.

McDade S.S., Daksha P., and McCance D.J. (2011) P63 Maintains Keratinocyte Proliferative Capacity through Regulation of Skp2-P130 Levels. *Journal of Cell Science*, **124**(Pt 10):1635-1643.

Morimoto R.I. (2012) The Heat Shock Response: Systems Biology of Proteotoxic Stress in Aging and Disease. *Cold Spring Harbor Symposia on Quantitative Biology*, **76**:91-9.

Ohga T., Uchiumi T., Makino Y., Koike K., Wada M., Kuwano M. and Kohno K. (1998) Direct Involvement of the Y-Box Binding Protein YB-1 in Genotoxic Stress-Induced Activation of the Human Multidrug Resistance 1 Gene. *Journal of Biological Chemistry,* **11**(273): 6030.

Palicharla V.R. and Subbareddy M. (2015) HACE1 Mediated K27 Ubiquitin Linkage Leads to YB-1 Protein Secretion. *Cellular Signalling,* **27**(12): 2355-2362.

Rauen T., Raffetseder U., Frye B.C., Djudjaj S., Mühlenberg P.J.T, Eitner F., Lendahl U., Bernhagen J., Dooley S., and Mertens P.R. (2009) YB-1 Acts as a Ligand for Notch-3 Receptors and Modulates Receptor Activation. *Journal of Biological Chemistry,* **284**(39):26928-26940.

Shurtleff M.J., Yao J., Qin Y., Nottingham R.M., Temoche-Diaz M.M., Schekman R., and Lambowitz A.M. (2017) Broad Role for YBX1 in Defining the Small Noncoding RNA Composition of Exosomes. *Proceedings of the National Academy of Sciences*, **114**(43): E8987-E8995.

Somasekharan S.P., El-Naggar A., Leprivier G., Cheng H., Hajee S., Grunewald T.G.P., Zhang F., Ng T., Delattre O., Evdokimova V., Wang Y., Gleave M., and Sorensen H.P. (2015) YB-1 Regulates Stress Granule Formation and Tumor Progression by Translationally Activating G3BP1. *Journal of Cell Biology*, **208**(7):913-929.

Szul T. and Sztul E. (2011) COPII and COPI Traffic at the ER-Golgi Interface. *Physiology*, **26**(5): 348-364.

Tartakoff A., Vassalli P., and Détraz M. (1978) Comparative Studies of Intracellular Transport of Secretory Proteins. *The Journal of Cell Biology*, **79**(3):694-707.

Thomas M.G., Loschi M., Desbats M.A., and Boccaccio G.L. (2011) RNA Granules: The Good, the Bad and the Ugly. *Cellular Signalling,* **3**(2):324-334.

Uings I.J. and Farrow S.N. (200) Cell Receptors and Cell Signalling. *Journal of Clinical Pathology - Molecular Pathology*, **53**(6):295-299.

Yang M. Chen J., Su F., Yu B., Su F., Lin L., Liu Y., Dong Huang J., and Song E. (2011) Microvesicles Secreted by Macrophages Shuttle Invasion-Potentiating MicroRNAs into Breast Cancer Cells. *Molecular Cancer,* **10**:117.

Rend. Acc. Sc. fis. mat. Napoli
Vol. LXXXVI, (2019) pp. 25-37

DOI 10.32092/1016

Single molecules methylation analysis

Nota di Ornella Affinito[1]*, Lorenzo Chiariotti[1,2], Sergio Cocozza[1]
(Adunanza del 15 marzo 2019)

Keywords: DNA methylation; qualitative analysis; methylation class; epialleles; methylation/demethylation dynamics; brain DNA methylation

Abstract - DNA methylation is involved in a broad range of biological processes. Traditional quantitative approach summarizes DNA methylation data as average percentage of methylated CpGs in specific genomic regions, or as methylation percentage for single CpG site. Such kind of approach gives important information on the general relationships between methylation and expression but might be not able to describe the complex epigenetic structure and dynamics within a cell population. In order to better decode epigenetic data, the analysis of DNA methylation from a qualitative point of view can provide an added value to the quantitative one. The qualitative approach allows methylation profiles of cell populations to be studied at the single molecule level and can be successfully applied in a broad range of biological systems, both physiological and pathological ones. In this way, it is possible to describe the methylation and demethylation dynamics, to investigate the epialleles distribution, to follow their evolution and to gain insight on epigenetic heterogeneity degree at specific loci. The tracking of the methylation profiles is more faithful to the epigenetic state of different loci and allows a more detailed overview of the methylation landscape in a tissue, which is composed by a mosaic of epigenetically different cells.

Riassunto - La metilazione del DNA gioca un ruolo fondamentale in molti processi biologici. Con l'approccio quantitativo tradizionale, la metilazione del DNA viene espressa come percentuale media di siti CpGs metilati in specifiche regioni genomiche, o come percentuale di metilazione per singolo sito CpG. Questo tipo di approccio fornisce importanti informazioni sulle relazioni generali tra metilazione ed espressione ma non è

[1] Department of Molecular Medicine and Medical Biotechnology, University of Naples "Federico II", 80131, Naples, Italy.
[2] Endocrinology and Molecular Oncology Institute (I.E.O.S.), National Research Council (C.N.R.), 80131, Naples, Italy.
*Vincitrice del Premio "Lisa De Conciliis" per il 2018.

sufficiente a descrivere la complessa struttura epigenetica all'interno di una popolazione cellulare. Al fine di decodificare meglio i dati epigenetici, l'analisi della metilazione del DNA da un punto di vista qualitativo può fornire un valore aggiunto a quello quantitativo. L'approccio qualitativo consente di studiare i profili di metilazione delle popolazioni cellulari a livello di singola molecola e può essere applicato con successo in differenti sistemi biologici, sia fisiologici che patologici. In questo modo, è possibile descrivere le dinamiche di metilazione e demetilazione, studiare la distribuzione di epialleli, seguire la loro evoluzione e ottenere informazioni sul grado di eterogeneità epigenetica in specifici loci. L'analisi dei profili di metilazione è più fedele allo stato epigenetico dei diversi loci e consente una panoramica più dettagliata del *landscape* di metilazione in un tessuto, che è composto da un mosaico di cellule epigeneticamente differenti.

1 - INTRODUCTION

Epigenetics is referred to changes in gene expression, which are heritable through multiple cell division cycles. These changes result from a set of reversible modifications that occur without alterations in the DNA sequence and include nucleic acid modification, chromatin remodelling and histone modifications. Regarding nucleic acid modification, DNA methylation is a common epigenetic mark in many eukaryotes, involved in the regulation of gene expression (Suzuki and Bird, 2008; Law and Jacobsen, 2010). DNA methylation has been recognized to play an important role in many biological processes, such as cellular differentiation (Khavari *et al.*, 2010), development (Smith and Meissner, 2013), disease (Robertson, 2005), aging (Fraga and Esteller, 2007), X-inactivation (Sharp *et al.*, 2011), imprinting (Li *et al.*, 1994), silencing of repetitive DNA (Slotkin and Martienssen, 2007) and chromosomal stability (Rizwana and Hahn, 1999).

In mammals, the most studied form of DNA methylation occurs on cytosine residues of CpG dinucleotides, by the addition of a methyl group at the C5 position. DNA methylation is mediated by the DNA methyltransferase (DNMT) family: DNMT3A and DNMT3B, responsible for the de novo methylation, and DNMT1, mainly involved in maintaining methylcytosine marks during DNA replication (Smith and Meissner, 2013). On the other side, DNA demethylation can take place through two mechanisms: passive and active demethylation. In the passive demethylation, 5-methylcytosine (5mC) can be lost or erased during cell division, while the active demethylation is mediated by Ten-11 translocation enzymes (TETs) (Kriaucionis. and Heintz, 2009).

In the human genome, both the CpG sites and their degrees of methylation are unevenly distributed in the genome (Bird *et al.*, 1985; Ehrlich *et al.*, 1982). Two fractions with distinct properties are distinguishable: a major fraction (~98%), in which CpGs are relatively infrequent (on average 1 per 100 bp) but highly methylated (approximately 70%–80% of all CpG sites), and a minor fraction

(<2%) that comprises short stretches of DNA (approximately 1 kb in length and longer than 200bp) in which CpG sites are frequent (~1 per 10 bp; CpG- rich regions), G+C base content is high (above 50% G+C content) and the observed-to-expected CpG ratio is greater than 60 %. The latter are known as CpG islands (CGIs) and they are usually methylation- free. They are found within the promoters of ~60-70% of human genes (Larsen *et al.*, 1992; Saxonov *et al.*, 2006). Due to their unmethylated status, CGI- promoters are characterised by a transcriptionally permissive chromatin state and are indeed generally associated with constitutively expressed genes in all cell type (housekeeping genes), but a subset of them may be subject to tissue- specific gain of methylation (Song *et al.*, 2005) or during the development (Li 2002), resulting in a stable transcriptional repression. However, CGI hypermethylation is required for the long-term silencing of genes located on the inactive X chromosome (Sharp *et al.*, 2011) or associated with imprinted loci (Li *et al.*, 1994), germline-specific genes (De Smet *et al.*, 1999) and pluripotency-associated genes (Mohn *et al.*, 2008).

Aberrant DNA methylation is associated with many human diseases and is a hallmark of cancer (Robertson, 2005). These epigenetic changes impact the biological activity of cells through their modification of transcriptional states and regulatory machinery. Hypermethylation of CGI promoters may contribute to carcinogenesis by inactivating tumor suppressor genes or DNA repair genes, while hypomethylation contributes to carcinogenesis by activating oncogene or promoting genomic instability.

2 - SINGLE MOLECULES METHYLATION ANALYSIS

DNA methylation has been extensively analysed from a genomic point of view both in normal and in pathogenic tissues (Bergman and Cedar, 2013; Shames *et al.*, 2007; Robertson and Wolfe, 2000), but the dynamics that form, maintain and reprogram differentially methylated regions are still not well- defined. Also, little is known about genome-wide variation of DNA methylation patterns.

Genome-wide techniques are unbiased relative to the sequence representation, but limited in the coverage/single locus. This limitation is essentially due to the fact that genome- wide methylomes cannot detect methylation profiles below a certain frequency. As a consequence, the vast majority of studies on DNA methylation used a quantitative approach, namely they took in consideration the average methylation level, summarizing data into average percentage of methylated CpGs in specific genomic regions, or the methylation percentage for single CpG site, or looking at CpGs genome-wide distribution with an only relatively high resolution (Ammerpohl *et al.*, 2016; Hannum *et al.*, 2013; Hua *et al.*, 2011; Woodfine *et al.*, 2011; Vaissière *et al.*, 2009; Shaw *et al.*, 2006). Such kind of approach is useful when methylation status is uniform in the population

of cells under study, but fails to dissect and recognise different DNA methylation patterns when a heterogeneous population is investigated. Indeed, percentage methylation described in most DNA methylation studies hides important pattern and positional information of DNA methylation with potential functional and regulatory relevance (Mikesa *et al.*, 2010).

In order to better decode epigenetic data, it could be useful to analyse DNA methylation with a qualitative approach. The qualitative approach allows methylation profiles of cell populations to be studied at the single molecule level, thus providing an added value to the quantitative one.

The key feature of the qualitative approach is to perform an in-depth methylation analysis and to obtain a very high coverage (about 200.000-300.000 reads/sample) of selected loci by means of the Deep Bisulfite Amplicon Sequencing (Deep- Bis). This technique leads to observations that are not achievable with the low coverage of the genome- wide techniques and allows to conduct DNA methylation analysis at single base resolution with high speed and high throughput.

The qualitative approach is based on the following idea. Each CpG site in an individual molecule may exist in a binary state (methylated or unmethylated) and each individual DNA molecule, containing a certain number of CpGs, is a combination of these states. Nevertheless, in many studies on DNA methylation (Ammerpohl *et al.*, 2016; Hannum *et al.*, 2013; Hua *et al.*, 2011; Woodfine *et al.*, 2011; Vaissière *et al.*, 2009; Shaw *et al.*, 2006), the methylation status of a cytosine is described as the average value of many different molecules. As a consequence, this kind of analysis does not take into account the combination of the binary states of CpG sites in each single molecule. On the contrary, a high-resolution approach, which specifically looks at the individual methylation conformation of single molecules, could provide additional information. Indeed, in principle each cell may bear a specific combination of methylated CpGs at specific loci (epiallele) that may reflect the origin of the cell and/or the functional state of a given gene in that cell. These epialleles differ in their pattern of methylated and unmethylated CpG positions. These molecules (epialleles) can be grouped in methylation classes, defined as number of methylated cytosines per molecule, independently of their position. This introduces the concept of epipolymorphism, by means that cells of a tissue may be considered a population of epigenetically heterogeneous cells in which each combination of ^{m}CpG at a given locus represent a specific epiallele. Considering that a single molecule corresponds to the configuration of a single epiallele in a single cell of the complex cell mixture present in an analysed tissue, such qualitative approach could be useful to recognise different methylation profiles inside a heterogeneous cell population (i.e., tissues). Furthermore, this approach could help to better understand the mechanisms underlying the changes of methylation state of these cells during methylation and demethylation processes and to evaluate the

stochastic and /or deterministic components of these phenomena.

Conceptual differences between quantitative and qualitative methylation analysis are shown in the Fig. 1.

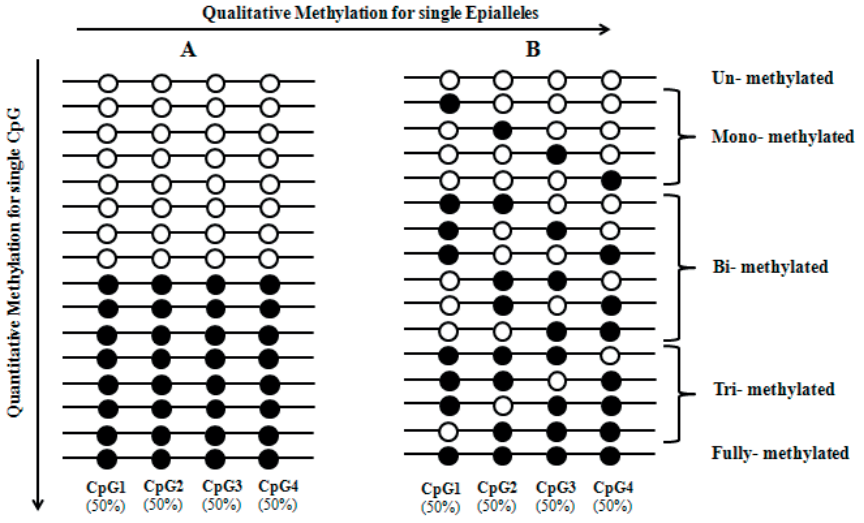

Fig. 1 – Scheme of the distributions of methylation profiles (epialleles) in two cell populations (A and B) and the corresponding methylation classes to which they belong. Empty and filled circles represent unmethylated and methylated CpGs, respectively. Each line represents a single molecule (epiallele). It should be noted that it is impossible to distinguish the DNA methylation scenarios of cell populations A and B by methodologies (e.g., pyrosequencing) that can quantify methylation at individual CpG sites.

Let's consider a locus composed by 4 CpG sites. By a quantitative point of view, both cell populations (A and B) have the same methylation value for each CpG site. However, from a qualitative point of view, DNA methylation scenarios in A and B are very different: in A two main epiallelic forms are present, while in B there is a great epiallelic diversity. In particular, as shown in B, these 4 CpGs can give arise to 16 possible methylation states or epialleles (2^{nCpGs}; 2^4) belonging to different methylation classes, including 1 unmethylated, 4 mono-methylated, 6 bi- methylated, 4 tri- methylated, 1 fully (tetra) – methylated. Thus, the methylation profiles inside the cell population B are very different and each one of the possible epialleles can have different frequency.

Qualitative approach allows to analyse DNA methylation at two different levels: i) methylation classes, defined as the number of methylated cytosine per molecule, independently of their position; 2) epialleles, defined as different combination of methylated CpG sites (^{m}CpGs) at a given locus.

Some applications of the qualitative approach are reported in the following paragraphs.

3 - MODELING DNA METHYLATION AND DEMETHYLATION DYNAMICS

DNA methylation has been extensively analyzed from a genomic perspective in both normal and pathological tissues (Bergman and Cedar, 2013; Shames *et al.*, 2007; Robertson and Wolffe, 2000), but the dynamics underlying the methylation and demethylation processes are still not well defined. The qualitative approach was applied to describe methylation and demethylation dynamics of Ddo (D-aspartate oxidase) genes occurring at various mouse developmental stages in 3 different tissues (brain, lung, and gut). Ddo is a flavin-adenine dinucleotide-containing enzyme that catalyzes the oxidative deamination of bicarboxylic D-amino acids, such as D-aspartate (D-Asp), N-methyl D-aspartate (NMDA) and D-glutamate (Still *et al.*, 1949; Van Veldhoven *et al.*, 1991, D'Aniello A *et al.*, 1993). During development, this gene undergoes methylation in lung and gut (Affinito *et al.*, 2016) and demethylation in brain (Punzo *et al*., 2016).

The complexity of the methylation and demethylation dynamics was markedly simplified by introducing the concept of methylation classes (MCs), defined as the number of methylated cytosines per molecule, irrespective of their position. The MC concept smooths the stochasticity of the system, allowing a more deterministic description. In this framework, it has been proposed a mathematical model based on the Markov chain (Fig. 2), which aims to identify the transition probability of a molecule from one MC to another during methylation and demethylation dynamics (Affinito *et al.*, 2016). This model suggests that these dynamics are ruled by a dominant class of phenomena, namely, the gain (loss) of one methyl group at a time for lung and gut (brain). Furthermore, the probability that a CpG becomes methylated or demethylated seems to depend on the existing methylation status of the whole molecule (Affinito *et al.*, 2016).

Regarding the methylation process, in the range from unmethylated to trimethylated, the lower is the existing methylation status and the lower is the probability for a molecule to become more methylated. Indeed, in the model, the class transition from an unmethylated to a monomethylated state occurs with very low probability. Upon proceeding toward a fully methylated state (from tri- to tetra-, from tetra- to penta- and from penta- to hexa-methylated MCs), the transition probability decreases. In the case of demethylation dynamics, the model shows a gradual decrease of the transition probability from an unmethylated class to a fully methylated one. In other words, the less methylated a molecule is, the higher the probability of it being further demethylated (Affinito *et al.*, 2016).

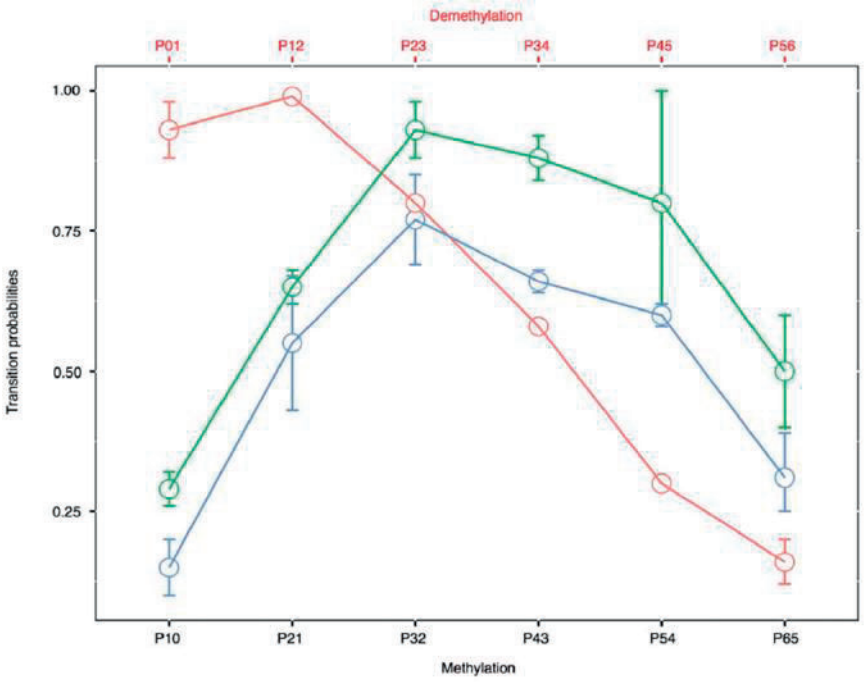

Fig. 2 – Transition probability during methylation and demethylation processes for the 3 tissues (violet = brain; green = gut; blue = lung) (Affinito *et al.*, 2016).

4 - TRACKING THE EVOLUTION OF EPIALLELES IN BRAIN CELL POPULATION

DNA methylation landscape is dynamically remodelled during the mammalian life cycle through distinct phases of reprogramming and *de novo* methylation (Hackett and Surani, 2012). This remodelling occurs through an establishment of a globally demethylated state during early embryogenesis. Then, at late stages of embryonic development and early post- natally, a lineage-specific methylome that maintains cellular identity is shaped (Mohn *et al.*, 2008; Liu *et al.*, 2015; Tanaka *et al.*, 2014; Ji *et al.*, 2010). Once such reconfiguration comes to end, it may be maintained throughout the life. Appropriate patterns of DNA methylation in the brain play an important role in neurodevelopment and neuropsychiatric conditions (Tsankova *et al.*, 2007; Mill *et al.*, 2008; Akbarian and Nestler, 2013; Nestler *et al.*, 2015), pointing out to the importance of correct formation and preservation of DNA methylation patterns in brain cells.

By performing an ultra-deep methylation analysis at single molecule level, it has been studied the promoter region of developmentally regulated D-Aspartate oxidase (Ddo) taking into account cell-to- cell heterogeneity and quantifying the frequency of each methylation pattern (epiallele) present in

mixed and pure populations during brain development and embryonic stem cell neural differentiation (Florio *et al.*, 2017). In this framework, an epiallele is defined as a specific combination of methylated CpG within Ddo locus and can represent the epigenetic haplotype revealing a cell-to-cell methylation heterogeneity. Using this approach, it has been found a high degree of polymorphism of methylated alleles (epipolymorphism) evolving in a remarkably conserved fashion during brain development. The different sets of epialleles mark developmental stage, brain areas, and cell type and unravel the possible role of specific CpGs in favoring or inhibiting local methylation (Florio *et al.*, 2017). Spatially specific methylation patterns emerge, by means that some CpGs are particularly sensitive to changes in methylation, creating an initiation point for methylation that then spreads over the region. This means that methylation profiles take origin by the spreading from susceptible sites that, when methylated, become able to influence nearby CpGs.

Undifferentiated embryonic stem cells show non-organized distribution of epialleles that apparently originated by stochastic methylation events on individual CpGs. Upon neural differentiation, the epiallele distribution is profoundly different, gradually shifting toward an ordered, non-stochastic, and less polymorphic epiallele profile (Fig. 3) (Florio *et al.*, 2017).

Overall, epiallele composition dynamics in brain cell population are very finely tuned and strikingly conserved. Moreover, tracking epiallele profiles may help get insight into the mechanisms underlying DNA methylation establishment, changes and, potentially, alterations of these processes that occur in neurodevelopmental diseases, which may not be revealed by conventional analyses of (gene-specific or genome-wide) average methylation.

5 - DNA METHYLATION LANDSCAPE OF DDO GENE IN POST-MORTEM BRAIN FROM CONTROLS AND SUBJECTS WITH SCHIZOPHRENIA

The spatio-temporal regulation of the D-aspartate oxidase (Ddo), a gene involved in the degradation of D-aspartate, plays a pivotal role in determining the correct levels of this D-amino acid in the human brain. Perturbation of D-Asp metabolism has been implicated as a contributor to the pathogenesis of this devastating mental illness (Balu and Coyle, 2015; Errico *et al.*, 2015). Epigenetic mechanisms could drive the appropriate spatio-temporal modulation of these genes in human brain. Therefore, it could be envisaged that altered epigenetic profiles at the Ddo gene may be associated with human brain disorders, including schizophrenia.

To finely map cell to cell methylation differences in specific brain areas and to evaluate whether methylation profiles may distinguish brain areas within each individual and/or be associated to schizophrenia diagnosis, it has been performed an ultra-deep analysis of DNA methylation of Ddo gene in three different post-mortem brain areas (hippocampus, dorsolateral prefrontal cortex, and

cerebellum) of patients with schizophrenia and non-psychiatric controls. DNA methylation analysis was performed at an ultradeep level, measuring individual epialleles frequency by single molecule approach (Keller *et al.*, 2018). Single-molecule methylation approach demonstrated that analysis of epiallele distribution of the Ddo gene was able to detect differences in DNA methylation representing area-specific methylation signatures, which are likely not detectable with targeted or genome-wide classic methylation analyses.

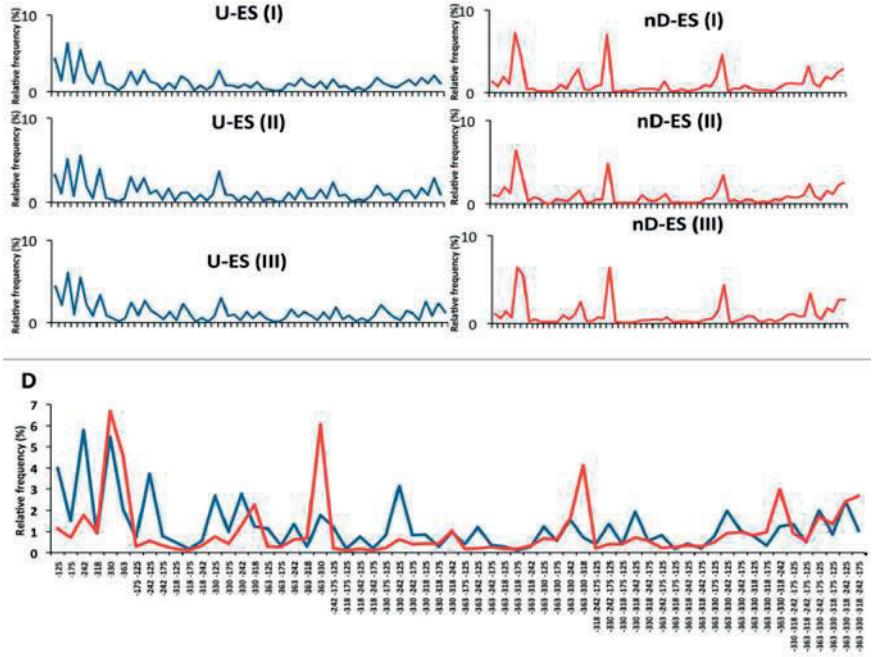

Fig. 3 – Epiallele frequency distribution in 3 independent ESCs differentiation experiments (I, II, and III). The line plots represent the frequency distribution of each epialleles (blue: undifferentiated ESC; red: differentiated ESCs). D) Comparison between average frequency distribution of each Ddo epialleles, from 3 independent experiments, in undifferentiated (blue line) vs. differentiated (red line) ESCs. The specific methyl CpG combinations of each epialleles are indicated on the x-axis (Florio *et al.*, 2017).

Average methylation is very low in cerebellum (about 5%) with no significant differences between schizophrenia and control groups (Fig. 4A). The average Ddo promoter methylation is significantly higher in the DLPFC than in the HIPP, both within control and schizophrenia groups. Moreover, there is a mild but significant increase in Ddo methylation levels in the HIPP of schizophrenia-affected patients, compared to control group, while no differences between diagnoses were found in the DLPFC (Nuzzo *et al.*, 2017; Keller *et al.*, 2018) (Fig. 4A). As expected by the lower average methylation, epialleles classes analysis shows that cerebellum displayed a clearly different pattern compared to HIPP

and DLPFC (Fig. 4B). However, although sharing a similar average methylation, DLPFC and hippocampus displayed significant differences in epialleles classes distribution (Fig. 4B) (Cramer test, $p < 0.05$). The PcoA plot confirmed that the CB clearly differed in terms of epialleles distribution from HIPP and DLPFC indicating that epiallelic patterns strongly typified CB cells with respect to the other two areas (Fig. 4C). Although schizophrenia-related patterns were not detected, the ability to detect brain region specific profiles in terms of individual cell methylation patterns, demonstrates the feasibility for an epiallelic approach to distinguish disease-related profiles at relevant loci in psychiatric conditions (Keller *et al.*, 2018).

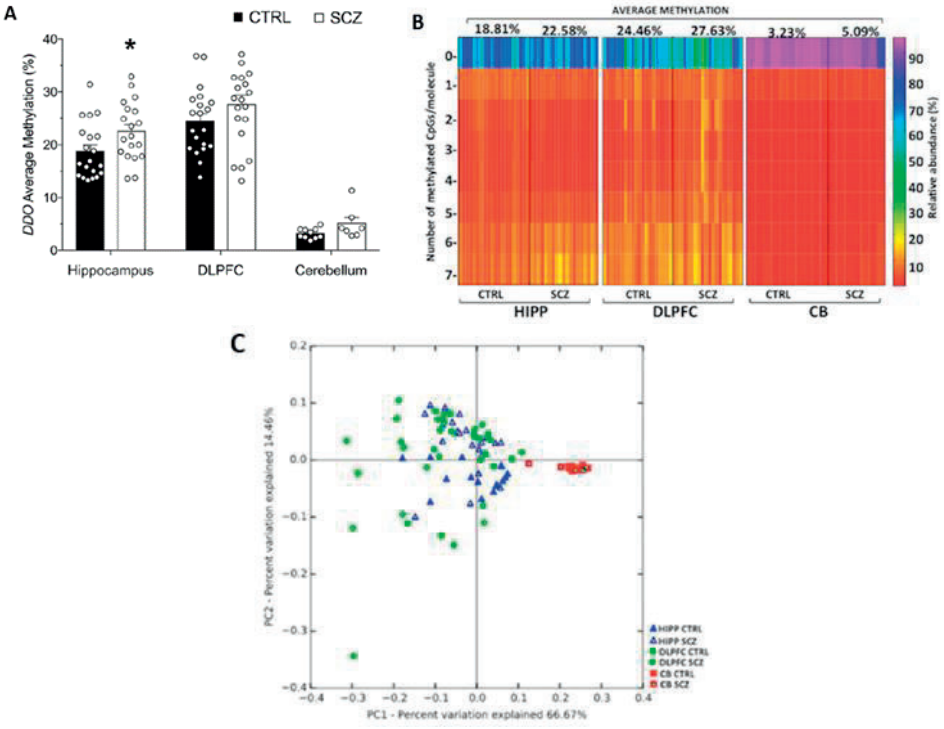

Fig. 4 – Methylation and Epiallele composition analyses in Ddo gene. A) Ddo average methylation is shown for both groups (non-psychiatric controls = CTRL and patients with schizophrenia = SCZ) and in each brain area (hippocampus = HIPP, dorso-lateral prefrontal cortex = DLPFC and cerebellum = CB) (Nuzzo *et al.*, 2017; Keller *et al.*, 2018). B) Heatmaps show the epiallelic classes abundance in HIPP, DLPFC and CB and for CTRL and SCZ groups. The color scale (from red to violet) indicates the frequency of each epiallelic class. On the top of the graph, the average methylation for CTRL and SCZ groups is reported for each brain area (Keller *et al.*, 2018). (C) DDO epiallelic composition is reported in Bray Curtis-based 2D Principal Coordinate Analysis (PCoA) plot. PC1 and PC2 in PCoA plot explained the percentage of the observed variance (Keller *et al.*, 2018).

6 - REFERENCES

Affinito O., Scala G., Palumbo D., Florio E., Monticelli A., Miele G., Avvedimento V.E., Usiello A., Chiariotti L. and Cocozza S. (2016) Modeling DNA methylation by analyzing the individual configurations of single molecules. *Epigenetics* **11**, 881-888.

Akbarian S. and Nestler E.J. (2013) Epigenetic mechanisms in psychiatry. *Neuropsychopharmacology* **38**, 1-2.

Ammerpohl O., Haake A., Kolarova J. and Siebert R. (2016) Quantitative DNA Methylation Profiling in Cancer. *Methods Mol Biol* **1381**, 75-92.

Balu D.T. and Coyle J.T. (2015) The NMDA receptor 'glycine modulatory site' in schizophrenia: D-serine, glycine, and beyond. *Curr Opin Pharmacol* **20**, 109-115.

Bergman Y. and Cedar H. (2013) DNA methylation dynamics in health and disease. *Nat Struct Mol Biol* **20**, 274-281.

Bird A., Taggart M., Frommer M., Miller O.J. and Macleod D. (1985) A fraction of the mouse genome that is derived from islands of nonmethylated, CpG-rich DNA. *Cell* **40**, 91-99.

D'Aniello A., Vetere A. and Petrucelli L. (1993) Further study on the specificity of D-amino acid oxidase and D-aspartate oxidase and time course for complete oxidation of D-amino acids. *Comp Biochem Physiol B* **105**, 731-734.

De Smet C., Lurquin C., Lethé B., Martelange V. and Boon T. (1999) DNA methylation is the primary silencing mechanism for a set of germ line- and tumor-specific genes with a CpG-rich promoter. *Mol Cell Biol* **19**, 7327-7335.

Ehrlich M., Gama-Sosa M.A., Huang L.H., Midgett R.M., Kuo K.C., McCune R.A. and Gehrke C. (1982) Amount and distribution of 5-methylcytosine in human DNA from different types of tissues of cells. *Nucleic Acids Res* **10**, 2709-2721.

Errico F., Mothet J.P. and Usiello A. (2015) D-Aspartate: An endogenous NMDA receptor agonist enriched in the developing brain with potential involvement in schizophrenia. *J Pharm Biomed Anal* **116**, 7-17.

Florio E., Keller S., Coretti L., Affinito O., Scala G., Errico F., Fico A., Boscia F., Sisalli M.J., Reccia M.G., Miele G., Monticelli A., Scorziello A., Lembo F., Colucci-D'Amato L., Minchiotti G., Avvedimento V.E., Usiello A., Cocozza S. and Chiariotti L. (2017) Tracking the evolution of epialleles during neural differentiation and brain development: D-Aspartate oxidase as a model gene. *Epigenetics* **12**, 41-54.

Fraga M.F. and Esteller M. (2007) Epigenetics and aging: the targets and the marks. *Trends Genet* **23**, 413-418.

Hackett J.A. and Surani M.A. (2013) DNA methylation dynamics during the mammalian life cycle. *Philos Trans R Soc Lond B Biol Sci* **368**, 20110328.

Hannum G., Guinney J., Zhao L., Zhang L., Hughes G., Sadda S., Klotzle B., Bibikova M., Fan J.B., Gao Y., Deconde R., Chen M., Rajapakse I., Friend S., Ideker T. and Zhang K. (2013) Genome-wide methylation profiles reveal quantitative views of human aging rates. *Mol Cell* **49**, 359-367.

Hua D., Hu Y., Wu Y.Y., Cheng Z.H., Yu J., Du X. and Huang Z.H. (2011) Quantitative methylation analysis of multiple genes using methylation-sensitive restriction enzyme-based quantitative PCR for the detection of hepatocellular carcinoma. *Exp Mol Pathol* **91**, 455-460.

Ji H., Ehrlich L.I., Seita J., Murakami P., Doi A., Lindau P., Lee H., Aryee M.J., Irizarry R.A., Kim K., Rossi D.J., Inlay M.A., Serwold T., Karsunky H., Ho L., Daley G.Q., Weissman I.L. and Feinberg A.P. (2010) Comprehensive methylome map of lineage commitment from haematopoietic progenitors. *Nature* **467**, 338-342.

Keller S., Punzo D., Cuomo M., Affinito O., Coretti L., Sacchi S., Florio E., Lembo F., Carella M., Copetti M., Cocozza S., Balu D.T., Errico F., Usiello A. and Chiariotti L. (2018) DNA methylation landscape of the genes regulating D-serine and D-aspartate metabolism in post-mortem brain from controls and subjects with schizophrenia. *Sci Rep* **8**, 10163.

Khavari D.A., Sen G.L. and Rinn J.L. (2010) DNA methylation and epigenetic control of cellular differentiation. *Cell Cycle* **9**, 3880-3883.

Kriaucionis S. and Heintz N. (2009) The nuclear DNA base 5-hydroxymethylcytosine is present in Purkinje neurons and the brain. *Science* **324**, 929-930.

Larsen F., Gundersen G., Lopez R. and Prydz H. (1992) CpG islands as gene markers in the human genome. *Genomics* **13**, 1095-1107.

Law J.A. and Jacobsen S.E. (2010) Establishing, maintaining and modifying DNA methylation patterns in plants and animals. *Nat Rev Genet* **11**, 204-220.

Li E., Beard C., Jaenisch R. (1994) Role for DNA methylation in genomic imprinting. *Trends in Genetics*. **10,** 78.

Li E. (2002) Chromatin modification and epigenetic reprogramming in mammalian development. *Nat Rev Genet* **3**, 662-673.

Liu H., Liu X., Zhang S., Lv J., Li S., Shang S., Jia S., Wei Y., Wang F., Su J., Wu Q. and Zhang Y. (2016) Systematic identification and annotation of human methylation marks based on bisulfite sequencing methylomes reveals distinct roles of cell type-specific hypomethylation in the regulation of cell identity genes. *Nucleic Acids Res* **44**, 75-94.

Mikeska T., Candiloro I.L. and Dobrovic A. (2010) The implications of heterogeneous DNA methylation for the accurate quantification of methylation. *Epigenomics* **2**, 561-573.

Mill J., Tang T., Kaminsky Z., Khare T., Yazdanpanah S., Bouchard L., Jia P., Assadzadeh A., Flanagan J., Schumacher A., Wang S.C. and Petronis A. (2008) Epigenomic profiling reveals DNA-methylation changes associated with major psychosis. *Am J Hum Genet* **82**, 696-711.

Mohn F., Weber M., Rebhan M., Roloff T.C., Richter J., Stadler M.B., Bibel M. and Schübeler D. (2008) Lineage-specific polycomb targets and de novo DNA methylation define restriction and potential of neuronal progenitors. *Mol Cell* 30, 755-766.

Nestler E.J., Peña C.J., Kundakovic M., Mitchell A. and Akbarian S. (2016) Epigenetic Basis of Mental Illness. *Neuroscientist* **22**, 447-463.

Nuzzo T., Sacchi S., Errico F., Keller S., Palumbo O., Florio E., Punzo D., Napolitano F., Copetti M., Carella M., Chiariotti L., Bertolino A., Pollegioni L. and Usiello A. (2017) Decreased free d-aspartate levels are linked to enhanced d-aspartate oxidase activity in the dorsolateral prefrontal cortex of schizophrenia patients. *NPJ Schizophr* **3**, 16.

Punzo D., Errico F., Cristino L., Sacchi S., Keller S., Belardo C., Luongo L., Nuzzo T., Imperatore R., Florio E., De Novellis V., Affinito O., Migliarini S., Maddaloni G., Sisalli M.J., Pasqualetti M., Pollegioni L., Maione S., Chiariotti L. and Usiello

A. (2016) Age-Related Changes in d-Aspartate Oxidase Promoter Methylation Control Extracellular d-Aspartate Levels and Prevent Precocious Cell Death during Brain Aging. *J Neurosci* **36**, 3064-3078.

Rizwana R. and Hahn P.J. (1999) CpG methylation reduces genomic instability. *J Cell Sci* **112 (Pt 24)**, 4513-4519.

Robertson K.D. (2005) DNA methylation and human disease. *Nat Rev Genet* **6**, 597-610.

Robertson K.D. and Wolffe A.P. (2000) DNA methylation in health and disease. *Nat Rev Genet* **1**, 11-19.

Saxonov S., Berg P. and Brutlag D.L. (2006) A genome-wide analysis of CpG dinucleotides in the human genome distinguishes two distinct classes of promoters. *Proc Natl Acad Sci U S A* **103**, 1412-1417.

Shames D.S., Minna J.D. and Gazdar A.F. (2007) DNA methylation in health, disease, and cancer. *Curr Mol Med* **7**, 85-102.

Sharp A.J., Stathaki E., Migliavacca E., Brahmachary M., Montgomery S.B., Dupre Y. and Antonarakis S.E. (2011) DNA methylation profiles of human active and inactive X chromosomes. *Genome Res* **21**, 1592-1600.

Shaw R.J., Liloglou T., Rogers S.N., Brown J.S., Vaughan E.D., Lowe D., Field J.K. and Risk J.M. (2006) Promoter methylation of P16, RARbeta, E-cadherin, cyclin A1 and cytoglobin in oral cancer: quantitative evaluation using pyrosequencing. *Br J Cancer* **94**, 561-568.

Slotkin R.K. and Martienssen R. (2007) Transposable elements and the epigenetic regulation of the genome. *Nat Rev Genet* **8**, 272-285.

Smith Z.D. and Meissner A. (2013) DNA methylation: roles in mammalian development. *Nat Rev Genet* **14**, 204-220.

Song F., Smith J.F., Kimura M.T., Morrow A.D., Matsuyama T., Nagase H. and Held W.A. (2005) Association of tissue-specific differentially methylated regions (TDMs) with differential gene expression. *Proc Natl Acad Sci U S A* **102**, 3336-3341.

Still J.L. and Buell M.V. (1949) Studies on the cyclophorase system; D-aspartic oxidase. *J Biol Chem* **179**, 831-837.

Suzuki M.M. and Bird A. (2008) DNA methylation landscapes: provocative insights from epigenomics. *Nat Rev Genet* **9**, 465-476.

Tanaka S., Nakanishi M.O. and Shiota K. (2014) DNA methylation and its role in the trophoblast cell lineage. *Int J Dev Biol* **58**, 231-238.

Tsankova N., Renthal W., Kumar A. and Nestler E.J. (2007) Epigenetic regulation in psychiatric disorders. *Nat Rev Neurosci* **8**, 355-367.

Vaissière T., Hung R.J., Zaridze D., Moukeria A., Cuenin C., Fasolo V., Ferro G., Paliwal A., Hainaut P., Brennan P., Tost J., Boffetta P. and Herceg Z. (2009) Quantitative analysis of DNA methylation profiles in lung cancer identifies aberrant DNA methylation of specific genes and its association with gender and cancer risk factors. *Cancer Res* **69**, 243-252.

Van Veldhoven P.P., Brees C. and Mannaerts G.P. (1991) D-aspartate oxidase, a peroxisomal enzyme in liver of rat and man. *Biochim Biophys Acta* **1073**, 203-208.

Woodfine K., Huddleston J.E. and Murrell A. (2011) Quantitative analysis of DNA methylation at all human imprinted regions reveals preservation of epigenetic stability in adult somatic tissue. *Epigenetics Chromatin* **4**, 1.

Rend. Acc. Sc. fis. mat. Napoli
Vol. LXXXVI, (2019) pp. 39-53

DOI 10.32092/1017

Xenobiotics involvement on human prostate cells functionality

Nota di Mariana Di Lorenzo[1]*, Vincenza Laforgia[1], Maria De Falco[1]
(Adunanza del 17 maggio 2019)

Keywords: EDCs, phthalates, alkylphenols, prostate.

Abstract - Alkylphenols and phthalates belong to the family of Endocrine Disruptor Chemicals (EDCs), a heterogeneous group of ubiquitous synthetic or natural substances which can affect multiple endocrine pathways, hormonal and homeostatic system. They particularly influence and perturb the reproduction since most of their effects are exerted through disturbance of estrogen or androgen-mediated processes. In prostate gland, both androgens and estrogens play a significant role in development and differentiation as well as in the maintenance of adult gland homeostasis. Therefore, even small changes in estrogen levels, including those of estrogen-mimicking chemicals, can lead to changes in prostate development, differentiation and function, but less is known about molecular pathways involved in the actions of these compounds in prostate models. Thus, the effects of two compounds with different action: the estrogenic nonylphenol (NP) and the antiandrogenic dibutylphthalate (DBP) have been investigated on human prostate non tumorigenic epithelial cells (PNT1A) and on adenocarcinoma prostate cells (LNCaP), respectively. Moreover, their effects have been compared with 17-β-estradiol (E2) action in order to investigate possible mimetical behaviour.

Riassunto - Gli alchilfenoli e gli ftalati appartengono alla famiglia dei distruttori endocrini (EDCs), un gruppo eterogeneo di sostanze sintetiche o naturali presenti in maniera ubiquitaria nell'ambiente ed in grado di influenzare il sistema endocrino a più livelli. In particolare, gli EDCs sono sostanze capaci di influenzare ed alterare la riproduzione in quanto possono interferire con i pathways degli estrogeni e degli androgeni. Nella ghiandola prostatica, sia gli androgeni che gli estrogeni giocano un ruolo significativo nello sviluppo e nella differenziazione, nonché nel mantenimento dell'omeostasi della ghiandola adulta. Pertanto, anche piccoli cambiamenti nei livelli di estrogeni, compresi quelli determinati da sostanze chimiche che mimano gli estrogeni, possono portare a cambiamenti nello sviluppo, nella differenziazione e nella funzione della ghiandola

[1] Dipartimento di Biologia, Università Federico II di Napoli, Complesso Universitario di Monte S. Angelo, via Cinthia, 80129 Napoli
*Vincitrice del Premio "Umberto Pierantoni" per il 2018.

stessa. Per tale ragione, sono stati valutati gli effetti di due composti con diversa azione: il nonilfenolo (NP), dotato di attività estrogenica, ed il dibutilftalato (DBP), dotato di attività antiandrogenica, rispettivamente su cellule epiteliali non tumorali di prostata umana (PNT1A) e su cellule di adenocarcinoma prostatico (LNCaP). Inoltre, i loro effetti sono stati confrontati con l'azione dell'ormone endogeno 17β-estradiolo (E2).

1- INTRODUCTION

In recent years, a growing number of studies has associated the worrisome trends in the incidence of reduced fertility rate observed in industrialized countries, with human exposure to specific chemicals identified as endocrine disruptors (EDCs).

EDCs are described as "exogenous chemicals or mixtures of chemicals that alter function(s) of the endocrine system and consequently cause adverse health effects in an intact organism, or its progeny, or (sub)populations" (World Health Organization, 2012).

EDCs are a heterogeneous group of compounds and they may be divided into anthropogenic and natural chemicals or classified based on your chemical properties, origin and applications.

EDCs can interfere with the endocrine system at multiple levels, by agonizing or antagonizing the target receptors or by disrupting the synthesis of the hormones or hormonal release, transport, metabolism and excretion (Giulivo *et al.*, 2016). The more frequent EDC targets are nuclear receptors such as thyroid receptors (TR), progesterone receptors (PR), estrogen receptors (ER), androgen receptors (AR) but they can also interact with membrane receptors, non-steroidal receptors and orphan receptors (Yang *et al.*, 2015). Moreover, several studies have demonstrated the ability of these substances to act on hormone metabolizing enzymes including aromatase, 5-reductase, 3-β-hydroxysteroid dehydrogenase (3βHSD), 11-β-hydroxysteroid dehydrogenase (11βHSD) (Guo *et al.*, 2012). Furthermore, EDCs can also act through epigenetic mechanisms which are particularly useful to understand how EDC exposure during the development can cause adverse effects in adulthood (Prusinski *et al.*, 2016). It is important to note that EDC responses do not follow the classical monotonic dose responses typically used in toxicological risk assessments. Experimental studies investigating EDC effects frequently detect non monotonic dose-response (NMDR) relationships (Lagarde *et al.*, 2015), indicating that Paracelsus principle of "the dose makes the poison" is not valid to assess their toxicity. NMDR relationship can result from multiple mechanisms and often presents a bell-shaped profile. U-shaped profiles are characterized by the highest response at low and high exposure levels; instead, inverted U-shape is characterized by response at intermediate dose(s) and a decrease response or no response at low and high exposure levels (Vandenberg *et al.*, 2013; Vandenberg, 2014).

EDCs are lipophilic compounds and thus they are persistent in the environment. They may biomagnificate and bioaccumulate during their production, use and disposal. The main source of human exposure to EDCs is estimated to be the diet, particularly ingestion of contaminated food and water (Rudel *et al.*, 2011), but they can be also exposed through indoor environment and skin contact (Nappi *et al.*, 2016).

The epidemic increase of male reproductive disorders, which cannot be explained by genetic changes, has occurred contemporaneously with cumulative exposures to various environmental factors through modern lifestyle. Increasing evidences demonstrate that males appear to be particularly vulnerable to exposure of certain compounds (Hauser *et al.*, 2015). Androgens are the most important hormones involved in the normal development and homeostasis of the male reproductive tract (Knez, 2013) but recently it has been proposed an equal role for estrogens (Zhang *et al.*, 2014). Specifically, both androgens and estrogens play a pivotal role in prostate gland development, differentiation and homeostasis, so *in vivo* and epidemiological studies suggest a relationship among EDC exposure and prostate diseases (Alavanja *et al.*, 2003).

Several compounds such as phthalates and alkylphenols belonging to EDCs. Phthalates (PAEs) are widely used in the manufacture of PVC and are considered to be one of the major groups of antiandrogenic substances and among these, di-2-ethylhexyl phthalate (DEHP) and dibutylphthalate (DBP) are the most commonly found in the environment (Chen *et al.*, 2011; Knez, 2013). Alkylphenols (AP), which include bisphenol A (BPA), nonylphenol (NP) and octylphenol (OP) are widely used in plastic formulation as non-ionic surfactants, in agricultural products, in personal care products and they also have been found in rivers, lakes, sea and sediments as surfactants (Careghini *et al.*, 2015).

Considered this background, in our studies we evaluated the effect of two different compound with different activities: the estrogenic nonylphenol (NP) and the antiandrogenic dibutylphthalate (DBP) on human prostate cells.

2- METHODS

The effects of NP and DBP were investigated on human prostate non tumorigenic epithelial cells (PNT1A) and on adenocarcinoma prostate cells (LNCaP)and were compared with 17-β-estradiol (E2).

Cell viability was evaluated using MTT assay. PNT1A cells were treated for 24 h with NP or E2 from 10^{-12}M to 10^{-6} M, with or without 10^{-5}M of the Estrogen selective antagonist ICI182780. LNCaP cells were treated with DBP and E2 from 10^{-5} M to 10^{-13} M for 24 h. MTT assay allowed us to establish NP, DBP and E2 concentration to use for the further experiments.

Then, the expression of genes and proteins involved in the cell cycle regulation was evaluated after 24h of exposure. Moreover, in order to investigate a

possible interaction between NP, DBP and E2 with estrogen and androgen receptors, immunofluorescence and western blot experiments were performed after different time of exposure.

Each experiment was carried out in triplicate. Data reported in graphs are expressed as mean values ± SEM for the indicated number of independent determinations. The statistical significance was calculated by the one-way ANOVA with Bonferroni's multiple comparison test, and differences were considered statistically significant when the P value was at least <0.05.

3 - RESULTS

In order to determine E2 and NP effects on cellular proliferation, PNT1A cells were treated with increasing concentration of E2 and NP (from 10^{-12}M to 10^{-6}M) for 24 h. The same experiments were also carried out in presence or absence of 10^{-5}M ICI.

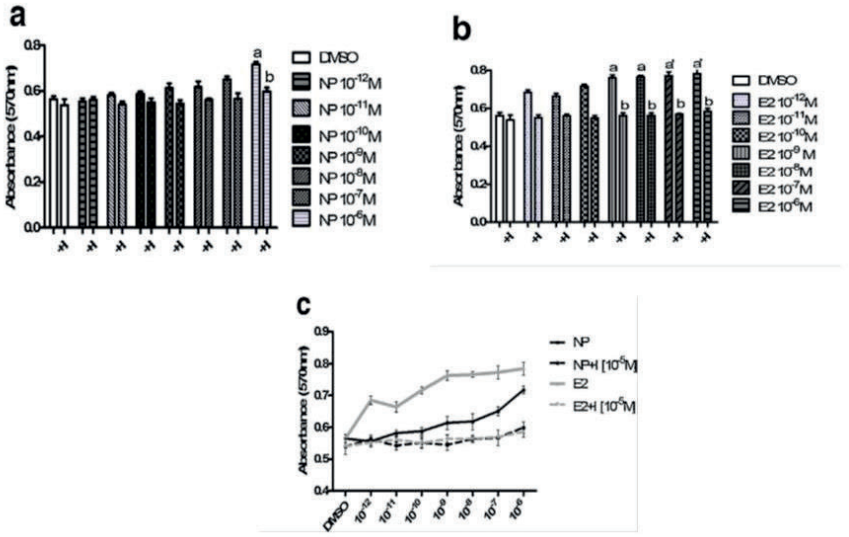

Fig.1 – MTT assay after 24 h of exposure to nonylphenol (NP) and 17β-estradiol (E2) alone or in combination with ICI 182, 780 (+I). In graph is reported the absorbance measured at 570 nm which correlates with the number of living cells. a, response significantly different than the vehicle control ($P < 0.05$); a', response significantly different than the vehicle control ($P < 0.01$); b, response significantly different than cells without ICI ($P < 0.05$).

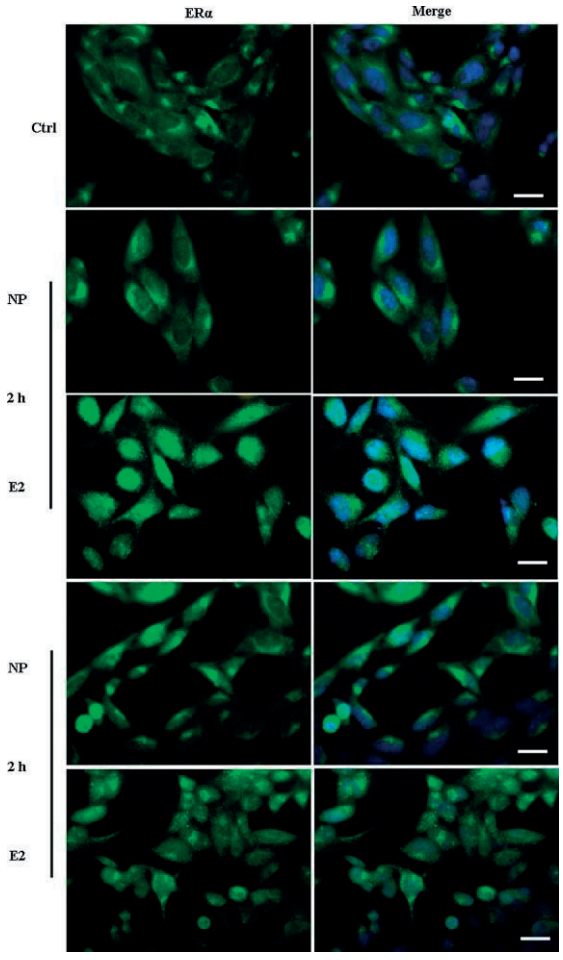

Fig. 2 – Localization of ERα after 2 and 6 h of exposure to NP and E2. E2 promotes translocation of ERα to the nucleus at both time of treatment, while NP at 6 h. ERα (Alexa Fluor 488) and nuclear staining (Höechst) were analyzed by immunofluorescence. Scale bar 10 mm.

E2 stimulated PNT1A cells proliferation from 10^{-9}M to 10^{-6}M, with the greatest effect showed at 10^{-6}M (Fig. 1b). E2 induced proliferation is strongly inhibited by adding ICI. NP stimulated PNT1A cells proliferation at the highest concentration of10^{-6}M (Fig.1a). At lower concentrations, we did not observe any significant effects when compared to control group. 10^{-5}M ICI inhibited the proliferation induced by 10^{-6}M NP. In the graph in Fig.1c is also possible to note that E2 has a greater effect compared to NP onPNT1A cells proliferation. Using immunofluorescence and western blot, we studied the localization and expression of ERα and ERβ after 2h and 6h of exposure to NP and E2 at 10^{-6}M. Immunofluorescence showed that after 2 h of treatment, NP did not affect ERα cellular localization, that was localized in the cytoplasm as in control cells. On the contrary, in E2 treated cells for 2 h, ERα is localized predominantly in the nucleus (Fig.2). After 6 h of exposure, in PNT1A cells treated with NP and E2,

ERα shifted from the cytoplasm to the nucleus that appeared to be strongly positive, with a weak cytoplasmic fluorescence if compared to control (Fig.2). ERβ after treatment with 10^{-6}M NP and 10^{-6}M E2 for both 2 h and 6 h was localized in the cytoplasm (data not shown).

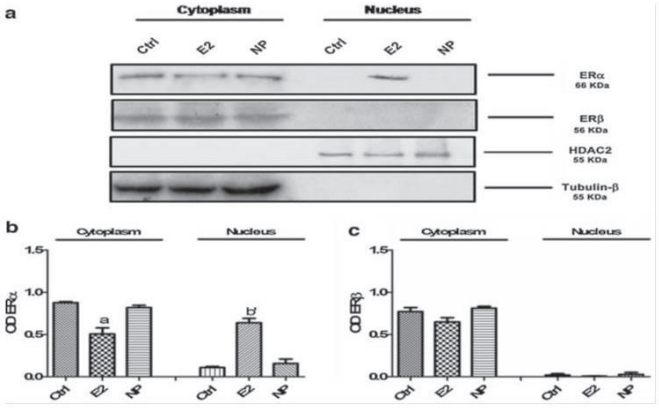

Fig. 3 – Western blot analysis and nuclear and cytoplasmic quantification of ERα and ERβ after 2 h of exposure to 10^{-6}M NP and E2. a, response significantly different than the cytoplasmatic control ($P < 0.05$); b', response significantly different than the nuclear control ($P < 0.01$).

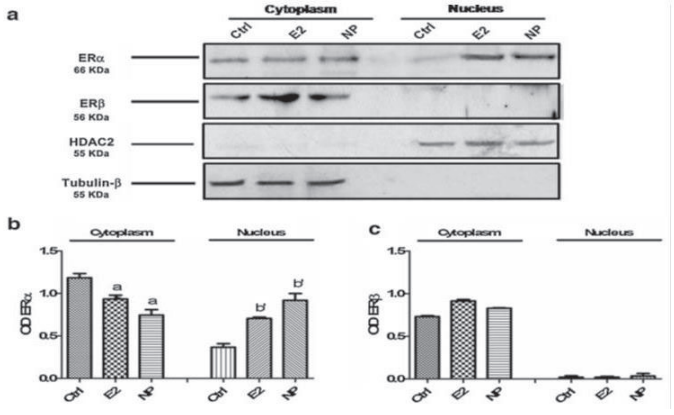

Fig. 4 – Western blot analysis and nuclear and cytoplasmic quantification of ERα and ERβ after 6 h of exposure to 10^{-6}M NP and E2. a, response significantly different than the cytoplasmatic control ($P < 0.05$); b', response significantly different than the nuclear control ($P < 0.01$).

In order to confirm immunofluorescence data, after separation of cytoplasmic and nuclear proteins we performed a translocation study of ERα and ERβ with western blot analysis. Densitometric analyses were normalized for cytoplasmic and nuclear extracts with β-tubulin (55 KDa) and HDAC2 (55 KDa), respectively. After 2 h of exposure (Fig. 3) we found ERα protein (66 KDa) in the cytoplasm of NP treated and non-treated PNT1A cells whereas optical density values were significantly lower in E2 treated cells (Fig. 3 a,b). Moreover, after 2 h nuclear proteins revealed a signal only in E2 treated cells (Fig. 3a). ERβ (56 KDa) after 2 h of treatment was found only in cytoplasmic fractions (Fig. 3a,c). After 6 h of exposure (Fig. 4) we observed a nuclear translocation of ERα both in NP and E2 treated cells (Fig. 4a,b). However, densitometry did not reveal significant differences in nuclear extracts between NP and E2 treated cells (Fig. 4 b). In contrast, values were significantly lower in the cytoplasm in treated cells compared to control (Fig. 4 b). ERβ was found only in cytoplasmatic fractions (Fig. 4a,c) and there were not significant differences in optical density between treated and non-treated cells (Fig. 4c).

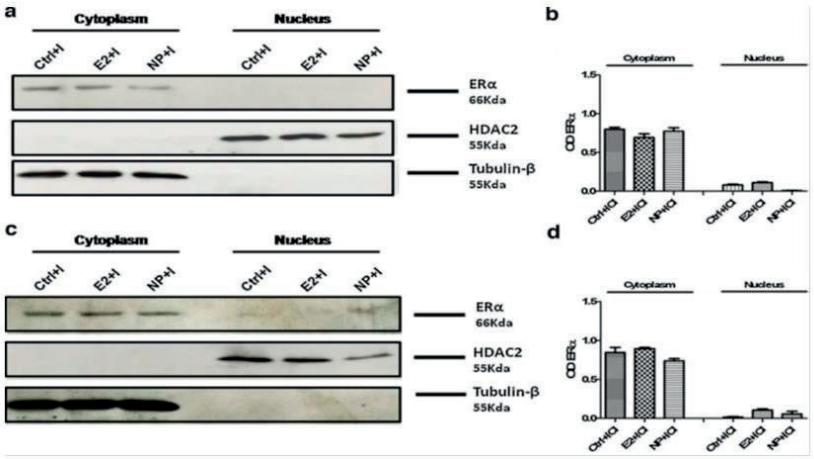

Fig. 5 – Western blot analysis and nuclear and cytoplasmic quantification of ERα after pre-treatment with 10^{-5} M ICI 182,780 (+I).

Western blot for ERα localization performed in presence of 10^{-5}M ICI after 2 (Fig. 5a,b) and 6 h of treatment (Fig. 5c,d) revealed ERα exclusively in the cytoplasm, with a weak signal in the nuclear extracts after 6 h of exposure (Fig. 5c).

In order to investigate if NP is able to affect gene expression, RT-qPCR analysis of genes involved in cell cycle regulation and in pathological states of prostate was performed after 24 h of exposure. NP enhanced mRNA levels of Cyclin D (Fig. 6a), Cyclin E (Fig. 6b), Ki67 (Fig. 6c) and IL1-b (Fig. 6e) while it did not affect p53 expression (Fig. 6d). Interestingly, ICI reduced gene ex-

pression of Cyclin D (Fig. 6a) and Ki67 (Fig. 6c) in PNT1A cells treated with NP, while it did not inhibit gene expression of Cyclin E (Fig. 6b) or IL1-b (Fig. 6e). E2 significantly affected gene expression up-regulating Cyclin D (Fig. 6a) and Ki67 (Fig. 6c). This induction was strongly inhibited by ICI (Fig. 6a,c).

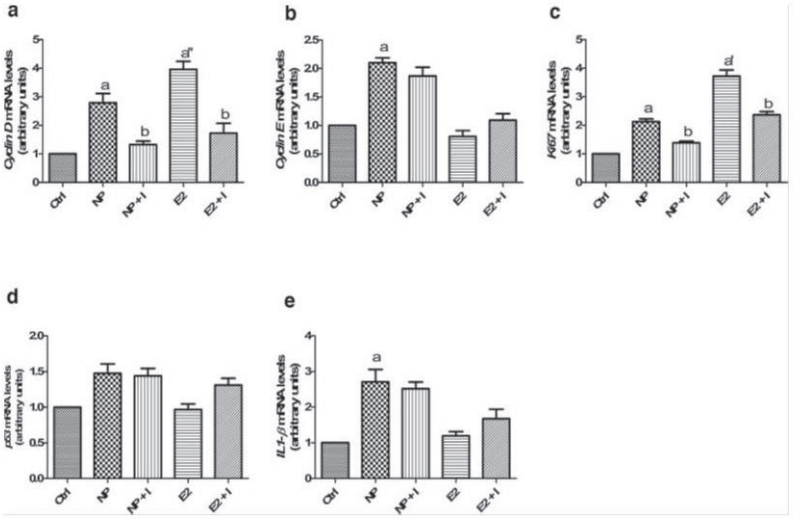

Fig. 6 – RT-qPCR analysis after 24 h of exposure to 10^{-6} M NP and E2, alone or in combination with 10^{-5}M ICI (+I). Cyclin D (a), Cyclin E (b), Ki67 (c), p53 (d) and IL1b (e) relative mRNA levels were normalized using GAPDH as housekeeping gene. a, response significantly different than the vehicle control (P< 0.05); a',response significantly different than the vehicle control (P < 0.01); a", response significantly different than the vehicle control (P < 0.001) b, response significantly different than cells without ICI (P < 0.05); b', response significantly different than cells without ICI (P < 0.01).

In order to investigate the effects of an antiandrogenic compound, LNCaP cells were exposed to DBP and E2 range from10^{-5} M to 10^{-13} M. After 24 h of exposure, E2 increased LNCaP viability with the higher effect showed at 10−9 M (Fig. 7b). Instead, DBP induced a decreased cells viability with the greatest effect at 10^{-8} M (Fig. 7a).

In order to investigate a possible interaction among DBP with estrogen and androgen receptors in the cells, we performed immunofluorescence after 30 minutes, 2 h and 4 h of exposure to DBP 10^{-8} M and E2 10^{-9}M. After 30 min of treatment, control cells and treated with DBP and E2 showed ERα in the cytoplasm. After 2 h DBP did not affect ERα localization, that was localized in the cytoplasm as in control cells. ERα shifted from cytoplasm to nucleus after 4 h of treatment with DBP. On the contrary, both after 2 h and 4 h, E2 induced ERα translocation from the cytoplasm to the nucleus that appeared to be strongly

positive (Data not shown). DBP did not affect ERβ localization at any time of exposure: ERβ was localized in the cytoplasm of LNCaP cells with no fluorescent signal in cell nuclei as in control cells. Instead E2 translocated ERβ from the cytoplasm to the nucleus after 4 h (Data not shown). AR localization was also investigated, and data showed that DBP did not interfere with AR localization which was perinuclear in both control and treated cells after 30′, 2 h and 4 h of exposure. Only after 4 h of treatment E2, AR translocated from the cytoplasm to the nucleus (Data not shown).

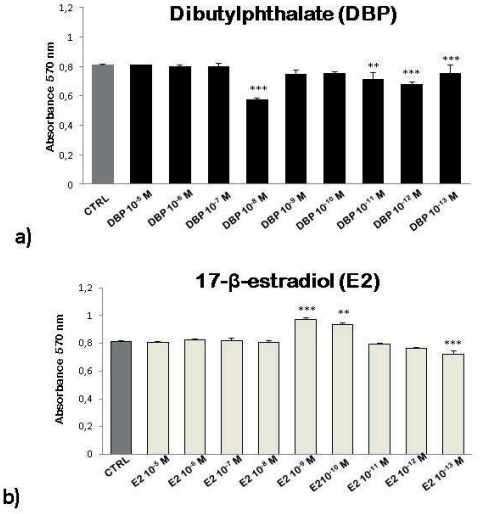

Fig. 7 – MTT assay after 24 h of exposure to DBP and E2 from 10^{-5} M to 10^{-13} M. In graphs are reported the absorbencies measured at 570 nm which correlates with number of living cells. (**p<0,01; ***p<0,001).

Western blot analysis was performed after 24 h of exposure with DBP 10^{-8} M and E2 10^{-9} M in order to evaluate the expression of MCT4 and Cyclin D1 involved in cell cycle regulation, the expression of pro-apoptotic proteins such as Bax and Bak and protein expression of estrogen and androgen receptors. Densitometric analysis was normalized with β-actin (42 kDa). The densitometric analysis revealed higher levels of MCT4 and Cyclin D1 proteins in E2 treated cells (Figs. 8 b, c) compared to DBP treated and control cells. Treatment with DBP significantly enhanced both Bax (Fig. 8 d) and Bak (Fig. 8 e) protein expressions, instead treatment with E2 significantly decreased Bax expression (Fig. 8 d) and didn't interfere with Bak expression (Fig. 8 e). ERα protein expression was drastically reduced by DBP treatment (Fig. 8 f), in contrast E2 strongly increased its expression (Fig. 8 f). Regarding to ERβ and AR only the treatment with E2 induced a significant increase of their expressions (Fig. 8 g, h).

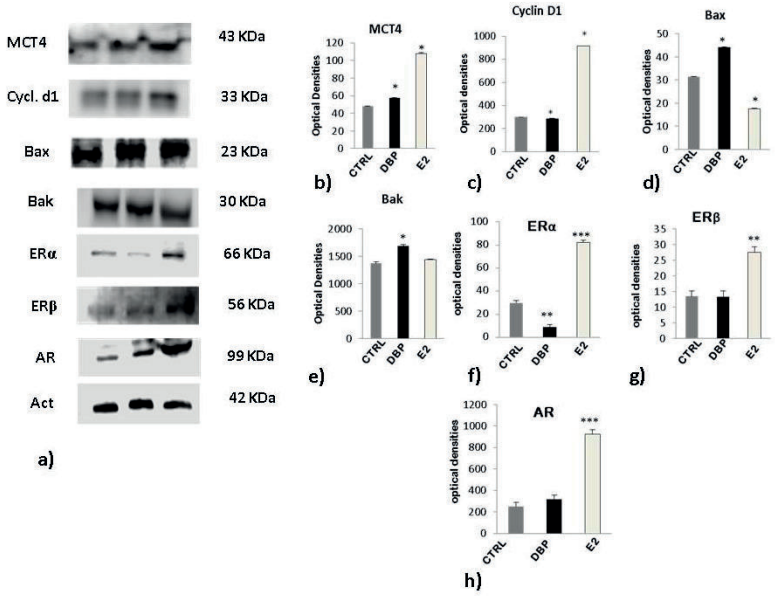

Fig. 8 – Western blot analysis after 24 h of exposure to DBP 10^{-8} M and E2 10^{-9} M. The graphs represented the optical density (O.D.) ratio of MCT4 (b), cyclin D1 (c), Bax (d), Bak (e), ERα (f), ERβ (g), AR (h) normalized on β actin. (*p<0,05; ** p<0,01; ***p<0,001).

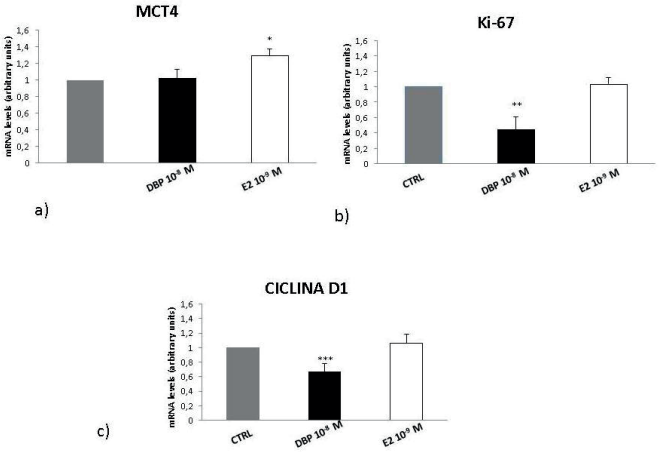

Fig. 9 – RT-qPCR analysis after 24 h of exposure to DBP 10^{-8} M and E2 10^{-9} M. (*p<0,05; ** p<0,01; ***p<0,001).

Finally, after 24 h of exposure with DBP 10^{-8}M and E2 10^{-9}M, RT-qPCR was performed to evaluate expression of genes involved in cell cycle regulation such as MCT4, Ki67 and Cyclin D1. DBP didn't interfere on mRNA levels of MCT4 (Fig. 9a); on the contrary DBP strongly decreased expression of Ki67 (Fig. 9b) and Cyclin D1 (Fig. 9c) of 50% and 40% respectively. Conversely, E2 enhanced MCT4 expression of 30% (Fig. 9a), and it didn't significantly interfere on Ki67 (Fig. 9b) and Cyclin D1 expression (Fig. 9c).

4 - CONCLUSIONS

Prostate gland plays a key role in male fertility. Its main function is to produce secretion (20–30% of the total ejaculation) that provides essential components for sperm quality and survival. Androgens have a significant function in prostate development and differentiation. Also estrogens have been demonstrated to have direct effects on prostate gland development and adult homeostasis but small changes in their levels might play a role in the aetiology of prostatic diseases (McPherson *et al*., 2008; Prins, Korach, 2008). Several epidemiological studies reveal that chronic or intermittent exposure to different classes of EDCs may affect the development and progression of prostate disorders (Van Maele-Fabry *et al.*, 2006).

Hence the aim of our project was to evaluate the effect of nonylphenol (NP) and dibutylphthalate (DBP) on human prostate cells. To better understand exogenous and endogenous compounds involvement in prostate gland and to investigate possible mimetical behaviour by NP and DBP, cells were also treated with the endogenous hormone 17 β-estradiol (E2).

Regarding NP, obtained results suggest that NP was able to stimulate PNT1A cells proliferation after 24 h of exposure at 10^{-6}M as well as E2 did. However, E2 affected PNT1A cells proliferation also at lower concentrations. Interestingly, ICI reverted NP and E2 proliferative stimuli indicating that both compounds were able to bind ER receptors. We studied the localization and the expression of estrogen receptors demonstrating that E2 induced cytoplasm-nucleus translocation of ERα at both 2h and 6h, while NP only after 6h. Surprisingly, both E2 and NP did not affect ERβ localization. ICI inhibited the ERα translocation observed with NP and E2 alone. Both proliferation and localization data confirm the estrogenic activity of NP. However, the greatest biological responses showed by E2 can be explained by its best binding affinity with ERs compared to NP (Laws, 2000). To assess if the presence of ERα in the nucleus led to the activation of transcription, we analysed gene expression of E2 gene targets also known to be deregulated in pathological state of the prostate. We demonstrated that NP was able to upregulate Cyclin D, Cyclin E, Ki67 and IL1-b gene expression whereas E2 induced upregulation only of Cyclin D and Ki-67. Moreover, we showed that up-regulation of Cyclin D and Ki67 is mediated

by estrogen signaling pathways, while the induction of Cyclin E and IL1-b involved an estrogen independent pathways, since ICI did not revert this induction. These results of gene expression were in agreement with the showed induced proliferation caused by NP and E2. In this regard, it is well known that Cyclin D and Cyclin E promoting G1/S phase transition of cell cycle (Kastan and Bartek, 2004) and are often used to screening the carcinogenic potential of EDCs (Diamanti-Kandarakis *et al*., 2009).

Differently DBP act on LNCaP cells with different effects than E2. DBP reduces LNCaP cellular viability at 10^{-8} M; on the contrary E2 at 10^{-9} M stimulated cellular viability of prostate cell line. Then, in order to evaluate expression of genes and proteins involved in cellular proliferation and in cell cycle regulation, after 24 h of treatment with DBP 10^{-8} M and E2 10^{-9} M, we performed two different approaches: RT-qPCR and western blot analysis. DBP treatment did not interfere with MCT4 gene and protein expression, instead E2 enhanced both of them. MCT4 belongs to the family of the monocarboxylate transporter and it is thought to be involved in the cellular efflux of lactic acid/H+; highly MCT4 expression has been associated in cancer progression by promoting several oncogenic processes (Sanità *et al*., 2014). Gene expression of Ki67, a well-known marker of cell proliferation, is decreased after treatment with DBP but not after E2 treatment. Some studies have shown that estrogens might play a decisive role in some processes such as the development of prostate cancer (Susa *et al*., 2015). DBP was able to decrease gene and protein expression of cyclin D1, on the contrary E2induced a strongly increase of cyclin D1 protein expression. Cyclin D1 is an estrogen response target and it promotes G1/S phase transition of cell cycle (Kastan, Bartek, 2004). To better understand trough which pathway DBP induced a decreased cell viability, we evaluated protein expression of two different pro-apoptotic proteins involved in intrinsic apoptosis pathway: Bax and Bak. DBP, contrarily to E2, strongly enhanced their expression, suggesting a DBP involvement in programmed cell death processes. Moreover, to assess estrogen (ER) and androgen (AR) receptors participation, we evaluated the expression of ERs and AR with western blot. We showed a reduced expression of ERα after treatment with DBP and a significant increase of its expression after E2 treatment. It has been demonstrated that ERα appears to be involved in cellular proliferation and carcinogenesis of prostate (Prins, Korach, 2008). Furthermore, DBP did not interfere with ERβ and AR expression, instead E2 increased the expression of both of them. The E2 action on both ERs and AR expression is in agreement with Susa *et al.* (2015) that showed E2 involvement in the activation of AR pathway (Susa *et al.*, 2015). Finally, we studied ERα, ERβ and AR localization after 30 min, 2 h and 4 h of treatment. DBP induced ERα cytoplasm-nucleus translocation only after 4 h of treatment; conversely E2 affected ERα localization after 2 h and 4 h. ERα nuclear transloca-

tion is linked to its activation and it was not surprising that E2 had highest effects than DBP.

DBP did not interfere with ERβ and AR localization indicating that its effects on LNCaP cells are not linked with AR interaction as also reported by Hrubá *et al.* (2014). On the contrary E2 was able to induce ERβ and surprisingly also AR cytoplasm-nucleus translocation after 4 h. It has been demonstrated that AR might be activated by other steroid hormones and E2 shows affinity for its LBD domain so it can be able to activate transcription of AR target genes (Susa *et al.*, 2015).

In conclusion, we demonstrated that NP and DBP acts on PNT1A and LNCaP cells through the activation of ERα pathway and they may be involved in a deregulation of cell cycle which in turn may contribute to pathological states of prostate gland.

However, more cellular and *in vivo* models will be needed in order to best characterize the risk of NP and DBP exposure for prostate diseases.

Alkylphenols and phthalates are only two of the components of the mixture of EDCs which human population is non-stop exposed. Thus, it is very important to compare the effects of environmental compounds with anti-estrogenic and anti-androgenic properties in order to explore the crosstalk between different hormonal signaling pathways.

5 - REFERENCES

Alavanja M.C., Samanic C., Dosemeci M., Lubin J., Tarone R., Lynch C.F., Knott C., Thomas K., Hoppin J.A., Barker J., Coble J., Sandler D.P., Blair A., 2003. Use of agricultural pesticides and prostate cancer risk in the Agricultural Health Study cohort. *American Journal of Epidemiology*, **157(9)**:800-814.

Careghini A., Mastorgio A.F., Saponaro S., Sezenna E., 2015. Bisphenol A, nonylphenols, benzophenones and benzotriazoles in soils, groundwater, surface, water, sediments, and food: a review. *Environmental Science and Pollution Research International*, **22**, 5711-5741.

Chen X., An H., Ao L., Sun L., Liu W., Zhou Z., Wang Y., Cao J., 2011.The combined toxicity of dibutylphthalate and benzo(a)pyrene on the reproductive system of male Sprague Dawley rats in vivo. *Journal of Hazardous Materials***186**, 835–841.

Diamanti-Kandarakis E., Bourguignon J.-P., Giudice L.C., Hauser R., Prins, G.S., Soto A.M., Zoeller R.T., Gore, A.C., 2009. Endocrine-disrupting chemicals: an endocrine society scientific statement. *Endocrine Reviews* 293–342.

Giulivo M., Lopez de Alda M., Capri E., Barceló D., 2016. Human exposure to endocrine disrupting compounds: their role in reproductive systems, metabolic syndrome and breast cancer. A review. *Environmental Research***151**, 251-264.

Guo J., Yuan W., Qiu L., Zhu W., Wang C., Hu G., Chu Y., Ye L., Xu Y., Ge R.S., 2012. Inhibition of human and rat 11beta-hydroxysteroid dehydrogenases activities by bisphenol A. *Toxicology Letters* **215 (2)**, 126–130.

Hrubá E., Pernicová Z., Pálková L., Souček K., Vondráček J., Machala M., 2014.Phthalates deregulate cell proliferation, but not neuroendocrine transdifferentiation,in human LNCaP prostate cancer cell model.*Folia Biologica,***60 (1)**, 56–61.

Kastan M.B., Bartek J., 2004. Cell-cycle checkpoints and cancer. *Nature***432**, 316–323.

Knez J., 2013. Endocrine-disrupting chemicals and male reproductive health. *Reproductive Biomedicine Online***26**, 440–448.

Kortenkamp A., 2007. Ten years of mixing cocktails: a review of combination effects of endocrine-disrupting chemicals. *Environmental Health Perspectives*, **115 (1)**, 98-105.

Lagarde F., Beausoleil C., Belcher S.M., Belzunces L.P., Emond C., Guerbet M., Rousselle C., 2015. Non monotonic dose-response relationships and endocrine disruptors: a qualitative method of assessment. *Environmental Health*, **14,** 13.

Laws S.C., 2000. Estrogenic activity of octylphenol, nonylphenol bisphenol a andmethoxychlor in rats. *Toxicological Sciences,***54**, 154–167.

Mantovani A., 2016. Endocrine Disrupters and the Safety of Food Chains. *Hormone Research in Paediatrics***86**, 279–288.

McPherson S.J., Ellem S.J., Risbridger G.P., 2008. Estrogen-regulated development and differentiation of prostate. *Differentiation*, **76(6),** 660–670.

Nappi F., Barrea L., Di Somma C., Savanelli M.C., Muscogiuri G., Orio F., Savastano S., 2016. Endocrine aspects of environmental "obesogen" pollutants. *International Journal of Environmental Research and Public Health***13**, 765-781.

Prins G.S., Korach K.S., 2008. The role of estrogens and estrogen receptors in normal-prostate growth and disease. *Steroids*, **73**, 233–244.

Prusinski L., Al-Hendy A., Yang Q., 2016. Developmental exposure to endocrine disrupting chemicals alters the epigenome: identification of reprogrammed targets. *Gynecology and Obstetrics Research***3(1)**, 1-6.

Rudel R.A., Gray J.M., Engel C.L.,Rawsthorne T.W., Dodson R.E., Ackerman J.M., Rizzo J., Nudelman J.L., Brody J.G., 2011. Food packaging and bisphenol A and bis(2-ethyhexyl) phthalate exposure: Findings from a dietary intervention. *Environmental Health Perspectives*,**119**, 914–920.

Sanità P., Capulli M., Teti A., Galatioto G.P., Vicentini C., Chiarugi P., Bologna M., Angelicci A., 2014. Tumor-stroma metabolic relationship based on lactate shuttle can sustain prostate cancer progression. *BMC Cancer*, **14**, 154.

Susa T., Ikaga R., Kajitani T., Ilzuka M., Okinaga H., Tamamori-Adachi M., Okazaki T., 2015. Wild-type and specific mutant androgen receptors mediates transcription via 17β-estradiol in sex hormone-sensitive cancer cells. *Journal of cellular phisiology*, **230**, 1595-1606.

Vandenberg L.N., 2014. Non-monotonic dose responses in studies of endocrine disrupting chemicals: Bisphenol A as a case study. *Dose-Response***12**, 259–276.

Vandenberg L. N, Colborn T., Hayes T.B., Heindel J.J., Jacobs Jr D.R., Lee, D.H., Myers J.P., Shioda T., Soto A.M., von Saal F.M., Welshons W.V., Zoeller R.T., 2013.Regulatory decisions on endocrine disrupting chemicals should be based on the principles of endocrinology. *Reproductive Toxicology*, **38**:1–15.

Van Maele-Fabry G., Libotte V., Willems J., Lison D., 2006. Review and meta-analysisof risk estimates for prostate cancer in pesticide manufacturing workers. *Cancer Causes Control,***17**, 353–373.

World Health Organization (WHO), 2012. State of the Science of Endocrine Disrupting Chemicals – 2012, http://www.who.int/ceh/publications/endocrine/en/.

Yang O., Kim H.L., Weon J.I., Seo Y.R., 2015. Endocrine-disrupting chemicals: review of toxicological mechanisms using molecular pathway. *Journal of Cancer Prevention,* **20 (1)**, 12–24.

Zhang L., Dong L. Ding S., Qiao P., Wang C., Zhang M., Zhang L., Du Q., Li Y., Tang N., Chang B., 2014.Effects of n-butylparaben on steroidogenesis and spermatogenesis through changed E2 levels in male rat offspring. *Environmental Toxicology and Pharmacology*, **37**, 705–717.

Rend. Acc. Sc. fis. mat. Napoli
Vol. LXXXVI, (2019) pp. 55-59

DOI 10.32092/1018

Brain metabolic DNA is reverse transcribed by mitochondrial telomerase

Joyce Casalino[1], Marina Prisco[1], Salvatore Valiante[1], Marianna Crispino[1] and Antonio Giuditta[2]

Presentata dal socio Antonio Giuditta
(Adunanza del 21 giugno 2019)

Keywords: mtDNA, BMD, telomerase, mitochondria, reverse transcription.

Abstract - Brain metabolic DNA is synthesized by a cytoplasmic RNA-dependent DNA polymerase present in synaptic regions. Preliminary immunofluorescence analyses suggest that BMD reverse transcription is catalyzed by mitochondrial telomerase. The data are in agreement with additional observations.

Riassunto - Il DNA metabolico del cervello è sintetizzato da una DNA polimerasi RNA dipendente presente nelle regioni sinaptiche. Analisi preliminari di immunofluorescenza suggeriscono che la trascrizione inversa del BMD è catalizzata dalla telomerasi mitocondriale. Tale dato concorda con diverse altre osservazioni.

1 - INTRODUCTION

In experiments made in the early seventies the distribution of brain metabolic DNA (BMD) in subcellular fractions indicated its prevalence in mitochondrial fractions (Rutigliano and Giuditta, 2015; Giuditta *et al.*, 2017), thus raising the possibility that it could be related to mitochondrial DNA. The possibility of a direct connection with mtDNA replication was discarded in view of the considerably faster rate of BMD synthesis. In any case, the distribution of BMD

---

[1]Dipartimento di Biologia, Università Federico II di Napoli; [2]giuditta@unina.it.

and mitochondrial cytochrome-oxidase in subcellular fractions turned out to be completely different, thus negating any indirect connection (Rutigliano and Giuditta, 2015). It should however be mentioned that at that time cytochrome-oxidase and the entire electron transport chain were assumed to be exclusively present in mitochondria while in recent studies they have been identified in several different locations of the nervous system, including myelin and retinal photoreceptors (Ravera *et al.*, 2011; Calzia *et al.*, 2014). Hence, earlier results cannot be considered to have invalidated the possible connection between BMD and mitochondria.

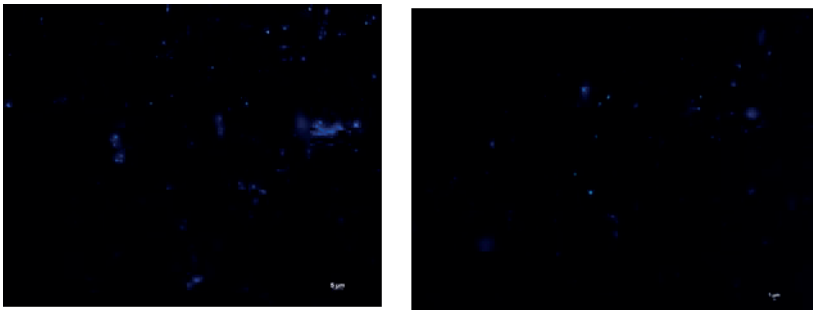

Fig. 1 – Purified brain synaptosomes from an adult rat. Left panel, dsDNA is visualized with Hoechst; right panel, dsDNA is almost completely lost after DNase treatment.

Previous experiments have also demonstrated that newly synthesized BMD originates from a cytoplasmic reverse transcriptase eliciting the synthesis of a DNA-RNA hybrid eventually attaining the double stranded configuration before being partly transferred to nuclei (Giuditta and Rutigliano, 2018). The initial presence of the hybrid configuration was subsequently confirmed by the colocalization of BrdU-labeled BMD with DR hybrids (Prisco *et al.*, 2019) which allowed to use anti-DR-hybrid antibodies as markers of newly synthesized BMD. Additional experiments have shown that BrdU-labeled BMD colocalizes with synaptophysin and GFAP (Prisco *et al.*, 2019), thus implying its localization in presynaptic and astroglial synaptosomes. BMD is also present in a variety of squid optic lobe synaptosomes, including those derived from the large nerve terminals of retinal photoreceptors (Cefaliello *et al.*, 2019).

The recent discovery that telomerase is not exclusively localized in mammalian nuclei but it is also exerting its reverse transcription in mitochondria (Sharma *et al.*, 2012; Saretzki G. 2014; Eitan *et al.*, 2016) has suggested that BMD might be synthesized by the mitochondrial telomerase. The possibility has been evaluated by determining the colocalization of synaptosomal DR hybrids with mitochondrial telomerase.

2 - METHODS

Purified brain synaptosomes were prepared from an adult male Wistar rat and a young male C57 mouse by using a standard protocol (Eyman *et al.*, 2007). The presence of synaptosomal dsDNA was established by treating rat synaptosomes with Hoechst (1 μg/ml, 5 min) and exposing a different synaptosomal aliquot with 1U DNase (Thermo Fisher, 1U/μl; 37 °C, 30 min).

The rabbit anti-telomerase antibody (Abcam) was identified by the anti-rabbit green fluorescent Alexafluor 488 secondary antibody (Abcam), while the mouse anti-DR hybrid antibody (Kerafast) was identified by the anti-mouse red fluorescent Alexafluor 594 secondary antibody (Abcam).

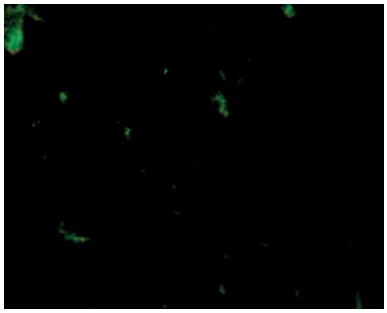

Fig. 2 – Colocalization of DNA-RNA hybrids (red fluorescence) with telomerase (green fluorescence) in a purified synaptosomal fraction from a young mouse.

3 - RESULTS

The first experiment aimed at visualizing double stranded DNA in purified brain synaptosomes by treating them with Hoechst. The wide distribution of Hoechst generated blue fluorescence is clearly shown in Fig. 1, left panel; its almost complete disappearance after DNase treatment further confirmed its nature (Figure 1, right panel). Comparable data were previously obtained by cesium gradient analyses of rat BMD (Giuditta and Rutigliano, 2018) and immunofluorescence experiments with mice BMD (Prisco *et al.*, 2019).

The possible colocalization of DR hybrids with the mitochondrial telomerase was examined in purified synaptosomes from a young mouse. As shown in Fig. 2, the green fluorescent anti-telomerase antibody colocalized with the red fluorescent anti-DR-hybrids antibody, thus indicating that mitochondrial telomerase colocalized with DR hybrids previously shown to originate from newly synthesized BMD (Prisco *et al.*, 2019).

The latter result was confirmed by an additional visualization of the purified synaptosomes in a Zeiss Axioskop fluorescence microscope and a Zeiss Z.1 Light sheet microscope (Fig. 3).

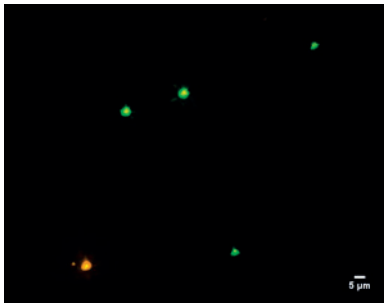

Fig. 3 – Colocalization of DNA-RNA hybrids (red fluorescence) with telomerase (green fluorescence) in purified synaptosomes from a young mouse.

4 - DISCUSSION

The involvement of mitochondrial telomerase in the reverse transcription of BMD is suggested by the colocalization of anti-telomerase and anti-DR hybrids antibodies in purified brain synaptosomes. While this result is encouraging, additional evidence will be needed to further support this conclusion. Nonetheless, it may be worth mentioning that this suggestion is in full agreement with a number of observations that have recently been made or have been erroneously interpreted in the past.

One observation regards the chromosomal alignment of BMD sequences obtained from learning and control mice (Angelini *et al.*, 2018). Values of aligned sequences, duly standardized to chromosome size and sequencing depth, were closely comparable in most chromosomes, with the exception of chromosomes 2 and 9 in which values doubled, and chromosomes X e Y in which values halved. The only substantial exception regarded mitochondria which exhibited values several orders of magnitude larger than in all other chromosomes. This unique extremely high concentration of BMD sequences is likely to indicate the crowed mitochondrial origin of all sequences.

An additional indication was provided by the considerably higher BMD content of purified mitochondria with respect to synaptosomes of adult rats (Giuditta and Rutigliano, 2018). These surprising data were however attributed to tissue fragments contaminating the mitochondrial fraction since at that time (early seventies) the different subcellular distribution of BMD and cytochrome oxidase excluded any connection between mitochondria and BMD, as already mentioned in the Introduction.

The third stronger indication concerned the electrophoretic mobility of cytoplasmic BMD purified from learning and control mice. In all mice it corresponded to about 17 kbp (Giuditta *et al.*, in preparation), that is essentially the same of mtDNA (16,660 bp). Provided this result will not turn out to be a mere coincidence, BMD reverse transcription should be attributed to mitochondrial telomerase using as RNA template the polycistronic mtDNA transcript clearly endowed with the same size of mtDNA.

5 - BIBLIOGRAFIA

Angelini C., Casalino J., Giuditta A. (2018) BMD sequences from learning mice differ from those of control mice. *Rend. Acc. Sc. fis. mat.* **LXXXV**: 71-76.

Calzia D., Garbarino G., Caicci F., Manni L., Candiani S., Ravera S., Morelli A., Traverso C.E., Panfoli I. (2014) Functional expression of electron transport chain complexes in mouse rod outer segments. *Biochimie* **102**: 78-82.

Cefaliello C., Prisco M., Crispino M., Giuditta A. (2019) DNA in squid synaptosomes. *Mol. Neurobiol.* **56**:56-60. doi: 10.1007/s12035-018-1071-3. Epub 2018 Apr 19.

Eyman M., Cefaliello C., Ferrara E., De Stefano R., Crispino M., Giuditta A. (2007) Synaptosomal protein synthesis is selectively modulated by learning. *Brain Res*. **1132**:148-57.

Eitan E., Braverman C., Tichon A., Gitler D., Hutchison E.R., Mattson M.P., Priel E. (2016) Exitotoxic and radiation stress increase TERT levels in the mitochondria and cytosol of cerebellar Purkinje neurons. *Cerebellum* **15**:509-517.

Giuditta A., Grassi-Zucconi G., Sadile A. (2017) Brain metabolic DNA in memory processing and genome turnover. *Rev. Neurosci.* **28**:21-30. doi: 10.1515/revneuro-2016-0027.

Giuditta A., Rutigliano B. (2018) Brain metabolic DNA in rat cytoplasm. *Mol. Neurobiol.* **55**:7476-7486. doi: 10.1007/s12035-018-0932-0. Epub 2018 Feb 9.

Prisco M., Casalino J., Cefaliello C., Giuditta A. (2019) Brain etabolic DNA is reverse transcribed in cytoplasm: Evidence by immunofluorescence analysis. *Mol. Neurobiol.* doi: 10.1007/s12035-019-1569-3.

Ravera S., Panfoli I., Aluigi M.G., Calzia D., Morelli A. (2011) Characterization of myelin sheath F_0F_1-ATP synthase and its regulation by IF_1. *Cell Biochem. Biophys.* **59**: 63-70.

Rutigliano B., Giuditta A. (2015) The unexpected recovery of misplaced data on brain metabolic DNA. *Rend. Acc. Sc. fis. mat. Napoli*, **LXXXII**: 99-106.

Saretzki G. (2014) Extra-telomric function of human telomerase: cancer, mitochondria and oxidative stress. *Curr. Pharm. Des* **20**: 6386-6403.

Sharma N.K., Reyes A., Green P., Caron M.J., Bonini M.G., Gordon D.M., Holt I.J., Santos J.H. (2012) Human telomerase acts as a hTR-independent reverse-transcriptase in mitochondria. *Nucleic Acids Res*. **40**:712-725.

Rend. Acc. Sc. fis. mat. Napoli
Vol. LXXXVI, (2019) pp. 61-75

DOI 10.32092/1018

Le RIP (proteine inattivanti i ribosomi): struttura e potenziali applicazioni biotecnologiche

Nota del socio Alberto Di Donato[1] e di Antimo Di Maro[2]
(Adunanza del 20 dicembre 2019)

Keywords: immunotoxins, ribosome inactivating proteins, ricin.

Abstract - Ribosome inactivating proteins (RIP), found in many plants, are able to alter 28S rRNA, by depurinating a single adenine (N-β-glycosidase activity) and making ribosomes unable to operate protein synthesis. They include type 1 RIP, consisting of a single chain, and type 2, consisting of an A chain with N-glycosidase activity bound to a lectin B chain able to bind glycidic chains with galactosyl residues. B chain binds receptors on cell surface, allowing A chain to enter cytoplasm and exert its enzymatic activity. For this reason, many type 2 RIP are powerful toxins (e.g.: ricin), whereas type 1 RIP are less toxic because of their difficulty to enter the cell. Due to their properties, RIPs can be used for different biotechnological applications such as: i) possible antiviral agents in both plants and animals; ii) conjugated to carrier molecules in biomedical applications.

Riassunto – Le proteine inattivanti i ribosomi (ribosome inactivating proteins, RIP), isolate da numerose piante, alterano l'rRNA 28S, depurinando una specifica adenina (attività N-β-glicosidasica), rendendo i ribosomi incapaci di operare la sintesi proteica. Le RIP possono essere di tipo 1, costituite da una sola catena, o di tipo 2, costituite da una catena A con attività N-β-glicosidasica unita ad una catena B lectinica capace di legare catene glucidiche con residui di galattosio. La catena B si lega a recettori sulla superficie cellulare, permettendo l'entrata nel citoplasma della catena A, dove esercita la sua attività enzimatica. Per questo motivo, molte RIP di tipo 2 sono potenti tossine (es., la ricina); mentre le RIP di tipo 1 penetrano con difficoltà nelle cellule e di conseguenza sono relativamente poco tossiche. Per le loro proprietà, le RIP possono essere utilizzate per possibili

[1] Dipartimento di Biologia, Università Federico II di Napoli, Complesso Universitario di Monte S. Angelo, via Cinthia, 80126 Napoli e Accademia di Scienze Fisiche e Matematiche della Società Nazionale di Scienze, Lettere e Arti in Napoli, via Mezzocannone 8, 80134 Napoli.
[2] Dipartimento di Scienze e Tecnologie Ambientali Biologiche e Farmaceutiche, Università degli Studi della Campania Luigi Vanvitelli, Via Vivaldi 43, 81100 Caserta.

applicazioni biotecnologiche come: i) possibili agenti antivirali sia in piante che animali; ii) coniugati a molecole vettrici in applicazioni biomediche.

1 - INTRODUZIONE

Le tossine di origine vegetale sono molecole prodotte e secrete dalle piante superiori per difendersi dai predatori. Esse includono molecole che hanno un effetto tossico sugli organismi bersaglio, siano essi microbi, insetti, animali o piante parassite. Le tossine vegetali possono essere sia piccole molecole organiche (metaboliti secondari) che macromolecole complesse, come proteine/enzimi che riconoscono peculiari bersagli in grado di arrestare la crescita dei parassiti o provocarne la morte. Tra queste, le RIP '*ribosome inactivating proteins'* sono le tossine più studiate date le loro peculiarità strutturali ed enzimatiche alla base di interessanti applicazioni, sia nel settore farmaceutico che in campo agricolo. Lo studio delle RIP prosegue da decenni, poiché è importante comprenderne il ruolo biologico nelle piante e i meccanismi struttura/funzione alla base della loro citotossicità. D'altro canto la loro tossicità è nota da oltre un secolo, quando fu isolata la prima RIP dai semi di ricino, una proteina tossica, poi chiamata ricina.

2 - ATTIVITA' ENZIMATICA, STRUTTURA E DISTRIBUZIONE

Le proteine inattivanti i ribosomi conosciute con l'acronimo di RIP, appartengono a una classe di enzimi (EC 3.2.2.22) ampiamente distribuita in piante, funghi (Girbes et al. 2004) e ritrovata fino ad ora in un'unica alga (Liu et al. 2002). Le RIP presentano un'attività rRNA N-β-glicosidasica, che porta alla scissione di un singolo residuo di adenina in un sito conservato dell'rRNA 28S denominato Loop α-Sarcina Ricina (SRL) (Endo e Tsurugi 1987). In particolare, l'adenina scissa nell'rRNA 28S di ratto è la numero 4324 (Fig. 1).

La scissione del singolo legame N-β-glicosidico è irreversibile e l'assenza della singola adenina, impedisce l'associazione dei fattori di allungamento con il ribosoma (EF-G e EF-2 in procarioti ed eucarioti, rispettivamente) portando al blocco della sintesi proteica, provocando la morte cellulare per apoptosi (Montanaro et al. 1975). Oltre agli effetti citotossici alcune RIP hanno effetti biologici specifici su differenti linee cellulari e/o su organismi *in toto*. Tuttavia, queste attività aggiuntive possono in alcuni casi non dipendere direttamente dall'attività N-β-glicosidasica. Inoltre, in letteratura è riportato che alcune RIP sono attive su substrati differenti dall'rRNA (Barbieri et al. 1994). In alcuni casi si è riscontrata la capacità di alcune RIP di agire su DNA, lipidi, chitina e ione superossido, esibendo quindi attività DNasica, fosfatasica, chitinasica e superossido dismutasica (Stirpe 2013).

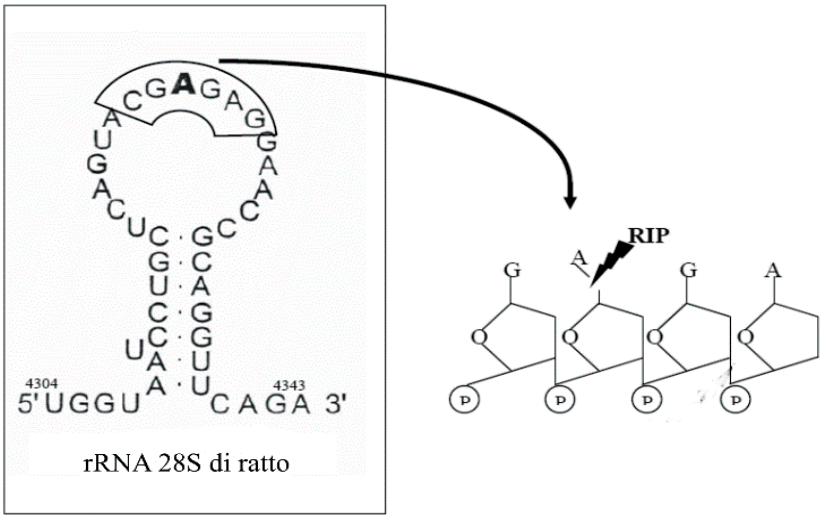

Fig. 1 – Struttura secondaria dell'rRNA 28S di ratto nel quale il residuo di adenina (evidenziato in grassetto) viene eliminato dall'azione delle RIP.

La maggior parte delle RIP può essere classificata in due gruppi, che si distinguono in base all'assenza (RIP di tipo 1) o alla presenza (RIP di tipo 2) di una catena lectinica (la catena B) legata ad una catena "tossica" (catena A) tramite interazioni idrofobiche e un ponte disolfurico intracatena (Fig. 2) (Barbieri et al. 1993). La catena enzimatica A promuove il rilascio del residuo di adenina e quindi possiede l'attività rRNA N-β-glicosidasica tossica. La catena lectinica B, dove presente, si lega in modo specifico a recettori galattosil terminali presenti sulla superfice cellulare dei mammiferi, promuovendo l'ingresso della catena A nelle cellule (IC_{50}[3] sulla linea cellulare Hela 0,0003-1,7 nM) (Stirpe e Gilabert-Oriol 2017). L'assenza della catena lectinica B limita in modo significativo l'accesso delle RIP di tipo 1 nelle cellule, determinando una loro minore citotossicità (IC_{50} sulla linea cellulare Hela 170-3300 nM) (Stirpe e Gilabert-Oriol 2017). Oltre ai due principali gruppi, alcune RIP come la b-32 isolata dal mais presentano una struttura risultante dall'unione di due polipeptidi (di circa 15 e 9 kDa) dotati di attività N-β-glicosidasica. Queste RIP costituiscono secondo alcuni autori il gruppo delle RIP di tipo 3, mentre per altri rappresentano soltanto un singolare sottogruppo di RIP di tipo 1 (Hey et al. 1995; Chaudhry et al. 1994).

Le RIP di tipo 1 sono proteine a catena singola di circa 30 kDa con un punto isoelettrico basico e un IC_{50} *in vitro* minore di 0,01 - 4,0 nM (Stirpe e Gilabert-Oriol 2017). Tra le più note vi sono la PAP (da *Phytolacca americana* L.), la

[3] Concentrazione di inibitore (farmaco, enzima, tossina o veleno) necessaria ad inibire il 50% del bersaglio in esame (enzima, cellula, recettore o microrganismo).

tricosantina (da *Trichosanthes kirilowii* L.), la gelonina (da *Gelonium multiflorum* L.), le PD-S/PD-Ls (da *Phytolacca dioica* L.), e le saporine (da *Saponaria officnalis* L.).

La maggior parte delle RIP di tipo 2 provenienti da piante superiori ha una struttura dimerica (circa 60 kDa), un punto isoelettrico compreso tra 6 e 8 e valori di IC_{50} *in vitro* compresi tra 43 e 88 nM (Stirpe e Gilabert-Oriol 2017). Tra le più note vi sono la ricina (da *Ricinus communis* L.), l'abrina (da *Abrus precatorius* L.) e l'ebulina (da *Sambucus ebulus* L.).

Alcune RIP di tipo 2 sono costituite da una singola catena A con attività N-β-glicosidasica che interagisce con più catene B capaci di legare differenti recettori glicosil terminali sulla superficie cellulare. Esempi di tali proteine, dotate di struttura quaternaria complessa includono, RIP tetrameriche e ottameriche isolate dal genere *Sambucus* (Girbes et al. 1993).

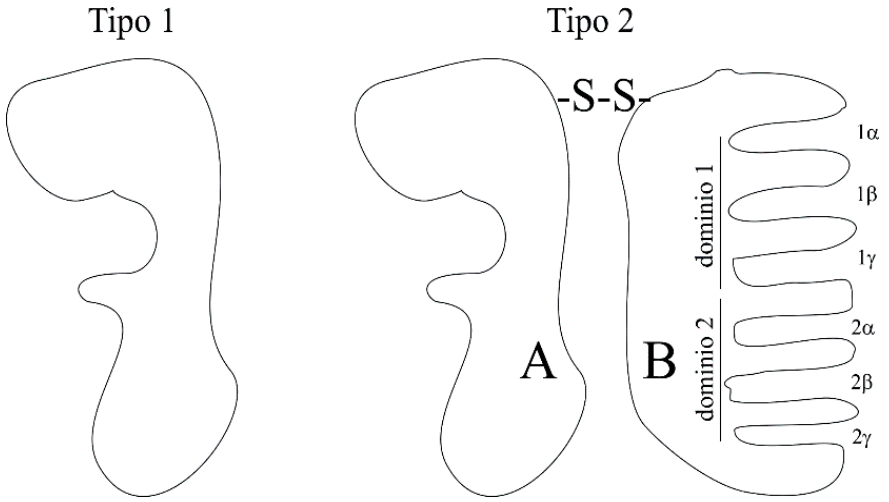

Fig. 2 – Rappresentazione delle RIP di tipo 1 e di tipo 2 (con catena enzimatica A e lectinica B). Per la catena B lectinica è messa in evidenza l'organizzazione in domini e motivi alla base del riconoscimento degli zuccheri.

Le strutture tridimensionali delle RIP di tipo 1 sono accumunate da uno stesso ripiegamento, noto come 'RIP fold'. In particolare, il 'RIP fold' è costituito da un dominio N-terminale risultante dall'unione di α-eliche e β-foglietti e un dominio C terminale dove sono presenti prevalentemente α-eliche (Monzingo et al. 1993). Un residuo di glutammato, di arginina e di triptofano sono strutturalmente conservati nel sito catalitico e la specificità enzimatica delle diverse RIP è determinata da piccole variazioni conformazionali della struttura delle singole catene polipeptidiche, in particolare in regioni circostanti il sito catalitico, che influenzano il legame enzima-substrato (Di Maro et al. 2014). Ciò è confermato da studi

strutturali effettuati utilizzando analoghi dei substrati. Tali studi indicano che la specificità enzimatica di ogni singola RIP dipende dalla stabilità degli stati di transizione durante il processo di legame substrato-enzima e durante la catalisi (Ghosh e Batra 2006; Guo et al. 2003). Questi studi indicano che differenti valori di pH ottimali per l'attività enzimatica e diverse modalità di legame degli analoghi dei substrati originano da differenze strutturali che riguardano il sito attivo (Gu e Xia 2000; Watanabe et al. 1994).

Per quanto riguarda le caratteristiche strutturali delle RIP di tipo 2, la catena A è strutturalmente simile alla struttura delle RIP di tipo 1, mentre la catena B è una proteina globulare con due domini (domino 1 e 2) omologhi presenti all'N- e al C terminale, ciascuno costruito da tre motivi omologhi, chiamati α, β e γ, che probabilmente derivano da eventi di duplicazione genica da un motivo ancestrale di riconoscimento dei carboidrati (Rutenber et al. 1987). Ciascun dominio è costituito da circa 40 residui amminoacidici. Sebbene i sottodomini α, β e γ abbiano la stessa conformazione di base, solo i motivi 1α e 2γ, alle estremità della catena B, hanno la capacità di legare monosaccaridi facenti parte di catene glicidiche complesse legate a proteine di membrana (Fig. 3). La catena B, che non influenza in alcun modo l'attività N-β-glicosidasica delle RIP di tipo 2, riveste un ruolo rilevante nella capacità di rendere le RIP di tipo II altamente tossiche nei confronti di determinate linee cellulari dato che i motivi 1α e 2γ possono riconoscere recettori contenuti nelle strutture glicidiche contenenti galattosio, mannosio o acido sialico con differente capacità di legame. Inoltre, sostituzioni amminoacidiche nei motivi 1α e 2γ, che ne compromettono la struttura, rendono alcune RIP di tipo 2 poco tossiche perdendo la capacità di interagire con le catene glicidiche complesse (Iglesias et al. 2018).

Il maggior numero di RIP è stato isolato dalle Angiosperme, in particolare in alcune famiglie (Caryophyllaceae, Sambucaceae, Cucurbitaceae, Euphorbiaceae, Phytolaccaceae e Poaceae) mentre non sono state isolate RIP dalle Gimnosperme (Di Maro et al. 2014). Molti di questi enzimi sono generalmente espressi in differenti tessuti della pianta (ad esempio le saporine sono presenti in foglie, semi e radici di *Saponaria officinalis* L.) (Ferreras et al. 1993) sebbene siano noti esempi di piante che ne mostrano la presenza solo in tessuti specifici (ad es. la ricina nei semi di *Ricinus comunis* L.). La loro espressione è strettamente correlata all'omeostasi, essendo la risposta a condizioni di stress abiotico e biotico come calore, stress osmotico, freddo, salinità, o in seguito all'attacco di virus, microrganismi, insetti e funghi patogeni (Stirpe et al. 1996).

La maggior parte delle RIP è risultata citotossica nei confronti di differenti linee cellulari tumorali *in vitro* ed *in vivo* (Gilabert-Oriol et al. 2014). Da quanto riportato in letteratura, sembra che la citotossicità sia dovuta alla loro attività enzimatica di danneggiare i ribosomi nel citoplasma, ma è anche fortemente correlata al percorso di internalizzazione cellulare. Infatti, la loro entrata nel citoplasma promuove l'inattivazione dei ribosomi con conseguente morte cellulare per

apoptosi (Lord e Spooner 2011). Ciò è confermato dall'esistenza di RIP di tipo 2 non tossiche, identificate in alcune piante (ad es. *Sambucus*), che pur possedendo attività rRNA N-β-glicosidasica, non sono tossiche perché sono degradate a seguito di un'internalizzazione con percorsi intracellulari non ancora del tutto chiari, differenti dalle RIP di tipo 2 tossiche (Girbes et al. 1993; Tejero et al. 2015).

Tuttavia, la possibilità di dirigere selettivamente le RIP verso specifici bersagli cellulari da eliminare, come indicato dai diversi percorsi di internalizzazione, mette in risalto le grosse potenzialità di questi enzimi per possibili applicazioni in campo biomedico, come dimostrato da numerosi studi preclinici e clinici (Gilabert-Oriol et al. 2014). Sulla base di tali osservazioni e tenendo conto delle tecniche biotecnologiche ad oggi disponibili, che permettono di scegliere selettivamente le popolazioni cellulari da eliminare con specifici vettori, le RIP sono sempre più utilizzate (Polito et al. 2016). In parallelo, l'ingegneria proteica sta migliorando nel contempo il meccanismo di ingresso cellulare di questi preparati tossici, la loro specificità, così come la loro emivita nel plasma e la loro resistenza alle proteasi nei liquidi extracellulari o nel citoplasma, riducendone la loro antigenicità.

3 - POTENZIALITA' APPLICATIVE DELLE RIP

La citotossicità delle RIP è stata studiata *in vivo* e *in vitro* su un ampio numero di linee cellulari cancerose e non, mostrando che ogni RIP è in grado di danneggiare (azione citostatica) o uccidere (azione citotossica) differenti linee cellulari. Queste azioni richiedono l'entrata delle RIP di tipo 1 o della catena A delle RIP di tipo 2 nel citoplasma delle cellule bersaglio per esplicare l'attività rRNA N-β-glicosidasica sui ribosomi. Il passaggio dall'esterno all'interno della cellula è uno dei punti nevralgici alla base della differente citotossicità delle RIP di tipo 1 e di tipo 2, ed è strettamente correlata con il percorso intracellulare, una volta attraversata la membrana plasmatica. Tale percorso può variare sia in base alle caratteristiche strutturali delle RIP, sia in base all'ultrastruttura delle cellule in esame, e dipende: i) dai ligandi sulla superficie cellulare; ii) dall'indirizzamento dei complessi RIP-recettore nella cellula bersaglio; e iii) dal numero di catene integre (RIP di tipo 1 o catena A delle RIP di tipo 2) capaci di esplicare la loro azione enzimatica nel citoplasma (de Virgilio et al. 2010).

In generale, i macrofagi e i trofoblasti sono risultati le cellule con maggiore sensibilità alle RIP, probabilmente a causa della loro capacità di interagire con un vasto numero di molecole esterne, data la presenza di un elevato e diversificato numero di recettori o strutture recettoriali sulla loro superficie (Barbieri et al. 1993). In genere, le RIP entrano nella cellula legandosi prima a recettori o strutture della superficie cellulare, dopodiché attraversano la membrana plasmatica

mediante endocitosi ed infine, vengono traslocate nel citoplasma, fluendo attraverso un determinato compartimento intracellulare (che di preferenza è il Golgi) (de Virgilio et al. 2010). Le RIP di tipo 2 (ad es. la ricina) interagiscono con la membrana plasmatica, dopo essersi legate a strutture contenenti galattosio, riconosciute dalla catena lectinica B, attraversano la membrana plasmatica per endocitosi e arrivano alle vescicole dell'apparato del Golgi. Il contenuto delle vescicole viene quindi rilasciato e trasportato mediante un successivo trasporto vescicolare retrogrado fino al reticolo endoplasmatico (RE). Una volta nel lume del RE, le catene A e B delle RIP di tipo 2 subiscono un processo di dissociazione, ed infine, una minima quantità di catena A trasloca nel citoplasma dove, esplicando la sua attività rRNA N-β-glicosidasica, danneggia i ribosomi (Sowa-Rogozinska et al. 2019).

Al contrario, data la loro struttura monomerica, le RIP di tipo 1 mancano della catena lectinica B, mostrando una maggiore difficoltà ad entrare nelle cellule (motivo per cui sono meno tossiche). Tuttavia, la maggior parte degli studiosi concorda sul fatto che le RIP di tipo 1 necessitano di specifici meccanismi di accesso, ancora poco noti o sconosciuti. Una volta internalizzate, le RIP di tipo 1 vengono rilasciate nel citoplasma attraverso un percorso diverso da quello utilizzato dalla catena A della ricina, indipendente dalla via del Golgi, che ne limita la tossicità, portando ad un inefficiente rilascio nel citoplasma (Polito et al. 2013).

4 - UTILIZZO DELLE RIP IN CAMPO BIOMEDICO (IMMUNOTOSSINE E CONIUGATI)

Un approccio ipotizzato da Paul Ehrlich all'inizio del 1900 per lo sviluppo di farmaci mirati ('magic bullet' in inglese) volto a migliorare l'efficacia terapeutica di nuovi farmaci, utili a bloccare o eliminare cellule dannose dell'organismo (ad esempio le cellule cancerose), è la combinazione di molecole capaci di riconoscere uno specifico bersaglio cellulare con un'altra/altre capace/i di attività citotossica nei confronti delle cellule che presentano tale bersaglio (Strebhardt e Ullrich 2008). Un esempio è rappresentato dalle immunotossine, macromolecole chimeriche ottenute combinando un anticorpo (vettore) con una tossina. Queste macromolecole chimeriche si basano sulla capacità della tossina legata all'anticorpo di entrare nelle cellule bersaglio e di esplicare, dopo internalizzazione, l'azione citotossica sulle cellule bersaglio. La specificità del bersaglio è data dall'affinità dell'anticorpo selezionato nei confronti di uno specifico bersaglio (recettore, proteina di membrana o specifici polisaccaridi o lipidi complessi). Queste molecole bifunzionali hanno una potente azione citotossica *in vitro*, ma il loro uso *in vivo* è spesso limitato o presenta problemi, data la capacità di indurre la risposta immunitaria, tossica per il fegato, così come la capacità di danneggiare i vasi sanguigni e bassa attività sui tumori solidi dati i problemi di diffusione nei tessuti.

Negli ultimi anni, i progressi dell'ingegneria proteica, per la produzione di anticorpi ricombinanti e delle tecniche biochimiche, per ottenere proteine di fusione, hanno portato ad un rapido aumento di biomolecole capaci di riconoscere specifici bersagli, avendo maggior affinità per il bersaglio e di cui è più facile studiare la farmacocinetica. In particolare, si sono ottenuti progressi nel diminuire sia la grandezza delle molecole chimeriche, sia la loro antigenicità. Oggi le immunotossine sono considerate potenti 'immunofarmaci' specifici contro cellule cancerose e utili per il trattamento di malattie virali o parassitarie.

Tale processo di evoluzione molecolare *in vitro*, ha portato le RIP di tipo 1 e le catene A delle RIP di tipo 2, ad essere attori di primo piano per un ampio spettro di applicazioni. Infatti, tra le prime immunotossine prodotte, ci sono molecole chimeriche basate sulle RIP generate accoppiando le RIP di tipo 1 o la catena A delle RIP di tipo 2, con un anticorpo nativo (inizialmente da topo) attraverso leganti covalenti, generalmente ponti disolfurici, tra le due molecole (Fig. 3) (Vitetta et al. 1982).

Inoltre, le iniziali immunotossine basate sulle RIP, prevedevano l'utilizzo di tossine deglicosilate, al fine di ridurre legami non specifici o reazioni aspecifiche o per diminuirne l'antigenicità che comprometterebbe l'azione di questi immunoconiugati. In particolare, tra le prime immunotossine ottenute vi è quella basata sulla catena A della ricina deglicosilata legata ad un anticorpo monoclonale anti-CD22 murino (un recettore presente sulle cellule tumorali della maggior parte dei pazienti con leucemia linfoblastica acuta) (Ghetie et al. 1988). Successivamente, avendo a disposizione un numero sempre maggiore di RIP di tipo 1, che evitano procedure di separazione della catena A dalla catena lectinica B, sono state prodotte nuove immunotossine. Inoltre, la loro purificazione da piante differenti (la saporina da *S. officinalis*, la PAP da *P. americana* e la tricosantina da *T. kirilowii*), permetteva in linea di principio di poter avviare cicli di cure in cui gli immunoconiugati erano realizzati con RIP di tipo 1 differenti e quindi in grado di sfuggire alla risposta anticorpale del paziente (Stirpe 2013).

Nonostante i risultati incoraggianti ottenuti, questi primi approcci sperimentali misero in evidenza svariati problemi per queste prime immunotossine, definite di prima generazione (Fig. 3). Tra i principali problemi riscontrati c'erano: i) scarsa stabilità dovuta al legame tra anticorpo e tossina; ii) composizione eterogenea e ridotta affinità di legame, causata da una non specifica coniugazione chimica; iii) scarsa penetrazione nella massa tumorale solida per le grosse dimensioni delle macromolecole (circa 100 kDa); iv) immunogenicità; e v) difficoltà di produzione su larga scala.

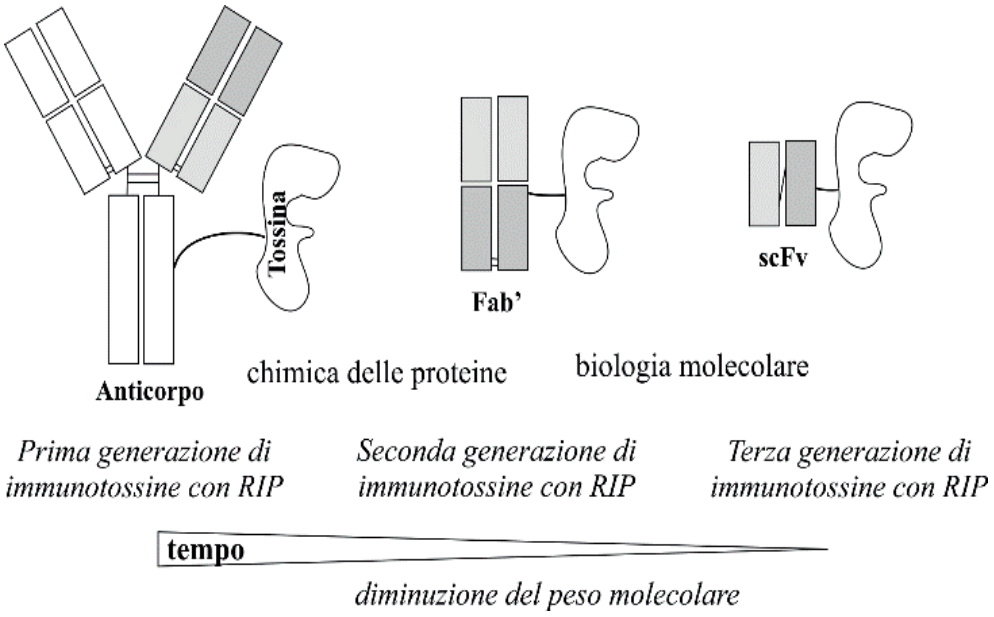

Fig. 3 – Evoluzione schematica delle immunotossine basate sulle RIP.

Per migliorare la farmacocinetica e ridurre gli effetti collaterali di queste immunotossine, sono stati fatti grandi sforzi per produrre una nuova generazione di immunotossine basate sulle RIP, mediante l'utilizzo di tecniche del DNA ricombinante e ottimizzazione dei sistemi di espressione che utilizzano lievito, batteri, cellule di ovaio di criceto o cellule di insetto. Lo sviluppo di queste nuove immunotossine basate sulle RIP comporta due passaggi critici: i) progettazione e costruzione di frammenti di anticorpi come i frammenti Fab' (seconda generazione di immunotossine) e poi i mini anticorpi (svFc; terza generazione) ottenuti con metodi ricombinanti, con peso molecole ridotto; ii) sviluppo di metodologie per la produrre anticorpi umanizzati; e iii) miglioramento dell'espressione e delle metodologie di purificazione di questi costrutti chimerici in sistemi eterologhi di espressione. In tale contesto, le RIP si sono rivelate uno strumento adatto a validare le ipotesi alla base di queste nuove idee e per mettere a punto gli iniziali protocolli per lo sviluppo di nuove generazioni di immunotossine (Antignani e Fitzgerald 2013).

Come esempio, ricordiamo lo sviluppo di immunoconiugati costruiti utilizzando la saporina S6, RIP di tipo 1, utilizzata in molecole chimeriche differenti, in cui veniva cambiato l'anticorpo selettivo (anticorpo o parte di esso) rendendola capace di divenire tossica per differenti tipi di cellule maligne o tumori solidi. La scelta della saporina S6, è dovuta alle sue intrinseche caratteristiche strutturali e funzionali, come un'alta resistenza alla denaturazione e alla proteolisi, nonché

alla sua forte efficacia catalitica accoppiata a una citotossicità meno accentuata su cellule non cancerose. Nel 1985, la saporina S6, fu coniugata per la prima volta all'anticorpo monoclonale murino anti-Thy 1.1 e al suo frammento Fab' (Thorpe et al. 1985). Da allora, la saporina S6 è stata ampiamente utilizzata come parte tossica in una varietà di immunoconiugati che colpiscono le molecole della superficie cellulare (marcatori CD, o marcatori dei gruppi di differenziazione) di diverse cellule ematiche maligne e tumori solidi. La maggior parte dei marcatori CD riconosciuti da immunotossine saporina S6/anticorpo sono recettori o molecole di adesione cellulare o specifici ligandi. Successivamente, al fine di eliminare la risposta anticorpale umana nei confronti degli anticorpi murini (mAB), sono stati sviluppati nel tempo nuovi immunoconiugati chimerici, sostituendo domini costanti degli anticorpi murini con domini costanti umanizzati. Negli ultimi anni, infine, sono stati utilizzati parti variabili di anticorpi ricombinanti, in cui solo la parte ipervariabile era murina (anticorpi umanizzati) diminuendo ancora di più la grandezza molecolare e l'antigenicità di tali immunotossine.

Per evitare l'eterogeneità, migliorare la penetrazione nel tumore e aumentare la complessità della produzione, le tecniche del DNA ricombinante sono state applicate per produrre l'ultima generazione di immunotossine formate dalla saporina S6 e frammenti variabili a catena singola (noti come mini anticorpi) (Fig. 3). In questi costrutti il dominio di legame cellulare della tossina viene sostituito con la porzione Fv dell'anticorpo in cui si trovano i suoi frammenti variabili a catena leggera e pesante collegati con peptidi. I costrutti sono realizzati mediante sintesi proteica utilizzando un'unica molecola di RNA messaggero (Gilabert-Oriol et al. 2014).

Diverse RIP e la saporina S6 sopra descritta, sono state usate per costruire immunotossine contro diversi bersagli in molti studi preclinici, portando a risultati promettenti nella maggior parte dei casi. La grande efficacia di questo approccio è stata riportata in particolare nella cura di diversi modelli tumorali ematologici. Negli esperimenti condotti su topi, i trattamenti con le immunotossine basate sulle RIP, sono stati in grado di ridurre fortemente la dimensione dei tumori trapiantati in tutti i casi e in diversi modelli sperimentali si è arrivati alla totale eliminazione delle masse tumorali.

Oltre ad essere utilizzati per la produzione di immunotossine, alcune RIP sono state coniugate (sia chimicamente o mediante tecniche di ingegneria proteica) con molecole diverse da un anticorpo, ottenendo specifici agenti bifunzionali, citotossici e selettivi per una determinata popolazione cellulare, come ad esempio ligandi di recettori cellulari, inibitori di proteasi, ormoni, ecc. La prima RIP utilizzata a tale scopo è stata la saporina S6 fusa con l'urochinasi (uPA) una proteasi in grado di degradare sia la fibrina che il fibrinogeno esercitando così un'azione fibrinolitica. Il prodotto chimerico ottenuto si è dimostrato molto efficace su cellule che esprimevano il recettore per uPA (noto come uPAR), mentre

le linee cellulari prive di uPAR non erano influenzate dal coniugato (Cavallaro et al. 1993).

La transferrina è una proteina coinvolta nell'assorbimento del ferro da parte delle cellule, con la capacità, in seguito al legame con uno specifico recettore di membrana, di trasportare all'interno della cellula due ioni ferro nella forma ferrica (Fe^{3+}). Il recettore della transferrina, ampiamente distribuito in diversi tipi cellulari, è di solito iperespresso in cellule maligne. Pertanto, la transferrina è stata utilizzata per costruire coniugati contenenti RIP, come la saporina S6 e la catena A della ricina (Polito et al. 2013). Gli studi condotti su entrambi i coniugati hanno dimostrato un'alta selettività di questi coniugati su varie linee cellulari tumorali che esprimevano il recettore della transferrina, con differenti meccanismi di indirizzamento intracellulare.

Un approccio simile è stato usato con la curcina, una RIP di tipo 1 isolata dai semi di *Jatropa curcas* L., in grado di inibire la proliferazione delle cellule tumorali, portando alla morte cellulare per apoptosi. Poiché la citotossicità della curcina non è selettiva essa è stata fusa ad uno specifico peptide molto affine al recettore per la transferrina (TfRBP) rendendo altamente selettiva la molecola chimerica nei confronti di popolazioni cellulari iperesprimenti il recettore della transferrina, ottenendo anche una notevole riduzione del peso molecolare del costrutto chimerico (Zheng et al. 2013).

Un approccio alternativo per la costruzione di coniugati basati sulle RIP prevede il potenziamento della loro resistenza alla proteolisi. Infatti, è stato ampiamente dimostrato che la citotossicità delle RIP dipende non solo dal modo con cui entrano nelle cellule ed arrivano al citoplasma, ma anche dalla loro intrinseca resistenza agli agenti proteolitici durante il percorso cellulare (Santanche et al. 1997). Infatti, vari coniugati basati sulle RIP di tipo 1 fusi con inibitori di proteasi, hanno mostrato un aumento della loro citotossicità *in vitro* rispetto alle RIP di tipo 1 non coniugate (Tamburino et al. 2012).

Infine, negli ultimi anni, sono stati compiuti notevoli sforzi nello sviluppo di nanosistemi in grado di migliorare il riconoscimento e il rilascio di farmaci in specifiche cellule bersaglio, nella terapia antitumorale. Diversi nanomateriali sintetici sono stati sintetizzati basandosi su liposomi, polimeri organici e nanoparticelle inorganiche (Minko et al. 2013; Uddin et al. 2016). Inoltre, vale la pena anche evidenziate che le diverse nanoparticelle sono in grado di attraversare la barriera emato-encefalica, aprendo nuove prospettive per il trasporto di farmaci al cervello. Le dimensioni nanometriche delle particelle consentono anche un accesso facilitato nella cellula e in vari compartimenti cellulari, incluso il nucleo. Una alternativa ai coniugati contenenti esclusivamente anticorpi è la costruzione di nanoconiugati delle RIP che contengono nanomateriali[4] (Pizzo e Di Maro

[4] I nanomateriali sono sostanze chimiche o materiali composti da particelle con dimensioni comprese tra 1 e 100 nanometri (nm).

2016). Ad esempio, la curcina, una RIP di tipo 1, è stata utilizzata con successo nella costruzione di nanoparticelle d'oro coniugate con l'acido folico e l'anticorpo antitransferrina, per ottenere una doppia e mirata nanoformulazione diretta verso i gliomi (Mohamed et al. 2014b). In questo costrutto, la proteina è stata coniugata in nanoparticelle tramite legami sensibili al pH per minimizzare la diffusione sistemica non specifica della tossina durante la circolazione e massimizzare l'efficienza del trasporto mirato dei farmaci alla zona invasa dal tumore. Un altro esempio sono i nanosistemi colloidali ibridi, costituiti da componenti polimerici lipidici altamente compatibili con le cellule endoteliali e neuronali umane. Quando queste nanoparticelle a base lipidica sono coniugate alla curcina, la nanoformulazione ottenuta si è dimostrata settivamente attiva contro le cellule di gliomi (Mohamed et al. 2014a).

5 - CONCLUSIONI

Le proteine inattivanti i ribosomi rappresentano una classe di enzimi, ampiamente distribuita nelle piante ed in misura minore, in altri organismi. Finora, molte informazioni strutturali e funzionali su queste proteine sono state accumulate; tuttavia, come di regola nella ricerca scientifica, le nuove domande poste dai risultati, probabilmente superano le risposte ottenute finora. Probabilmente la domanda più importante riguarda la funzione delle RIP in natura. Sono state avanzate diverse ipotesi ma predomina l'ipotesi della loro presenza per la difesa contro predatori, parassiti e virus. È possibile che le RIP di tipo 2 possano dissuadere gli animali dal mangiare piante in cui sono presenti, ma ciò non è facilmente verificabile per le RIP di tipo 1. Queste ultime, verosimilmente possono prevenire le infezioni virali, ma questa regola non è valida per tutti gli organismi che producono RIP di tipo 1. Il fatto che l'espressione delle RIP aumenti in condizioni di stress, porta a supporre che siano d'aiuto per le piante in condizioni ambientali sfavorevoli.

Comunque, dalla scoperta della ricina (Stillmark, 1888 e 1889), molto è stato compreso sulla struttura e sui meccanismi di questi enzimi. Inoltre, le loro attività antivirali e citotossiche sono da sempre al centro dell'interesse da parte della comunità scientifica, sia per applicazioni in campo biomedico, che in campo agricolo. Infatti, la moderna medicina non si focalizza solo sull'ottenimento di 'piccoli farmaci' ma anche su chemioterapici selettivi e senza effetti genotossici, come i differenti coniugati antitumorali delle RIP prodotti dallo sviluppo di metodi efficaci per ottenere specifici coniugati usando anticorpi, ormoni o nanostrutture hanno messo in evidenza che le RIP possono essere utilizzate nella terapia antitumorale mirata.

6 - BIBLIOGRAFIA

Antignani A., Fitzgerald D. (2013) Immunotoxins: the role of the toxin. Toxins (Basel) 5 (8):1486-1502.

Barbieri L., Battelli M.G., Stirpe F. (1993) Ribosome-inactivating proteins from plants. Biochim. Biophys. Acta 1154 (3-4):237-282.

Barbieri L., Gorini P., Valbonesi P., Castiglioni P., Stirpe F. (1994) Unexpected activity of saporins. Nature 372 (6507):624.

Cavallaro U., del Vecchio A., Lappi D.A., Soria M.R. (1993) A conjugate between human urokinase and saporin, a type-1 ribosome-inactivating protein, is selectively cytotoxic to urokinase receptor-expressing cells. J. Biol. Chem. 268 (31):23186-23190.

Chaudhry B., Muller-Uri F., Cameron-Mills V., Gough S., Simpson D., Skriver K., Mundy J. (1994) The barley 60 kDa jasmonate-induced protein (JIP60) is a novel ribosome-inactivating protein. Plant J. 6 (6):815-824.

de Virgilio M., Lombardi A., Caliandro R., Fabbrini M.S. (2010) Ribosome-inactivating proteins: from plant defense to tumor attack. Toxins (Basel) 2 (11):2699-2737.

Di Maro A., Citores L., Russo R., Iglesias R., Ferreras J.M. (2014) Sequence comparison and phylogenetic analysis by the Maximum Likelihood method of ribosome-inactivating proteins from angiosperms. Plant Mol. Biol. 85 (6):575-588.

Endo Y., Tsurugi K. (1987) RNA N-glycosidase activity of ricin A-chain. Mechanism of action of the toxic lectin ricin on eukaryotic ribosomes. J. Biol. Chem. 262 (17):8128-8130.

Ferreras J.M., Barbieri L., Girbes T., Battelli M.G., Rojo M.A., Arias F.J., Rocher M.A., Soriano F., Mendez E., Stirpe F. (1993) Distribution and properties of major ribosome-inactivating proteins (28 S rRNA N-glycosidases) of the plant *Saponaria officinalis* L. (Caryophyllaceae). Biochim. Biophys. Acta 1216 (1):31-42.

Ghetie M.A., May R.D., Till M., Uhr J.W., Ghetie V., Knowles P.P., Relf M., Brown A., Wallace P.M., Janossy G., et al. (1988) Evaluation of ricin A chain-containing immunotoxins directed against CD19 and CD22 antigens on normal and malignant human B-cells as potential reagents for *in vivo* therapy. Cancer Res. 48 (9):2610-2617.

Ghosh P., Batra J.K. (2006) The differential catalytic activity of ribosome-inactivating proteins saporin 5 and 6 is due to a single substitution at position 162. Biochem. J. 400 (1):99-104.

Gilabert-Oriol R., Weng A., Mallinckrodt B., Melzig M.F., Fuchs H., Thakur M. (2014) Immunotoxins constructed with ribosome-inactivating proteins and their enhancers: a lethal cocktail with tumor specific efficacy. Curr. Pharm. Des. 20 (42):6584-6643.

Girbes T., Citores L., Ferreras J.M., Rojo M.A., Iglesias R., Munoz R., Arias F.J., Calonge M., Garcia J.R., Mendez E. (1993) Isolation and partial characterization of nigrin b, a non-toxic novel type 2 ribosome-inactivating protein from the bark of *Sambucus nigra* L. Plant Mol. Biol. 22 (6):1181-1186.

Girbes T., Ferreras J.M., Arias F.J., Stirpe F. (2004) Description, distribution, activity and phylogenetic relationship of ribosome-inactivating proteins in plants, fungi and bacteria. Mini Rev. Med. Chem. 4 (5):461-476.

Gu Y.J., Xia Z.X. (2000) Crystal structures of the complexes of trichosanthin with four substrate analogs and catalytic mechanism of RNA N-glycosidase. Proteins 39 (1):37-46.

Guo Q., Zhou W., Too H.M., Li J., Liu Y., Bartlam M., Dong Y., Wong K.B., Shaw P.C., Rao Z. (2003) Substrate binding and catalysis in trichosanthin occur in different sites as revealed by the complex structures of several E85 mutants. Protein Eng. 16 (6):391-396.

Hey T.D., Hartley M., Walsh T.A. (1995) Maize ribosome-inactivating protein (b-32). Homologs in related species, effects on maize ribosomes, and modulation of activity by pro-peptide deletions. Plant Physiol. 107 (4):1323-1332.

Iglesias R., Ferreras J.M., Di Maro A., Citores L. (2018) Ebulin-RP, a novel member of the Ebulin gene family with low cytotoxicity as a result of deficient sugar binding domains. Biochim. Biophys. Acta Gen. Subj. 1862 (3):460-473.

Liu R.S., Yang J.H., Liu W.Y. (2002) Isolation and enzymatic characterization of lamjapin, the first ribosome-inactivating protein from cryptogamic algal plant *(Laminaria japonica* A). Eur. J. Biochem. 269 (19):4746-4752.

Lord J.M., Spooner R.A. (2011) Ricin trafficking in plant and mammalian cells. Toxins (Basel) 3 (7):787-801.

Minko T., Rodriguez-Rodriguez L., Pozharov V. (2013) Nanotechnology approaches for personalized treatment of multidrug resistant cancers. Adv. Drug. Deliv. Rev. 65 (13-14):1880-1895.

Mohamed M.S., Veeranarayanan S., Baliyan A., Poulose A.C., Nagaoka Y., Minegishi H., Iwai S., Shimane Y., Yoshida Y., Maekawa T., Kumar D.S. (2014a) Structurally distinct hybrid polymer/lipid nanoconstructs harboring a type-I ribotoxin as cellular imaging and glioblastoma-directed therapeutic vectors. Macromol. Biosci. 14 (12):1696-1711.

Mohamed M.S., Veeranarayanan S., Poulose A.C., Nagaoka Y., Minegishi H., Yoshida Y., Maekawa T., Kumar D.S. (2014b) Type 1 ribotoxin-curcin conjugated biogenic gold nanoparticles for a multimodal therapeutic approach towards brain cancer. Biochim. Biophys. Acta 1840 (6):1657-1669.

Montanaro L., Sperti S., Mattioli A., Testoni G., Stirpe F. (1975) Inhibition by ricin of protein synthesis in vitro. Inhibition of the binding of elongation factor 2 and of adenosine diphosphate-ribosylated elongation factor 2 to ribosomes. Biochem. J. 146 (1):127-131.

Monzingo A.F., Collins E.J., Ernst S.R., Irvin J.D., Robertus J.D. (1993) The 2.5 A structure of pokeweed antiviral protein. J. Mol. Biol. 233 (4):705-715.

Pizzo E., Di Maro A. (2016) A new age for biomedical applications of Ribosome Inactivating Proteins (RIPs): from bioconjugate to nanoconstructs. J. Biomed. Sci. 23 (1):54.

Polito L., Bortolotti M., Mercatelli D., Battelli M.G., Bolognesi A. (2013) Saporin-S6: a useful tool in cancer therapy. Toxins (Basel) 5 (10):1698-1722.

Polito L., Djemil A., Bortolotti M. (2016) Plant Toxin-Based Immunotoxins for Cancer Therapy: A Short Overview. Biomedicines 4 (2).

Rutenber E., Ready M., Robertus J.D. (1987) Structure and evolution of ricin B chain. Nature 326 (6113):624-626.

Santanche S., Bellelli A., Brunori M. (1997) The unusual stability of saporin, a candidate for the synthesis of immunotoxins. Biochem. Biophys. Res. Commun. 234 (1):129-132.
Sowa-Rogozinska N., Sominka H., Nowakowska-Golacka J., Sandvig K., Slominska-Wojewodzka M. (2019) Intracellular Transport and Cytotoxicity of the Protein Toxin Ricin. Toxins (Basel) 11 (6).
Stillmark H. (1888) Über Ricin, ein giftiges Ferment aus den Samen von Ricinus comm. L. und einigen anderen Euphorbiaceen (tesi di dottorato). University of Dorpat, Dorpat.
Stillmark H. (1889) In: R. Kobert (ed) Arbeiten des pharmakologischen Institutes zu Dorpat. Enke, Stuttgart. vol. 3, pp 57-62.
Stirpe F. (2013) Ribosome-inactivating proteins: from toxins to useful proteins. Toxicon 67:12-16.
Stirpe F., Barbieri L., Gorini P., Valbonesi P., Bolognesi A., Polito L. (1996) Activities associated with the presence of ribosome-inactivating proteins increase in senescent and stressed leaves. FEBS Lett. 382 (3):309-312.
Stirpe F., Gilabert-Oriol R. (2017) Ribosome-Inactivating Proteins: An Overview. In: Carlini CR, Ligabue-Braun R (eds) Plant Toxins. Springer Netherlands, Dordrecht, pp 153-182.
Strebhardt K., Ullrich A. (2008) Paul Ehrlich's magic bullet concept: 100 years of progress. Nat. Rev. Cancer. 8 (6):473-480.
Tamburino R., Pizzo E., Sarcinelli C., Poerio E., Tedeschi F., Ficca A.G., Parente A., Di Maro A. (2012) Enhanced cytotoxic activity of a bifunctional chimeric protein containing a type 1 ribosome-inactivating protein and a serine protease inhibitor. Biochimie 94 (9):1990-1996.
Tejero J., Jimenez P., Quinto E.J., Cordoba-Diaz D., Garrosa M., Cordoba-Diaz M., Gayoso M.J., Girbes T. (2015) Elderberries: A Source of Ribosome-Inactivating Proteins with Lectin Activity. Molecules 20 (2):2364-2387.
Thorpe P.E., Brown A.N., Bremner J.A., Jr., Foxwell B.M., Stirpe F. (1985) An immunotoxin composed of monoclonal anti-Thy 1.1 antibody and a ribosome-inactivating protein from Saponaria officinalis: potent antitumor effects in vitro and in vivo. J. Natl. Cancer Inst. 75 (1):151-159.
Uddin I., Venkatachalam S., Mukhopadhyay A., Usmani M.A. (2016) Nanomaterials in the pharmaceuticals: Occurrence, behaviour and applications. Curr. Pharm. Des.
Vitetta E.S., Krolick K.A., Uhr J.W. (1982) Neoplastic B cells as targets for antibody-ricin A chain immunotoxins. Immunol. Rev. 62:159-183.
Watanabe K., Dansako H., Asada N., Sakai M., Funatsu G. (1994) Effects of chemical modification of arginine residues outside the active site cleft of ricin A-chain on its RNA N-glycosidase activity for ribosomes. Biosci. Biotechnol. Biochem. 58 (4):716-721.
Zheng Q., Xiong Y.L., Su Z.J., Zhang Q.H., Dai X.Y., Li L.Y., Xiao X., Huang Y.D. (2013) Expression of curcin-transferrin receptor binding peptide fusion protein and its anti-tumor activity. Protein Expr. Purif. 89 (2):181-188.

Parte B
Scienze Matematiche

Rend. Acc. Sc. fis. mat. Napoli
Vol. LXXXVI, (2019) pp. 79-102

DOI 10.32092/1019

Categories of results in variable Lebesgue spaces theory

Nota del socio Alberto Fiorenza[1,2]

(Adunanza del 18 gennaio 2019)

Key words: Classical Lebesgue spaces, variable exponents, measurable functions.

Abstract – Variable (exponent) Lebesgue spaces represent a relevant research area within the theory of Banach function spaces. Much attention is devoted to look for sufficient conditions on the variable exponent to establish the assertions within the theory. In this Note we try to show the beauty of the research in this field, mainly quoting some known results organized into “categories", each of them characterized by a common typology of conditions on the variable exponent. New results involve the failure of rearrangement-invariant property, the rearrangement of the exponent, and a generalization of a formula known for constant exponents.

Riassunto – Gli spazi di Lebesgue con esponente variabile rappresentano un settore di rilievo nell’ambito della teoria degli spazi funzionali di Banach. Di notevole interesse é la ricerca di condizioni, da imporre alla funzione esponente, sufficienti ad assicurare il verificarsi di determinate affermazioni. In questa Nota ci proponiamo di mostrare il fascino della ricerca in questo settore, segnalando essenzialmente alcuni noti risultati organizzati in “categorie", ognuna delle quali caratterizzata da una comune tipologia di condizioni sulla funzione esponente. I risultati originali sono relativi alla non invarianza per riordinamento, al riordinamento dell’esponente e ad una generalizzazione di una formula nota per esponenti costanti.

1 - A SHORT HISTORY OF VARIABLE LEBESGUE SPACES

The introduction of a number of topological spaces, among which some families of Banach function spaces, contributed indubitably to the development of

[1]Dipartimento di Architettura, Università di Napoli Federico II, via Monteoliveto, 3, 80134 Napoli e Istituto per le Applicazioni del Calcolo “Mauro Picone", sezione di Napoli, Consiglio Nazionale delle Ricerche, via Pietro Castellino, 111, 80131 Napoli e Accademia di Scienze Fisiche e Matematiche della Societá Nazionale di Scienze, Lettere e Arti in Napoli, via Mezzocannone 8, 80134 Napoli. e-mail: fiorenza@unina.it

[2]This Note contains an updated and enlarged revision of the introduction of the talk, given by the author, at the AMS-EMS-SPM International Meeting 2015, 10-13 June, Porto, Portugal, entitled *On “essentially variable" variable Lebesgue space problems.*

the Functional Analysis. The continuous need to improve and refine mathematical models gave the opportunity to extend to more general frameworks several classical results of Mathematical Analysis. In this order of ideas a fruitful research area is that one of variable exponent Lebesgue spaces (variable Lebesgue spaces, in short), actually available through several references (see, for instance, Antontsev and Shmarev [10], Cruz-Uribe and the author [27], [31], Diening, Harjulehto, Hästö and Růžička [39], Edmunds, Lang and Méndez [46], Izuki, Nakai and Sawano [72], Kokilashvili, Meskhi, Rafeiro and Samko [76, 77], Lang and Edmunds [85], Meskhi [95], Pick, Kufner, John and Fučík [104], Rădulescu and Repovš [106], Růžička [111]).

Strictly speaking, variable Lebesgue spaces were born in a paper by Orlicz [103] in 1931, where in a remark about functions f such that $|f(x)|^{p(x)} \in L^1(0,1)$, $1 < p(x) < \infty$, he established essentially a kind of sharpness of Hölder's inequality. However, Orlicz is actually known for the spaces called Orlicz spaces, which he also introduced in 1931 in a joint paper with Birnbaum [16] (for the early history of these spaces, see Krasnosel′skiĭ and Rutickiĭ [84]; for treatments on Orlicz spaces, see e.g. also Maligranda [91], Rao and Ren [108], Harjulehto and Hästö [68]).

An important step in the development of the variable Lebesgue spaces came two decades later in the work of Nakano [98, 99] who originated the theory of modular spaces, sometimes referred to as Nakano spaces. A modular space is a topological vector space equipped with a "modular": a generalization of a norm. An important example of a modular space is the function space consisting of all functions f on a (Lebesgue) measurable set $\Omega \subset \mathbf{R}^n$ (in the following we will assume that Ω has positive measure) such that for some $\lambda > 0$,

$$\int_\Omega \Phi\left(x, \frac{|f(x)|}{\lambda}\right) dx < \infty,$$

where $\Phi : \Omega \times [0,\infty) \to [0,\infty]$ is a function such that for almost every $x \in \Omega$, $\Phi(x,\cdot)$ behaves like a Young function (i.e., roughly speaking, a convex function whose graph has the shape "similar" to that one of a power having constant exponent greater or equal than 1). These spaces are referred to as Musielak-Orlicz spaces or generalized (or variable) Orlicz spaces (see e.g. Musielak [97], Harjulehto and Hästö [68]). They contain a number of function spaces as special cases. If $\Phi(x,t) = \Phi(t)$ is just a function of t, they are the Orlicz spaces, and if $\Phi(x,t) = t^p w(x)$, they become the weighted Lebesgue spaces. In [98], Nakano introduced the variable Lebesgue spaces as specific examples of modular spaces: if $\Phi(x,t) = t^{p(x)}$, where $1 \le p(x) < \infty$ is a measurable function on Ω, they are the variable Lebesgue spaces $L^{p(\cdot)}(\Omega)$, which are therefore defined as the set of all measurable functions f on Ω such that for some $\lambda > 0$,

$$\int_\Omega \left|\frac{f(x)}{\lambda}\right|^{p(x)} dx < \infty. \tag{1}$$

$L^{p(\cdot)}(\Omega)$ becomes a *Banach function space* (i.e. a Banach space, whose elements are measurable functions and whose norm verifies some further conditions; see

e.g. Bennett and Sharpley [15]) when equipped with the Luxemburg norm

$$\|f\|_{L^{p(\cdot)}(\Omega)} = \inf\left\{\lambda > 0 : \int_\Omega \left|\frac{f(x)}{\lambda}\right|^{p(x)} dx \le 1\right\}. \tag{2}$$

When $p(\cdot) \equiv p$, p being a constant greater or equal than 1, then $L^{p(\cdot)}(\Omega) = L^p(\Omega)$ and (2) reduces to the classical norm on $L^p(\Omega)$. This notion can be simply adapted to allow $p(x) = \infty$ for a.e. x in a set $\Omega_\infty \subset \Omega$ (see Kováčik and Rákosník [83]), replacing the left hand side in (1) (and the corresponding term in (2)) by

$$\int_{\Omega\setminus\Omega_\infty} \left|\frac{f(x)}{\lambda}\right|^{p(x)} dx + \left\|\frac{f(x)}{\lambda}\right\|_{L^\infty(\Omega_\infty)}.$$

A different way to allow the case $p(x) = \infty$ on some subset of Ω, nicer from the formal point of view, has been suggested in Diening [38] (see also Diening, Harjulehto, Hästö, Mizuta and Shimomura [44]): the positions (1) and (2) *can* remain as they are, the trick is just to make the

$$\text{convention}: \quad t^{+\infty} = \begin{cases} 0 & \text{if} \quad 0 < t \le 1 \\ +\infty & \text{if} \quad t > 1 \end{cases} \quad ; \tag{3}$$

the resulting norm is slightly different, but the resulting space $L^{p(\cdot)}(\Omega)$ is the same, up to equivalence of norms.

The variable Lebesgue spaces appeared independently in the Russian literature, where they were studied as spaces of interest in their own right. They were introduced by Tsenov [123] in 1961, in the study of a minimization problem. In 1979, Sharapudinov [119] begun to develop the function space theory of the variable Lebesgue spaces on intervals on the real line, introducing the Luxemburg norm (drawing on ideas of Kolmogorov [78]), and showing that when $p(\cdot)$ is bounded, $L^{p(\cdot)}([0,1])$ is separable and its dual space is $L^{p'(\cdot)}([0,1])$, where $p'(\cdot)$ denotes the variable exponent $p'(\cdot) = p(\cdot)/(p(\cdot)-1)$. In [120] he was the first to consider questions that involved the regularity of the exponent function $p(\cdot)$, and introduced the local log-Hölder continuity condition,

$$|p(x) - p(y)| \le \frac{C_0}{-\log(|x-y|)}, \qquad \forall x, y : |x-y| < \frac{1}{2}, \tag{4}$$

that has proved to be of critical importance in the theory of variable Lebesgue spaces. The most influential work is due to Zhikov, who, starting from [124], begun to apply the variable Lebesgue spaces to problems in the Calculus of Variations.

The "modern" period in the study of variable Lebesgue spaces begun with the foundational paper of Kováčik and Rákosník [83] from 1991.

In the early 1990's, Samko and Ross [118, 109] (see also Samko [113, 116]) introduced a Riemann-Liouville fractional derivative of variable order and the

corresponding variable Riesz potential. Investigating the behavior of these operators led naturally to the study of convolution and potential operators on the variable Lebesgue spaces: see Samko [114, 115] and Edmunds and Meskhi [48].

In the mid 1990's, functionals with non-standard growth and the $p(\cdot)$-Laplacian were studied by Fan [54, 55], Fan and Zhao [58, 59], Marcellini [92, 93].

Partial differential equations with non-standard growth conditions have been considered, among others, in Fan [56], Harjulehto, Hästö, Lê and Nuortio [69], Mingione [96], Antontsev and Shmarev [10].

Interest in the variable Lebesgue spaces has increased since the 1990's because of their use in a variety of applications. Foremost among these is the mathematical modeling of electrorheological fluids, namely, fluids whose viscosity changes when exposed to an electric field: see Růžička [111, 112], Diening and Růžička [40, 43, 41, 42], Acerbi and Mingione [1, 2, 3].

The variable Lebesgue spaces have also been used to model the behavior of other physical problems. Some examples include quasi-Newtonian fluids (see Zhikov [125]), the thermistor problem (see Zhikov [126]), fluid flow in porous media (see Amaziane, Pankratov and Piatnitski [6], Antontsev and Shmarev [11]), magnetostatics (see Çekiç, Kalinin, Mashiyev and Avci [22]), and the study of image processing (see Blomgren, Chan, Mulet and Wong [17]).

2 - A LIST OF CATEGORIES

Roughly speaking, from the pure mathematical point of view, the attempts to generalize known classical statements to the variable exponent context lead in a natural way to the problem of looking for sufficient conditions on the variable exponent to establish the assertions within the theory. In the following we will quote some known results organized into "categories", each of them characterized by a common typology of conditions on the variable exponent; their number shows the richness of the phenomena encountered by researchers in the theory.

Before the beginning of our presentation, we recall that a kind of exposition into categories appears in Section 1.3 of the book by Diening, Harjulehto, Hästö and Růžička [39]; even if the present Note has some overlap with such reference, the reader here finds a discussion on the results considered and a finer classification, rather than just few collections of results.

This Note is based on the following observation: statements in terms of classical Lebesgue spaces (hence, say, true for constant exponents) may

(i) ... remain true for variable exponents and the extension is trivial

(ii) ... remain true for variable exponents but the proof needs some more effort

(iii) ... remain true only for *certain* variable exponents

(iv) ... are *never* true when exponents are not constant

The theory of variable Lebesgue spaces admits also another category of results, which do not come from the classic theory and their main feature is based specifically on the variability of the exponents:

(v) ... have no interest when exponents are constant

In Section we will shortly describe each of the above categories: we will treat ***(i)***-***(v)*** in paragraphs 4.1-4.5, respectively. For the completeness of the exposition, we need few prerequisites, which are the object of next Section .

3 - SOME STATEMENTS INVOLVING CLASSICAL LEBESGUE SPACES

For further needs, let us recall few definitions and results. Lebesgue spaces are part of standard knowledge in Mathematical Analysis and are presented in many textbooks and tracts, see e.g. Brezis [18, 19], Castillo and Rafeiro [21], DiBenedetto [35], Okikiolu [102], Pick, Kufner, John and Fučík [104], Rudin [110]. We will use also the notion of decreasing rearrangement, which is e.g. in Bennett and Sharpley [15], Kawohl [73], Korenovskii [81], Leoni [86], Rakotoson [107].

The well known formula (see e.g. DiBenedetto, p.149 [35], Stein p.7 [121], Lieb-Loss p.26 [90], Ambrosio, Fusco and Pallara p.34 [7], Okikiolu p.236 [102])

$$\int_\Omega |f(x)|^p\,dx = p\int_0^\infty t^{p-1}|\{x\in\Omega\,:\,|f(x)|>t\}|\,dt \tag{5}$$

shows that classical Lebesgue spaces are rearrangement-invariant Banach function spaces (see e.g. p.59 in Bennett and Sharpley [15]): in fact, the key property needed to define these spaces is that the norms of every pair of functions f,g equimeasurable, i.e. such that

$$|\{x\in\Omega : |f(x)|>t\}| = |\{x\in\Omega : |g(x)|>t\}| \qquad\qquad \forall t\geq 0\,,$$

coincide. As a further consequence of this formula, the norm of every function f in every rearrangement-invariant Banach function space coincides with that one of its decreasing rearrangement, which we denote by f_*. The importance of this class of spaces is the characterization given through the fundamental interpolation theorem: on one hand every rearrangement-invariant Banach function space is an interpolation space between L^1 and L^∞, and on the other every Banach function space which is an interpolation space between L^1 and L^∞ is rearrangement-invariant. Being interpolation space implies, in turn, the boundedness of a wide class of operators acting on them (see e.g. Ch.3 in Bennett and Sharpley [15] for details).

However, even without involving directly the machinery of interpolation theory, (5) can be used directly for proving a result which is a milestone in real-variable Harmonic Analysis. Given a function $f\in L^1_{loc}(\mathbf{R}^n)$, the (uncentered) Hardy-Littlewood maximal function Mf is defined by

$$Mf(x) = \sup_{Q\ni x}\frac{1}{|Q|}\int_Q |f(y)|dy \qquad\qquad \forall x\in\mathbf{R}^n\,,$$

where the supremum is taken over all cubes $Q \subset \mathbf{R}^n$ containing x and whose sides are parallel to the coordinate axes. If $f \in L^1_{loc}(\Omega)$, then Mf is defined by extending f to be identically 0 on $\mathbf{R}^n \setminus \Omega$. The following boundedness result holds (see e.g. Stein [121, 122]):

Theorem 1. *If $f \in L^p(\mathbf{R}^n)$, with $1 < p \leq \infty$, then $Mf \in L^p(\mathbf{R}^n)$ and*

$$\|Mf\|_{L^p(\mathbf{R}^n)} \leq C\|f\|_{L^p(\mathbf{R}^n)} \tag{6}$$

where C depends only on p and the dimension n.

It would be impossible to describe in few lines the importance of this classical result, which is a fundamental tool for proving, sometimes in a direct way, the boundedness of many operators in Harmonic Analysis (see e.g. Cruz-Uribe, Martell and Pérez [33], Duoandikoetxea [45], Kokilashvili and Krbec [75], Kokilashvili, Meskhi, Rafeiro and Samko [76, 77], Stein [121, 122]); for our goals we observe that since it provides an alternative proof of the classical Sobolev inequality and its consequences (see e.g. Ziemer [128]), its versions for other Banach function spaces, including variable Lebesgue spaces (see e.g. next Theorem 3), became a tool for extensions of the Sobolev inequality and several other classical results.

Incidentally, even if it is not among the goals of this Note, we notice that Theorem 1 is someway involved also to get packing results in Geometry of fractal sets (see Section 7.5 p. 109 in Falconer [53]).

4 - THE CATEGORIES IN DETAIL

The straightforward generalizations

When making research in Mathematics, sometimes the generalizations of theorems can be proved without any effort: one discovers that a certain argument can work “as it is" because it has in fact a greater validity. Of course formally such new theorems are “better" than the original ones, however, they can be classified as simple remarks, because no new ideas are needed to get the proofs. This is the case, for instance, of the proof of the completeness of variable Lebesgue spaces:

Theorem 2. *If $\Omega \subset \mathbf{R}^n$ and $p(\cdot) : \Omega \to [1, \infty]$ is a measurable function, then $L^{p(\cdot)}(\Omega)$ is complete: every Cauchy sequence in $L^{p(\cdot)}(\Omega)$ converges in norm.*

The proof of Theorem 2 can be found, for instance, in Cruz-Uribe and the author [27] (see Theorem 2.71 therein). It is nice to observe that formally replacing $p(\cdot)$ by p in any line of this reference, one gets the original proof which works for classical Lebesgue spaces.

This kind of results occupies a minor part of the theory of variable Lebesgue spaces; the proofs which can be written almost automatically have, of course, not so much interest.

The case of longer proofs

The existence of much literature involving variable Lebesgue spaces (see e.g. the enormous references list in the book by Cruz-Uribe and the author [27] or in the book by Diening, Harjulehto, Hästö and Růžička [39]) is justified by the fact that the majority of the results cannot be proved as Theorem 2. Maybe the first reason is that the formal substitution of p into $p(x)$ does not work already since the beginning of the theory, namely, with the expression of the norm: the "transformation"

$$\left(\int_\Omega |f(x)|^p\,dx\right)^{\frac{1}{p}} \quad \to \quad \left(\int_\Omega |f(x)|^{p(x)}\,dx\right)^{\frac{1}{p(x)}} \tag{7}$$

does not give, as "output", a number, but a function. Note also that homogeneity is lost: multiplying, for instance, f by 2 in the expression on the right, one does not get the double.

However, the expression of the norm in (2) has been obtained using exactly the formal substitution of p into $p(x)$, which works fine if one, previously, writes

$$\left(\int_\Omega |f(x)|^p\,dx\right)^{\frac{1}{p}}$$

in the different form

$$\inf\left\{\lambda>0:\ \int_\Omega \left|\frac{f(x)}{\lambda}\right|^p\,dx\le 1\right\}.$$

This trick, which is successful also in the case of Orlicz spaces and more generally in the context of modular spaces (see e.g. Maligranda [91]), has a deep topological validity (see Kolmogorov [78]); however, it reveals once more the usual way to construct generalizations, which is to use some characterization and to "discover" that the equivalent form is adapt to a new framework. A much more known example in this sense is the notion of weak derivative to define Sobolev spaces (see e.g. Brezis [18]).

In some cases the characterization leads to a significant change of the expression which is just apparent. Generalizations follow using the same ideas of the classical argument: just some small extra effort is needed.

For instance, let $1<p<\infty$ and consider the classical Hölder's inequality

$$\int_\Omega |f(x)g(x)|\,dx \le \left(\int_\Omega |f(x)|^p\,dx\right)^{\frac{1}{p}}\left(\int_\Omega |g(x)|^q\,dx\right)^{\frac{1}{q}}$$

where $\dfrac{1}{p}+\dfrac{1}{q}=1$. Its standard proof (see e.g. Brezis [18]) starts from the concavity of the logarithm, from which one gets the Young's inequality

$$ab\le \frac{1}{p}a^p+\frac{1}{q}b^q \qquad \forall\, a\ge 0,\ b\ge 0.$$

Then one replaces a with $|f(x)|$, b with $|g(x)|$, and integrate. The conclusion follows applying the previous argument to $\lambda|f(x)|$ and $\frac{|g(x)|}{\lambda}$, λ being a positive parameter, and finally choosing the "best" λ.

Looking at the corresponding result in the variable case (see e.g. Theorem 2.26 in Cruz-Uribe and the author [27]), when $1 < p(x) < \infty$ the method does not change: the Young's inequality is applied pointwise and therefore one gets

$$ab \leq \frac{1}{p(x)}a^{p(x)} + \frac{1}{q(x)}b^{q(x)} \qquad \forall\, a \geq 0\,,\ b \geq 0\,,\ x \in \Omega\,,$$

where $\frac{1}{p(x)} + \frac{1}{q(x)} = 1$ and, as before, one integrates over Ω.

It is clear that we are not in the same situation as in the previous paragraph: the proof does not work *word by word*, because integrating, now, one does not find immediately the norm. The fact that the expression of the norm is different makes the proof a little bit longer (see details in [27]), and some small extra effort must be spent to get the statement in the variable exponent case.

In some applications the effort to pass from the constant case to the variable case must be much higher, even when the exponent is relatively "nice". For instance, this may happen for exponents being continuous until the boundary of the domain: see e.g. El Hamidi [50], where existence results to elliptic systems involving the $p(x)-$laplacian are obtained.

The heart of the theory

Maybe the nicest feature of variable Lebesgue spaces theory is that the extension of results involving classical Lebesgue spaces does not hold for *all* variable exponents, but just for a *certain class* of exponents. It may be a hazard to make general assertions about mathematical theories, but, at least starting from our experience, this category of results includes the majority of the literature in this field. The main features of a result in this category are:

- The result holds for constant exponents
- The result does not hold for all possible variable exponents (and therefore an example is given)
- The result holds for *some* "really variable" (= not constant) exponents
- The class of exponents is studied: it is larger than the classes of exponents, previously known, involved in sufficient conditions for the validity of certain assertions, or it is smaller than the classes of exponents, previously known, involved in necessary conditions. The "full" result characterizes the class of exponents for which a certain assertion holds

A consequence of the features above is that several results do not admit just one variable version, but each of them may admit various "not full" extensions.

An entire “community" may work on the same assertion, producing results which may improve (or simply overlap with) already existing ones.

Let us draw our attention to an example of result in this category. We choose, because of its importance highlighted in Section , Theorem 1: the central problem is therefore that one to study conditions on an exponent $p(\cdot)$ so that the Hardy-Littlewood maximal operator is bounded on $L^{p(\cdot)}(\mathbf{R}^n)$. The first major result in this direction was due to Diening [36], who showed that it is sufficient to assume that $p(\cdot)$ satisfies the local log-Hölder condition (4), is constant outside of a large ball, and, finally, is bounded (i.e. $\operatorname{ess\,sup} p(\cdot) < \infty$) and bounded away from 1 (i.e. $\operatorname{ess\,inf} p(\cdot) > 1$). This result was generalized by Cruz-Uribe, Neugebauer and the author in [29] (see also Capone, Cruz-Uribe and the author [20] for a simpler proof), where a nearly optimal sufficient condition on the exponent $p(\cdot)$ is given: it was shown that it is sufficient to assume (besides the boundedness and the boundedness away from 1) that (4) holds and $p(\cdot)$ is log-Hölder continuous at infinity, namely, there exist constants p_∞ and C_∞ such that

$$|p(x) - p_\infty| \leq \frac{C_\infty}{\log(e+|x|)} \qquad \forall x \in \mathbf{R}^n\,. \tag{8}$$

A generalization which includes the constant case $p(\cdot) \equiv +\infty$ taking into account of the

$$\text{convention}: \quad \frac{1}{+\infty} = 0\,, \tag{9}$$

and involves the log-Hölder continuity both locally (see (4)) and at infinity (see (8)), is the following:

Theorem 3. *Given an open set $\Omega \subset \mathbf{R}^n$, if $p(\cdot) : \Omega \to [p_-, +\infty]$ is such that $p_- > 1$ and such that $1/p(\cdot)$ is log-Hölder continuous both locally and at infinity, then M is bounded on $L^{p(\cdot)}(\Omega)$:*

$$\|Mf\|_{L^{p(\cdot)}(\Omega)} \leq C\|f\|_{L^{p(\cdot)}(\Omega)}. \tag{10}$$

The proof of Theorem 3 borrows ideas from several papers. Expositions, eventually with small variants in the assumptions, are e.g. in Diening, Harjulehto, Hästö, Mizuta and Shimomura [44] (see Theorem 1.2 therein), in Cruz-Uribe and the author [27] (see Theorem 3.16 therein), in Cruz-Uribe, Diening and the author [24], in Izuki, Nakai and Sawano [72], in Harjulehto and Hästö [68] (see Corollary 4.5.5 therein), in Diening, Harjulehto, Hästö and Růžička [39] (see Theorem 4.3.8 and Remark 4.3.10 therein). The condition $p_- > 1$ for the maximal operator to be bounded is known to be necessary: this was first proved in Cruz-Uribe, Neugebauer and the author [29, 30] with the additional assumption that $p(\cdot)$ is upper semi-continuous. This hypothesis was removed by Diening [38] (see also Diening, Harjulehto, Hästö, Mizuta and Shimomura [44]). The same references have to be quoted for the case when $\operatorname{ess\,sup} p(\cdot) = \infty$ and the idea of the requirement of the log-Hölder continuity imposed to $1/p(\cdot)$. A very different proof of this theorem when $\operatorname{ess\,sup} p(\cdot) < \infty$, gotten by viewing $L^{p(\cdot)}$

from the perspective of abstract Banach function spaces, was given by Lerner and Pérez [89]. Independently, Nekvinda [100] showed that it was sufficient to assume that $p(\cdot)$ satisfies a somewhat weaker integral decay condition. The log-Hölder conditions are the sharpest possible pointwise conditions (see Pick and Růžička [105] and Cruz-Uribe, Neugebauer and the author [29, 30]) but they are not necessary: see Nekvinda [101], Kopaliani [79] and Lerner [88]. Diening [37] has given a necessary and sufficient condition that is difficult to check but has important theoretical consequences. The importance of these results was reinforced by the work in Cruz-Uribe, Martell, Pérez and the author [28], Cruz-Uribe and Hästö [32], where it was shown that the theory of Rubio de Francia extrapolation could be extended to the variable Lebesgue spaces and generalized Orlicz spaces. This allows the theory of weighted norm inequalities to be used to prove the boundedness of a multitude of operators (such as singular integrals) whenever the maximal operator is.

Of course, especially when full results are missing, in plenty of papers which need the boundedness of the maximal operator, the authors assume it directly (just to quote an example, see Kopaliani and Chelidze [80], where a Gagliardo-Nirenberg inequality with norms having variable exponents is obtained). This solution is reasonable as soon as from the literature it is known at least a set of sufficient conditions for such boundedness, because this way, in principle, any future result giving sufficient conditions can provide a new good set of assumptions. Such policy appears frequently in literature. As a further example, some results in the 2002 paper by the author [61] (see Hästö and Ribeiro [71], Ferreira, Hästö and Ribeiro [60], Harjulehto and Hästö [68] as other references dealing with the same topic) hold assuming the density of smooth functions in variable *Sobolev* spaces and even actually - in spite of various papers on this subject, for instance Cruz-Uribe and the author [26], Edmunds and Rákosník [49], Fan, Wang and Zhao [57], Hästö [70], Samko [117], Zhikov [127], the latest being Kostopoulos and Yannakakis [82] - a full result is still missing (while a full result exists for variable *Lebesgue* spaces, see Edmunds, Lang and Nekvinda [47]). Another paper where density of smooth functions in variable Sobolev spaces plays a key role is by Giannetti [67], who proved a modular version of the Gagliardo-Nirenberg inequality.

We mention now a “full" result in the sense above, due to Diening ([38]): in this case there is no sequence of papers trying to find the exact class of exponents, because it has been found already in the first reference on the topic. Consider the problem to establish the embedding between classical Lebesgue spaces. The result is simple to state and to be proved (see e.g. Theorem 3.10 in Castillo and Rafeiro [21]): for Ω of finite measure, if $1 \leq r \leq p \leq \infty$, then $L^p(\Omega) \subset L^r(\Omega)$ (note that the inclusion as sets is equivalent to the continuous embedding because they are particular Banach function spaces over the same measure space, see Theorem 1.8 in Bennett and Sharpley [15]). Whatever proof of the result for classical Lebesgue spaces is chosen (one may split Ω into the sets where $|f| \leq 1$ and $|f| > 1$, or one may use Hölder's inequality), the extension can be done without too much effort. The surprise is that while for classical Lebesgue spaces this result solves completely the problem to characterize the embedding (because

when Ω has not finite measure, two classical Lebesgue spaces over Ω cannot be compared), in the case of variable Lebesgue spaces this is not true. Namely, the embedding can hold in the case of exponents which become close each other, *very fast at infinity*, in a sense we are going to make precise. This can never happen for different, constant exponents: their distance is always constant. The "full" result for variable Lebesgue spaces (whose proof is quite technical) is the following (see Theorem 2.45 in Cruz-Uribe and the author [27], which is from Diening [38])

Theorem 4. *Given $\Omega \subset \mathbf{R}^n$ and $p(\cdot), q(\cdot) : \Omega \to [1,\infty]$, then $L^{q(\cdot)}(\Omega) \subset L^{p(\cdot)}(\Omega)$ and there exists $K > 1$ such that for all $f \in L^{q(\cdot)}(\Omega)$, $\|f\|_{p(\cdot)} \leq K\|f\|_{q(\cdot)}$, if and only if:*

1. *$p(x) \leq q(x)$ for almost every $x \in \Omega$;*
2. *there exists $\lambda > 1$ such that*

$$\int_D \lambda^{-r(x)}\,dx < \infty, \tag{11}$$

where $D = \{x \in \Omega : p(x) < q(x)\}$ and $r(\cdot)$ is the defect exponent defined by

$$\frac{1}{p(x)} = \frac{1}{q(x)} + \frac{1}{r(x)}.$$

In the same order of ideas we recall the following extension of (6): the inequality

$$\int_{\mathbf{R}^n} Mf(x)^p\,dx \leq c_1 \int_{\mathbf{R}^n} |f(x)|^q\,dx + c_2$$

holds for every $f \in L^q(\mathbf{R}^n)$ and for some positive constants c_1, c_2 independent of f if and only if $1 < p = q$. We stress that it is an extension: in fact, if $1 < p = q$, from the existence of some positive constants c_1, c_2 such that

$$\int_{\mathbf{R}^n} Mf(x)^p\,dx \leq c_1 \int_{\mathbf{R}^n} |f(x)|^p\,dx + c_2 \qquad \forall\, f \in L^p(\mathbf{R}^n) \tag{12}$$

one gets that also (6) is true, applying (12) to λf, dividing both sides by λ^p, and letting $\lambda \to \infty$. We remark that such homogeneization procedure can be applied in a general context (see e.g. D'Aristotile and the author [34]). The proof of such extension is a consequence of the following "full" result (see Cruz-Uribe, Di Fratta and the author [25])

Theorem 5. *Let $p(\cdot), q(\cdot) : \mathbf{R}^n \to [1,\infty[$. The inequality*

$$\int_{\mathbf{R}^n} Mf(x)^{p(x)}\,dx \leq c_1 \int_{\mathbf{R}^n} |f(x)|^{q(x)}\,dx + c_2$$

holds for every $f \in L^{q(x)}(\mathbf{R}^n)$ and for some positive constants c_1, c_2 independent of f if and only if $L^{q(\cdot)}(\mathbf{R}^n) \subset L^{p(\cdot)}(\mathbf{R}^n)$ and $p(\cdot)$ and $q(\cdot)$ "touch at infinity", namely, for every $E \subset \mathbf{R}^n$ having infinite measure,

$$\operatorname*{ess\,sup}_E p(\cdot) = \operatorname*{ess\,sup}_{\mathbf{R}^n} p(\cdot) = \operatorname*{ess\,inf}_{\mathbf{R}^n} q(\cdot) = \operatorname*{ess\,inf}_E q(\cdot).$$

Let us close this paragraph with one more result, where again the class of exponents has been fully characterized. Here the symbol $L^{p(\cdot)}_w(\Omega)$ stands for the weighted version of $L^{p(\cdot)}(\Omega)$, built as in Section using

$$\int_{\Omega\setminus\Omega_\infty}\left|\frac{f(x)}{\lambda}\right|^{p(x)}w(x)dx+\left\|\frac{f(x)}{\lambda}w(x)\right\|_{L^\infty(\Omega_\infty)},$$

where w is a weight, i.e. $w:\Omega\to]0,\infty[$, $w\in L^1_{loc}(\Omega)$.

Theorem 6. *Let $\Omega\subset\mathbf{R}^n$, and let $p(\cdot):\Omega\to[1,\infty]$ be such that $\operatorname{ess\,sup}_{\Omega\setminus\Omega_\infty}p(\cdot)<\infty$. The weight w is noneffective, i.e. $L^{p(\cdot)}(\Omega)=L^{p(\cdot)}_w(\Omega)$, if and only if $w\approx$ constant.*

For the proof and the details about the optimality of the condition $\operatorname{ess\,sup}_{\Omega\setminus\Omega_\infty}p(\cdot)<\infty$ see Krbec and the author [64].

Classic statements are the best ones

One of the features of the previous category of results is that the generalization to the variable setting holds for some non-constant exponents. However, there are results which, if written in terms of variable exponents, hold if and only if the exponents are constant. A collection of results in this category appears explicitly in Section 1.3 of the book by Diening, Harjulehto, Hästö and Růžička [39] already quoted above, and an overlapping collection is someway "hidden" in the Subject Index of the book by Cruz-Uribe and the author [27] (see *non-constant vs. constant* in p. 306 therein).

It is not our goal to make one, maybe more complete, list of results in this category. Just to give an idea of the category, we state and prove the following

Theorem 7. *Let $\Omega\subset\mathbf{R}^n$ and $p(\cdot):\Omega\to[1,\infty]$. The space $L^{p(\cdot)}(\Omega)$ is rearrangement-invariant if and only if $p(\cdot)$ is constant.*

Its proof is in Kováčik and Rákosník [83], where an extra assumption of continuity of the exponent appears, and another proof, where the exponent is assumed just measurable, is in Cruz-Uribe and the author [27] (see Example 3.14 p. 87 therein), but it is wrong. In the case $\Omega=\mathbf{R}^n$, Theorem 7 can be seen as a corollary of Proposition 3.6.1 p. 95 in Diening, Harjulehto, Hästö and Růžička [39], where it is shown that if an exponent $p(\cdot)$ is such that every translation operator maps $L^{p(\cdot)}(\mathbf{R}^n)$ to $L^{p(\cdot)}(\mathbf{R}^n)$, then it must be constant. In fact, suppose that $L^{p(\cdot)}(\mathbf{R}^n)$ is rearrangement-invariant. Since every translation of any $f\in L^{p(\cdot)}(\mathbf{R}^n)$ is equimeasurable with f, its norm equals that one of f. Therefore every translation operator maps $L^{p(\cdot)}(\mathbf{R}^n)$ to $L^{p(\cdot)}(\mathbf{R}^n)$ from which, by the proposition above, $p(\cdot)$ must be constant.

Here we are going to show a direct argument.

Proof.
Fix $E \subset \Omega$ of finite measure on which $p(\cdot)$ is non-constant, so that

$$p_+ := \operatorname{ess\,sup}_E p(\cdot) > \operatorname{ess\,inf}_E p(\cdot) =: p_- .$$

Let $p_*(\cdot)$ be the decreasing rearrangement of the restriction of $p(\cdot)$ to E, $p_*(\cdot)$ being defined in $(0,|E|)$. Let $\overline{p} \in (p_-, p_+)$. Since $p_*(\cdot)$ is a decreasing function, then it is limit a.e. of an increasing sequence of step functions, therefore there exists $s_1(\cdot)$ step function such that

$$s_1(t) = \sum_{i=1}^{K_1} \alpha_i \chi_{(t_{i-1}^{(1)}, t_i^{(1)})} \leq p_*(t), \qquad t_0^{(1)} = 0 < t_1^{(1)} < \cdots < t_{K_1}^{(1)} = |E|,$$

and such that $p_*(t) > \alpha_1 > \overline{p}$ for $t \in (t_0^{(1)}, t_1^{(1)})$; arguing analogously on $-p_*(\cdot)$, we can get $s_2(\cdot)$ step function such that

$$s_2(t) = \sum_{j=1}^{K_2} \beta_j \chi_{(t_{j-1}^{(2)}, t_j^{(2)})} \geq p_*(t), \qquad t_0^{(2)} = 0 < t_1^{(2)} < \cdots < t_{K_2}^{(2)} = |E|,$$

and such that $p_*(t) < \beta_{K_2} < \overline{p}$ for $t \in (t_{K_2-1}^{(2)}, t_{K_2}^{(2)})$. Set

$$\varepsilon = \min\left\{ t_1^{(1)}, t_{K_2}^{(2)} - t_{K_2-1}^{(2)} \right\},$$

and set

$$g_1(t) = t^{-\frac{1}{\alpha_1}} \quad \forall t \in (0, \varepsilon)$$

$$g_2(t) = (|E| - t)^{-\frac{1}{\alpha_1}} \quad \forall t \in (|E| - \varepsilon, |E|).$$

Of course $g_1(\cdot)$ and $g_2(\cdot)$ are equimeasurable.

By Ryff's theorem (see e.g. Theorem 7.5 p. 82 in Bennett and Sharpley [15]), $p = p_* \circ \sigma$ where $\sigma : E \to (0,|E|)$ is a measure-preserving transformation, i.e. a map such that the measure of any subset in $(0,|E|)$ equals the measure of the pre-image in E. Set $f_1 = g_1 \circ \sigma$ and $f_2 = g_2 \circ \sigma$. By Proposition 7.2 p. 82 in Bennett and Sharpley [15], $f_1(\cdot)$ and $g_1(\cdot)$ are equimeasurable and, analogously, $f_2(\cdot)$ and $g_2(\cdot)$ are equimeasurable. Since $g_1(\cdot)$ and $g_2(\cdot)$ are equimeasurable, also $f_1(\cdot)$ and $f_2(\cdot)$ are as well.

On the other hand, for any $\lambda > 0$ the function $(\lambda f_1(\cdot))^{p(\cdot)} = (\lambda g_1 \circ \sigma)^{p_* \circ \sigma} = [(\lambda g_1)^{p_*}] \circ \sigma$ is not integrable, because again by the proposition above, it is equimeasurable with $(\lambda g_1)^{p_*}$ which is not integrable (because for t small we have that $(\lambda g_1(t))^{p_*(t)} > (\lambda t^{-\frac{1}{\alpha_1}})^{\alpha_1} = \lambda^{\alpha_1} t^{-1}$), while the function $(f_2(\cdot))^{p(\cdot)} = (g_2 \circ \sigma)^{p_* \circ \sigma} = [(g_2)^{p_*}] \circ \sigma$ is integrable, because it is equimeasurable with $(g_2)^{p_*}$ which is integrable (because $(g_2(t))^{p_*(t)} < (|E| - t)^{-\frac{\beta_{K_2}}{\alpha_1}}$ for t close to $|E|$, and $\beta_{K_2} < \overline{p} < \alpha_1$). The conclusion is that if $p(\cdot)$ is non-constant, there exist two

equimeasurable functions $f_1(\cdot)$ and $f_2(\cdot)$ such that $f_1 \notin L^{p(\cdot)}(\Omega)$, $f_2 \in L^{p(\cdot)}(\Omega)$, and the theorem is proved. □

One more result in this category is a consequence of Theorem 5 above (see Corollary 1.22 in Cruz-Uribe, Di Fratta and the author [25]), which generalizes a result by Lerner [87]:

Theorem 8. *Let $p(\cdot) : \mathbf{R}^n \to [1,\infty[$. The inequality*

$$\int_{\mathbf{R}^n} Mf(x)^{p(x)}\,dx \le c_1 \int_{\mathbf{R}^n} |f(x)|^{p(x)}\,dx + c_2$$

holds for every $f \in L^{p(x)}(\mathbf{R}^n)$ and for some positive constants c_1, c_2 independent of f if and only if $p(\cdot)$ equals a constant $p > 1$ almost everywhere.

We may insert in this category also another result, which holds if and only if the exponent is constant because it seems that it cannot even be stated in the variable setting. The result is formula (5) above, which we recall here:

$$\int_\Omega |f(x)|^p\,dx = p\int_0^\infty t^{p-1}|\{x \in \Omega : |f(x)| > t\}|\,dt\,.$$

Its generalization to the variable case seems "forbidden": in the book by Diening, Harjulehto, Hästö and Růžička [39] (see the *Warnings!* in p.9; see also p. 4 in Harjulehto and Hästö [68]) it is written that it has no variable exponent analogue, because of course the formula

$$\int_\Omega |f(x)|^{p(x)}\,dx = p\int_0^\infty t^{p(x)-1}|\{x \in \Omega : |f(x)| > t\}|\,dt$$

has no interest at all: similarly as in the case of (7), on the right hand side one has a function and not a number. Note that since (5) governs the proof of Theorem 1, the proofs of Theorem 3 must be done with much different arguments (and in fact they *use* Theorem 1).

In spite of the considerations above, we wish here to record the following simple formulas.

Proposition 1. *If $\Omega \subset \mathbf{R}^n$ and $p(\cdot) : \Omega \to [1,\infty[$, then for all measurable functions f in Ω the following equalities hold, the first one with the extra assumption $f(x) \neq 0$ for a.e. $x \in \Omega$:*

$$\int_\Omega |f(x)|^{p(x)}\,dx = \int_{\mathbf{R}} e^t |\{x \in \Omega : p(x)\log|f(x)| > t\}|\,dt \tag{13}$$

$$\int_\Omega |f(x)|^{p(x)}\,dx = \int_{\mathbf{R}} e^t |\{x \in \Omega : |f(x)| > e^{\frac{t}{p(x)}}\}|\,dt \tag{14}$$

$$\int_\Omega |f(x)|^{p(x)}\,dx = \int_0^{+\infty} |\{x \in \Omega : |f(x)| > t^{\frac{1}{p(x)}}\}|\,dt \tag{15}$$

Proof.

Proof of (13): for any measurable $g : \Omega \to \mathbf{R}$ we may apply (5) to the positive function $\exp(g(x))$, in the case $p = 1$. After the substitution $\log t = s$, we get

$$\int_\Omega \exp(g(x))\,dx = \int_{\mathbf{R}} e^s |\{x \in \Omega : g(x) > s\}|\,ds\,.$$

If $f : \Omega \to \mathbf{R}$ is a.e. nonzero, setting $g(x) = p(x)\log|f(x)|$ in the above equality we get the assertion.

Proof of (14): immediate after (13) for functions f such that $f(x) \neq 0$ for a.e. $x \in \Omega$. If $f(x) = 0$ in a set $\Omega_0 \subset \Omega$, equality (14) holds with Ω replaced by $\Omega \setminus \Omega_0$; however, the same equality is equivalent to the final assertion because the points of Ω_0 do not affect both members.

Proof of (15): apply the substitution $e^t = s$ in (14). □

We note that, in the case $p(\cdot)$ constant, the substitution $t^{\frac{1}{p}} = \tau$ in (15) gives back (5).

Finally, we remark that making the conventions in the spirit of (3), (9), one can extend the validity of (13): for instance, writing

$$\text{convention}: \quad \log 0 = -\infty\,,$$

one can remove the assumption $f(x) \neq 0$ for a.e. $x \in \Omega$ made for (13): in fact, the set $\Omega_0 \subset \Omega$ where $f = 0$ a.e. does not influence both sides of (13) (note that in the right hand side, for any given $t \in \mathbf{R}$, any x such that $f(x) = 0$ would never satisfy the inequality $p(x)\log|f(x)| = p(x)\log 0 = -\infty > t$).

Essentially variable results

This last category concerns results which – in some opposite sense with respect to the previous category – have no interest or no meaning at all when the exponent is constant.

Let us state and prove the following proposition, where the problem of comparability in the sense of inclusion (or, equivalently, the continuous embedding) is considered for two variable Lebesgue spaces whose exponents are linked by the decreasing rearrangement operator.

Proposition 2. *Let $p(\cdot) : (0,1) \to [1,\infty[$. The spaces $L^{p(\cdot)}(0,1)$ and $L^{p_*(\cdot)}(0,1)$ are never comparable, unless $p(\cdot) = p_*(\cdot)$, i.e. unless $p(\cdot)$ is decreasing.*

Proof.

Let us assume that they are comparable. By condition *1.* in Theorem 4, it must be $p(\cdot) \leq p_*(\cdot)$ or $p(\cdot) \geq p_*(\cdot)$. If the first option holds and the second one does

not, it would exist a set E, $|E|>0$, where $p(\cdot)<p_*(\cdot)$. As a consequence, since $p(\cdot)\le p_*(\cdot)$, it must be $\|p(\cdot)\|_{L^1(0,1)}<\|p_*(\cdot)\|_{L^1(0,1)}$, which is absurd because by Theorem 7 the space $L^1(0,1)$ is rearrangement-invariant. In the other case we can argue similarly, and the conclusion is that both options are true, hence $p(\cdot)=p_*(\cdot)$. □

As in the previous result, next one (see Theorem 3 in Rakotoson and the author [65]) involves, for a function f, the notion of decreasing rearrangement (denoted by f_*). Denoting by f^* the increasing rearrangement of f, all the norms in next chain of inequalities (16) coincide in the case of constant exponents:

Proposition 3. *If $\Omega\subset\mathbf{R}^n$, $p(\cdot):\Omega\to[1,\infty[$ and $f\ge 0$ in Ω, then*

$$\frac{1}{2(1+|\Omega|)}\|f_*\|_{L^{p^*(\cdot)}}\le\|f\|_{L^{p(\cdot)}}\le 2(1+|\Omega|)\|f_*\|_{L^{p*(\cdot)}}\,. \tag{16}$$

Other results involving rearrangement of exponents are in Rakotoson, Sbordone and the author [66].

The crucial notion of the last result (see Krbec and the author [62]) is the exponential summability: a function g measurable on $\Omega\subset\mathbf{R}^n$, $|\Omega|<\infty$, is said to belong to the Orlicz space $EXP_a(\Omega)$, $a>0$, if for some $\lambda>0$

$$\int_\Omega \exp\left(\lambda|g(x)|^a\right)dx<\infty\,.$$

Theorem 9. *Let $\Omega\subset\mathbf{R}^n$ be bounded and $p(\cdot)\in EXP_a(\Omega)$ for some $a>0$. If $f\in L^{p(\cdot)}(\Omega)$, $f\not\equiv 0$, then $p(\cdot)\log(Mf)\in EXP_{a/(a+1)}(\Omega)$.*

It is clear that if $p(\cdot)$ is constant and finite, it is in particular in $L^\infty(\Omega)$ which is contained in every $EXP_a(\Omega)$, $a>0$. In this case Theorem 9 tells that if $f\in L^p(\Omega)$, $f\not\equiv 0$, then $\log(Mf)\in EXP_{a/(a+1)}(\Omega)$, for every $a>0$. Note that $a/(a+1)<1$, hence the result is weaker than $\log(Mf)\in EXP_1(\Omega)$, which is true because, since Ω is bounded, Mf is bounded below by a positive number, and therefore by Theorem 1

$$\int_\Omega \exp\left(p|\log(Mf)|\right)dx<\infty\,.$$

The weakness of the thesis is readily explained: it is the "price" to pay because of the assumption $p(\cdot)\in EXP_a(\Omega)$, which includes a class of non-constant exponents (in fact, not bounded ones).

We close this Section pointing out that there exist essentially variable results which in the case of constant exponents have interest and meaning, but phenomena are new, the novelty being due exactly to the variability of the exponent. This happens for instance in Mercaldo, Rossi, Segura de León and Trombetti [94], where the authors consider an exponent having just two values, one of them being 1, in a Dirichlet problem involving the $p(x)-$laplacian.

5 - CONCLUSION AND NEW PERSPECTIVES

The categories of results in variable Lebesgue spaces theory presented in this Note could never pretend to be complete or rigorous. Moreover, even if nowadays the field is still very active, recently some new directions of research are becoming of interest among researchers. Just to quote a few of them, the interest in Musielak-Orlicz spaces is actually increasing, especially for their applications, because they are also the natural framework to generalize the conditions coming from variable Lebesgue spaces theory (see e.g. Ahmida, Chlebicka, Gwiazda and Youssfi [4], Baruah, Harjulehto, and Hästö [14], Cruz-Uribe and Hästö [32], Harjulehto and Hästö [68], Hästö[51, 52]); some special Musielak-Orlicz spaces, which are also generalizations of variable Lebesgue spaces, are generated by the functions $\Phi(x,t) = t^p + a(x)t^q$, $p < q$, which give raise to the double phase functional (see e.g. Baroni, Colombo and Mingione [12, 13], Colombo and Mingione [23]); there exist a huge development of variable variants of classical function spaces, for instance the Lorentz spaces with variable exponents (see Kempka and Vybíral [74]), grand variable Lebesgue spaces and their weighted version (see e.g. Kokilashvili, Meskhi and the author [63] and references therein) or the variable exponent Besov and Triebel-Lizorkin spaces (see e.g. Almeida, Diening and Hästö [5]).

Finally, let us mention that in principle, there are even papers where variable exponents appear, but the topic has no connections at all with variable Lebesgue spaces: for instance, in Anatriello, Chill and the author [8] (see also references therein), the norm $\|\cdot\|_{L^{p(x)}}$ which, for a given x, is a norm in the classical Lebesgue spaces, is considered. In Anatriello, Vincenzi and the author [9], starting from a variable exponent which is a simple function (i.e. with a finite number of values), the function spaces themselves "vary", and norms on product of quasinormed spaces which are roots of polynomials are considered.

Acknowledgment: The author thanks David Cruz-Uribe for the discussions about the proof of Theorem 7.

6 - REFERENCES

[1] E. Acerbi and G. Mingione. Regularity results for electrorheological fluids: the stationary case. *C. R. Math. Acad. Sci. Paris*, 334(9):817–822, 2002.

[2] E. Acerbi and G. Mingione. Regularity results for stationary electro-rheological fluids. *Arch. Ration. Mech. Anal.*, 164(3):213–259, 2002.

[3] E. Acerbi and G. Mingione. Gradient estimates for the $p(x)$-Laplacean system. *J. Reine Angew. Math.*, 584:117–148, 2005.

[4] Y. Ahmida, I. Chlebicka, P. Gwiazda, and A. Youssfi. Gossez's approximation theorems in Musielak-Orlicz-Sobolev spaces. *J. Funct. Anal.*, 275(9):2538–2571, 2018.

[5] A. Almeida, L. Diening, and P. Hästö. Homogeneous variable exponent Besov and Triebel-Lizorkin spaces. *Math. Nachr.*, 291(8-9):1177–1190, 2018.

[6] B. Amaziane, L. Pankratov, and A. Piatnitski. Nonlinear flow through double porosity media in variable exponent Sobolev spaces. *Nonlinear Anal. Real World Appl.*, 10(4):2521–2530, 2009.

[7] L. Ambrosio, N. Fusco, and D. Pallara. *Functions of bounded variation and free discontinuity problems*. Oxford Mathematical Monographs. The Clarendon Press, Oxford University Press, New York, 2000.

[8] G. Anatriello, R. Chill, and A. Fiorenza. Identification of fully measurable grand Lebesgue spaces. *J. Funct. Spaces*, pages 3, Art. ID 3129186, 2017.

[9] G. Anatriello, A. Fiorenza, and G. Vincenzi. Banach function norms via Cauchy polynomials and applications. *Internat. J. Math.*, 26(10), pages 20, 1550083, 2015.

[10] S. N. Antontsev and S. I. Shmarev. *Evolution PDEs with nonstandard growth conditions*, volume 4 of *Atlantis Studies in Differential Equations*. Existence, uniqueness, localization, blow-up. Atlantis Press, Paris, 2015.

[11] S. N. Antontsev and S. I. Shmarev. A model porous medium equation with variable exponent of nonlinearity: existence, uniqueness and localization properties of solutions. *Nonlinear Anal.*, 60(3):515–545, 2005.

[12] P. Baroni, M. Colombo, and G. Mingione. Nonautonomous functionals, borderline cases and related function classes. *Algebra i Analiz*, 27(3):6–50, 2015.

[13] P. Baroni, M. Colombo, and G. Mingione. Harnack inequalities for double phase functionals. *Nonlinear Anal.*, 121:206–222, 2015.

[14] D. Baruah, P. Harjulehto, and P. Hästö. Capacities in generalized Orlicz spaces. *J. Funct. Spaces*, pages 10, Art. ID 8459874, 2018.

[15] C. Bennett and R. Sharpley. *Interpolation of Operators*, volume 129 of *Pure and Applied Mathematics*. Academic Press Inc., Boston, MA, 1988.

[16] Z. W. Birnbaum and W. Orlicz. Über die Verallgemeinerung des Begriffes der zueinander konjugierten Potenzen. *Stud. Math.*, 3:1–67, 1931.

[17] P. Blomgren, T. Chan, P. Mulet, and C. K. Wong. Total variation image restoration: numerical methods and extensions. In *Proceedings of the 1997 IEEE International Conference on Image Processing*, volume III, pages 384–387, 1997.

[18] H. Brezis. *Analyse fonctionnelle*. Collection Mathématiques Appliquées pour la Maîtrise. [Collection of Applied Mathematics for the Master's Degree]. Masson, Paris, 1983. Théorie et applications. [Theory and applications].

[19] H. Brezis. *Functional analysis, Sobolev spaces and partial differential equations*. Universitext. Springer, New York, 2011.

[20] C. Capone, D. Cruz-Uribe, and A. Fiorenza. The fractional maximal operator and fractional integrals on variable L^p spaces. *Rev. Mat. Iberoam.*, 23(3):743–770, 2007.

[21] R. E. Castillo and H. Rafeiro. *An introductory course in Lebesgue spaces*. CMS Books in Mathematics/Ouvrages de Mathématiques de la SMC. Springer, [Cham], 2016.

[22] B. Çekiç, A. V. Kalinin, R. A. Mashiyev, and M. Avci. $l^{p(x)}(\omega$-estimates for vector fields and some applications to magnetostatics problems. *J. Math. Anal. Appl.*, 389(2):838–851, 2012.

[23] M. Colombo and G. Mingione. Bounded minimisers of double phase variational integrals. *Arch. Ration. Mech. Anal.*, 218(1):219–273, 2015.

[24] D. Cruz-Uribe, L. Diening, and A. Fiorenza. A new proof of the boundedness of maximal operators on variable Lebesgue spaces. *Boll. Unione Mat. Ital. (9)*, 2(1):151–173, 2009.

[25] D. Cruz-Uribe, G. Di Fratta, and A. Fiorenza. Modular inequalities for the maximal operator in variable Lebesgue spaces. *Nonlinear Anal.*, 177(part A):299–311, 2018.

[26] D. Cruz-Uribe and A. Fiorenza. Approximate identities in variable L^p spaces. *Math. Nachr.*, 280(3):256–270, 2007.

[27] D. V. Cruz-Uribe and A. Fiorenza. *Variable Lebesgue spaces*. Applied and Numerical Harmonic Analysis. Birkhäuser/Springer, Heidelberg, 2013. Foundations and harmonic analysis.

[28] D. Cruz-Uribe, A. Fiorenza, J. M. Martell, and C. Pérez. The boundedness of classical operators on variable L^p spaces. *Ann. Acad. Sci. Fenn. Math.*, 31(1):239–264, 2006.

[29] D. Cruz-Uribe, A. Fiorenza, and C. J. Neugebauer. The maximal function on variable L^p spaces. *Ann. Acad. Sci. Fenn. Math.*, 28(1):223–238, 2003. See also errata [30].

[30] D. Cruz-Uribe, A. Fiorenza, and C. J. Neugebauer. Corrections to: "The maximal function on variable L^p spaces" [Ann. Acad. Sci. Fenn. Math. **28** (2003), no. 1, 223–238;]. *Ann. Acad. Sci. Fenn. Math.*, 29(1):247–249, 2004.

[31] D. V. Cruz-Uribe, A. Fiorenza, M. Ruzhansky, and J. Wirth. *Variable Lebesgue spaces and hyperbolic systems*. Advanced Courses in Mathematics. CRM Barcelona. Birkhäuser/Springer, Basel, 2014. Selected lecture notes from the Advanced Courses on Approximation Theory and Fourier Analysis held at the Centre de Recerca Matemàtica, Barcelona, November 7–11, 2011, Edited by Sergey Tikhonov.

[32] D. Cruz-Uribe and P. Hästö. Extrapolation and interpolation in generalized Orlicz spaces. *Trans. Amer. Math. Soc.*, 370(6):4323–4349, 2018.

[33] D. Cruz-Uribe, J. M. Martell, and C. Pérez. *Weights, extrapolation and the theory of Rubio de Francia*, volume 215 of *Operator Theory: Advances and Applications*. Birkhäuser/Springer, [Cham], 2011.

[34] A. M. D'Aristotile and A. Fiorenza. A topology on inequalities. *Electron. J. Differential Equations*, pages 22, No. 85, 2006.

[35] E. DiBenedetto. *Real analysis*. Birkhäuser Advanced Texts: Basler Lehrbücher. [Birkhäuser Advanced Texts: Basel Textbooks]. Birkhäuser Boston, Inc., Boston, MA, 2002.

[36] L. Diening. Maximal function on generalized Lebesgue spaces $L^{p(\cdot)}$. *Math. Inequal. Appl.*, 7(2):245–253, 2004.

[37] L. Diening. Maximal function on Musielak-Orlicz spaces and generalized Lebesgue spaces. *Bull. Sci. Math.*, 129(8):657–700, 2005.

[38] L. Diening. *Lebesgue and Sobolev Spaces with Variable Exponent*. Habilitation, Universität Freiburg, 2007.

[39] L. Diening, P. Harjulehto, P. Hästö, and M. Růžička. *Lebesgue and Sobolev spaces with variable exponents*, volume 2017 of *Lecture Notes in Mathematics*. Springer, Heidelberg, 2011.

[40] L. Diening and M. Ružička. Calderón-Zygmund operators on generalized Lebesgue spaces $L^{p(\cdot)}$ and problems related to fluid dynamics. *J. Reine Angew. Math.*, 563:197–220, 2003.

[41] L. Diening and M. Ružička. Integral operators on the halfspace in generalized Lebesgue spaces $L^{p(\cdot)}$. I. *J. Math. Anal. Appl.*, 298(2):559–571, 2004.

[42] L. Diening and M. Ružička. Integral operators on the halfspace in generalized Lebesgue spaces $L^{p(\cdot)}$. II. *J. Math. Anal. Appl.*, 298(2):572–588, 2004.

[43] L. Diening and M. Ružička. Non-Newtonian fluids and function spaces. In *NAFSA 8—Nonlinear analysis, function spaces and applications. Vol. 8*, pages 94–143. Czech. Acad. Sci., Prague, 2007.

[44] L. Diening, P. Harjulehto, P. Hästö, Y. Mizuta, and T. Shimomura. Maximal functions in variable exponent spaces: limiting cases of the exponent. *Ann. Acad. Sci. Fenn. Math.*, 34(2):503–522, 2009.

[45] J. Duoandikoetxea. *Fourier Analysis*, volume 29 of *Graduate Studies in Mathematics*. American Mathematical Society, Providence, RI, 2001. Translated and revised from the 1995 Spanish original by David Cruz-Uribe.

[46] D. E. Edmunds, J. Lang, and O. Méndez. *Differential operators on spaces of variable integrability*. World Scientific Publishing Co. Pte. Ltd., Hackensack, NJ, 2014.

[47] D. E. Edmunds, J. Lang, and A. Nekvinda. On $L^{p(x)}$ norms. *R. Soc. Lond. Proc. Ser. A Math. Phys. Eng. Sci.*, 455(1981):219–225, 1999.

[48] D. E. Edmunds and A. Meskhi. Potential-type operators in $L^{p(x)}$ spaces. *Z. Anal. Anwendungen*, 21(3):681–690, 2002.

[49] D. E. Edmunds and J. Rákosník. Density of smooth functions in $W^{k,p(x)}(\Omega)$. *Proc. Roy. Soc. London Ser. A*, 437(1899):229–236, 1992.

[50] A. El Hamidi. Existence results to elliptic systems with nonstandard growth conditions. *J. Math. Anal. Appl.*, 300(1):30–42, 2004.

[51] P. Hästö. The maximal operator on generalized Orlicz spaces. *J. Funct. Anal.*, 269(12):4038–4048, 2015. See also corrigendum [52].

[52] P. Hästö. Corrigendum to "The maximal operator on generalized Orlicz spaces" [J. Funct. Anal. 269 (2015) 4038–4048]. *J. Funct. Anal.*, 271(1):240–243, 2016.

[53] K. J. Falconer. *The geometry of fractal sets*, volume 85 of *Cambridge Tracts in Mathematics*. Cambridge University Press, Cambridge, 1986.

[54] X. Fan. The regularity of Lagrangians $f(x,\xi) = |\xi|^{\alpha(x)}$ with Hölder exponents $\alpha(x)$. *Acta Math. Sinica (N.S.)*, 12(3):254–261, 1996. A Chinese summary appears in Acta Math. Sinica **4**0 (1997), no. 1, 158.

[55] X. Fan. Regularity of nonstandard Lagrangians $f(x,\xi)$. *Nonlinear Anal.*, 27(6):669–678, 1996.

[56] X. Fan. $p(x)$-Laplacian equations. In *Topological methods, variational methods and their applications (Taiyuan, 2002)*, pages 117–123. World Sci. Publ., River Edge, NJ, 2003.

[57] X. Fan, S. Wang, and D. Zhao. Density of $C^\infty(\Omega)$ in $W^{1,p(x)}(\Omega)$ with discontinuous exponent $p(x)$. *Math. Nachr.*, 279(1-2):142–149, 2006.

[58] X. Fan and D. Zhao. Regularity of minimizers of variational integrals with continuous $p(x)$-growth conditions. *Chinese J. Contemp. Math.*, 17(4):327–336, 1996.

[59] X. Fan and D. Zhao. Regularity of minimum points of variational integrals with continuous $p(x)$-growth conditions. *Chinese Ann. Math. Ser. A*, 17(5):557–564, 1996.

[60] R. Ferreira, P. Hästö, and A. M. Ribeiro. Characterization of generalized Orlicz spaces. *arXiv e-prints*, arXiv:1612.04566, December 2016.

[61] A. Fiorenza. A mean continuity type result for certain Sobolev spaces with variable exponent. *Commun. Contemp. Math.*, 4(3):587–605, 2002.

[62] A. Fiorenza. A local estimate for the maximal function in Lebesgue spaces with EXP-type exponents. *J. Funct. Spaces*, pages 5, Art. ID 581064, 2015.

[63] A. Fiorenza, V. Kokilashvili, and A. Meskhi. Hardy-Littlewood maximal operator in weighted grand variable exponent Lebesgue space. *Mediterr. J. Math.*, 14(3), pages 20, Art. 118, 2017.

[64] A. Fiorenza and M. Krbec. A note on noneffective weights in variable Lebesgue spaces. *J. Funct. Spaces Appl.*, pages 5, Art. ID 853232, 2012.

[65] A. Fiorenza and J. M. Rakotoson. Relative rearrangement and Lebesgue spaces $L^{p(\cdot)}$ with variable exponent. *J. Math. Pures Appl. (9)*, 88(6):506–521, 2007.

[66] A. Fiorenza, J. M. Rakotoson, and C. Sbordone. Variable exponents and grand Lebesgue spaces: some optimal results. *Commun. Contemp. Math.*, 17(6):1550023, 14, 2015.

[67] F. Giannetti. The modular interpolation inequality in Sobolev spaces with variable exponent attaining the value 1. *Math. Inequal. Appl.*, 14(3):509–522, 2011.

[68] P. Harjulehto and P. Hästö. Orlicz spaces and generalized Orlicz spaces. 2018.

[69] P. Harjulehto, P. Hästö, Ú. V. Lê, and M. Nuortio. Overview of differential equations with non-standard growth. *Nonlinear Anal.*, 72(12):4551–4574, 2010.

[70] P. Hästö. On the density of continuous functions in variable exponent Sobolev space. *Rev. Mat. Iberoam.*, 23(1):213–234, 2007.

[71] P. Hästö and A. M. Ribeiro. Characterization of the variable exponent Sobolev norm without derivatives. *Commun. Contemp. Math.*, 19(3):1650022, 13, 2017.

[72] M. Izuki, E. Nakai, and Y. Sawano. Function spaces with variable exponents—an introduction—. *Sci. Math. Jpn.*, 77(2):187–315, 2014.

[73] B. Kawohl. *Rearrangements and convexity of level sets in PDE*, volume 1150 of *Lecture Notes in Mathematics*. Springer-Verlag, Berlin, 1985.

[74] H. Kempka and J. Vybíral. Lorentz spaces with variable exponents. *Math. Nachr.*, 287(8-9):938–954, 2014.

[75] V. Kokilashvili and M. Krbec. *Weighted Inequalities in Lorentz and Orlicz Spaces*. World Scientific Publishing Co. Inc., River Edge, NJ, 1991.

[76] V. Kokilashvili, A. Meskhi, H. Rafeiro, and S. Samko. *Integral operators in non-standard function spaces. Vol. 1*, volume 248 of *Operator Theory: Advances and Applications*. Variable exponent Lebesgue and amalgam spaces. Birkhäuser/Springer, [Cham], 2016.

[77] V. Kokilashvili, A. Meskhi, H. Rafeiro, and S. Samko. *Integral operators in non-standard function spaces. Vol. 2*, volume 249 of *Operator Theory: Advances and Applications*. Variable exponent Hölder, Morrey-Campanato and grand spaces. Birkhäuser/Springer, [Cham], 2016.

[78] A. N. Kolmogorov. Zur Normierbarkeit eines allgemeinen topologischen linearen Räumes. *Studia Math.*, 5:29–33, 1934.

[79] T. Kopaliani. On the Muckenchaupt condition in variable Lebesgue spaces. *Proc. A. Razmadze Math. Inst.*, 148:29–33, 2008.

[80] T. Kopaliani and G. Chelidze. Gagliardo-Nirenberg type inequality for variable exponent Lebesgue spaces. *J. Math. Anal. Appl.*, 356(1):232–236, 2009.

[81] A. Korenovskii. *Mean oscillations and equimeasurable rearrangements of functions*, volume 4 of *Lecture Notes of the Unione Matematica Italiana*. Springer, Berlin; UMI, Bologna, 2007.

[82] T. Kostopoulos and N. Yannakakis. Density of smooth functions in variable exponent Sobolev spaces. *Nonlinear Anal.*, 127:196–205, 2015.

[83] O. Kováčik and J. Rákosník. On spaces $L^{p(x)}$ and $W^{k,p(x)}$. *Czechoslovak Math. J.*, 41(116)(4):592–618, 1991.

[84] M. A. Krasnosel′skiĭ and Ja. B. Rutickiĭ. *Convex Functions and Orlicz Spaces*. Translated from the first Russian edition by Leo F. Boron. P. Noordhoff Ltd., Groningen, 1961.

[85] J. Lang and D. Edmunds. *Eigenvalues, embeddings and generalised trigonometric functions*, volume 2016 of *Lecture Notes in Mathematics*. Springer, Heidelberg, 2011.

[86] G. Leoni. *A first course in Sobolev spaces*, volume 181 of *Graduate Studies in Mathematics*. American Mathematical Society, Providence, RI, second edition, 2017.

[87] A. K. Lerner. On modular inequalities in variable L^p spaces. *Arch. Math. (Basel)*, 85(6):538–543, 2005.

[88] A. K. Lerner. On some questions related to the maximal operator on variable L^p spaces. *Trans. Amer. Math. Soc.*, 362(8):4229–4242, 2010.

[89] A. K. Lerner and C. Pérez. A new characterization of the Muckenhoupt A_p weights through an extension of the Lorentz-Shimogaki theorem. *Indiana Univ. Math. J.*, 56(6):2697–2722, 2007.

[90] E. H. Lieb and M. Loss. *Analysis*, volume 14 of *Graduate Studies in Mathematics*. American Mathematical Society, Providence, RI, second edition, 2001.

[91] L. Maligranda. *Orlicz spaces and interpolation*, volume 5 of *Seminários de Matemática [Seminars in Mathematics]*. Universidade Estadual de Campinas, Departamento de Matemática, Campinas, 1989.

[92] P. Marcellini. Regularity and existence of solutions of elliptic equations with p,q-growth conditions. *J. Differential Equations*, 90(1):1–30, 1991.

[93] P. Marcellini. Regularity for elliptic equations with general growth conditions. *J. Differential Equations*, 105(2):296–333, 1993.

[94] A. Mercaldo, J. D. Rossi, S. Segura de León, and C. Trombetti. On the behaviour of solutions to the Dirichlet problem for the $p(x)$-Laplacian when $p(x)$ goes to 1 in a subdomain. *Differential Integral Equations*, 25(1-2):53–74, 2012.

[95] A. Meskhi. *Measure of non-compactness for integral operators in weighted Lebesgue spaces*. Nova Science Publishers, Inc., New York, 2009.

[96] G. Mingione. Regularity of minima: an invitation to the dark side of the calculus of variations. *Appl. Math.*, 51(4):355–426, 2006.

[97] J. Musielak. *Orlicz Spaces and Modular Spaces*, volume 1034 of *Lecture Notes in Mathematics*. Springer-Verlag, Berlin, 1983.

[98] H. Nakano. *Modulared Semi-Ordered Linear Spaces*. Maruzen Co. Ltd., Tokyo, 1950.

[99] H. Nakano. *Topology and Linear Topological Spaces*. Maruzen Co. Ltd., Tokyo, 1951.

[100] A. Nekvinda. Hardy-Littlewood maximal operator on $L^{p(x)}(R^n)$. *Math. Inequal. Appl.*, 7(2):255–265, 2004.

[101] A. Nekvinda. Maximal operator on variable Lebesgue spaces for almost monotone radial exponent. *J. Math. Anal. Appl.*, 337(2):1345–1365, 2008.

[102] G. O. Okikiolu. *Aspects of the Theory of Bounded Integral Operators in L^p-Spaces*. Academic Press, London - New York, 1971.

[103] W. Orlicz. Über konjugierte Exponentenfolgen. *Stud. Math.*, 3:200–211, 1931.

[104] L. Pick, A. Kufner, O. John, and S. Fučík. *Function spaces. Vol. 1*, volume 14 of *De Gruyter Series in Nonlinear Analysis and Applications*. Walter de Gruyter & Co., Berlin, extended edition, 2013.

[105] L. Pick and M. Růžička. An example of a space $L^{p(x)}$ on which the Hardy-Littlewood maximal operator is not bounded. *Expo. Math.*, 19(4):369–371, 2001.

[106] V. D. Rădulescu and D. D. Repovš. *Partial differential equations with variable exponents*. Variational methods and qualitative analysis. Monographs and Research Notes in Mathematics. CRC Press, Boca Raton, FL, 2015.

[107] J. M. Rakotoson. *Réarrangement Relatif*, volume 64 of *Mathématiques & Applications (Berlin) [Mathematics & Applications]*. Springer, Berlin, 2008.

[108] M. M. Rao and Z. D. Ren. *Theory of Orlicz spaces*, volume 146 of *Monographs and Textbooks in Pure and Applied Mathematics*. Marcel Dekker, Inc., New York, 1991.

[109] B. Ross and S. Samko. Fractional integration operator of variable order in the Hölder spaces $H^{\lambda(x)}$. *Internat. J. Math. Math. Sci.*, 18(4):777–788, 1995.

[110] W. Rudin. *Real and Complex Analysis*. McGraw-Hill Book Co., New York, third edition, 1987.

[111] M. Růžička. *Electrorheological fluids: modeling and mathematical theory*, volume 1748 of *Lecture Notes in Mathematics*. Springer-Verlag, Berlin, 2000.

[112] M. Růžička. Modeling, mathematical and numerical analysis of electrorheological fluids. *Appl. Math.*, 49(6):565–609, 2004.

[113] S. Samko. Fractional integration and differentiation of variable order. *Anal. Math.*, 21(3):213–236, 1995.

[114] S. Samko. Convolution and potential type operators in $L^{p(x)}(\mathbf{R}^n)$. *Integral Transform. Spec. Funct.*, 7(3-4):261–284, 1998.

[115] S. Samko. Convolution type operators in $L^{p(x)}$. *Integral Transform. Spec. Funct.*, 7(1-2):123–144, 1998.

[116] S. Samko. Differentiation and integration of variable order and the spaces $L^{p(x)}$. In *Operator theory for complex and hypercomplex analysis (Mexico City, 1994)*, volume 212 of *Contemp. Math.*, pages 203–219. Amer. Math. Soc., Providence, RI, 1998.

[117] S. Samko. Denseness of $C_0^\infty(\mathbf{R}^N)$ in the generalized Sobolev spaces $W^{M,P(X)}(\mathbf{R}^N)$. In *Direct and inverse problems of mathematical physics (Newark, DE, 1997)*, volume 5 of *Int. Soc. Anal. Appl. Comput.*, pages 333–342. Kluwer Acad. Publ., Dordrecht, 2000.

[118] S. Samko and B. Ross. Integration and differentiation to a variable fractional order. *Integral Transform. Spec. Funct.*, 1(4):277–300, 1993.

[119] I. I. Sharapudinov. The topology of the space $\mathcal{L}^{p(t)}([0,1])$. *Mat. Zametki*, 26(4):613–632, 655, 1979.

[120] I. I. Sharapudinov. The basis property of the Haar system in the space $\mathcal{L}^{p(t)}([0,1])$ and the principle of localization in the mean. *Mat. Sb. (N.S.)*, 130(172)(2):275–283, 286, 1986.

[121] E. M. Stein. *Singular integrals and differentiability properties of functions*. Princeton Mathematical Series, No. 30. Princeton University Press, Princeton, N.J., 1970.

[122] E. M. Stein. *Harmonic analysis: real-variable methods, orthogonality, and oscillatory integrals*, volume 43 of *Princeton Mathematical Series*. With the assistance of Timothy S. Murphy, Monographs in Harmonic Analysis, III. Princeton University Press, Princeton, NJ, 1993.

[123] I. V. Tsenov. Generalization of the problem of best approximation of a function in the space L^s. *Uch. Zap. Dagestan. Gos. Univ.*, 7:25–37, 1961.

[124] V. V. Zhikov. Problems of convergence, duality, and averaging for a class of functionals of the calculus of variations. *Dokl. Akad. Nauk SSSR*, 267(3):524–528, 1982.

[125] V. V. Zhikov. Meyer-type estimates for solving the nonlinear Stokes system. *Differ. Uravn.*, 33(1):107–114, 143, 1997.

[126] V. V. Zhikov. On some variational problems. *Russian J. Math. Phys.*, 5(1):105–116 (1998), 1997.

[127] V. V. Zhikov. On the density of smooth functions in Sobolev-Orlicz spaces. *Zap. Nauchn. Sem. S.-Peterburg. Otdel. Mat. Inst. Steklov. (POMI)*, 310(Kraev. Zadachi Mat. Fiz. i Smezh. Vopr. Teor. Funkts. 35 [34]):67–81, 226, 2004.

[128] W. P. Ziemer. *Weakly Differentiable Functions*, volume 120 of *Graduate Texts in Mathematics*. Springer-Verlag, New York, 1989.

Rend. Acc. Sc. fis. mat. Napoli
Vol. LXXXVI, (2019) pp. 103-121

DOI 10.32092/1020

Free boundary minimal surfaces: a survey of recent results

Nota di Alessandro Carlotto [1]

Presentata dal socio Luciano Carbone
(Adunanza del 15 febbraio 2019)

Key words: free boundary minimal surfaces, Steklov eigenvalues, Morse index, effective estimates.

Abstract – We present a wide-spectrum overview of some recent developments in the theory of free boundary minimal surfaces, with special emphasis on the problem of compactness under mild curvature conditions on the ambient manifold.

Riassunto – Presentiamo un ampio resoconto di alcuni sviluppi recenti nella teoria delle superfici minime a frontiera libera, con particolare riferimento al problema della compattezza sotto deboli ipotesi sulla curvatura sulla varietà ambiente.

1 - INTRODUCTION

Let Σ be a smooth manifold of dimension $k \geq 2$, let (X, g) be a smooth Riemannian manifold of dimension $d \geq 3$, and let $\varphi : \Sigma \to X$ be a proper immersion satisfying $\varphi(\Sigma) \cap \partial X = \varphi(\partial\Sigma)$ (i. e. the boundary of Σ is contained in the boundary of X, and there is no interior point of $\varphi(\Sigma)$ touching ∂X): we say that $\varphi : \Sigma \to X$ is a free boundary minimal immersion if it is a critical point for the k-dimensional area functional in the category of relative cycles, namely under all compactly supported variations (φ_t) subject to the constraint that $\varphi_t(\partial\Sigma) \subset \partial X$. Considering the first-variation formula it is easily seen that this happens if and only if $\varphi(\Sigma)$ has zero mean curvature and meets the ambient boundary orthogonally. We shall mostly be interested in the case when the map φ is an embedding, in which case we shall be talking about free boundary minimal submanifolds, and (with some abuse of language) identify the map in question with its image $\varphi(\Sigma)$.

Besides the self-evident geometric significance, which can be traced back at least to Courant [23, 24], free boundary minimal hypersurfaces also naturally arise in partitioning problems for convex bodies, in capillarity problems for fluids and, as has significantly emerged in recent years, in connection to extremal

[1] ETH - Department of Mathematics, Rämistrasse 101, 8092 Zürich, Switzerland; Institute for Advanced Study, 1 Einstein drive, 08540 Princeton, United States of America. e-mail: alessandro.carlotto@math.ethz.ch, alessandro.carlotto@ias.edu.

metrics for Steklov eigenvalues for manifolds with boundary (see primarily the works by Fraser-Schoen [33, 34, 36] and references therein).

A good point to start our discussion is provided by the unit ball in $\mathbb{R}^3$: in this case we have, modulo isometries, two simple examples of free boundary minimal surfaces. On the one hand, we have flat disks passing through the origin, while on the other we have the so-called *critical catenoids*, which are defined as the only catenoids centered at the origin and meeting the unit sphere orthogonally. Going beyond these classical examples, and producing free boundary minimal surfaces of topological type different from that of the disk or the annulus turns out to be a rather delicate task, that was only accomplished in recent years. In that respect, we mention the work by Fraser and Schoen [36] (genus zero and any number of boundary components), by Folha, Pacard and Zolotareva [29] (genus zero or one and any sufficiently large number of boundary components), by Ketover [50] and Kapouleas and Li [43] (arbitrarily large genus and three boundary components) and by Kapouleas and Wiygul [44] (arbitrarily large genus and one boundary component). In higher dimension, namely for $B^n \subset \mathbb{R}^{n+1}$ with $n \geq 4$, infinite families of examples have been found, via equivariant methods, by Freidin, Gulian and McGrath [37].

For general Riemannian manifolds, possibly subject to additional curvature conditions, in addition to older works mostly appealing to the parametric approach (cf. [23, 24, 30, 38, 47–49, 76, 78] and references therein) we have witnessed the implementation, for relative cyles, of powerful constructions like the min-max à la Almgren-Pitts or the degree-theoretic approach à la White: in that respect one should mention the work by Li [51], Li-Zhou [52], De Lellis-Ramic [25] and Maximo-Nunes-Smith [61]. In fact, there is good reason to believe that the min-max theory by Marques and Neves (see in part. [45,54,56,58,60]) should be pushed to the same impressive summits that have been achieved in the closed case, so to lead to a Weyl law for the (free boundary) volume spectrum, and to general density and equidistribution results.

Motivated by this variety of existence results, one is naturally lead to investigate some fundamental geometric questions which have to do with (what might be called) *the ensemble of free boundary minimal surfaces* inside a given Riemannian manifold (X, g):

1. When (X, g) is a space form, can one classify all free boundary minimal immersions having a pre-assigned topological type (namely: for fixed Σ)?

2. Under what curvature conditions (X, g) is the class of its free boundary minimal embeddings having a pre-assigned topological type *compact* in the sense of smooth, graphical one-sheeted convergence?

3. Are there universal bounds, only depending on the ambient manifold, relating the topological invariants of any free boundary minimal surface to its geometric data like e. g. area, spectral invariants, Morse index?

Each of these questions is already highly meaningful in the aforementioned special case of the unit ball in $\mathbb{R}^3$. To fix the ideas, one could ask, for instance,

whether (1)' the flat (equatiorial) disks are, in fact, the only contractible free boundary minimal surfaces in B^3, whether (2)' the space of free boundary minimal surfaces of genus five and three boundary components is strongly compact in the sense above, and whether (3)' the Morse index of any free boundary minimal surface is bounded from above and/or below by a linear function of its relative first Betti number.

The scope of this article is to describe various recent results related to the three questions above (and ramifications thereof), informally present some key ideas that come up in the corresponding proofs, and suggest a few related open problems.

Acknowledgements: This survey was written on the occasion of the conferral to its author of the *Riccardo De Arcangelis* prize in Mathematical Analysis by the *Accademia di Scienze Fisiche e Matematiche* of the *Società Nazionale di Scienze, Lettere ed Arti in Napoli*. The author is partly supported by the National Science Foundation (through grant DMS 1638352) and by the Giorgio and Elena Petronio Fellowship Fund.

2 - TOPOLOGICAL UNIQUENESS RESULTS

The first general problem we wish to discuss has to do with classifying special geometric objects: when (X, g) is a simple model space, like e. g. the unit ball B^3 or the hemisphere S^3_+ can we produce a complete list of all free boundary minimal immersions of fixed topological type? Besides the 'cheap' results one can obtain, in very special cases, via reflection methods (hence by reduction to the complete, or to the compact case), this question turns out to be very subtle. The first significant result, addressing the most basic of all such problems, was obtained by J. Nitsche [64] relying on a Hopf differential argument:

Theorem 1. *The only free boundary minimal immersions of a disk in the Euclidean unit ball are totally geodesic.*

The proof of this statement clearly resembles the one proposed by Almgren in 1966 [3] in the closed setting, in order to prove that the only minimally immersed two-spheres in the round three-sphere must be equatorial. This correspondence, i. e. the parallel between the theory of closed minimal surfaces in round S^3 and of free boundary minimal surfaces in B^3, turns out to be extremely rich, and surprisingly inspirational in the development of the subject. Within this framework, a fundamental conjecture was proposed in 2014 by Fraser and Li [32], to be thought in analogy with the theorem by Brendle [10] classifying the Clifford torus as the only minimally embedded torus in the sphere (as predicted by Lawson in 1970).

Conjecture 2. *The only free boundary minimal embeddings of an annulus in the Euclidean unit ball are, modulo isometries, reparametrizations of the critical catenoid.*

This result has very recently been claimed by Nadirashvili and Penskoi [63], and is currently under scrutiny. Although there are some serious concerns about the correctness of the proposed argument, it is interesting to remark that the authors show how confirming this conjecture would allow to prove a classification result for overdetermined elliptic boundary value problems on spherical domains, namely to determine all couples (Ω, v) for $\Omega \subset S^2$ a smooth simply-connected domain and v a smooth function solving a problem of the form

$$\begin{cases} \Delta v = -\lambda v & \text{in } \Omega, \\ v = \alpha & \text{on } \partial\Omega, \\ |\nabla v| = \beta & \text{on } \partial\Omega \end{cases}$$

for constants $\lambda, \alpha, \beta \in \mathbb{R}$. A similar result for scaling-invariant domains in $\mathbb{R}^3$ and degree one homogeneous functions, related to earlier work by Caffarelli, Jerison and Kenig [12], would also follow.

A different task concerns, instead, the generalization of Nitsche's theorem to higher dimension and/or codimension. If we stick to $k = 2$ (notation as in the Introduction) but allow for any $d \geq 3$, the question has been very satisfactorily addressed in yet another contribution by Fraser and Schoen [35]: the only free boundary minimal immersions of a disk in the Euclidean unit n-dimensional ball are totally geodesic.

This may sound like a very plausible and expected statement, but it is quite remarkable that, on the other hand, for any $d \geq 4$ there is plenty of non-trivial minimal immersions $\varphi : S^2 \to S^d$ (see Calabi [13]). Thereby, we face an interesting *broken symmetry* with respect to the parallelism described above.

Remark 3. In B^4 there are free boundary minimally embedded Möbius bands, hence free boundary minimally immersed annuli. Thus the conclusion of the conjecture above cannot possibly hold in higher codimension (at least not without additional assumptions).

Remark 4. The uniqueness results above, for disk-type free boundary minimal surfaces, actually holds true in the larger category of *branched* free boundary minimal immersions.

On the other hand, in the codimension one case i. e. if we take $k = d - 1$ and let $d \geq 4$ then the uniqueness problem for free boundary minimal immersions of simply-connected domains is completely open. Based on the analogy with the closed case, and specifically on the (abundant) existence of minimal hyperspheres in round S^4 that are *not* totally geodesic [41, 42], we are inclined to believe that rigidity should *not* hold. More precisely, there may be a chance of suitably desingularizing the cone, centered at the origin, over a non-equatorial minimal $(d-2)$-dimensional minimal hyperpshere in S^{d-1} to obtain a smooth free boundary minimal disk with the desired properties, at least for certain values of the integer d.

Remark 5. For an extension of Theorem 1 to the case of capillary surfaces, i. e. surfaces with constant mean curvature and a constant contact angle (not necessarily $\pi/2$) the reader may wish to consult Ros and Souam [70].

Remark 6. We still do not know whether for any (topological type of) compact surface with boundary Σ there exists a minimal immersion $\varphi : \Sigma \to B^3$. This is an interesting and challenging gap in the existence theory. For instance, it would be good to know whether there exist examples of free boundary minimal surfaces in B^3 with one boundary component and positive, but low genus.

3 - COMPACTNESS RESULTS

As a straightforward consequence of the classification result presented in the previous section, we notice that in B^3 the space of free boundary minimal disks is parametrized by a group of isometries (in fact by $SO(3)$) and, therefore, is compact with respect to the appropriate notion of convergence. The purpose of this section is to study such a problem in general Riemannian domains, where classification results cannot be expected. For the sake of simplicity and notational convenience, we will now restrict to free boundary minimal *embeddings* and work in codimension one.

Generalizing to the free boundary setting a foundational result by Choi and Schoen, Fraser and Li proved the following theorem:

Theorem 7. *[32] If (X,g) is a compact three-dimensional Riemannian manifold of non-negative Ricci curvature and convex boundary, then the space*

$$\mathfrak{M}_{\gamma,\rho} = \{\Sigma \in \mathfrak{M}(X) \ : \ genus(\Sigma) = \gamma, \#boundary\ components(\Sigma) = \rho\}$$

is strongly compact, in the sense of subsequential smooth graphical convergence with unit multiplicity.

In higher dimension, a conclusion of type cannot possibly hold because of the following two classes of counterexamples:

i) Given $m,n \geq 2$ such that $m+n < 8$, by work of Freidin-Gulian-McGrath [37], there exists an infinite family of distinct, free boundary minimal hypersurfaces in the Euclidean unit ball of dimension $m+n$, all having the topological type of $D^m \times S^{n-1}$ and converging (in the sense of varifolds) to a singular limit.

ii) The 'second principal family' constructed by Hsiang in 1983 provides infinite examples of free boundary minimal hypersurfaces all with the same topology (namely that of $D^2 \times S^1$) inside the upper hemisphere S^4_+, but the limit of these hypersurfaces is singular.

Therefore, we have counterexamples both in the case when either the Ricci tensor vanishes on the interior and the boundary is strictly convex, or the Ricci tensor is positive on the interior and the boundary is weakly convex. This evidence being provided, our idea (which goes back to [74] and [6]) was to approach the compactness problem from a somewhat different perspective, with less emphasis on the topological type and more on analytic bounds.

In order to introduce the fundamental notion of Morse index of a free boundary minimal hypersurface, let us consider a normal section $v \in \Gamma(N\Sigma)$ and compute the second variation of the area functional:

$$\begin{aligned} Q^{\Sigma}(v,v) :&= \int_{\Sigma} \Big(|\nabla^{\perp} v|^2 - (Ric_X(v,v) + |A|^2 |v|^2) \Big) + \int_{\partial\Sigma} \mathrm{II}_{\partial X}(v,v) \\ &= -\int_{\Sigma} g(v, L_{\Sigma}(v)) + \int_{\partial\Sigma} \Big(g(v, \nabla^{\perp}_{\tau} v) + \mathrm{II}_{\partial X}(v,v) \Big) \end{aligned}$$

for $L_{\Sigma} v := \Delta^{\perp}_{\Sigma} v + Ric^{\perp}_{X}(v,\cdot) + |A|^2 v$. If we consider the eigenvalue problem

$$\begin{cases} L_{\Sigma}(v) + \lambda v = 0 & \text{on} \quad \Sigma, \\ \nabla^{\perp}_{\tau} v = -(\mathrm{II}_{\partial X}(v,\cdot))^{\sharp} & \text{on} \quad \partial\Sigma. \end{cases} \qquad (*)$$

standard analytic results ensure the existence of a *discrete spectrum*: we have a complete basis of L^2 normal sections, say $\{v_j\}$, and an associated sequence $\{\lambda_j\}$ with $\lambda_j \to +\infty$ solving $(*)$. Thereby, one defines the Morse index of Σ as

$$index(\Sigma) = \#\{\lambda_j \text{ eigenvalue } :\ \lambda_j < 0\},$$

and the Morse nullity as

$$nullity(\Sigma) = \#\{\lambda_j \text{ eigenvalue } : \lambda_j = 0\}.$$

We shall say that Σ is stable if it has zero Morse index, and is unstable otherwise.

These definitions being given, one can informally rephrase the argument by Fraser-Li as follows: on the one hand a bound on the topology implies a uniform area bound, hence a weak form of convergence (as encoded in the context of *Geometric Measure Theory*), while on the other hand a bound on the topology implies a uniform bound on the Morse index, hence a subsequential convergence in the sense of laminations (cf. Colding-Minicozzi [22]). Roughly speaking, the combination of the two things allows to gain convergence to a smooth, free boundary minimal hypersurface, in the sense of smooth graphical convergence (possibly with multiplicity) away from finitely many points where *necks* may form, and whose number is controlled by the (uniform) index bound in question. This form of subsequential convergence for classes of the form

$$\mathfrak{M}_p(\Lambda, \mu) := \{\Sigma \in \mathfrak{M}(X) \ :\ \lambda_p(\Sigma) \geq -\mu \text{ and } \mathscr{H}^n(\Sigma) \leq \Lambda\}.$$

(which include, as a special case, sets of free boundary minimal hypersurfaces with uniformly bounded area and index) is the content of Theorem 2 and Theorem 5 in [8]. A fundamental point of our analysis was then the construction of Jacobi fields for the limit object, which in fact have a sign in the case when the limit is two-sided (i. e. when it has trivial normal bundle) and convergence happens with multiplicity $m \geq 2$. As a result of our study, we obtained the following strong compactness theorem:

Theorem 8. *Let $2 \leq n \leq 6$ and (X^{n+1}, g) a compact Riemannian manifold satisfying either of the following two assumptions*

1. *$Ric_X \geq 0$ with ∂X strictly convex, or*
2. *$Ric_X > 0$ with ∂X weakly convex and strictly mean convex.*

Then the corresponding class $\mathfrak{M}_p(\Lambda, \mu)$ is sequentially compact for geometric convergence and thus $\mathfrak{M}_p(\Lambda, \mu)$ consists of finitely many *diffeomorphisms classes.*

Here and below, we have employed the convenient phrase '*geometric convergence*' to refer to smooth, graphical convergence with multiplicity one.

In the so-called *bumpy* case, by which we mean that all free boundary minimal hypersurfaces (in the given ambient manifold (X, g)) do not have non-trivial Jacobi fields and the same is true for any finite covering thereof, one actually gets a much stronger finiteness result:

Theorem 9. *Let $2 \leq n \leq 6$ and (X^{n+1}, g) a compact Riemannian manifold such that ∂X is stricly mean convex. Suppose that for all $\Sigma \in \mathfrak{M}(X)$ and $\widetilde{\Sigma} \in \widetilde{\mathfrak{M}}(X)$ there exist no non-trivial Jacobi fields over Σ or $\widetilde{\Sigma}$. Then $|\mathfrak{M}_p(\Lambda, \mu)| < \infty$.*

Remark 10. This fact has a very interesting consequence: in the setting above the whole class $\mathfrak{M}(X)$ of free boundary minimal hypersurfaces is *countable*. The corresponding assertion in the closed case (which follows from [6, 74]) plays a key role in the proof of the density theorem in [45], which first settled Yau's 1982 conjecture in the generic case.

Obviously, this result poses the problem of understanding how restrictive the non-degeneracy assumption actually is. This is the object of the following *bumpy metric theorem* in the free boundary context:

Theorem 11. *Let X^{n+1} be a smooth, compact, connected manifold with non-empty boundary, and q denote a positive integer ≥ 3, or ∞.*

Let $\mathscr{B}^q$ be the subset of metrics g in Γ^q defined by the following property: no compact smooth manifolds with boundary that are C^q properly embedded as free boundary minimal hypersurfaces in (X, g), and no finite covers of any such hypersurface, admit a non-trivial Jacobi field. Then $\mathscr{B}^q$ is a comeagre subset of Γ^q.

The statement above is the free boundary counterpart of the bumpy metric theorem obtained by B. White in 1991 (for finite q) and in 2015 (for $q = \infty$). In simple terms, this theorem ensures that the notion of bumpyness given above is indeed *generic* in a set-theoretic sense (cf. Baire's category theorem).

Remark 12. B. White also proved, see [79] that if ∂X is mean convex then: X contains no closed smooth and embedded minimal hypersurface if and only if there exists some $C = C(X)$ such that for all free boundary minimal hypersurfaces Σ it holds that

$$\mathscr{H}^n(\Sigma) \leq C \mathscr{H}^{n-1}(\partial \Sigma).$$

Motivated by this result, one can define

$$\mathfrak{M}_p^{\partial}(\Lambda,\mu) := \{\Sigma \in \mathfrak{M}(X) \,:\, \lambda_p(\Sigma) \geq -\mu \text{ and } \mathscr{H}^{n-1}(\partial\Sigma) \leq \Lambda\}.$$

If $2 \leq n \leq 6$ and (X^{n+1}, g) is a compact Riemannian manifold with mean convex boundary and contains no closed minimal hypersurface, then Theorem 8 and Theorem 9 hold for the class $\mathfrak{M}_p^{\partial}(\Lambda,\mu)$ as well (hence also under a uniform index bound together with a uniform bound on the boundary mass).

4 - BUBBLING ANALYSIS AND QUANTIZATION

If one weakens the curvature condition that the Ricci curvature be positive, the conclusion of the compactness theorem by Choi-Schoen [19] is no longer true: indeed, Colding and De Lellis have constructed in [21] examples of three-dimensional manifolds (of positive *scalar* curvature) containing sequences of closed minimal surfaces of any pre-assigned fixed genus but arbitrarily large Morse index (and with a *lamination* limit). Although not yet in the literature, there is little doubt that a similar phenomenon (i. e. a similar lack of compactness, in spite of fixing the topological type) holds in the free boundary case as well: thus one cannot expect an *unconditional* result to hold. In this section, we will instead describe how *conditional* compactness results can be recovered, and how degenerations can be understood and described.

Embracing the same perspective as in the previous section, let us consider in a compact (X^3, g) a sequence of free boundary minimal surfaces with uniform bounds on the area and the Morse index (the topological type will come later into play). We already described how, at this level of generality (and without any curvature condition assumption) the sequence in question will subsequentially converge to a smooth limit, the convergence being smooth and graphical (with integer multiplicity $m \geq 1$) away from finitely many points where necks may form. The simplest local model to keep in mind is provided by the homothetic rescalings of a catenoid in $\mathbb{R}^3$ (in the free boundary case other basic examples are given by free boundary half-catenoids, either vertically or horizontally cut).

The way to proceed, and refine the *global* analysis described in the previous section, is to get a precise, qualitative and quantitative, understanding of what happens during the convergence process near the points where curvature concentration occurs. This has been done in [5] (which follows the study of the closed case, that was previously done in [4, 11]). The first result there is a quantization identity for the total curvature functional $\mathscr{A}(\cdot)$, the integral of the n-th power of the length of the second fundamental form.

Theorem 13. *Let $2 \leq n \leq 6$ and (X^{n+1}, g) be a compact Riemannian manifold with strictly mean convex boundary. For fixed $\Lambda, \mu \in \mathbb{R}_{\geq 0}$ and $p \in \mathbb{N}_{\geq 1}$, suppose that $\{\Sigma_k\}$ is a sequence in $\mathfrak{M}_p(\Lambda,\mu)$. Then there exist a $\Sigma \in \mathfrak{M}_p(\Lambda,\mu)$, $m \in \mathbb{N}$ and a finite set $\mathscr{Y} \subset X$ with cardinality $|\mathscr{Y}| \leq p-1$ such that, up to subsequence, $\Sigma_k \to \Sigma$ locally smoothly and graphically on $\Sigma \setminus \mathscr{Y}$ with multiplicity m. Moreover there exists a finite number of non-trivial bubbles or half-bubbles $\{\Gamma_j\}_{j=1}^J$ with*

$J \leq p-1$ *and*

$$\mathscr{A}(\Sigma_k) \to m\mathscr{A}(\Sigma) + \sum_{j=1}^{J} \mathscr{A}(\Gamma_j), \quad (k \to \infty).$$

For k sufficiently large, the hypersurfaces Σ_k of this subsequence are all diffeomorphic to one another (hence the class $\mathfrak{M}_p(\Lambda,\mu)$ is finite modulo diffeomorphisms).

Remark 14. The statement above is somewhat less general than what we proved in [5]: the assumption that the boundary of the ambient manifold be strictly mean convex is un-necessary, but avoids a digression on possibly improper limit surfaces.

Theorem 13 has a few straightforward geometric implications, which we present here as a list of remarks:

- In ambient dimension three (corresponding to $n = 2$), the total curvature of any bubble is an integer multiple of 8π (cf. [65, 66]) and thus the total curvature of any half-bubble is an integer multiple of 4π: hence Theorem 13 implies that for a sequence of surfaces that eventually satisfy $\mathscr{A}(\Sigma_k) \leq 4\pi - \delta$ for some $\delta > 0$, the set $\mathscr{Y}$ must be empty and the convergence to Σ is smooth and graphical everywhere (but possibly with higher multiplicity, which however will not happen if the limit is two-sided);
- In the very setting of the theorem, there exist:
  - a constant $C = C(p,\Lambda,\mu,X,g)$ such that the total curvature of any element in $\mathfrak{M}_p(\Lambda,\mu)$ is bounded from above by C.
  - a constant $I = I(p,\Lambda,\mu,X,g)$ such that the Morse index of any element in $\mathfrak{M}_p(\Lambda,\mu)$ is bounded from above by I.

The very last assertion in Theorem 13, about the unconditional finiteness of the diffeomorphisms types represented in $\mathfrak{M}_p(\Lambda,\mu)$ is justified by the following fine local description result:

Theorem 15. *With the setup as in Theorem 13, for each $y \in \mathscr{Y}$ there exist a finite number of point-scale sequences $\{(p_k^i, r_k^i)\}_{i=1}^{J_y}$ where $\sum_{y\in\mathscr{Y}} J_y \leq p-1$ with $\Sigma_k \ni p_k^i \to y$, $r_k^i \to 0$, and finite numbers of non-trivial bubbles and half-bubbles $\{\Gamma_i\}_{i=1}^{J_y}$, such that the following is true.*

- *For all $i \neq j$, we have*

$$\frac{r_k^i}{r_k^j} + \frac{r_k^j}{r_k^i} + \frac{dist_g(p_k^i, p_k^j)}{r_k^i + r_k^j} \to \infty.$$

  Taking normal coordinates centered at p_k^i, then $\widetilde{\Sigma}_k^i := \frac{\Sigma_k}{r_k^i}$ converges locally smoothly and graphically, away from the origin, to a disjoint union of

finitely many (half-)hyperplanes and at least one non-trivial bubble or half-bubble. The convergence to any non-trivial component of the limit occurs with multiplicity one.

- *Given any other sequence $\Sigma_k \ni q_k$ and $\rho_k \to 0$ with $q_k \to y$ and*

$$\min_{i=1,\dots J_y} \Big(\frac{\rho_k}{r_k^i} + \frac{r_k^i}{\rho_k} + \frac{dist_g(q_k, p_k^i)}{\rho_k + r_k^i} \Big) \to \infty$$

then taking normal coordinates at q_k, we obtain that $\widehat{\Sigma}_k := \frac{\Sigma_k}{\rho_k}$ converges to a collection of parallel (half-)hyperplanes.

When $n = 2$, any blow-up limit of $\widetilde{\Sigma}_k^i$ is always connected. The convergence is locally smooth, and of multiplicity one. Moreover we always have

$$(\dagger) \qquad \frac{dist_g(p_k^i, p_k^j)}{r_k^i + r_k^j} \to \infty.$$

Notice that condition $(\dagger)$ ensures that one can *separate* the bubble regions, so that in a certain sense there is no interaction between different regions of high curvature.

Let us focus on the case of ambient dimension three: in that case, one can rely on the Gauss-Bonnet theorem, and on the varifold convergence of the boundaries to rewrite the quantization identity in the form

$$\chi(\Sigma_k) = m\chi(\Sigma) + \sum_{j=1}^{J} (\chi(\Gamma_j) - b_j),$$

where $\chi(\Gamma_j)$ denotes the Euler characteristic of Γ_j and b_j denotes the number of its ends.

Let us now see a simple application of this machinery. Since one can fully classify bubbles and half-bubbles of Morse index less than two, we were able to obtain novel geometric convergence results for sequences of free boundary minimal surfaces of low index. To shorten the statement it is convenient to introduce the following notation:

$$\mathfrak{M}(\Lambda, I) := \{\Sigma \in \mathfrak{M}(X) \ : \ index(\Sigma) \leq I \text{ and } \mathscr{H}^n(\Sigma) \leq \Lambda\}.$$

Theorem 16. *Let (X^3, g) be a compact Riemannian manifold, with non-empty boundary ∂X. Assume that:*

a) *either the scalar curvature of (X, g) is positive and ∂X is mean convex with no minimal component;*

b) *or the scalar curvature of (X, g) is non-negative and ∂X is strictly mean convex.*

Then, for any $\Lambda > 0$ the following assertions hold:

1. *The class $\mathfrak{M}(\Lambda,0)$ is sequentially compact in the sense of smooth multiplicity one convergence. Similarly, any subclass of $\mathfrak{M}(\Lambda,1)$ of fixed topological type is sequentially compact, in the sense of smooth multiplicity one convergence, for all given topological types except those of the disk and of the annulus. In particular, we obtain unconditional sequential compactness for any class of non-orientable surfaces of given topological type.*

2. *Let $\{\Sigma_k\}$ be a sequence of disks (respectively: annuli) in $\mathfrak{M}(\Lambda,1)$. Then:* either *a subsequence converges smoothly, with multiplicity one, to an embedded minimal disk (respectively: annulus) of index at most one* or *there exists a subsequence converging smoothly, with multiplicity two and exactly one vertically cut catenoidal half-bubble (respectively: exactly one catenoidal bubble), to a properly embedded, free boundary stable minimal disk. As a result, if X contains no stable, embedded, minimal disks then strong compactness holds.*

All conclusions still hold true without assuming any a priori upper area bound if X is simply connected and, in case b), if moreover there is no closed minimal surface in X.

Remark 17. It would be interesting to know if the *degenerations* listed above actually occur, i. e. to provide a construction of degenerating disks or annuli of Morse index one (and uniformly bounded) area with a point of bad convergence. There is a chance this may be achieved via a (rather subtle) gluing/desingularization scheme.

We refer the reader to [5] for a list of other interesting applications of the quantization identity.

5 - ESTIMATES INVOLVING THE MORSE INDEX

An interesting aspect of our analysis of the limit behaviour of sequences of index one free boundary minimal surfaces (Theorem 16) is that, in many interesting cases, an a priori area estimate is not needed for one can prove it using a variation of the Hersch trick. In fact, one gets an effective estimate: if we set $\rho := \inf R$ and $\sigma := \inf H$, both assumed to be non-negative numbers, then any index one, orientable free boundary minimal surface Σ satisfies

$$\frac{\rho}{2}\mathscr{H}^2(\Sigma) + \sigma\mathscr{H}^1(\partial\Sigma) \leq 2\pi(8 - \#\text{boundary components}(\Sigma)) \leq 16\pi.$$

An estimate of this type is not known for surfaces of higher index, i. e. for free boundary minimal surfaces whose Morse index is bounded from above by a given integer k. Nevertheless, an *ineffective* estimate can be proven via refined surgery techniques following the work by Chodosh-Ketover-Maximo for the closed case [17]. These results, and their applications, are the object of a forthcoming article by the author and Franz. However, such a priori area estimate are only one of the two key ingredient needed to extend Theorem 16 to the case of higher

index. The second one, which compensates for a lack of classification results for bubbles of index ≥ 4, is a general index-topology inequality for complete minimal surfaces in $\mathbb{R}^3$ due to Chodosh-Maximo [18]. Their work fits in a very active area of research, which we shall now briefly describe with special focus on the free boundary setting. We will present a network of results in this spirit, which fit in a general program of the author of comparing different *notions of complexity* for minimal submanifolds.

Except in very few, special circumstances (including the critical catenoid, see [26, 62, 75]) the Morse index of a free boundary minimal hypersurface is unlikely to be computable, or even to be effectively estimated. Thus, it is of some importance to develop more general methods to bound it, from above and/or from below, in terms of other data of the surface in question, like e. g. its topology. We shall describe the topology of a manifold with boundary by means of its (real) homology groups. As it is well-known, in the most basic case of orientable surfaces with boundary the topological type can be completely described by means of two numbers, namely the genus and the number of boundary components of the surface in question.

There are some general results about the geometry and topology of stable and index one compact free boundary minimal surfaces in general three-manifolds whose boundary satisfies some convexity assumption. For example, by a variation of the Schoen-Yau rearrangement trick it is known that stable compact two-sided free boundary minimal surfaces in mean convex domains of three-manifolds with non-negative scalar curvature must be topological disks or totally geodesic annuli. Moving one step further, Cheng, Fraser and Pang showed in [16] that there exists an explicit upper bound on the genus and the number of boundary components of index one compact two-sided free boundary minimal surfaces in such manifolds. Related results about the topology of free boundary volume-preserving stable CMC surfaces in strictly mean convex domains of the three-dimensional Euclidean space were obtained by Ros in [69]. Going beyond the low index regime, but adding suitable curvature assumptions on the ambient manifold, in [9] we obtained general linear inequalities for the Morse index. For the sake of simplicity, anad to avoid an unnecessary digression on the methods we had introduced in [8] for the closed case, we shall simply stick to the special case of compact, regular domains in $\mathbb{R}^3$.

Theorem 18. *Let Ω^{n+1} be a strictly mean convex domain of the $(n+1)$-dimensional Euclidean space, $n \geq 2$. Let Σ^n be a compact, orientable, properly embedded free boundary minimal hypersurface in Ω. Then*

$$index(\Sigma) \geq \frac{2}{n(n+1)} dim H_1(\Sigma, \partial\Sigma; \mathbb{R}).$$

The dimension of the homology group $H_1(\Sigma, \partial\Sigma; \mathbb{R})$ can be explicitly computed in terms of the homology groups of Σ and $\partial\Sigma$. In particular, we can obtain an estimate for the index in terms of the number of boundary components. Furthermore, in the special case of free boundary minimal surfaces ($n = 2$), the

estimate also involves the genus of the surface and can in fact be upgraded to the more general scenario when the ambient domain is only *weakly* mean convex. This requires an *ad hoc* argument, and relies on a result of Ros [68].

Theorem 19. *Let Ω^3 be a mean convex domain of the three-dimensional Euclidean space. Let Σ^2 be a compact, orientable, properly embedded free boundary minimal surface in Ω with genus γ and $\rho \geq 1$ boundary components. Then*

$$index(\Sigma) \geq \frac{1}{3}(2\gamma + \rho - 1).$$

The conclusion of this theorem coincide with the one obtained by Ros and Vergasta [71] in the special case of index one free boundary minimal surfaces in strictly convex domains of $\mathbb{R}^3$ (which contain no stable free boundary minimal surfaces).

Remark 20. In the case of the unit ball in $\mathbb{R}^3$, one should be able to improve the estimate above in analogy with Theorem 1.3 in [72], concerning the index of closed minimal surfaces in the round three-dimensional sphere. In terms of *absolute* lower bounds (i. e. estimates not brining topology into play) Fraser and Schoen [36] have proven that if $\Sigma^n \subset B^{n+1}$ (a free boundary minimal hypersurface in the unit ball of $\mathbb{R}^{n+1}$) then either Σ^n is a flat disk (whose index is one) or its Morse index is at least $n+2$.

Remark 21. The above theorem can be used to understand the behaviour of the index of some known examples of free boundary minimal surfaces constructed in the unit ball in $\mathbb{R}^3$. In particular, it implies that the examples in any of the families of free boundary minimal surfaces obtained in [36], [29], [43] and [44] have arbitrarily large Morse indices.

Remark 22. All the main results in [5] actually hold for properly *immersed* free boundary minimal hypersurfaces. The necessary modifications to our proofs are of purely notational character.

Remark 23. For (strictly) two-convex domains of the Euclidean space one can actually improve the estimate in Theorem 18 replacing, in the right-hand side, $\dim H_1(\Sigma, \partial\Sigma; \mathbb{R})$ by means of $\max\{\dim H_1(\Sigma, \partial\Sigma; \mathbb{R}),\ \dim H_{n-1}(\Sigma, \partial\Sigma; \mathbb{R})\}$.

The ideas behind the proof of Theorem 18 (hence Theorem 19) have their roots in earlier work by Ros [68], Savo [72] and, as mentioned above, by Ambrozio, Sharp and the author [8] in the study of a well-known conjecture by Schoen on the index of closed minimal hypersurfaces inside three-dimensional manifolds of positive Ricci curvature. Let us explain it, very briefly, in the simpler case of Theorem 19.

Roughly speaking, given a harmonic one-form $\omega \in \mathscr{H}^1_T(\Sigma, g)$ subject to suitable boundary conditions, one considers its projections with respect to some orthonormal basis $\{\theta_i\}$ of $\mathbb{R}^3$ and proves, via a direct calculation, an identity for the mean value $\sum Q^\Sigma(u_i, u_i)$ where Q^Σ is the Jacobi form arising in the second variation of the area of Σ and $u_i = \langle \omega, \theta_i \rangle$. Thereby, the geometric assumption that the domain be strictly mean convex ensures that this sum must be *negative*.

Now, let us assume that Σ^2 has index k, and denote by $\{\phi_q\}_{q=1}^{\infty}$ an L^2-orthonormal basis of eigenfunctions of the Jacobi operator of Σ satisfying the Robin boundary conditions $(*)$ (see Section). Let then Φ denote the linear map defined by

$$\begin{array}{rccc} \Phi: & \mathscr{H}^1_T(\Sigma,g) & \to & \mathbb{R}^{3k} \\ & \omega & \mapsto & [\int_\Sigma \langle \omega, \theta_i\rangle \phi_q], \end{array}$$

where q varies from 1 to k. Clearly, by linear algebra

$$dim\mathscr{H}^1_T(M,g) \leq dimKer(\Phi) + 3k$$

Since $\mathscr{H}^1_T(\Sigma,g) \simeq H_1(\Sigma,\partial\Sigma;\mathbb{R})$, and thus both spaces have dimension $2\gamma+\rho-1$, the result will follow once we prove injectivity of the map Φ.

Let then ω be an element of the kernel of the map Φ. This means that all functions u_i are orthogonal to the first k eigenfunctions, namely $\phi_1,\ldots,\phi_k$. Since $index(\Sigma) = k$, we must have

$$Q(u_i,u_i) \geq \lambda_{k+1}\int_\Sigma u_i^2 d\mathscr{H}^2 \geq 0, \quad \text{for } i = 1,2,3,$$

by the variational characterization of the eigenvalues for problem $(*)$. On the other hand, we have already observed that the assumption $H^{\partial\Omega} > 0$ implies that the above inequality can only possibly hold if $|\omega|$ vanishes identically on ∂M. But then $\omega = 0$ on Σ by suitably applying the maximum principle. Hence, if the domain is strictly mean convex, Φ has trivial kernel, and the conclusion follows.

General estimates of the type above are not known in higher codimension, or under weaker curvature assumptions. However, we remark that some interesting results on the index of free boundary minimal submanifolds of higher codimension have been proven in [31] and [36], Theorem 3.1.

Besides the index estimates provided above, we further know, thanks to recent work [53] by V. Lima, extending to the free boundary setting the results by Eijiri-Micallef [28] and Cheng-Tysk [15], that a uniform bound both on the area and on the topology of a sequence of orientable free boundary minimal surfaces implies a uniform bound on the Morse index. We note that when $n = 2$ and one considers convex domains in Euclidean space the theorem by V. Lima can be regarded as a partial converse to Theorem 19 above.

Lastly, let us mention some very recent work by Aiex and Hong [1] presenting index estimates in the spirit of [8, 9] for *constant mean curvature* surfaces in three-dimensional manifolds, both in the closed and in the free boundary case (see [14] for earlier contributions in the case of mean convex domains in $\mathbb{R}^3$). Of course, in the stable case these estimates recover much more basic results concerning the topology of isoperimetric surfaces in Euclidean bodies.

6 - REFERENCES

[1] N. Aiex, H. Hong, *Index estimates for surfaces with constant mean curvature in 3-dimensional manifolds*, preprint (arXiv: 1901.00944).

[2] A. Aché, D. Maximo, H. Wu, *Metrics with nonnegative Ricci curvature on convex three-manifolds*, Geom. Topol. **20** (2016), no. 5, 2905-2922.

[3] F. Almgren, *Some interior regularity theorems for minimal surfaces and an extension of Bernstein's theorem*, Ann. of Math. (2) **84** (1966), 277-292.

[4] L. Ambrozio, R. Buzano, A. Carlotto, B. Sharp, *Geometric convergence results for closed minimal surfaces via bubbling analysis*, preprint (arXiv: 1803.04956).

[5] L. Ambrozio, R. Buzano, A. Carlotto, B. Sharp, *Bubbling analysis and geometric convergence results for free boundary minimal surfaces*, J. Éc. polytech. Math. **6** (2019), 621-664.

[6] L. Ambrozio, A. Carlotto, B. Sharp, *Compactness of the space of minimal hypersurfaces with bounded volume and p-th Jacobi eigenvalue*, J. Geom. Anal. **26** (2016), no. 4, 2591-2601.

[7] L. Ambrozio, A. Carlotto, B. Sharp, *Compactness analysis for free boundary minimal hypersurfaces*, Calc. Var. PDE **57** (2018), no. 1, 1-39.

[8] L. Ambrozio, A. Carlotto, B. Sharp, *Comparing the Morse index and the first Betti number of minimal hypersurfaces*, J. Differential Geom., **108** (2018), no. 3, 379-410.

[9] L. Ambrozio, A. Carlotto, B. Sharp, *Index estimates for free boundary minimal hypersurfaces*, Math. Ann., **370** (2018), no. 3-4, pages 1063-1078.

[10] S. Brendle, *Embedded minimal tori in S3 and the Lawson conjecture*, Acta Math. **211** (2013), no. 2, 177-190.

[11] R. Buzano, B. Sharp, *Qualitative and quantitative estimates for minimal hypersurfaces with bounded index and area*, Trans. Amer. Math. Soc., **370** (2018), 4373-4399.

[12] L. Caffarelli, D. Jerison, C. Kenig, *Global energy minimizers for free boundary problems and full regularity in three dimensions.* Noncompact problems at the intersection of geometry, analysis, and topology, 83-97, Contemp. Math., 350, Amer. Math. Soc., Providence, RI, 2004.

[13] E. Calabi, *Minimal immersions of surfaces in Euclidean spheres*, J. Differential Geometry **1** (1967), 111-125.

[14] M. Cavalcante, D. de Oliveira, *Index estimates for free boundary constant mean curvature surfaces*, preprint (arXiv: 1803.05995).

[15] S. Y. Cheng and J. Tysk, *Schrödinger operators and index bounds for minimal submanifolds*, Rocky Mountain J. Math. **24** (1994), no. 3, 977-996.

[16] J. Chen, A. Fraser, C. Pang, *Minimal immersions of compact bordered Riemann surfaces with free boundary*, Trans. Amer. Math. Soc., **367** (2014), no. 4, 2487-2507.

[17] O. Chodosh, D. Ketover, D. Maximo, *Minimal surfaces with bounded index*, Invent. Math. **209** (2017), no. 3, 617-664.

[18] O. Chodosh, D. Maximo, *On the topology and index of minimal surfaces*, J. Differential Geom. **104** (2016), no. 3, 399-418.

[19] H. Choi, R. Schoen, *The space of minimal embeddings of a surface into a three-dimensional manifold of positive Ricci curvature*, Invent. Math. **81** (1985), no. 3, 387-394.

[20] H. Choi, A. Wang, *A first eigenvalue estimate for minimal hypersurfaces*, J. Differential Geom. **18** (1983), no. 3, 559-562.

[21] T. Colding, C. De Lellis, *Singular limit laminations, Morse index, and positive scalar curvature*, Topology **44** (2005), no. 1, 25-45.

[22] T. Colding, W. Minicozzi, *A course in minimal surfaces*, Graduate Studies in Mathematics, 121. American Mathematical Society, Providence, RI, 2011. xii+313 pp.

[23] R. Courant, *The existence of minimal surfaces of given topological structure under prescribed boundary conditions*, Acta Math. **72** (1940), 51-98.

[24] R. Courant, *Dirichlet's Principle, Conformal Mapping, and Minimal Surfaces. Appendix by M. Schiffer*, Interscience Publishers, Inc., New York, N.Y., 1950. xiii+330 pp.

[25] C. De Lellis, J. Ramic, *Min-max theory for minimal hypersurfaces with boundary*, preprint (arXiv:1611.00926).

[26] B. Devyver, *Index of the critical catenoid*, preprint (arXiv: 1609.02315).

[27] M. do Carmo, C. K. Peng, *Stable complete minimal surfaces in* $\mathbb{R}^3$ *are planes*, Bull. Amer. Math. Soc. (N.S.) **1** (1979), no. 6, 903-906.

[28] N. Ejiri and M. Micallef, *Comparison between second variation of area and second variation of energy of a minimal surface*, Adv. Calc. Var. **1** (2008), no. 3, 223-239.

[29] A. Folha, F. Pacard, T. Zolotareva, *Free boundary minimal surfaces in the unit* 3*-ball*, Free boundary minimal surfaces in the unit 3-ball, Manuscripta Math. **154** (2017), no. 3-4, 359-409.

[30] A. Fraser, *On the free boundary variational problem for minimal disks*, Comm. Pure Appl. Math. **53** (2000), no. 8, 931-971.

[31] A. Fraser, *Index estimates for minimal surfaces and k-convexity*, Proc. Amer. Math. Soc. **135** (2007), no. 11, 3733-3744.

[32] A. Fraser, M. Li, *Compactness of the space of embedded minimal surfaces with free boundary in three-manifolds with nonnegative Ricci curvature and convex boundary*, J. Differential Geom. **96** (2014), no. 2 , 183-200.

[33] A. Fraser, R. Schoen, *The first Steklov eigenvalue, conformal geometry, and minimal surfaces*, Adv. Math. **226** (2011), no. 5, 4011-4030.

[34] A. Fraser, R. Schoen, *Minimal surfaces and eigenvalue problems. Geometric analysis, mathematical relativity, and nonlinear partial differential equations*, 105?121, Contemp. Math. **599**, Amer. Math. Soc., Providence, RI, 2013.

[35] A. Fraser, R. Schoen, *Uniqueness theorems for free boundary minimal disks in space forms*, Int. Math. Res. Not. IMRN 2015, no. 17, 8268-8274.

[36] A. Fraser, R. Schoen, *Sharp eigenvalue bounds and minimal surfaces in the ball*, Invent. Math. **203** (2016), no. 3, 823-890.

[37] B. Freidin, M. Gulian, P. McGrath, *Free boundary minimal surfaces in the unit ball with low cohomgeneity*, Proc. Amer. Math. Soc. **145** (2017), no. 4, 1671-1683.

[38] M. Grüter, J. Jost, *On embedded minimal disks in convex bodies*, Ann. Inst. H. Poincaré Anal. Non Linéaire **3** (1986), no. 5, 345-390.

[39] Q. Guang, X. Zhou, *Compactness and generic finiteness for free boundary minimal hypersurfaces*, preprint (arXiv:1803.01509).

[40] D. Hoffman, W. H. Meeks III, *The strong halfspace theorem for minimal surfaces*, Invent. Math. **101** (1990), no. 2, 373-377.

[41] W.-Y. Hsiang, *Minimal cones and the spherical Bernstein problem*, I. Ann. of Math. (2) **118** (1983), no. 1, 61-73.

[42] W.-Y. Hsiang, *Minimal cones and the spherical Bernstein problem. II*, Invent. Math. **74** (1983), no. 3, 351-369.

[43] N. Kapouleas, M. Li *Free boundary minimal surfaces in the unit three-ball via desingularization of the critical catenoid and equatorial disk*, preprint (arXiv: 1709.08556).

[44] N. Kapouleas, D. Wygul *Free-boundary minimal surfaces with connected boundary in the 3-ball by tripling the equatorial disc*, preprint (arXiv: 1711.00818).

[45] K. Irie, F. C. Marques, A. Neves, *Density of minimal hypersurfaces for generic metrics*, Ann. Math. **187** (2018), no. 3, 963-972.

[46] L. Jorge, W. H. Meeks III, *The topology of complete minimal surfaces of finite total Gaussian curvature*, Topology **22** (1983), no. 2, 203-221.

[47] J. Jost, *Existence results for embedded minimal surfaces of controlled topological type. I*, Ann. Scuola Norm. Sup. Pisa Cl. Sci. (4) **13** (1986), no. 1, 15-50.

[48] J. Jost, *Existence results for embedded minimal surfaces of controlled topological type. II*, Ann. Scuola Norm. Sup. Pisa Cl. Sci. (4) **13** (1986), no. 3, 401-426.

[49] J. Jost, *Existence results for embedded minimal surfaces of controlled topological type. III*, Ann. Scuola Norm. Sup. Pisa Cl. Sci. (4) **14** (1987), no. 1, 165-167.

[50] D. Ketover, *Free boundary minimal surfaces of unbounded genus*, preprint (arXiv:1612.08691).

[51] M. Li, *A general existence theorem for embedded minimal surfaces with free boundary*, Comm. Pure Appl. Math. **68** (2015), no. 2, 286-331.

[52] M. Li, X. Zhou, *Min-max theory for free boundary minimal hypersurfaces I - regularity theory*, preprint (arXiv:1611.02612).

[53] V. Lima, *Bounds for the Morse index of free boundary minimal surfaces*, preprint (arXiv: 1710.10971).

[54] Y. Liokumovich, F. C. Marques, A. Neves, *Weyl law for the volume spectrum*, Ann. Math. **187** (2018), no. 3, 933-962.

[55] F. Marques, *Minimal surfaces - variational theory and applications*, Proceedings of the International Congress of Mathematicians, Seoul 2014.

[56] F. Marques, A. Neves, *Existence of infinitely many minimal hypersurfaces in positive Ricci curvature*, Invent. Math. **209** (2017), no. 2, 577-616.

[57] F. Marques, A. Neves, *Min-max theory and the Willmore conjecture*, Ann. of Math. (2) **179** (2014), no. 2, 683-782.

[58] F. Marques, A. Neves, *Morse index and multiplicity of min-max minimal hypersurfaces*, Camb. J. Math. **4** (2016), no. 4, 463-511.

[59] F. Marques, A. Neves, *Rigidity of min-max minimal spheres in three-manifolds*, Duke Math. J. **161** (2012), no. 14, 2725-2752.

[60] F. C. Marques, A. Neves, A. Song, *Equidistribution of minimal hypersurfaces for generic metrics*, preprint (arXiv: 1712.06238).

[61] D. Máximo, I. Nunes, G. Smith, *Free boundary minimal annuli in convex three-manifolds*, J. Differential Geom. **106** (2017), no. 1, 139-186.

[62] P. McGrath, *A characterization of the critical catenoid*, preprint (arXiv:1603.04114v2).

[63] N. Nadirashvili, A. Penskoi, *Free boundary minimal surfaces and overdetermined boundary value problems*, preprint (arXiv: 1812.08943).

[64] J. Nitsche, *Stationary partitioning of convex bodies*, Arch. Rational Mech. Anal. **89** (1985), no. 1, 1-19.

[65] R. Osserman, *On complete minimal surfaces*, Arch. Rational Mech. Anal. **13** (1963), 392-404.

[66] R. Osserman, *Global properties of minimal surfaces in E^3 and E^n*, Ann. of Math. (2) **80** (1964), 340-364.

[67] J. Pitts, *Existence and regularity of minimal surfaces on Riemannian manifolds*, Princeton University Press, Princeton, N.J.; University of Tokyo Press, Tokyo. Mathematical Notes **27** (1981).

[68] A. Ros, *One-sided complete stable minimal surfaces*, J. Differential Geom. **74** (2006), no. 1, 69-92.

[69] A. Ros, *Stability of minimal and constant mean curvature surfaces with free boundary*, Mat. Contemp. **35** (2008), 221-240.

[70] A. Ros, R. Souam, *On stability of capillary surfaces in a ball*, Pacific J. Math. **178** (1997), no. 2, 345-361.

[71] A. Ros, E. Vergasta, *Stability for hypersurfaces of constant mean curvature with free boundary*, Geom. Dedicata **56** (1995), no. 1, 19-33.

[72] A. Savo, *Index bounds for minimal hypersurfaces of the sphere*, Indiana Univ. Math. J. **59** (2010), no. 3, 823-837.

[73] R. Schoen, L. Simon, *Regularity of stable minimal hypersurfaces*, Comm. Pure Appl. Math. **34** (1981), no. 6, 741-797.

[74] B. Sharp, *Compactness of minimal hypersurfaces with bounded index*, J. Differential Geom. **106** (2017), no. 2, 317-339.

[75] G. Smith, D. Zhou, *The Morse index of the critical catenoid*, preprint (arXiv:1609.01485).

[76] M. Struwe, *On a free boundary problem for minimal surfaces*, Invent. Math. **75** (1984), no. 3, 547-560.

[77] J. Tysk, *Finiteness of index and total scalar curvature for minimal hypersurfaces*, Proc. Amer. Math. Soc. **105** (1989), no. 2, 428-435.

[78] G. Wang, *Birkhoff minimax principle for minimal surfaces with a free boundary*, Math. Ann. **314** (1999), no. 1, 89-107.

[79] B. White, *Which ambient spaces admit isoperimetric inequalities for submanifolds?*, J. Diff. Geom. **83** (2009), no. 1 213-228.

Rend. Acc. Sc. fis. mat. Napoli
Vol. LXXXVI, (2019) pp. 123-146

DOI 10.32092/1021

A review about public cryptography protocols based on RSA or elliptic curves

Nota di Antonio Corbo Esposito[1], Cristian Tirelli[1]

Presentata dal socio Antonio Corbo Esposito
(Adunanza del 15 novembre 2019)

Key words: RSA, Diffie-Hellman, Discrete Logarithm, Elliptic Curve, ECDSA

Abstract – We provide the basic definitions regarding computational complexity theory and review some basic cryptography protocols based on RSA or elliptic curves. These protocols summarize the history of the last fifty years in cryptography and are actually ubiquitous in applications, as for example SSL (secure socket layers), smartcards, creation of a bitcoin wallet etc. Since it is known they are in the polynomial class for the Shor's algorithm, the possible development of quantum computers, needed to run such algorithm, will represent a dramatic shift in cryptography research and in applications.

Riassunto – In questa nota forniamo le definizioni di base relative alla teoria della complessitá computazionale ed esaminiamo alcuni semplici protocolli crittografici basati su RSA e curve ellittiche. Questi protocolli riassumono la storia degli ultimi cinquant'anni della crittografia e sono onnipresenti nelle applicazioni, come ad esempio SSL (secure socket layers), smartcards, creazione di portafogli per bitcoin etc. Poiché é noto che rientrano nella classe di problemi polinomiali per l'algoritmo di Shor, un possibile sviluppo dei computer quantistici, necessari per eseguire questi algoritmi, rappresenterebbe un drammatico cambiamento nella ricerca crittografica e nelle applicazioni.

1 - INTRODUCTION

In this review we summarize the basic concepts about complexity theory and provide an overview of main public cryptography protocols actually used for a widespread range of applications, from the protections of money transactions over internet to the creation of a bitcoin wallet to the digital signature of documents.
While these algorithms are ubiquitous in the present ICT world they all share a common feature: they are all vulnerable to the Shor's algorithm, meaning that if

[1]Dipartimento di Ingegneria Elettrica e dell' Informazione "Maurizio Scarano", Università degli studi di cassino e del Lazio meridionale, Via G. Di Biasio 43, 03043, Cassino, Italia. e-mail: corbo@unicas.it, cristiantirelli@gmail.com

a "quantum computer" is ever realized managing a suitable number (i.e. >128) of qubits, the complexity to solve these problems will fall into the polynomial class.
The only problems present in this review which will resist to "quantum computers" are NP-complete problems, as MQ problem. However MQ problem, as other "post quantum" cryptographic problems has failed so far to provide adequate and practical public cryptography protocols. This review therefore provides an outlook directed to the recent history of cryptography: this history has provided exceptionally beautiful topics in mathematics, as RSA algorithm or the theory of elliptic curves, while the fate of the protocols based upon these algorithms is already sealed.
The world of cryptography is actively preparing for the upcoming paradigm shift. New algorithms are proposed and NIST (National Institute of Standards and Technology) has already started the selection for the next generation of protocols that will resist even attacks running on "quantum computers".
The present situation and perspectives will be addressed in an upcoming report.

2 - COMPUTATIONAL COMPLEXITY THEORY

Computational complexity theory is a tool that help us to classify and analyze computational problem to their inherent difficulty.
Information Theory tells us that every cryptographic algorithm is insecure, but with the study of computational complexity we can tell after how much time this algorithm can be broken.

2.1 - Algorithms complexity

The complexity of an algorithm is defined like the power needed to compute it. Usually it's measured considering two variables: T the time complexity and S the spatial complexity. The complexity of an algorithm is expressed using the Big O notation, that allow us to approximate the result using a superior limit.

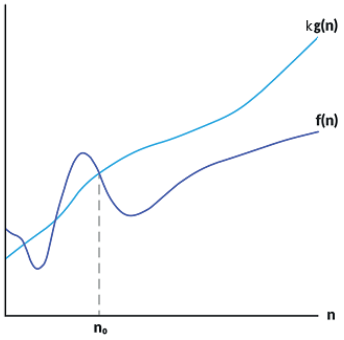

Figure 1: Big O notation

Definition 1. *$f(n) = \mathcal{O}(g(n))$ means that $k \cdot g(n)$ is the superior limit of $f(n)$. So there exists a constant k such that $f(n) \leq k \cdot g(n)$ for values bigger enough of n*

Definition 2. *$f(n) = \Omega(g(n))$ means that $k \cdot g(n)$ is the inferior limit of $f(n)$. So there exists a constant k such that $f(n) \geq k \cdot g(n)$, for values bigger enough of n*

Definition 3. *$f(n) = \Theta(g(n))$ means that $k_1 \cdot g(n)$ is the superior limit of $f(n)$ and $k_2 \cdot g(n)$ is the inferior limit for each $n \geq n_0$. So there exists some constants k_1 and k_2 for which $f(n) \leq k_1 \cdot g(n)$ and $f(n) \geq k_2 \cdot g(n)$ with this we can say $g(n)$ is a good approximation of $f(n)$.*

This notation is usefull to group in the same class of complexity different algorithm. The most common class of complexity are:

- Constant functions: $f(n) = 1$ when we don't have a dependence of n
- Logarithmic functions: $f(n) = \log n$
- Linear functions: $f(n) = n$
- Superlinear functions: $f(n) = n \log n$
- Quadratic functions: $f(n) = n^2$
- Cubic functions: $f(n) = n^3$
- Exponential function: $f(n) = c^n$
- Factorial functions: $f(n) = n!$

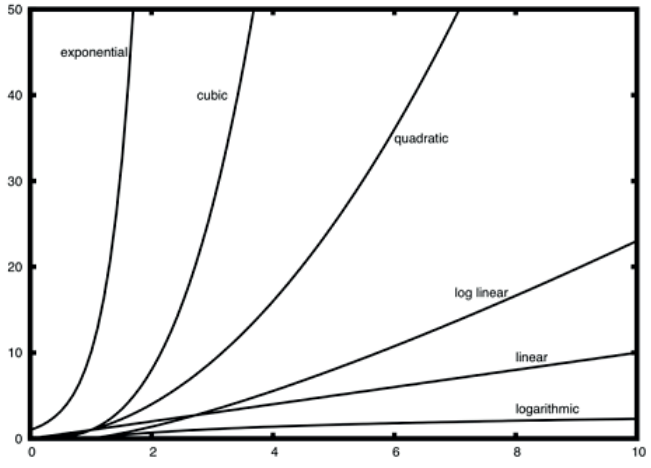

Figure 2: Execution time

To have a better gasp of the running time associate to each complexity function we can read the following table:

Classes	Complexity	#operation for $n = 10^6$	Time
Constant	$\mathcal{O}(1)$	1	1 μsec.
Linear	$\mathcal{O}(n)$	10^6	1 sec.
Quadratic	$\mathcal{O}(n^2)$	10^{12}	11.6 days
Cubic	$\mathcal{O}(n^3)$	10^{18}	32000 yrs.
Exponential	$\mathcal{O}(2^n)$	10^{301030}	10^{301006} y.u.

We can see that bruteforce attack for problems of exponential complexity are not practically possible, since they will require enormous amount of time, in fact this is the strengths of cryptographic algorithms.

2.2 - Complexity class

Cryptography is a science that was developed together with writing, in fact there are numerous example of "secret writing" in the history. In the past all the algorithm used to communicate secretly where based on the secrecy of the algorithm itself, but right know it's the complete opposite. Modern cryptography made possible for two strangers to communicate securely using a channel secured by the application of some mathematical problems and everything is done with public algorithms.

Computational complexity theory classify not only the complexity of algorithms, but also the complexity of problems in general. The objective is to find, using less time and space possible , the solution to a problem on a theoretic computer called Turing machine. Problems are divided in various class of complexity, determinated on the base of their difficulty. In the following image we can see various class and their relation, however mathematical a lot of topics still need to be demonstrated.

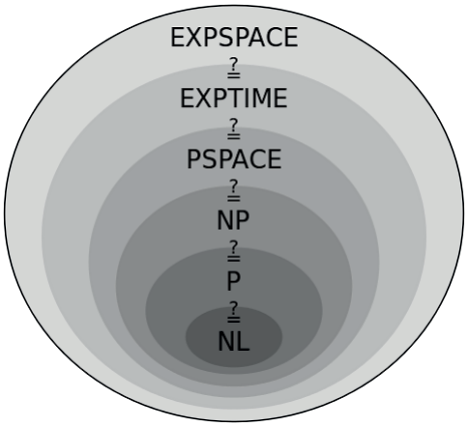

Figure 3: Diagram of the complexity class

2.3 - P vs NP

Definition 4. *The class P contains all the problem that can be solved in a polynomial time.*

Definition 5. *The class NP contains all the problem of which the solution can be verified in a polynomial time.*

Like we can guess from the definitions the membership to a class NP require less then the memebershipt to the class P. The class NP contains P because every problem that can be resolved in polynomial time can also be verified in polynomial time. It seems easy to prove that NP problems are more difficult of P problems, but right now a mathematical demonstration still has to be made. If $NP = P$ will be demonstrated, a lot o cryptographic algorithms could become useless. Some of this NP problems are more difficult than others and are called $NP - complete$.

Definition 6. *A P problem is called $NP - complete$ is every other problem Q, contained in NP, can be reduced to P in a polynomial time*

Example 1. *NP-complete problems:*

- *The knapsack problem. Given a set of items, each with a weight and a value, determine the number of each item to include in a collection so that the total weight is less than or equal to a given limit and the total value is as large as possible*
- *Graph coloring problem. Given n colors, find a way to color the vertex of a graph such that two adjacent vertex doesn't have the same color.*
- *Travelling salesman problem. A traveler need to visit n different cities following the shortest route possible.*

If at least one of this problems would be verified with an algorithm that run in polynomial time, then we can say that $NP \neq P$. All this problems are easy to verify, but hard to solve. They complexity is exponential, but that doens't mean that every NP problem is exponential and this is what brings us to ask ourselves if $P = NP$. Nowday no mathematical demonstration has succeeded in giving us an answer.

2.4 - Boolean satisfiability problem

Boolean satisfiability problem (**SAT**) is a fundamental problem in the mathematical logic and in the theory of computational complexity. In practice it's a tool used for a variety of problems, for example there are numerous application of it for solving design problem of integrated circuits.
Given a set of n variables: $x_1, \ldots, x_n$, a set of literals (a literals is a variable $Q = x$), a set of distinct rules $C_1, \ldots, C_n$, and each rules is a set of literals bound together by the logic operation or ($\vee$).
The objective of SAT problems is to find the value that associate to the literals, make the following formula true.

$$C_1 \wedge C_2 \wedge \ldots \wedge C_m$$

2.5 - Multivariate quadratic polinomial (MQ) problem

Another importan $NP-Complete$ problem is the Multivariate Quadratic polinomial (MQ) problem that sees its application in the public key cryptography. A system of this kind have a set of quadratic polynomials on a finite field and solving this problems on a finite field is not easy. This kind of problem is considered to be one of the few that could resist to a quantic computer. The public key cryptosystem depends on the existance of a class of function called *trapdoor*; this function are easy to calculate, but very difficult to invert (for example the multiplication between two prime numbers). In the PKV (public key cryptosystem) that uses MQ systems, the trapdoor function is a polynomial equation with more then one boolean variables. Usually the key is generated with a system of quadratic polynomials:

$$\mathscr{P} = (p_1(\omega_1, \ldots, \omega_n), \ldots, p_m(\omega_1, \ldots, \omega_n))$$

where p_i is a non linear quadratic polynomial system over $w = (\omega_1, \ldots, \omega_n)$:

$$p_k(w) := \sum_i P_{ik}\omega_i + \sum_i Q_{ik}\omega_i^2 + \sum_{i>j} R_{ijk}\omega_i\omega_j$$

in which each coefficient and each variable is in $\mathbb{F}_q$.

3 - CRYPTOGRAPHIC PROTOCOLS

Sharing data and information on a secure channel between two endpoint was something needed also during the egyptian times and only with the evolution of society and the improvement in technologies was possible to create more sophisticated methodologies to communicate. The real breakthrough there was in the 1976 with the publication of the **Diffie-Hellman** algorithm which got us a secure way to exchange information on an insecure channel and after a few years, in the 1978 another important algorithm, **RSA**(from it's creators *Rivest, Shamir e Adleman*) was born. The publication of this algorithms helped to develop and research new area of math, contributing with the improvement of the general cryptography technique. We can divide cryptographic protocol in two big branches: **symmetric** and **asymmetric** cryptography. In the symmetric cryptography the key used to encrypt the data is also used to decrypt it, meaning that the two part need to share the same key. However with asymmetric cryptography we don't have this problem since it uses two different keys, one to encrypt and one to decrypt. Usually this is used only to exchange the key and then use symmetric cryptography, since asymmetric cryptography it's not so efficient when dealing with large quantities of data.

3.1 - Prime number generation

Prime number play an important role in cryptography, but generating those number in a deterministic way and in a small amount of time is not possible; what we can to is do generate random number and then check if they are prime with a probability test.

Theorem 1. ***Prime number theorem***

This theorem describe the asymptotic distribution of prime number and gives use an approximation of how many prime exists under a certain integer n.
Let $\pi(x)$ be the prime-counting function then

$$\lim_{x\to\infty} \frac{\pi(x)}{\frac{x}{\log(x)}} = 1$$

That can be approximated like this $\pi(x) \approx \frac{x}{\log(x)}$

Algorithms like **RSA** and **D-H** use prime number of 512 bit that, using the previous theorem, gives us around 10^{150} prime number that we can pick. Generating prime number is not easy, we could pick a random number and then try to factorize it, but with number of 512 bit this is not possible since this operation while require too much time. We need to use some probabilistic algorithms like the following one.

Lehmann Algorithm

1. Pick a random number a less then p
2. Compute $a^{\frac{p-1}{2}} \pmod p$
3. If $a^{\frac{p-1}{2}} \neq \pmod p$ or $a^{\frac{p-1}{2}} \neq -1 \pmod p$ then p is not prime
4. If $a^{\frac{p-1}{2}} \equiv 1 \pmod p$ or $a^{\frac{p-1}{2}} \equiv -1 \pmod p$ then the probability that p is not prime doesn't exceed 50%

Repeating this algorithm decrease the probability of p to not be prime.

Rabin-Miller Algorithm Let's pick a random number p. Compute b that is the number of times that 2 divide $p-1$ e let's compute m so that $p = 1+2^b m$.

1. Pick a random number a less then p
2. $j = 0$ and $z = a^m \pmod p$
3. If $z = 1$ or $z = p-1$ then p is probably prime
4. If $j > 0$ and $z = 1$ then p is not prime
5. $j = j+1$
6. If $j < b$ and $z \neq p-1$ then $z = z^2 \pmod p$ and repeat from the third point. If $z = p-1$ then p is probably prime.
7. If $j = b$ and $z \neq p-1$ then p is not prime.

This is the most used algorithm because the probability of a number to not be prime decrease faster than other algorithms, since it's about $\frac{1}{4^t}$ where t is the number of iteration.

3.2 - RSA

The security of this particular algorithm is based on the difficulty to factorize large number. There are some technique developed trying to break this algorithm, but right now nobody found a solution that can be run on polynomial time.
RSA is not so difficult to understand, there are just three main step:

1. ***Generation of the public and private key***
   - Generate two big number p and q both with the same lenght in bit.
   - Compute $n = pq$ and $\phi = (p-1)(q-1)$
   - Pick a random integer e such that $1 < e < \phi$ and $gcd(e, \phi) = 1$
   - With the extended Euclidean algorithm compute d such that $1 < d < \phi$ and $ed \equiv 1 \pmod{\phi}$
   - The *public key* is given by the pair (n, e), while the *private key* is d
2. ***Data Encryption***
   - The part interested in the communication get the public key (n, e)
   - Represented the message like a big integer $m \in [0, n-1]$
   - Compute $c = m^e \pmod{n}$
   - The encrypted message to send is c
3. ***Data Decryption***
   - The receiver, who provided the public key and who recived the encrypted text c, can get the original text use its private key d to get $m = c^d \pmod{n}$.

Demonstration

Since $ed \equiv 1 \pmod{\phi}$ exist a value k such that $ed = q + k\phi$. If $gcd(m, p) = 1$ then for Fermat's last theorem we have:

$$m^{p-1} \equiv 1 \pmod{p}$$

raising for $k(q-1)$ and multiplicand for m we get:

$$m^{1+k(p-q)(q-1)} \equiv m \pmod{p}$$

Else if $gcd(m, p) = p$ then the last congruency hold since its congruent to 0 modulo p. So we always have that:

$$m^{ed} \equiv m \pmod{p}$$
$$m^{ed} \equiv m \pmod{q}$$
$$m^{ed} \equiv m \pmod{n}$$

So it holds that:

$$c^d \equiv (m^e)^d \equiv m \pmod{n}$$

The encryption phare used in RSA can be speed up if we choose e equal to 4, 16 or 65537 since are more easy to calculate and they choice don't make weak, from a secuirty prospective, the algorithm.

3.3 - Diffie-Hellman

The first public key protocol was published in 1976 by **Whitfield Diffie** e **Martin Hellman** and its the first example of public key exchange. Usually a secure communication required a key exchange on a physical channel, but with the introduction of **D-H** it become possible to exchange a secret key on a public(insecure) channel.
Conceptually the algorithm is represented in the following image

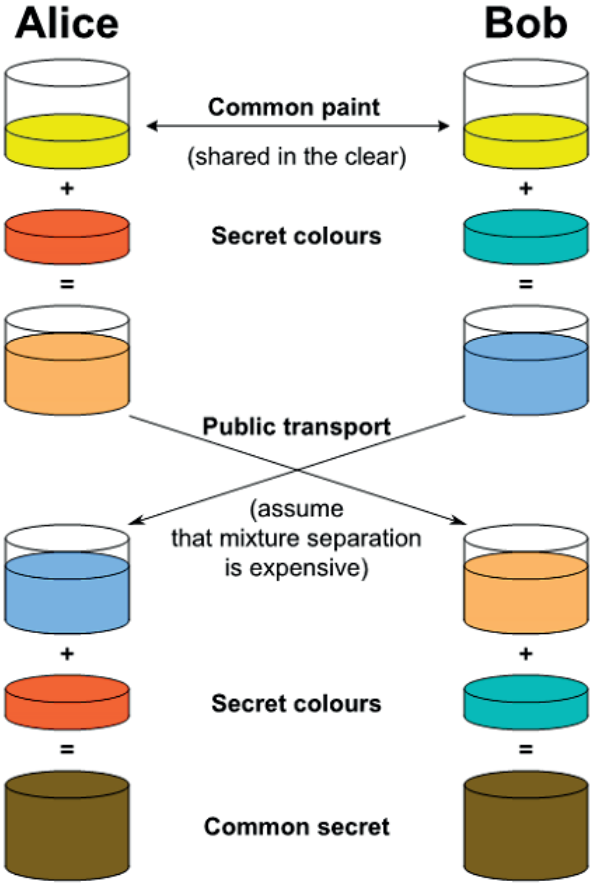

Figure 4: Diffie-Hellman key exchange

Mathematically we define **D-H** algorithm on a multiplicative group of a finete

set of prime number. The two part **Alice** (A) and **Bob**(B) choose a big prime number n and g such that g is a primitive element of G. The values n and g must be kept secret and can be shared on a public channel following this procedure:

- **A** Pick a big integer x and sends to **B** $X = g^x \pmod n$
- **B** Pick a big integer y and sends to **A** $Y = g^y \pmod n$
- **A** Compute $k_0 = Y^x \pmod n$
- **B** Compute $k_1 = X^y \pmod n$

Since $(g^x)^y = (g^y)^x = g^{xy}$ we have that $k = k_0 = k_1$. Knowing only n, g, X and Y is not possible find x or y without first solving a discrete logarithm problem.

3.4 - Man in the middle

One thing that **D-H** cannot do is to protect ourself from MITM attack.

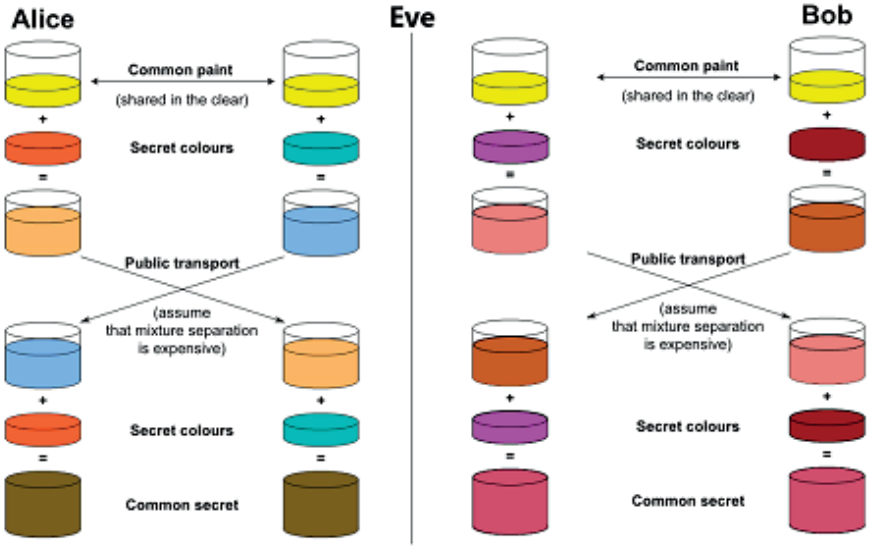

Figure 5: Diffie-Hellman MitM

Looking at the image is easy to notice that Alice cannot know if she is communicating with Eve or Bob, the only way to know the other interlocutor is to meet him physically, same thing for Bob.

3.5 - Discrete logarithm problem

The **D-H** algorithm is the application of a mathematical problem called *discrete logarithm*.

Definition 7. *Let $(G, \circ)$ be a cyclic group of order n and let g be a generator of G. Having $y = g^x = g \circ g ... \circ g$ find x.*

We basically need to calculate $x = \log_g y$ (discrete logarithm). One thing to notice is that the solution to this problem is not unique. If G is a cyclic group with g as generator then $g^x = g^z \Leftrightarrow x \equiv z \pmod{n}$. The difficulty in solving a discrete logarithm problem depends also from the chosen group and from the operation defined in it. In fact solving the **DLP** on additive group modulo n is a lot easier that solving **DLP** on multiplicative group(like in *D-H*).

4 - ELLIPTIC CURVE

A lot of public key algorithms, protocols and cryptocurrency (recently born) are based on elliptic curve that allows to have a security level comparable with the one offered by **RSA** and **D-H**, but with faster encryption and decryption time.

Definition 8. *An elliptic curve E on a field $\mathbb{K}$ written as $E/\mathbb{K}$ is given by the Weierstraβ equation:*

$$E : y^2 + a_1xy + a_3y = x^3 + a_2x^2 + a_4x + a_6$$

with $a_1, a_2, a_3, a_4, a_6 \in \mathbb{K}$ such that for every point (x_1, y_1) with coordinate in $\overline{\mathbb{K}}$ satisfy E and its partial derivatives $2y_1 + a_1x_1 + a_3$ and $3x_1^2 + 2a_2x_1 + a_4 - a_1y_1$ do not become null.
Another condition to satisfy is that of **non-singularity**. A point of a curve is singular if both the partial derivatives are null. More formally we can write:

Definition 9. *Let:*

$$\begin{aligned} b_2 &= a_1^2 + 4a_2 \\ b_4 &= a_1a_3 + 2a_4 \\ b_6 &= a_3^2 + 4a_6 \\ b_8 &= a_1^2a_6 - a_1a_3a_4 + 4a_2a_6 + a_2a_3^2 + a_4^2 \end{aligned}$$

Using the transformation $y \to y - (a_1x + a_3)/2$ we get an isomorphic curve

$$y^2 = x^3 + \frac{b_2}{4}x^2 + \frac{b_4}{2}x + \frac{b_6}{4}$$

whose cubic polynomial have the roots in the closure of $\overline{\mathbb{K}}$ if and only if the discriminant is not null.

The equation is useful to find out if a curve is elliptic or not.

Definition 10. *Let E a curve defined over $\mathbb{K}$. The discriminant of E denoted by Δ satisfies*

$$\Delta = -b_2^2b_8 - 8b_4^3 - 27b_6^2 + 9b_2b_4b_6$$

The curve is not singular and so its elliptic if and only if Δ is not null. That assure the existence of one unique tangent for each point on the curve.

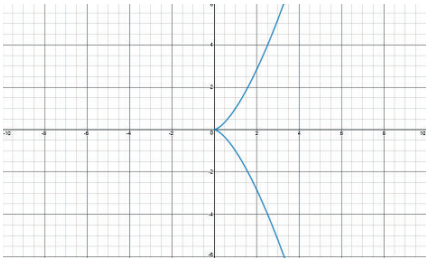

Figure 6: Curve $y^2 = x^3$ with a singular point of cusp $y^2 = x^3 - 3x + 2$

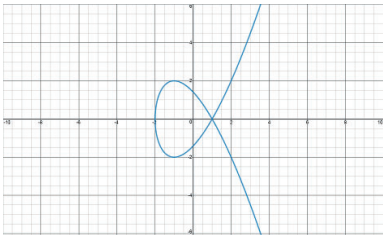

Figure 7: Curve $y^2 = x^3 - 3x + 2$ with a node(singular point)

4.1 - Group law

The set of point described by the curve together with a group operation define a group on $\mathbb{R}$. Since we are in an abelian group we can write $P + Q + R = \Theta$ like $P + Q = -R$. This allows us to derive a geometric way to sum two points $P(x_1, y_1)$ and $Q = (x_2, y_2)$. The result of the operation can be obtained by drawing a straight line that pass on the two points P and Q, the third point R is given by the intersection of the straight line with the curve. The result of the sum is the point R with its y coordinate multiplied by -1.

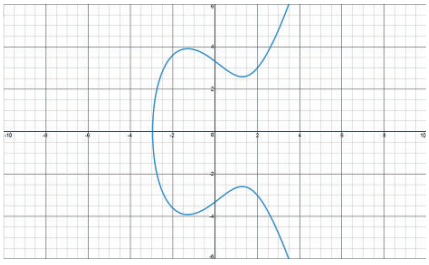

Figure 8: Curve over $\mathbb{R}$

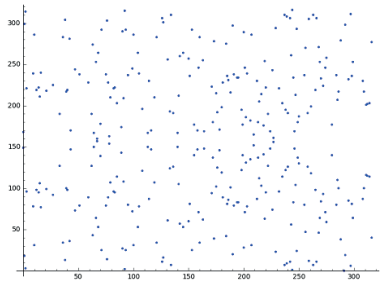

Figure 9: Curve over $\mathbb{F}$

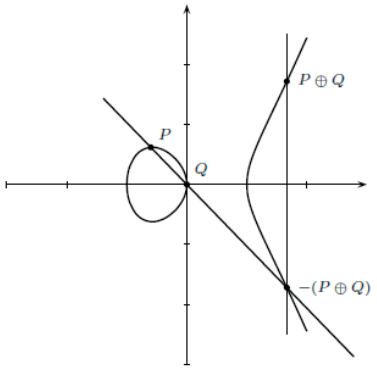

Figure 10: Sum over $\mathbb{R}$

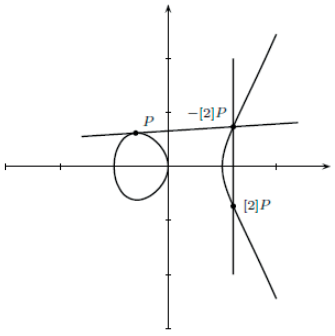

Figure 11: Doubling over $\mathbb{F}$

From the *Weierstraβ* equation we can obtain different kind of curve and each curve have a different group law which depends on the group.

Group law on a field $\mathbb{K} = \mathbb{F}_p$ with p>3

$$y^2 = x^3 + ax + b$$

1. Identity: $P + \Theta = P$ for every P on the curve
2. Opposite: Let $P = (x,y)$ then $(x,y) + (x,-y) = \Theta$. The point $(x,-y)$ is written as $-P$
3. Addition: Let $P = (x_1,y_1)$ and $Q = (x_2,y_2)$ points on the curve with $P \neq \pm Q$. Then $R = P + Q = (x_3,y_3)$ with:

$$x_3 = \left(\frac{y_2 - y_1}{x_2 - x_1}\right)^2 - x_1 - x_2$$
$$y_3 = \left(\frac{y_2 - y_1}{x_2 - x_1}\right)(x_1 - x_3) - y_1$$

4. Doubling: Let $P = (x_1,y_1)$ a point on the curve and $P \neq -P$. Then $R = P + P = (x_3,y_3)$ with:

$$x_3 = \left(\frac{3x_1^2 + a}{2y_1}\right)^2 - 2x_1$$
$$y_3 = \left(\frac{3x_1 + a}{2y_1}\right)(x_1 - x_3) - y_1$$

Group law of super singular curve over $\mathbb{K} = \mathbb{F}_{2^m}$

$$y^2 + cy = x^3 + ax + b$$

1. Identity: $P+\Theta=P$ for every P on the curve
2. Opposite: Let $P=(x,y)\in E$, the point $P^{'}=(x,x+c)$ be on the curve and $P+P^{'}=\Theta$. $P^{'}$ is the opposite of P and is written as $-P$
3. Addition: Let $P=(x_1,y_1)$ and $Q=(x_2,y_2)$ points on the curve, $P\neq\pm Q$. Then $R=P+Q=(x_3,y_3)$ where:

$$x_3=\left(\frac{y_2+y_1}{x_2+x_1}\right)^2+x_1+x_2$$
$$y_3=\left(\frac{y_2+y_1}{x_2+x_1}\right)(x_1+x_3)+y_1+c$$

4. Doubling: Let $P=(x_1,y_1)$ a point on the curve and $P\neq -P$. Then $R=P+P=(x_3,y_3)$ with:

$$x_3=\left(\frac{x_1^2+a}{c}\right)^2$$
$$y_3=\left(\frac{x_1^2+a}{c}\right)(x_1+x_3)+y_1+c$$

Group law of non super singular curve over $\mathbb{K}=\mathbb{F}_{2^m}$

$$y^2+cy=x^3+ax+b$$

1. Identity: $P+\Theta=P$ for every P on the curve
2. Opposite: Let $P=(x,y)\in E$ the point $P^{'}=(x,x+c)$ is a point on the curve and $P+P^{'}=\Theta$. $P^{'}$ is the opposite of P witten as $-P$
3. Addition: Let $P=(x_1,y_1)$ and $Q=(x_2,y_2)$ points on the curve, $P\neq\pm Q$. Then $R=P+Q=(x_3,y_3)$ where:

$$x_3=\lambda^2+\lambda+x_1+x_2+a$$
$$y_3=\lambda(x_1+x_3)+x_3+y_1$$

with $\lambda=(y_1+y_2)/(x_1+x_2)$

4. Doubling: Let $P=(x_1,y_1)$ a point on the curve and $P\neq -P$. Then $R=P+P=(x_3,y_3)$ with:

$$x_3=\lambda^2+\lambda+a=x_1^2+\frac{b}{x_1^2}$$
$$y_3=x_1^2+\lambda x_3+x_3$$

where $\lambda=x_1+y_1/x_2$

Observation 1. *From the group law we can obtain another operation i.e. the scalar multiplication:*

$$n \cdot P = \underbrace{P + P + ... + P}_{n \text{ times}}$$

Looking at the formula we can notice that if n have k bit then the sum would spend about $\mathcal{O}(2^k)$, that's practically not feasible. What we can to do speed up this operation is to use a technique similar to the *Square and Multiply*.

Example 2. *Let $n = 151$, in binary becomes 10010111_2 that we can write like:*

$$151 = 1 \cdot 2^7 + 0 \cdot 2^6 + 0 \cdot 2^5 + 1 \cdot 2^4 + 0 \cdot 2^3 + 1 \cdot 2^2 + 1 \cdot 2^1 + 1 \cdot 2^0$$

and in our case:

$$151 \cdot P = 2^7 P + 2^4 P + 2^7 P + 2^2 P + 2^1 P + 2^0 P$$

That's a lot easier to calculate and take only $\mathcal{O}(\log n)$ to be computed.

4.2 - Order of a group

In general is not easy to calculate how many points are on a **EC**, what we can to is to write and approximation of it using the following theorem:

Theorem 2. ***Hasse-Wail theorem***
Let E an elliptic curve define over $\mathbb{F}_q$. Then

$$|E(\mathbb{F}_q)| = q + 1 - t$$

with $|t| \leq 2\sqrt{q}$

4.3 - Discrete logarithm problem

Definition 11. *Let $(G, \oplus)$ a cyclic group of order p, with p prime. Let $P, Q \in G$ and let P be a generator of G.*
*The **DL** in G of Q respect to P is $n = \log_P Q$ so that:*

$$Q = n \cdot P = \underbrace{P \oplus P \oplus ... \oplus P}_{n \text{ times}}$$

We need to find n, modulo p, knowing only P and Q.

The security of a system that uses a **DLP** on elliptic curve depends also from the group operation $\oplus$ and from the choice of G.
In our case we have:

$$Q = \underbrace{P + P + ... + P}_{\text{n times}} = n \cdot P$$

4.4 - Elliptic curve over finite fields

We only talked about elliptic curve defined over $\mathbb{R}$ but real application uses only finite fields.

Definition 12. *An elliptic curve on $\mathbb{F}_p$ with $p > 3$ is the set of all the point $(x, y) \in F_p$*

$$y^2 \equiv x^3 + ax + b \pmod{p}$$

together with an imaginary point at infinity and with $a, b \in \mathbb{F}_p$ and $4a^4 + 27b^2 \neq 0 \pmod{p}$

5 - STUDY OF A CURVE

Let's take for example the curve $y^2 = x^2 - 5x + 11$ over $\mathbb{F}_{317}$. Graphically on the set of real number and in the finite set we have:

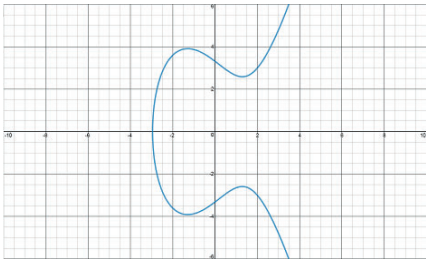

Figure 12: Curve over $\mathbb{R}$

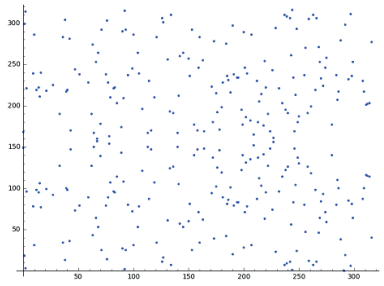

Figure 13: Curve over $\mathbb{F}$

Graphically representing the sum and the doubling we get:

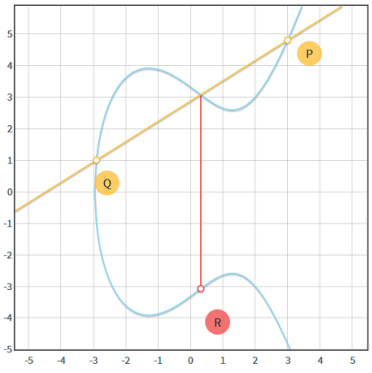

Figure 14: Sum over $\mathbb{R}$

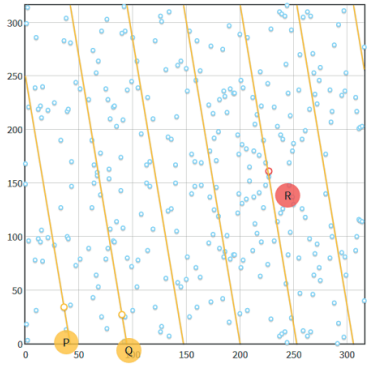

Figure 15: Sum over $\mathbb{F}$

Applying the formulas defined in the group law we get:

- Real field:

$$
\begin{aligned}
&P = (3, 4.7958) \\
&Q = (-2.9054, 1) \\
&R = P + Q = (x_3, y_3) \\
&x_3 = \left(\frac{4.7958 - 1}{2.9054 - 3}\right)^2 - 3 + 2.9054 = 0.3186 \\
&y_3 = \left(\frac{1 - 4.7958}{-2.9054 - 3}\right)(3 - 0.3186) - 4.7958 = -3.0723 \\
&R = (0.3186, -3.0723)
\end{aligned}
$$

- Finite field:

$$
\begin{aligned}
&P = (36, 34) \\
&Q = (90, 27) \\
&R = P + Q = (x_3, y_3) \\
&x_3 = \left(\frac{34 - 27}{90 - 36}\right)^2 - 36 - 90 = 227 \pmod{317} \\
&y_3 = \left(\frac{27 - 34}{90 - 36}\right)(36 - 227) - 34 = 161 \pmod{317} \\
&R = (227, 161)
\end{aligned}
$$

For the doubling:

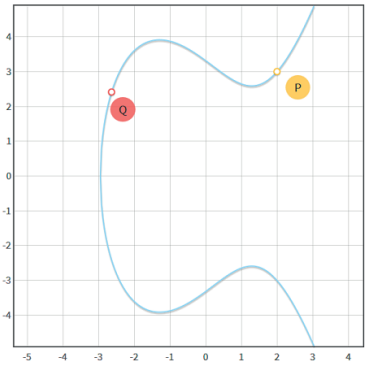

Figure 16: Doubling over $\mathbb{R}$

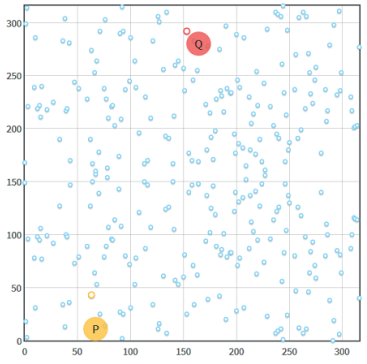

Figure 17: Doubling over $\mathbb{F}$

- Real field:

$$
\begin{aligned}
&P = (2,3)\\
&R = 2 \cdot P = (x_2, y_2)\\
&x_2 = \left(\frac{3 \cdot 2^2 - 5}{2 \cdot 3}\right)^2 - 2 \cdot 2 = -2.6388\\
&y_2 = \left(\frac{3 \cdot 2^2 - 5}{2 \cdot 3}\right)(2 + 2.6388) - 3 = 2.4120\\
&R = (-2.6388, 2.4120)
\end{aligned}
$$

- Finite field:

$$
\begin{aligned}
&P = (63,43)\\
&R = 2 \cdot P = (x_2, y_2)\\
&x_2 = \left(\frac{3 \cdot 63^2 - 5}{2 \cdot 43}\right)^2 - 2 \cdot 63 = 153 \pmod{317}\\
&y_2 = \left(\frac{3 \cdot 63^2 - 5}{2 \cdot 43}\right)(63 - 153) - 43 = 292 \pmod{317}\\
&R = (153, 292)
\end{aligned}
$$

To estimate the order of the curve we use the *Hasse-Weil theorem* and we get that :

$$282 \leq |E(\mathbb{F}_q)| \leq 353$$

Calculating the exact order of a curve is not an easy task, to get a precise result we could calculate and the count every point in the group, but this is not feasible we using group with a big prime number.
In our case since p is very small this approach can be used and after calculating and counting every point we get 312.

6 - ELLIPTIC CURVE APPLICATION IN CRYPTOGRAPHY

A lot of the algorithms defined on finite field can be readapted to be used on group build upon elliptic curve. In the following section we will see two application of it, just to have an idea and to see how much they differ from they corresponding defined only on finite filed.

6.1 - Diffie-Hellman

Compared to the original algorithm, the basic principle is the same we only need to change the group and its operations.
Let's considere the curve $y^2 \equiv x^3 + ax + b \pmod{p}$ with $p > 3$. Alice (**A**) and Bob (**B**) choose a primitive elements P of G then:

- **A** and **B** generate their private key d_A and d_B

- **A** and **B** generate their public key $Q_A = d_A P$ and $Q_B = d_B P$, with $P \in G$ public
- **A** and **B** exchange Q_A and Q_B
- **A** compute $S = n_A Q_B$ and **B** compute $S = n_B Q_A$

Since P is know by multiplying with they private key the message of the other they get a common key to use to encrypt data and after that they can start to communicate.

6.2 - ECDSA

A digital signature is a mathematical scheme used to verify the authenticity of a message. It guarantees to the receiver that the sender is authentic and that the message didn't change on the communication channel.
There are numerous **DSA** (*Digital Signature Algorithm*) based, for example, on elliptic curve, but the overall procedure is the same.

Algorithm

Let's suppose that Alice wants to send a signed message to Bob, the first thing that they have to do is decide the parameters of the curve, (C, G, n) where:

- C is the equation of the elliptic curve and it include the field on which is defined
- G is a generatore of the curve with order n
- n is an integer that's the order of G and that verify: $nG = 0$

Then Alice generate a private key $d_A \in [1, n-1]$ and a public key $Q_A = d_A \cdot G$. Since the parameters Q_A and G are public in theory it's possible to find the secret key d_A and so impersonate Alice.
In practice this is not possible, since finding d_A means solving a *discrete logarithm problem on elliptic curve*. In the following chapter we will see some common algorithm that try to solve the **DLP** and they execution time.

6.3 - Signature

Alice can sign a massage m by following this steps:

1. Compute $e = HASH(m)$ with an hashing function (like SHA)
2. Let z composed by the L_n leftmost bit of e where L_n is the length in bit of the order of the group n.
3. Pick a random integer $k \in [1, n-1]$
4. Compute the point $(x_1, y_1) = k \cdot G$
5. Compute $r = x_1 \pmod n$. If $r = 0$ go back to 3
6. Compute $s = k^{-1}(z + rd_A) \pmod n$. If $s = 0$ go back to 3

7. The digital signature is the pair (r,s)

The parameter k doesn't have to be private, but it's important that it's different every time that we sign a message else we can compute d_A with the information of two signed message.

Verification of the signature
To verify the signature of Alice, Bob must have the point Q_A then checks if the point is on the curve:

- Check that Q_A is not the identity
- Check that Q_A is on the curve
- Check that $n \cdot Q_A = 0$

Next he verify the digital signature.

1. Checks that r and s are both integer in $[1, n-1]$. If this is not the case then the signature is not valid.
2. Compute $e = HASH(m)$ where the hashing function is the same used for the signature
3. Compute $w = s^{-1} \pmod{n}$
4. Compute $u_1 = zw \pmod{n}$ and $u_2 = rw \pmod{n}$
5. Compute a point on the curve $(x_1, y_1) = u_1 \cdot G + u_2 \cdot Q_A$. If $(x_1, y_1) = \Theta$ then the signature is not valid
6. The signature is valid if $r \equiv x_1 \pmod{n}$ else is not valid

It's easy to verify that the algorithm gives the correct result.

$$\begin{aligned} C &= u_1 \cdot G + u_2 \cdot G = (u_1 + u_2 d_A) \cdot G \\ &= \left(zs^{-1} + rd_A s^{-1}\right) \cdot G = (z + rd_A)\, s^{-1} \cdot G \\ &= (z + rd_A)\,(z + rd_A)^{-1} \left(k^{-1}\right)^{-1} \cdot G \\ &= k \cdot G \end{aligned}$$

7 - COMPUTING THE DISCRETE LOGARITHM

The best algorithms to solve discrete logarithm problem on cyclic group have a complexity of $\mathcal{O}(\sqrt{n})$ and they are called *square root algorithms*. In general those algorithm use the birthday paradox as main idea, trying to exploit the collision during the execution. The most famous are: *giant-step, baby-step* and *Pollard-*ρ.

7.1 - Baby-step, giant-step

This algorithm use as main idea the following remark:

Observation 2. *Let x a positive integer. We can write x like :*

$$x = am + b$$

with a, m, b *integer*

We can define the DLP on elliptic curve such as:

$$\begin{aligned} Q &= xP \\ Q &= (am+b)P \\ Q &= amP + bP \\ Q - amP &= bP \end{aligned}$$

The steps that we need to follow to execute our algorithm are:

- Compute $m = \sqrt{n}$
- For each b in $0...m$ compute bP and save the result into an hash table
- For each a in $0, ..., m$ compute:
  - amP
  - $Q - amP$
  - Check if in the hash table exist a point such that $Q - amP = bP$
  - If it exist then we found $x = am + b$

The points bP are the baby step (computed with small increments), while in the second part of the algorithm we calculate the giant step (computed with big increments) A more direct way to explain the overall algorithm is the following. Let's take the equation $Q = amP + bP$ and consider the case:

- When $a = 0$ we check that Q is equal to bP with b in $0, ..., m$. So we are comparing Q with the points ranging from $0P$ to mP
- When $a = 1$ we check that Q is equal to $mP + bP$. So we are comparing Q with all the points ranging from mP to $2mP$
- When $a = 2$ we are comparing Q with all the points ranging from $2mP$ to $3mP$
- ...
- When $a = m - 1$ we are comparing Q with all the points ranging from $(m-1)mP$ to $m^2P = nP$

7.2 - Pollard-ρ

This algorithm use as main idea the birthday paradox.

Definition 13. ***Birthday paradox***
Given a set of n random people we need to find a pair of person with the same birthday. For the pigeonhole principle we have a probability of 100% *if n is 367, but we can get to* 99.9% *only with 70 people.*

This algorithm have the same time complexity of baby-step giant-step, but it doesn't require large amount of space since its spatial complexity is negligible. We divide a group G in three subset S_1, S_2, S_3 of approximately the same order. Let's also suppose that $1 \notin S_2$ and define the sequence $x_0, x_1, ..., x_h, ...$ with $x_0 = 1$ and

$$x_{i+1} = f(x_i) = \begin{cases} \beta \cdot x_i, & \text{if } x_i \in S_1 \\ x_i^2, & \text{if } x_i \in S_2 \\ \alpha \cdot x_i, & \text{if } x_i \in S_3 \end{cases}$$

with $i \geq 0$, $ord(G) = n$, α generator of G and β in G. This sequence, in turn, defines another two sequence $a_0, a_1, \ldots$ and $b_0, b_1, \ldots$ that fulfill $x_i = \alpha^{a_i}\beta^{b_i}$ for $i \geq 0$. Then defining $a_0 = 0, b_0 = 0$ for $i \geq 0$ we get:

$$a_{i+1} = \begin{cases} a_i, & \text{if } x_i \in S_1 \\ 2a_i \pmod n, & \text{if } x_i \in S_2 \\ a_i + 1 \pmod n, & \text{if } x_i \in S_3 \end{cases}$$

$$b_{i+1} = \begin{cases} b_i + 1 \pmod n, & \text{if } x_i \in S_1 \\ 2b_i \pmod n, & \text{if } x_i \in S_2 \\ b_i, & \text{if } x_i \in S_3 \end{cases}$$

We can now use the **Floyd's algorithm** to find two elements on the group, x_i and x_{2i}, such that $x_i = x_{2i}$. So we obtain $\alpha^{a_i}\beta^{b_i} = \alpha^{a_{2i}}\beta^{b_{2i}}$ that we can write as $\beta^{b_i - b_{2i}} = \alpha^{a_2 i - a_i}$. After doing the logarithm in base α on both side, we get:

$$(b_i - b_{2i}) \cdot \log_\alpha \beta \equiv (a_{2i} - a_i) \pmod n$$

Considering $b_i \not\equiv b_{2i} \pmod n$ (the probability that they are equal is very low so we can neglect it).

On elliptic curve the problem is the same. We need to find an x that satisfy $Q = xP$, to do so we use some integer a, b, A, B such that $aP + bQ = AP + BQ$. In short we have:

$$\begin{aligned} aP + bQ &= AP + BQ \\ aP + bxP &= AP + BxP \\ (a - A)P &= (B - b)xP \end{aligned}$$

Then:

$$a - A \equiv (B - b)x \pmod{n}$$
$$x = (a - A)(B - b)^{-1} \pmod{n}$$

where n is the order of the cyclic group G that we are using.
There are different versions of this algorithm but the overall behavior is the same.

7.3 - Baby-step giant-step vs Pollard-ρ vs bruteforce

In this final section we report some execution times of the previous algorithms run on PC for some quite small groups:

Example 3. *Low order curve*
Curve order: 10331
Using bruteforce
Computing all logarithms: 100.00% done
Took 2m 31s (5193 steps on average)
Using babygiantstep
Computing all logarithms: 100.00% done
Took 0m 6s (152 steps on average)
Using pollardsrho
Computing all logarithms: 100.00% done
Took 0m 21s (138 steps on average)

Example 4. *High order curve*
Curve order: 123779
Using bruteforce
Computing all logarithms: 100.00% done
Took 5h 51m 31s (61866 steps on average)
Using babygiantstep
Computing all logarithms: 100.00% done
Took 3m 56s (527 steps on average)
Using pollardsrho
Computing all logarithms: 100.00% done
Took 14m 11s (481 steps on average)

The worst algorithm is the brute force one, like we expected and we can notice that Baby-step Giant-Step is three times faster then Pollard-ρ.
To understand this result we must remind that the advantage of Pollard-ρ over *BS-GS* is the requirement in terms of memory. One require a huge amount of memory(which depends on the order of the group) the other require a negligible amount of memory and so can be used with larger group.
The last thing to notice is the number of steps that each algorithm took to run; we can see that the square root methods needed about half of the step of the brute force, in according with the theory.

8 - REFERENCES

Bernstein D.J., Buchmann J., Dahmen E. (2009) *Post-Quantum Cryptography*. Springer, pp.1-32

Blackburn S. R., Cid C., Mullan C. (2010) *Group Theory in Cryptography*. Department of Mathematics, Royal Holloway, University of London Egham, Surrey TW20 0EX, United Kingdom, pp. 2-6

Cohen H., Frey G., Avanzi R., Doche C., Lange T., Nguyen K., Vercauteren F. (2005) *Handbook of Elliptic and Hyperelliptic Curve Cryptography*. Chapman and Hall/CRC, pp. 19-35, 268-285, 591-607

Corbellini A. (2015) Elliptic Curve Cryptography: A gentle introduction *http://andrea.corbellini.name/2015/05/17/elliptic-curve-cryptography-a-gentle-introduction*

Hankerson D., Menezes A., Vanstone S.A. (2004) *Guide to Elliptic Curve Cryptography*, Springer-Verlag, pp. 76-83

Koblitz N. (1998), *Algebraic Aspects of Cryptography*. Springer(Corrected Second Printing 1999),pp. 18-21, 133-136

McEliece R. J. (1979) *Finite Fields for Computer Scientists and Engineers*. Springer, pp. 3-28

Mermin N. D. (March 28, 2006). *Breaking RSA Encryption with a Quantum Computer: Shorś Factoring Algorithm*, Cornell University, Physics 481-681 Lecture Notes

Schneier B. (1996), *Applied Cryptography*. John Wiley & Sons, pp. 238-241, 233-263

Shor P.W. (1994) *Algorithms for quantum computation: Discrete logarithms and factoring*, Proc. 35th Annu. Symp. Foundations of Computer Science, pp. 124-134.

Silverman J. H. (1986). *The Arithmetic of Elliptic Curves. Graduate Texts in Mathematics*, Springer-Verlag, pp. 137-139

Rend. Acc. Sc. fis. mat. Napoli
Vol. LXXXVI, (2019) pp. 147-164

DOI 10.32092/1022

L'importanza delle definizioni in Matematica

Nota di Margherita Guida[1], Emanuela Romano[2] e del socio Carlo Sbordone[3]
(Adunanza del 20 dicembre 2019)

Keywords: Theorems, proofs, definitions in Mathematics

Abstract - The purpose and nature of definitions, theorems and mathematical proofs are considered. It is our duty as teachers to support students to overcome the difficulties when accepting a "hundred percent precise" definition or recognizing the difference between an empirical argument and the rigorous proof. It is very important to avoid an excess of unnecessary notions in the presentation of single chapters of Mathematics.

Riassunto: Si considerano alcuni aspetti dell'insegnamento della matematica ritenuti essenziali per consentire agli allievi una migliore comprensione della materia. Dalla necessità di dare definizioni precise "al cento per cento", all'opportunità di limitare un eccesso di definizioni (per evitare il rischio di nozionismo matematico). Si raccomanda la massima cura da parte dell'insegnante per un corretto passaggio da considerazioni empiriche, basate su esempi particolari, alle dimostrazioni complete e rigorose.

1 - INTRODUZIONE

Una delle critiche comunemente rivolte alla Matematica ed agli insegnanti di Matematica è che tale disciplina si possa ridurre ad una lista di teoremi tra loro non chiaramente collegati. Tale critica in parte è dovuta alle presentazioni della nostra materia che non si preoccupano di dare definizioni precise delle no-

[1] I.S.I.S. "Elena di Savoia", Largo S. Marcellino 15, Napoli, Università degli Studi di Napoli Federico II, Dipartimento di Matematica e Applicazioni "R. Caccioppoli", Complesso Monte S. Angelo, via Cintia, 80126 Napoli, maguida@unina.it.

[2] Scuola Secondaria di I grado "San Tommaso", Piazza Ettore Imperio 4, Mercato San Severino (SA), emanuela.romano3@istruzione.it.

[3] Università degli Studi di Napoli Federico II, Dipartimento di Matematica e Applicazioni "R. Caccioppoli", Complesso Monte S. Angelo, via Cintia, 80126 Napoli, sbordone@unina.it.

zioni matematiche. Per definizione precisa, qui si intende "precisa al cento per cento". Trattare il tema delle "definizioni precise" significa pensare alle difficoltà che gli studenti possono incontrare nell'apprendimento di certe nozioni matematiche, analizzando gli errori e i fraintendimenti più comuni. In particolare, se l'insegnante sceglie di indicare particolari rappresentazioni di ciò che è oggetto di definizione, quali rappresentazioni può scegliere per la nozione oggetto di studio e come può evitare che l'allievo identifichi l'oggetto con una sua rappresentazione?

La soluzione rigorosa di tale problema si ottiene scegliendo di dare come **definizione** uno dei possibili enunciati e poi dimostrando mediante teoremi che gli altri enunciati sono a loro volta veri, secondo il metodo naturale della matematica che si sviluppa per teoremi.

È ovvio che queste questioni dipendono sia dalla nozione da definire che da altre condizioni, come ad esempio, l'età degli studenti, il percorso didattico seguito, le esperienze matematiche vissute. È anche evidente che, dal punto di vista didattico, nessuna delle precedenti questioni può essere sottovalutata e che, in generale, tali problematiche coinvolgono aspetti di carattere logico, cognitivo ed epistemologico. In mancanza del requisito della precisione nelle definizioni è difficile, anche per uno studente dotato, dare delle spiegazioni logiche, fare ragionamenti corretti.

La matematica è un libro aperto. È accessibile a chiunque sia disposto a rispettare le regole esplicite del gioco. Gli studenti devono acquisire questa consapevolezza prima di impegnarsi a studiarla. Perché ciò accada, gli insegnanti di matematica dovrebbero per primi avere tale convinzione.

Qui di seguito consideriamo due esempi: la nozione di frazione, la nozione di area di una figura piana e, più in generale, descriviamo alcune questioni di geometria.

La nozione di frazione

Dal punto di vista della matematica di livello universitario, la definizione di frazione (o di numero razionale) è la seguente:

frazione = classe di equivalenza

tra coppie ordinate di interi rispetto ad un'opportuna relazione binaria.
Non si può pretendere di presentare a livello così astratto le frazioni in una classe di scuola secondaria di primo grado.
Infatti, i ragazzi concepiscono le frazioni come "parte di un tutto" e questa giusta concezione intuitiva è molto lontana dal mondo delle coppie ordinate e delle relazioni di equivalenza.

La nozione di area di una figura piana

Dal punto di vista della matematica di livello universitario, la definizione di area di un poligono del piano è la seguente:

area = classe di equivalenza

tra poligoni rispetto alla relazione di congruenza fra insiemi misurabili.
Non si può presentare in modo così astratto la nozione di area in una classe di scuola secondaria di primo grado.

Infatti, i ragazzi percepiscono che l'area di un rettangolo con lati di lunghezza intera (ad esempio 4 cm e 3 cm) intesa come numero di quadrati unitari necessari a ricoprire il rettangolo completamente e senza sovrapposizioni, misura 12 centimetri quadri (Fig. 1).

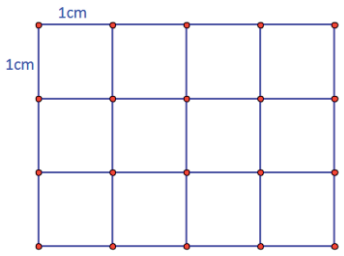

Fig. 1 – Rettangolo di lati di lunghezza 3 cm e 4 cm.

Le definizioni devono esser precise, ma possono avere diversi gradi di accuratezza e completezza a seconda dei destinatari. Una cosa sono gli studenti universitari, altra cosa sono gli allievi di una secondaria di primo grado. Per questi ultimi è opportuno inizialmente limitare ai poligoni le definizioni di area perché, per tali figure geometriche, l'area può essere calcolata esattamente, una volta nota l'area dei rettangoli (base per altezza).

Il riferimento poi alle figure circolari va fatto menzionando procedimenti di approssimazione (basati sulla nozione di limite). Si perviene così ad una definizione incompleta di area, ma almeno la definizione è del tutto corretta. Spesso occorre fare scelte didattiche tra due situazioni del tipo di quella appena descritta. Da un lato la massima correttezza e completezza e dall'altro la necessità di mettere l'ascoltatore in condizioni di capire.

Quali sono i problemi che incontrano i docenti di matematica nelle scuole? Proveremo ad analizzare questo quesito, ponendo l'accento sulle definizioni di nozioni e sulle dimostrazioni di teoremi.

2 - IL RUOLO DELLE DEFINIZIONI

La maggior parte degli insegnanti deve risolvere autonomamente il problema di colmare il divario tra ciò che viene insegnato loro durante il percorso universitario e ciò che essi insegnano agli studenti nelle scuole. Probabilmente va dedicato maggior impegno per consentire ai futuri insegnanti di valorizzare le

caratteristiche essenziali della matematica: la sua precisione, l'importanza del ragionamento logico e la sua coerenza come disciplina. La matematica dovrebbe essere per sua natura un argomento di grande chiarezza. Eppure, essa viene spesso presentata agli studenti delle scuole in modo confuso. Riteniamo auspicabile una solida condivisione delle seguenti caratteristiche della matematica:

1) le definizioni precise costituiscono la base di qualsiasi spiegazione matematica e senza spiegazioni la matematica diventa difficile da imparare;
2) il ragionamento logico è l'essenza della matematica;
3) nozioni ed enti della matematica sono organizzati come parte di un insieme coerente, in modo che la comprensione di qualsiasi nozione richieda anche la comprensione di tutti i legami con altre nozioni ed enti.

Come già accennato, talvolta gli insegnanti non si soffermano con sufficiente enfasi ed efficacia sulle definizioni. Per esempio, nell'introdurre un nuovo ente matematico, a volte gli insegnanti ricorrono ad una presentazione discorsiva e troppo articolata soprattutto se scelgono di descrivere tutte insieme le diverse prestazioni del nuovo ente. *La procedura corretta è invece quella di dare una sola definizione e poi di ottenere attraverso teoremi le proprietà che individuano le altre prestazioni.* In altre parole, occorre che solo una di esse sia adottata come definizione e quindi usata per spiegare perché anche le altre siano valide. Qui consideriamo con attenzione l'insegnamento delle frazioni e della geometria nelle scuole secondarie di primo grado.

Una frazione viene spesso presentata come un ente matematico con diverse identità allo stesso tempo:

1) Una frazione è parte di un tutto (la frazione $\frac{2}{3}$ rappresenta due parti, quando il tutto è diviso in tre parti uguali e poiché non è chiaro cosa intendere per "il tutto", spesso si fa riferimento alla metafora della "pizza");
2) Una frazione è un rapporto (la frazione $\frac{2}{3}$ rappresenta una situazione: vi sono due banchi per ogni terzetto di studenti);
3) Una frazione corrisponde ad una divisione tra due numeri interi di cui il secondo diverso da zero (la frazione $\frac{2}{3}$ rappresenta l'operazione "2 diviso 3").

La terza interpretazione può generare un equivoco. Infatti, gli allievi si apprestano allo studio delle frazioni subito dopo aver appreso la divisione fra numeri interi $m : n$ con n diverso da zero. Pertanto, sono portati ad interpretare la

frazione come suddivisione in gruppi uguali solo se *m* è multiplo di *n.* In caso contrario, la divisione *m : n* è da riguardarsi come divisione con resto e quindi coinvolge **due** numeri: il quoziente *q* ed il resto *r*.

Ad esempio, riguardare 2:3 come un solo ente numerico e tentare di definire $\frac{2}{3}$ come 2:3 è fuorviante.

In realtà l'uguaglianza

$$m : n = \frac{m}{n}$$

è frutto di un **Teorema.**

Alle volte si trova anche scritto che il termine "frazione" si riferisce ad un "operatore" per esempio la frazione $\frac{1}{2}$ corrisponde all'operatore che dimezza gli oggetti. Altre volte si dice che la frazione rappresenta una certa forma di scrittura di numeri. In questo senso una frazione è una coppia di numeri interi *a* e *b* scritti nella forma $\frac{a}{b}$, con la condizione che il numero al denominatore deve essere diverso da zero.

Alla luce di queste difficoltà è matematicamente più appropriato utilizzare la retta dei numeri per definire una frazione come punto su questa retta, come segue. Sulla retta dei numeri fissato un punto origine detto zero ed indicato con 0, per esempio $\frac{1}{3}$ è il primo punto di suddivisione a destra di zero, quando il segmento da 0 a 1 è diviso in tre segmenti di uguale lunghezza (Fig. 2):

Fig. 2 – Costruzione sequenza dei terzi

Analogamente, se dividiamo in tre parti di uguale lunghezza tutti i segmenti [1,2], [2,3], [3,4], … otteniamo la sequenza dei terzi:

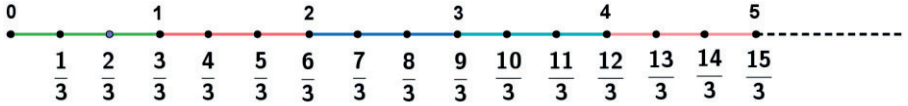

Fig. 3 – Sequenza dei terzi.

Ogni punto della sequenza (Fig. 3) misura la sua distanza da zero, ad esempio $\frac{5}{3}$ è la lunghezza di [0, $\frac{5}{3}$], ma $\frac{5}{3}$ è anche 5 volte la lunghezza di [0, $\frac{1}{3}$], e inoltre è la quinta frazione, nella sequenza dei terzi, a destra di zero.

I numeri $\frac{m}{3}$ sono i multipli di $\frac{1}{3}$ al variare di $m \in N$.

A partire da questo esempio appare chiaro che è possibile dare la seguente definizione di frazione:

Definizione 2.1 *Dati i numeri naturali m ed n, costruiamo la sequenza degli n-simi:* $\frac{1}{n}, \frac{2}{n}, \frac{3}{n}$, *..., dividendo i segmenti* [0,1], [1,2], [2,3], ... *in n parti uguali.*

La frazione $\frac{m}{n}$ *è l'm-simo punto, nella sequenza degli n-simi, a destra di zero.*

In questo modo, fissato n in *N*, al variare di $m \in N \cup \{0\}$ si ottengono tutti i multipli interi positivi $\frac{m}{n}$ di $\frac{1}{n}$ e zero. Esattamente come per *n=1* al variare di $m \in N \cup \{0\}$, si ottengono tutti gli interi positivi m e zero.

Questa definizione di frazione, confrontata con quella che si basa su un pezzo di torta è più facile da applicare: abbiamo scelto di dividere un segmento in n parti di uguale lunghezza piuttosto che un cerchio in n parti congruenti.

Osservazione 2.2 *Per dividere il segmento unitario in un dato numero di parti uguali possiamo usare o il metodo classico delle proiezioni parallele, basato sul Teorema di Talete, oppure il metodo ricorsivo illustrato di seguito (Guida, Sbordone, 2016), che è una versione semplificata dell'algoritmo scoperto in classe da due ragazzi americani, Daniel Litchfield e Dave Goldenheim, che con l'aiuto del loro insegnante Charles Dietrich pubblicarono nel 1997 un articolo sulla rivista Mathematics Teacher* (Litchfield *et al*.,1997).

Versione semplificata algoritmo C. Dietrich, D. Goldenhein, D. Litchfield

Sia AB il segmento unitario [0;1], per determinare la posizione di $\frac{1}{3}$:

- Costruiamo il quadrato ABCD e tracciamo le diagonali DB e AC. Detto V il punto di incontro delle diagonali, indichiamo con M la proiezione ortogonale di V su AB, il punto M sarà il punto medio di AB e quindi $\overline{AM} = \frac{1}{2}$;

- Congiungiamo il punto D con il punto M. Detto G il punto di incontro di DM con AC, indichiamo con H la proiezione ortogonale di G su AB. Per la similitudine dei triangoli AGM e CGD otteniamo $\overline{AH} = \frac{1}{3}$.
- Con analogo procedimento si determinano $\frac{1}{4}, \frac{1}{5}, \ldots$ del segmento unitario.

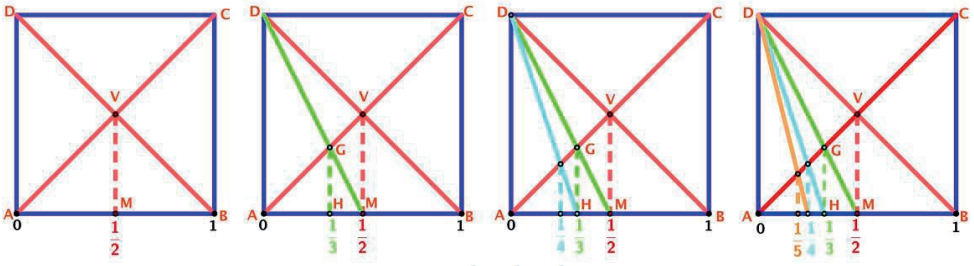

Fig. 4: Determinazione posizione di $\frac{1}{3}, \frac{1}{4}, \frac{1}{5}, \ldots$ del segmento unitario.

3 - ADDIZIONE DI FRAZIONI

Quando si definiscono le operazioni di addizione e moltiplicazione di due frazioni $\frac{m}{n}$ e $\frac{k}{l}$, è ingannevole dare tali definizioni usando rispettivamente le formule

$$\frac{m}{n} + \frac{k}{l} = \frac{ml + nk}{nl}$$

e

$$\frac{k}{l} \times \frac{m}{n} = \frac{km}{ln}$$

che sono frutto di **teoremi**.

L'allievo attento che si vedesse presentare le formule precedenti come **definizioni** di addizione e moltiplicazione, noterebbe subito che quella per l'addizione è più elaborata ed artificiosa di quella della moltiplicazione. Il che è in stridente contrasto con ciò che viene detto a proposito della moltiplicazione e cioè che essa è un'operazione più complessa dell'addizione che a volte viene presentata come un'addizione ripetuta. Gli studenti si domanderebbero: perché non adottare una formula analoga a quella della moltiplicazione (numeratore =

prodotto dei numeratori e denominatore = prodotto dei denominatori) anche per l'addizione e cioè:

$$\frac{m}{n}+\frac{k}{l}=\frac{m+k}{n+l}$$? (FORMULA ERRATA!)

La risposta corretta è che la definizione di somma di due frazioni va data diversamente e deve avere il requisito che, quando le due frazioni da addizionare hanno denominatore uguale a 1, la definizione deve coincidere con quella precedentemente studiata di addizione tra interi.

Vogliamo segnalare che il secondo membro di tale formula (somma dei numeratori fratto somma dei denominatori), come notato da McKay (Sherzer, 1973), tuttavia ha un significato interessante, in quanto a partire da due frazioni positive ridotte ai minimi termini $\frac{m}{n}$ e $\frac{k}{l}$ tale secondo membro costituisce una frazione **compresa** tra esse, che nella pratica è molto più agevole da calcolare rispetto alla media aritmetica tra i due addendi.

Tornando alla definizione di addizione, ci serviamo ora della rappresentazione dei numeri come punti della retta reale.

Il primo caso che esamineremo, nel seguente esempio, è quello più semplice, ossia quello della somma di frazioni con lo stesso denominatore.

Esempio 3.1: La somma $\frac{2}{9}+\frac{5}{9}$ può essere interpretata come la lunghezza della *concatenazione* di due segmenti adiacenti, aventi rispettivamente lunghezza $\frac{2}{9}$ e $\frac{5}{9}$ del segmento unitario [0, 1]. Infatti, se dividiamo in 9 parti uguali il segmento [0, 1] e su di esso evidenziamo in rosso prima i $\frac{2}{9}$ del segmento e poi altri $\frac{5}{9}$ otteniamo che la lunghezza della concatenazione delle due frazioni è la loro somma (Fig. 5).

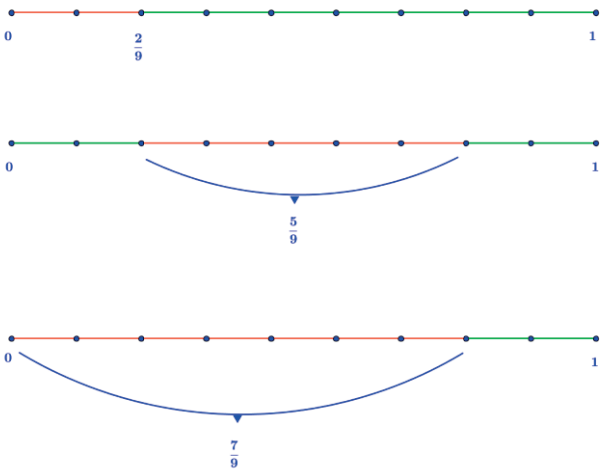

Fig. 5 – Somma delle frazioni: $\frac{2}{9}+\frac{5}{9}$

Da ciò risulta chiaro che in generale la definizione di somma deve essere compatibile con quella illustrata nell'Esempio 3.1.

Definizione 3.2 *Date due frazioni* $\frac{m}{n}$ *e* $\frac{k}{l}$ *, la loro somma* $\frac{m}{n}+\frac{k}{l}$ *è la lunghezza della concatenazione dei due segmenti adiacenti di lunghezze rispettive* $\frac{m}{n}$ *e* $\frac{k}{l}$.

Introdotta tale definizione, usando il Teorema sulla semplificazione di frazioni si ottiene che per l'addizione di frazioni vale la formula illustrata nel seguente Teorema:

Teorema 3.3 *Date due frazioni* $\frac{m}{n}$ *e* $\frac{k}{l}$ *, con* $m,k \in N \cup\{0\}$ *ed* $l,n \in N$*, allora vale la seguente formula per l'addizione:*

$$\frac{m}{n}+\frac{k}{l}=\frac{ml+nk}{nl}$$

4 – MOLTIPLICAZIONE DI FRAZIONI

Esaminiamo ora il caso del prodotto di due frazioni partendo da un esempio.

Esempio 4.1: Consideriamo il prodotto $\frac{1}{4} \times \frac{3}{7}$ che è definito come $\frac{1}{4}$ di $\frac{3}{7}$, ed è la lunghezza di una parte del segmento $[0, \frac{3}{7}]$ quando tale segmento è diviso in 4 parti di uguale lunghezza (Fig. 6).

Fig. 6: Prodotto delle frazioni: $\frac{1}{4} \times \frac{3}{7}$.

Precisamente, sulla retta dei numeri a partire dal segmento [0, 1] si disegna il punto $\frac{3}{7}$ e poi si divide il segmento $[0, \frac{3}{7}]$, in 4 segmenti di uguale lunghezza, il primo segmento evidenziato nella figura 3 è $\frac{3}{28}$ di [0,1] cioè $\frac{1}{4} \times \frac{3}{7}$ (Fig. 6).

Osservazione 4.2 *Si potrebbe anche presentare la moltiplicazione in quattro fasi:*

- *prima fase: eseguire il prodotto dei denominatori delle frazioni che si vanno a moltiplicare;*
- *seconda fase: suddividere l'unità per tale prodotto;*
- *terza fase: eseguire il prodotto dei numeratori;*
- *quarta fase: addizionare un numero di parti dell'unità frazionaria ottenuta pari al prodotto dei numeratori.*

I primi due passaggi possono allora riconnettersi a quella che generalmente viene chiamata frazione di frazione.
Nella definizione (Guida, Sbordone, 2016, Definizione 1.18*) si potrebbe allora dire:*
Date due frazioni $\frac{m}{n}$ *e* $\frac{k}{l}$, *con* $m, k \in N \cup \{0\}$ *ed* $l, n \in N$, *il prodotto* $\frac{k}{l} \times \frac{m}{n}$ *è uguale alla totalità di km parti, quando il segmento [0, 1] è diviso in ln parti di uguale lunghezza, come da utile suggerimento del Prof. Luciano Carbone, che ringraziamo.*

In generale, si ha quindi la seguente definizione di prodotto di due frazioni.

Definizione 4.3 *Date due frazioni* $\frac{m}{n}$ *e* $\frac{k}{l}$ *, con* $m, k \in N \cup \{0\}$ *ed* $l, n \in N$*, il prodotto* $\frac{k}{l} \times \frac{m}{n}$ *ossia* $\frac{k}{l}$ *di* $\frac{m}{n}$ *è dato dalla totalità di km parti, quando il segmento* [0, 1] *è diviso in ln parti di uguale lunghezza.*

Osservazione 4.4 *Dalla Fig. 3 risulta chiaro che se utilizziamo* $\frac{3}{7}$ *come unità di misura sulla retta dei numeri, otteniamo una nuova retta dei numeri dove l'unità è* $\frac{3}{7}$ *e rispetto a questa nuova unità* $\frac{1}{4}$ *è la lunghezza di una parte quando il segmento [0,* $\frac{3}{7}$*] è ripartito in 4 parti di uguale lunghezza. Tale parte ha lunghezza* $\frac{1}{4} \times \frac{3}{7}$*, quindi* $\frac{1}{4}$ *in termini della nuova unità è* $\frac{1}{4} \times \frac{3}{7}$ *.*

Usando la definizione, si dimostra che il prodotto di due frazioni è dato dalla formula illustrata nel Teorema 4.5.

Teorema 4.5 *Date due frazioni* $\frac{m}{n}$ *e* $\frac{k}{l}$ *, con* $m, k \in N \cup \{0\}$ *ed* $l, n \in N$ *, allora vale la seguente formula per il prodotto:*

$$\frac{k}{l} \times \frac{m}{n} = \frac{km}{ln}$$

5 – DIVISIONE DI FRAZIONI

Esaminiamo ora la divisione di due frazioni partendo da un quesito:

Domanda:
Come giustificare l'uguaglianza

$$\frac{\frac{a}{b}}{\frac{c}{d}} = \frac{a}{b} \times \frac{d}{c}$$

brevemente soprannominata "inverti e moltiplica"?

Consideriamo il caso concreto

$$\frac{\frac{2}{3}}{\frac{3}{4}} = \frac{2}{3} \times \frac{4}{3} = \frac{8}{9}$$

che schematizza la situazione seguente:

Un tale ha un certo budget per acquistare un pezzo di terreno. Gli viene detto che con $\frac{2}{3}$ di quel budget potrà acquistare $\frac{3}{4}$ del terreno.

Domanda: "Quale frazione del budget servirà per acquistare l'intero pezzo di terreno?"

Risposta: impostiamo la proporzione

$$\frac{2}{3} : \frac{3}{4} = x : 1$$

Allora si avrà che x è uguale al rapporto considerato.

D'altra parte, riflettendo sul fatto che egli acquisisce 3 parti su 4 dell'intero terreno con $\frac{2}{3}$ del budget (Fig. 7)

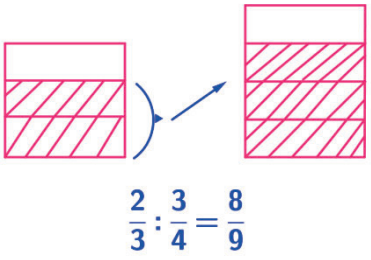

Fig. 7 – Divisione tra $\frac{2}{3}$ e $\frac{3}{4}$

per determinare la frazione del budget che serve a comprare ciascuna di quelle parti, si deve

1) dividere $\frac{2}{3}$ per 3, ottenendo

$$\frac{\frac{2}{3}}{3}$$

2) moltiplicare per 4 quanto appena trovato,

$$\frac{\frac{2}{3}}{3} \times 4 = \frac{\frac{2}{3} \times 4}{3} = \frac{2}{3} \times \frac{4}{3}$$

in quanto si vogliono comprare tutte e 4 le parti.

Gli esempi precedenti mostrano come sia possibile dare una sola definizione di frazione e ottenere attraverso teoremi le proprietà che individuano le altre prestazioni. Questa procedura migliora la comprensione della nozione in questione, perché sottolinea l'interazione logica dei diversi significati. Infatti, è generalmente riconosciuto che l'attuale crisi di educazione matematica deriva dall'assenza di ragionamento logico nelle aule di matematica. È importante anche presentare ogni argomento nuovo di matematica partendo da qualche problema concreto e applicativo, che ne giustifichi l'utilità e lo studio. Generalmente, per conoscere l'utilità della matematica basterebbe un solo esempio significativo per indicare il motivo per cui è importante per poi passare subito alla definizione rigorosa.

In particolare, lo studio della geometria nella scuola merita una considerazione a parte. Il problema principale riguarda l'approccio universitario: se nel corso degli studi universitari la geometria non viene insegnata adeguatamente, l'unica esperienza di "geometria per la scuola" che gli insegnanti di matematica della secondaria di primo grado hanno nel loro bagaglio culturale è la loro stessa esperienza di ex allievi di scuola superiore.

Si può osservare quindi come le questioni riguardanti le frazioni e quelle riguardanti la geometria euclidea abbiano un elemento in comune: un loro insegnamento inadeguato diverrà responsabile del rifiuto dello studio matematica da parte degli studenti per tutto il successivo percorso di studi.

6 - DIMOSTRAZIONI EMPIRICHE E DIMOSTRAZIONI MATEMATICHE

La geometria è fondamentale come studio e comprensione dello spazio che ci circonda ed è uno dei più complessi edifici concettuali sviluppati dall'uomo. La crisi della Geometria dipende dalla difficoltà che presentano le dimostrazioni nella pratica di tale ramo della matematica. A differenza di quanto avviene in aritmetica o in algebra, le dimostrazioni geometriche presentano la caratteristica dell'interazione tra immagine visive e aspetti analitici. È molto difficile arrivare ad una autonoma capacità dimostrativa in mancanza di esperienza di geometria sperimentale. Inoltre, senza una buona dose di intuizione geometrica non c'è verso di portare a termine una dimostrazione. Non sembra possibile, da vari studi eseguiti da matematici professionisti, che l'intuizione geometrica si possa acquisire attraverso animazioni ottenute al computer. Nonostante le animazioni contengano importanti ed innovativi elementi di apprendimento, sembra fondamentale per acquisire sicurezza in geometria (specialmente dello spazio) la costruzione a mano di modelli e l'uso di riga e compasso. Sin dalla scuola primaria occorre una frequente esperienza geometrica. Le dimostrazioni geometriche non si basano su un insieme di tecniche e algoritmi. Per tale ragione, in molte circostanze lo studente non sa da dove cominciare il processo dimostrativo. È opportuno apprendere e ripetere più volte le dimostrazioni in geometria. Obiettivo importante dell'insegnante è quello di comunicare correttamente la natura delle dimostrazioni in Matematica, far comprendere gli enunciati dei teoremi e le loro dimostrazioni agli allievi. La difficoltà che si incontra sta nelle differenze che sussistono tra contesto matematico e realtà quotidiana. Infatti, nella vita quotidiana la nozione di "ragionamento corretto" non è ovvia, perché partendo dalle stesse premesse si può arrivare a conclusioni diverse. In matematica, invece, un "ragionamento matematico corretto" porta ad un'unica conclusione. In molti casi, l'azione di dimostrazione intrapresa dagli studenti è quella di partire da esempi particolari in cui il teorema funziona per poi dedurre l'universale. Sebbene tale approccio abbia i suoi lati positivi, perché se non altro semplifica la situazione, deve esser ben chiaro a tutti che un enunciato è vero se lo è in tutti i casi possibili, senza eccezione alcuna. Dunque, bene partire dal particolare per congetturare l'universale, in quanto è come aver fatto una "dimostrazione empirica". Nel seguito mostriamo come sia diverso il concetto di "dimostrazione" quando si fa Matematica da quando si fa Fisica.

In Matematica, se proviamo a scomporre un numero pari (maggiore di 2) nella somma di una coppia di numeri dispari, notiamo che fra queste coppie è sempre possibile trovarne una o più d'una costituita da due numeri primi:

- $10 = 3+7$
- $28 = 11+17$

- 100 = 53+47 = 59+41 = 71+29 = 83+17 = 89+11

- 1000 = 491+509 = 479+521 = 443+557 = 431+569 = 383+617 = 359+641 = 353+ 647 = 347+653 = 317+683 = 281+719 = 257+743 = 239+761 = 227+773 = 191+809 = 179+821 = 173+827 = 137 + 863 = 113+887 = 89+911 = 71+929 = 59+941 = 53+947 = 47+953 = 29+971= 23+977 = 17+983 = 3+997

Se si effettuano moltissime prove su numeri pari, si controlla che ciò è vero senza nessuna eccezione. In altre parole, non è stato mai trovato un numero pari che non sia scomponibile nella somma di due numeri primi. Quindi, è naturale dire che:

A) OGNI NUMERO PARI (MAGGIORE DI 2) È SCOMPONIBILE NELLA SOMMA DI DUE NUMERI PRIMI

In Fisica, analogamente, cioè eseguendo moltissime prove, si controlla la validità della legge della caduta libera dei gravi nel vuoto. Perciò i fisici dicono:

B) OGNI GRAVE CADE LIBERAMENTE NEL VUOTO CON MOTO UNIFORMEMENTE ACCELERATO, E OGNUNO CON LA STESSA ACCELERAZIONE

La proposizione **B)** viene ritenuta vera perché dimostrata sperimentalmente, la proposizione **A)** per i matematici è solo una congettura (la congettura di Goldbach).

Per i matematici non basta aver fatto un enorme quantità di verifiche per avere la certezza che essa valga sempre (cioè per tutti i numeri pari), dato che l'insieme dei numeri pari è **infinito**, mentre le prove che noi possiamo fare sono sempre in numero finito.

La circonferenza della matematica ha una perfezione irraggiungibile mediante i modelli che di volta in volta possiamo realizzare.

Siamo in presenza di un fenomeno interessante: gli enti geometrici vengono definiti e trattati con un linguaggio astratto, ma noi non siamo in grado di concretizzare questi enti nel nostro mondo sensibile.

La Matematica a volte viene sviluppata indipendentemente dalle sue applicazioni agli altri rami del sapere e spesso i suoi risultati trovano riscontro sensibile solo in epoche successive.

Il Teorema di Pitagora, ad esempio, secondo il quale: "*il quadrato costruito sull'ipotenusa c di un triangolo rettangolo è equivalente alla somma dei quadrati costruiti sui cateti a e b*" è stato talvolta concretamente presentato in qual-

che “Science Centre”, realizzando un dispositivo del tipo in nella Fig. 8 e facendolo ruotare adeguatamente.

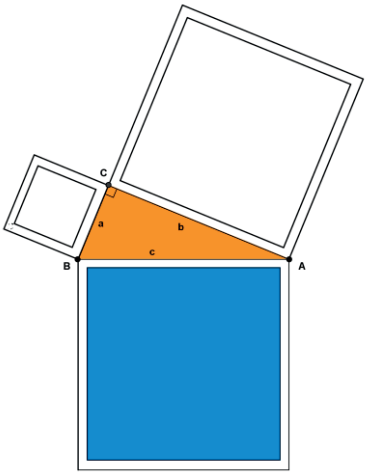

Fig. 8 – Teorema di Pitagora con liquidi

Il liquido, che inizialmente riempie il recipiente a forma di quadrato costruito sulla ipotenusa, previa una rotazione, va a riempire i due recipienti quadrati costruiti sui cateti. Si ottiene così una prova “tangibile” del teorema di Pitagora: Prima di passare ad approfondire tale “prova sperimentale” e di mostrarne i limiti, presentiamo una ben nota dimostrazione rigorosa e semplice, relativo al caso particolare che il triangolo rettangolo sia anche isoscele, cioè che abbia i cateti uguali (Fig. 9).

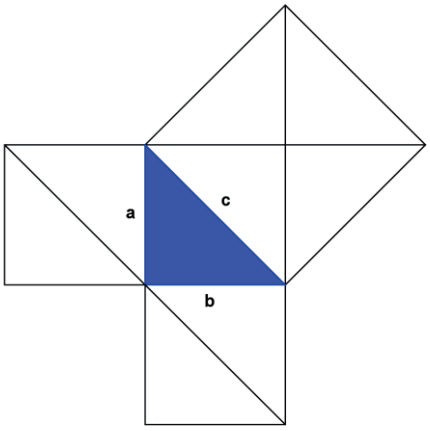

Fig. 9 – Teorema di Pitagora per triangolo rettangolo isoscele

Il quadrato costruito sull'ipotenusa c viene scomposto in quattro triangoli equivalenti a quello dato, mentre ciascuno dei due quadrati costruiti sui cateti è scomponibile in due triangoli equivalenti a quello dato. Ne segue il teorema.

Eppure, il dispositivo non funziona perfettamente. Si vede chiaramente che spostando il liquido dal quadrato grande in quelli piccoli, ve ne è una piccola quantità che avanza (Fig. 10):

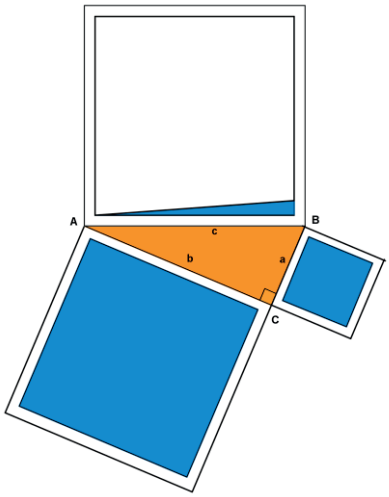

Fig. 10 – Teorema di Pitagora (dimostrazione con liquidi)

Il motivo è il seguente. Un qualsiasi contenitore di liquido deve avere delle pareti con certo spessore. Dunque anche i contenitori a sezione quadrata costruiti nel dispositivo avranno uno spessore e se le loro pareti esterne misurano a, b, c con $a^2+b^2=c^2$, le loro pareti interne misureranno per lati non a, b, c ma $a-\varepsilon, b-\varepsilon, c-\varepsilon$.

Si verifica subito che a fronte dell'uguaglianza pitagorica $a^2+b^2=c^2$ si ha invece la disuguaglianza

$$(a-\varepsilon)^2+(b-\varepsilon)^2 < (c-\varepsilon)^2$$

per ε sufficientemente piccolo.

Per convincerci con un esempio di questo fatto, immaginiamo di partire dalla terna pitagorica $a=3, b=4, c=5$ ($3^2+4^2=5^2$) e supponiamo che sia $\varepsilon=1$.
Si ha:

$$a-\varepsilon=3-1=2,\ \ b-\varepsilon=4-1=3,\ \ c-\varepsilon=5-1=4$$

dunque

$$2^2 + 3^2 = 13 < 16 = 4^2$$

Dunque la terna 2,3,4 non è una pitagorica e la somma delle aree dei quadrati di lato 2 e 3 è inferiore all'area del quadrato di lato 4.

In sostanza il dispositivo non riproduce una dimostrazione esatta del Teorema di Pitagora, ma ne costituisce una prova sperimentale approssimativa, che suscita anche interesse, perché mette in luce un'ulteriore proprietà delle terne pitagoriche.

In conclusione, per quel che concerne la matematica non possiamo non rilevare un dato estremamente positivo per la scuola italiana: con il corso di laurea in Scienze della formazione primaria lo spazio di crediti (CFU) di matematica è notevole, raggiungendo il numero di 20 in molte sedi. In tale contesto, si riesce a dare una buona formazione sulle nozioni matematiche ai futuri insegnanti della scuola primaria.

7 - BIBLIOGRAFIA

Guida M., Sbordone C. (2015) La Matematica e le sue attrattive per i giovani, *Quale Scuola? Le proposte dei Lincei per l'italiano, la matematica, le scienze*. *Introduzione di Tullio De Mauro.* A cura di F. Clementi, L. Serianni, Collana: Sfere (105), Casa editrice Carocci, Roma, pp.85–101.

Guida M., Sbordone C. (2016) Sull'insegnamento delle frazioni nella scuola secondaria, *Orizzonti Matematici. Tra didattica e divulgazione. A cura di S. Cuomo, S. Rionero, C. Sbordone*, Società Nazionale di Scienze, Lettere e Arti in Napoli, Memorie dell'Accademia di Scienze Fisiche e Matematiche, Giannini Editore, Napoli, pp.105-126.

Litchfield D.C., Goldenheim D.A., Dietrich C.H. (1997) Euclid Fibonacci Sketchpad, *The Mathematics Teacher*, **Vol. 90**, N.1, 8–12.

Sherzer L. (1973) McKay's Theorem, *Mathematics Teacher*, **Vol. 66**, 229–230.

Wu H. (2011) *Understanding Numbers in Elementary School Mathematics*, American Mathematical Society, Providence, Rhode Island, 551 pp.

Rend. Acc. Sc. fis. mat. Napoli
Vol. LXXXVI, (2019) pp. 165-198

DOI 10.32092/1023

Il Fondo Stampacchia

Nota di Luciano Carbone[12*], Maria Rosaria Enea[3] e Nicla Palladino[4]
(Adunanza del 20 dicembre 2019)

Keywords: History of Mathematics, Guido Stampacchia.

Abstract - In this work, we want to describe documents that the heirs of the mathematician Guido Stampacchia donated to the Department of Mathematics and Applications "Renato Caccioppoli" of the University of Naples "Federico II". The archive consists, *e. g.,* of Stampacchia's papers and preliminary versions of papers, conference reports, letters with more than 300 correspondents, documents concerning his activities within organizations as U.M.I., C.I.M.E., I.A.C and his university career.

Riassunto - In questa nota, descriviamo i documenti acquisiti dal Dipartimento di Matematica e Applicazioni "Renato Caccioppoli" dell'Università "Federico II" di Napoli appartenuti al matematico Guido Stampacchia. Il fondo, donato dagli eredi del matematico, consiste prevalentemente di lavori e versioni preliminari di lavori, relazioni a congressi, lettere con più di 300 corrispondenti, documenti riguardanti le sue attività all'interno di organismi quali l'U.M.I., il C.I.M.E., l'I.A.C. e la sua carriera.

1 - INTRODUZIONE

Guido Stampacchia (1922-1978) è stato senza dubbio uno degli studiosi di analisi matematica più influenti nel terzo quarto del Novecento. Nato a Napoli da famiglia ebrea per parte di madre e protestante per parte di padre, frequentò

[1]Dipartimento di Matematica e Applicazioni "Renato Caccioppoli", Università degli Studi di Napoli "Federico II", Complesso Universitario di Monte Sant'Angelo, Via Cintia, Napoli.

[*]Corrispondenza a luciano.carbone@unina.it.

[3]Dipartimento di Matematica, Informatica ed Economia, Università degli Studi della Basilicata, Macchia Romana, via dell'Ateneo Lucano, Potenza.

[4]Dipartimento di Matematica e Informatica, Università di Perugia, Via Vanvitelli 1 Perugia.

il liceo Giambattista Vico, ove ebbe come docente di filosofia un giovane Giuseppe Martano, che avrebbe lasciato una traccia importante nella sua formazione. Entrato nella Scuola Normale Superiore di Pisa nel 1940, ebbe come maestro Leonida Tonelli dal quale attinse interesse per i metodi diretti nel calcolo delle variazioni.

I casi della guerra lo riportarono a Napoli e presso l'Università di Napoli completò gli studi in matematica nel 1944 sotto la guida di Carlo Miranda, grazie ai cui insegnamenti imparò a maneggiare con maestria le tecniche di teoria del potenziale e, soprattutto, di Renato Caccioppoli che lo introdusse ad una visione analitico-funzionale. A Napoli rimase fino al 1952, anno nel quale vinse un concorso di professore straordinario. Si trasferì allora all'università di Genova, ove divenne ordinario. Nel 1960 passò all'università di Pisa, nel 1968 a quella di Roma e nel 1970 infine fu di nuovo a Pisa ma alla Scuola Normale. La morte lo colse a Parigi, ove si trovava per un periodo di ricerca, ad appena 56 anni. Per suo espresso desiderio è stato sepolto a Napoli nel cimitero britannico.

Tra le varie importanti funzioni svolte vale la pena di menzionare almeno quella di presidente dell'Unione Matematica Italiana dal 1967 al 1973.

Nella sua vasta attività scientifica vanno segnalati almeno i contributi dati da un lato alla soluzione del diciannovesimo problema di Hilbert, sia direttamente sia come stimolo all'attività di Renato Caccioppoli e di Ennio de Giorgi (al quale ultimo viene correntemente attribuito il passo finale nella soluzione di tale problema), dall'altro alla fondazione della teoria delle disequazioni variazionali. Va inoltre esplicitamente segnalata la vasta rete di importanti collaborazioni scientifiche internazionali che egli costruì a partire dagli anni Sessanta del Novecento e della quale poterono godere anche i suoi numerosi allievi.

Alla figura di Guido Stampacchia sono dedicati numerose biografie e vari ricordi (cfr. De Giorgi 1978, 1980; Garroni 2005; Kinderlehrer 1988; Lions 1978; Magenes 1978a, 1978b, 2005, 2018; Mancino 2005; Mazzone 2005, 2019; Moscariello, Sbordone 2018; Nirenberg 1996-97, 2005; Sbordone 2005; Stampacchia Giulia 2005, ai quali rinviamo per approfondimenti. Le sue opere sono state raccolte per conto dell'Unione Matematica Italiana in due volumi: Stampacchia 1996-97, a cura di L. Boccardo, G. Da Prato, U. Mosco, V. Murthy, M. G. Platone, C. Sbordone e, per conto del Dipartimento di Matematica e Applicazioni "Renato Caccioppoli" dell'Università di Napoli "Federico II", a cura di G. Moscariello e C. Sbordone (Moscariello, Sbordone 2018b).

I materiali conservati nel suo studio presso la Scuola Normale furono donati dalla famiglia subito dopo la sua morte a questa istituzione; i materiali invece custoditi presso la sua abitazione accompagnarono nel corso degli anni sua moglie Sara Naldini. Alla scomparsa di quest'ultima, i figli Mauro, Renata, Giulia e Franca in considerazione anche dei profondi legami che il loro genitore aveva con la sua città natale e con il suo maestro Renato Caccioppoli hanno ritenuto opportuno farne dono proprio al Dipartimento di Matematica "Renato Cacciop-

poli" dell'Università degli Studi di Napoli "Federico II". Recentemente infine un nucleo di circa trecento volumi a stampa, appartenuti a Stampacchia, è stato individuato presso la Biblioteca di Matematica, Fisica ed Informatica dell'Università degli Studi di Pisa.

2 - PRINCIPI DI RIORDINO E CATALOGAZIONE DEL FONDO

Va innanzi tutto osservato che il fondo, costituito da sette plichi voluminosi, è stato parzialmente ordinato da Mauro Stampacchia che ha cercato di conservare quelle unità in qualche modo già costituite da suo padre. Va anche notato che la documentazione è stata precedentemente esplorata in maniera approfondita da Silvia Mazzone che l'ha utilizzata nel comporre le biografie prima menzionate e ha dato un contributo alla riorganizzazione di parte dei materiali stessi.

Nel riordinare e catalogare il fondo, si è cercato in qualche modo di contemperare due esigenze tendenzialmente in contrasto, quella cioè di dar conto dell'attività di Guido Stampacchia e quella invece di offrire a studiosi di altre tematiche e altre figure la possibilità di verificarne la presenza nel fondo stesso. A tale scopo si sono costituiti, ad esempio, dei fascicoli tematici, utilizzando il lavoro già svolto, e contemporaneamente dei repertori per la corrispondenza ed i lavori. Un opportuno sistema di rinvii consente di integrare i fascicoli con i repertori e viceversa.

Diamo qui di seguito una descrizione del fondo articolata in varie sezioni.

3 - DESCRIZIONE DEL FONDO

3.1 - Versioni preliminari di libri di Stampacchia

- Equations elliptiques du second ordre à coefficients discontinus. 1966.
- (con Kinderlehrer) An introduction to variational inequalities and their applications. Ed. Academic Press.
- (con J. Cecconi) Lezioni di Analisi matematica. Vol. I, ed. Liguori, Napoli 1966.
- (con J. Cecconi) Lezioni di Analisi matematica. Vol. II, ed. Liguori, Napoli 1980.

3.2 - Minute di corsi e cicli di conferenze tenuti da Stampacchia

- Appunti del corso di Analisi superiore, Università di Pisa 1963/64. Ne esistono una versione dattiloscritta, una manoscritta in italiano ed una manoscritta in inglese.
- Appunti del corso di Analisi superiore (teoria della misura), Università di Genova prima del 1960. Ne esistono una versione dattiloscritta e una manoscritta.

- Equazioni differenziali ellittiche del secondo ordine, Università di Pisa 1963/64.
- Appunti per le ultime lezioni in Francia, 28 febbraio e 2 marzo 1978.
- Théorie de inéquations variationnelles. Collège de France (Parigi) 1976.
- Second order elliptic differential equations. Università del Minnesota 1962.
- Some regular variational problems. Courant Institute (New York) 1962.
- Teoria delle funzioni di più variabili complesse. Quaderno manoscritto. Forse parte di un corso di Istituzioni di analisi superiore.
- I punti all'infinito. Quaderno manoscritto. Forse parte di un corso di Istituzioni di analisi superiore.
- Corso sulle equazioni a derivate parziali. Dattiloscritto con correzioni manoscritte. Forse parte di un corso di Istituzioni di analisi superiore.

3.3 - Corsi e conferenze seguiti da Stampacchia (appunti manoscritti)

- Algebra complementare. Corso tenuto da L. Giuliano presso la Scuola Normale di Pisa presumibilmente tra il 1940 e il 1943.
- Equazioni differenziali nel campo reale (1943).
- Matematiche complementari. Corso tenuto da F. Cecioni presumibilmente tra il 1940 e il 1943.
- Complementi alle lezioni di Analisi matematica, 2ª parte. Corso risalente presumibilmente agli anni 1940-1943.
- Quaderno di appunti di corsi su similitudini, frazioni continue, prodotti infiniti, risalenti presumibilmente agli anni 1940-1943.
- Conferenza tenuta da A. Andreotti (1965).
- Conferenza tenuta da di F. E. Browder.
- Congetture relative a una conferenza tenuta da De Giorgi (probabilmente risalente agli inizi degli anni Sessanta).
- Corso tenuto da J. Dieudonné (probabilmente seguito a Grenoble intorno al 1965).
- Conferenza tenuta da L. Nirenberg
- Corso tenuto da L. Schwartz.

3.4 - Cicli di seminari (note dattiloscritte)

- The coerciveness problem for integro-differential forms. Di S. Agmon, Jerusalem 1958.
- Questioni di Analisi funzionale. Lezioni tenute da L. Amerio, Roma 1954.
- On moduli of Riemann surfaces. Lectures di L. Bers, Zurigo 1964.
- Problemi matematici della teoria delle particelle e dei campi. Corso diretto da A. Borsellino, Varenna 1958.
- Lectures on potential theory. Lezioni tenute da M. Brelot, Bombay 1960.

- Appunti sulla teoria delle superficie continue. Lezioni tenute da L. Cesari, Roma 1955.
- Appunti sulla teoria delle superficie continue e questioni connesse. Lezioni tenute da L. Cesari, Varenna 1954.
- Appunti sulla teoria degli spazi lineari topologici e delle distribuzioni. Lezioni tenute da E. Magenes, Saltino di Vallombrosa 1961.
- Lecture Notes on the theory of elliptic partial differential equations. Lezioni tenute da C.B. Morrey, Chicago 1960.
- Matematica y fisica quantica. Lezioni tenute da L. Schwartz, Buenos Aires 1958.
- Su alcuni problemi della teoria delle equazioni differenziali lineari di tipo ellittico. Lezioni tenute da L. Schwartz, Genova 1957.
- Problèmes de Cauchy et problèmes mixtes en theorie des distibutions. Lezioni tenute da F. Trèves, Berkeley 1959.
- Lectures on linear partial equations with constant coefficients. Lezioni tenute da F. Trèves, Rio de Janeiro 1961.
- Lezioni sulle equazioni alle derivate parziali. (di autore non identificato).

3.5 - Lavori e versioni preliminari di lavori di Stampacchia e materiali ad essi correlati

1. Sulle condizioni che determinano gli integrali di un sistema di due equazioni differenziali ordinarie del primo ordine. Atti Accad. Naz. Lincei. Rend. Cl. Sci. Fis. Mat. Nat. (8) 2, (1947) pp. 411-418.
2. Sulla definizione assiomatica dell'area di una superficie rettificabile. Atti Accad. Naz. Lincei. Rend. Cl. Sci. Fis. Mat. Nat. (8) 2, (1947) pp. 542-546.
3. Sulla semicontinuità degli integrali doppi, in forma ordinaria, nel calcolo delle variazioni. Atti Accad. Naz. Lincei. Rend. Cl. Sci. Fis. Mat. Nat. (8) 3, (1947) pp. 247-253.
4. Alcuni teoremi sull'estremo assoluto degli integrali doppi del calcolo delle variazioni dipendenti dalle derivate del secondo ordine. Giorn. Mat. Battaglini (4) 1(77), (1947) pp. 36-54.
5. Un teorema di calcolo delle variazioni ed applicazioni a problemi al contorno per equazioni alle derivate parziali del tipo iperbolico. Giorn. Mat. Battaglini (4) 2(78), (1948) pp. 81-96.
6. Un'osservazione su un problema ai limiti per l'equazione: $y^{(n)}=\lambda f(x, y, y', \cdots, y^{(n-1)})$. Boll. Un. Mat. Ital. (3) 4, (1949) pp. 235-239.
7. Sulle successioni di funzioni continue rispetto ad una variabile e misurabili rispetto ad un'altra. Atti Accad. Naz. Lincei. Rend. Cl. Sci. Fis. Mat. Nat. (8) 6, (1949) pp.198-201.
8. Le trasformazioni funzionali che presentano il fenomeno di Peano. Atti Accad. Naz. Lincei. Rend. Cl. Sci. Fis. Mat. Nat. (8) 7, (1949) pp. 80-84.

9. Il problema di Goursat per un'equazione alle derivate parziali del secondo ordine di tipo iperbolico. Giorn. Mat. Battaglini (4) 3(79), (1950) pp. 66-85.
10. Gli integrali doppi del calcolo delle variazioni in forma ordinaria. Atti Accad. Naz. Lincei. Rend. Cl. Sci. Fis. Mat. Nat. (8) 8, (1950) pp. 21-26.
11. Criteri di compattezza per gli insiemi di funzioni continue rispetto alle variabili separatamente. Rend. Sem. Mat. Univ. Padova 19, (1950) pp. 201-213.
12. Sopra una classe di funzioni in due variabili. Applicazioni agli integrali doppi del calcolo delle variazioni. Giorn. Mat. Battaglini (4) 3(79), (1950) pp. 169-208.
13. Problema di Dirichlet e proprietà qualitative della soluzione. Giorn. Mat. Battaglini (4) 4(80), (1951) pp. 226-237.
14. Sopra una classe di funzioni in *n* variabili. Ricerche Mat. 1, (1952) pp. 27–54.
15. Sopra una classe di funzioni in *n* variabili e su alcune questioni di calcolo delle variazioni. Atti IV congr. Un. Mat. Ital. Ed. Cremonese, Roma vol.II (1953) pp. 232-238.
16. Problemi al contorno per equazioni di tipo ellittico a derivate parziali e questioni di calcolo delle variazioni connesse. Ann. Mat. Pura Appl. (4) 33, (1952) pp. 211-238.
17. Approssimazione di una funzione su una superficie. Rend. Accad. Sci. Fis. Mat. Napoli (4) 19 (1952) pp. 90-97.
18. Sistemi di equazioni di tipo ellittico a derivate parziali del primo ordine e proprietà delle estremali degli integrali multipli. Ricerche Mat. 1, (1952) pp. 200-226.
19. Problemi variazionali per gli integrali multipli in forma non parametrica. Univ. e Politec. Torino. Rend. Sem. Mat. 13, (1954) pp. 19-29.
20. Sopra una generalizzazione dei problemi ai limiti per i sistemi di equazioni differenziali ordinarie. Ricerche Mat. 3, (1954) pp. 76–94.
21. Problèmes de Neumann relatifs aux équations du calcul des variations. Proc. intern. Math. Cong. Amsterdam 1954, vol. II p. 172.
22. Problemi al contorno misti per equazioni del calcolo delle variazioni. Ann. Mat. Pura Appl. (4) 40 (1955) pp. 193-209.
23. Osservazioni sull'esistenza e sull'unicità della soluzione dei problemi al contorno misti per equazioni a derivate parziali del secondo ordine di tipo ellittico. Rend. Accad. Sci. Fis. Mat. Napoli (4) 22 (1955) pp. 144–148.
24. Proprietà differenziali delle estremali degli integrali multipli del calcolo delle variazioni. Atti V Congr. Un. Mat. Ital. Ed. Cremonese, Roma (1956) p. 183.
25. Problemi ai limiti per i sistemi di equazioni differenziali ordinarie. Le Matematiche Catania 11 (1956) pp. 121-134.

26. Su un problema relativo alle equazioni di tipo ellittico del secondo ordine. Ricerche Mat. 5 (1956) pp. 3-24.
27. Recensione a P.S. Alexandroff Einführung in die Mengenlehre und die Theorie der reellen Funktionen. Boll. Un. Mat. Ital. (3) 11, (1956) pp. 4-5.
28. Completamenti funzionali ed applicazione alla teoria dei potenziali di dominio. Rend. Mat. e Appl. (5) 16 (1957) pp. 415-429.
29. Risposta a quesito di M. Rionero "conduttori e superfici unilatere". Giornale di Fisica (1957) pp. 299-300.
30. Recensione a G. Sansone, R. Conti, Equazioni differenziali non lineari. Boll. Un. Mat. Ital. (3) 12, (1957) pp. 6-8.
31. (con E. Magenes) I problemi al contorno per le equazioni differenziali di tipo ellittico. Ann. Scuola Norm. Sup. Pisa (3) 12 (1958) pp. 247-358.
32. Contributi alla regolarizzazione delle soluzioni dei problemi al contorno per equazioni del secondo ordine ellittiche. Ann. Scuola Norm. Sup. Pisa (3) 12 (1958) pp. 223-245.
33. I problemi al contorno per le equazioni differenziali di tipo ellittico. Atti VI Congr. Un. Mat. Ital. Ed. Cremonese, Roma (1960) pp. 1-24.
34. I problemi di trasmissione per le equazioni di tipo ellittico. Confer. Sem. Mat. Univ. Bari No. 58 (1960) pp. 1-12.
35. Sur des espaces de fonctions qui interviennent dans les problèmes aux limites elliptiques. Colloque sur l'Analyse Fonctionnelle, Centre Belge Rech. Math. (1961) pp. 81-89.
36. Problemi al contorno ellittici, con dati discontinui, dotati di soluzioni hölderiane. Ann. Mat. Pura Appl. (4) 51 (1960) pp. 1-37.
37. Regolarizzazione delle soluzioni di problemi ai limiti ellittici a dati discontinui. Versione italiana del lavoro Régularisation des solutions de problèmes aux limites elliptiques à données discontinues. Proc. Internat. Sympos. Linear Spaces (1961) pp. 399-408.
38. Équations elliptiques à coefficients discontinus. Sem. Schwartz, 5 n.4 (1960-61) pp. 1-16.
39. Recensione a L. Tonelli, Opere scelte. Boll. Un. Mat. Ital. (3) 16, (1961) pp. 3-4.
40. Second order elliptic equations and boundary value problems. Proc. Internat. Congr. Mathematicians, Stockholm, Inst. Mittag-Leffler, Djurshojm (1962) pp. 405-413.
41. On some regular multiple integral problems in the calculus of variations. Comm. Pure Appl. Math. 16 (1963) pp. 383-421.
42. Some limit cases of L^p-estimates for solutions of second order elliptic equations. Comm. Pure Appl. Math. 16 (1963) pp. 505-510.
43. (con W. Littman e H.F. Weinberger) Regular points for elliptic equations with discontinuous coefficients. Ann. Scuola Norm. Sup. Pisa (3) 17 (1963) pp. 43-77.

44. $L^{(p,\lambda)}$-spaces and interpolation. Comm. Pure Appl. Math. 17 (1964) pp. 293-306.
45. Un problema di interpolazione. Atti VII Congr. Un. Mat. Ital. Ed. Cremonese, Roma (1963) p. 347.
46. Équations elliptiques du second ordre à coefficients discontinus. Sem. Equat. Derivées Part., Collège de France (1963-64), III pp. 1-77.
47. Formes bilinéaires coercitives sur les ensembles convexes. C. R. Acad. Sci. Paris 258 (1964) pp. 4413-4416.
48. Le problème de Dirichlet pour les équations elliptiques du second ordre à coefficients discontinus. Ann. Inst. Fourier 15 (1965) fasc. 1 pp. 189-258.
49. Il principio di minimo nel calcolo delle variazioni. Atti Convegno Lagrangiano Atti Accad. Sci. Torino (1964) pp. 1-20.
50. The spaces $L^{(p,\lambda)}$, $N^{(p,\lambda)}$ and interpolation. Ann. Scuola Norm. Sup. Pisa (3) 19 (1965) pp. 443-462.
51. (con E. De Giorgi) Sulle singolarità eliminabili delle ipersuperficie minimali. Atti del Convegno su le Equazioni alle Derivate Parziali. Cremonese, Roma (1965) pp. 55-58.
52. (con J.L. Lions) Inéquations variationnelles non coercives. C. R. Acad. Sci. Paris 261 (1965) pp. 25-27.
53. Équations elliptiques du second ordre à coefficients discontinus. Les presses de l'université de Montréal (1966) pp. 1-326.
54. (con P. Hartman) On some non-linear elliptic differential-functional equations. Acta Math. 115 (1966) pp. 271-310.
55. Note sull'insegnamento della matematica. Boll. Un. Mat. Ital. (3) 21, (1966) pp. 186-190.
56. (con J.L. Lions) Variational inequalities. Comm. Pure Appl. Math. 20 (1967) pp. 493-519.
57. The $L^{p,\lambda}$-spaces and applications to the theory of partial differential equations. Equadiff II Acta Fac. rerum Natur. Univer. comemanae, Math., XVII (1967) pp. 129-141.
58. Su un problema di disequazioni variazionali. Atti del VIII Congresso dell'U.M.I. Trieste 1867, (1968).
59. (con M.K.V. Murthy) Equazioni ellittiche che degenerano. Atti del Convegno sulle Equazioni alle Derivate Parziali, Edizioni Cremonese, Roma (1965) pp. 90-96.
60. (con M.K.V. Murthy) Boundary value problems for some degenerate-elliptic operators. Ann. Mat. Pura Appl. (4) 80 (1968) pp. 1-122.
61. Discorso del prof. Stampacchia presidente dell'U.M.I. Atti dell'VIII congr. dell'Unione Matematica Italiana, Trieste 1967. Bologna (1968) pp. 17-19.
62. Variational inequalities. In Theory and Applications of Monotone Operators (Proc. NATO Advanced Study Inst., Venice, 1968), Edizioni Oderisi, Gubbio (1969) pp. 101-192.

63. (con H. Lewy) On the regularity of the solution of a variational inequality. Comm. Pure Appl. Math. 22 (1969) pp. 153-188.
64. Regularity of solutions of some variational inequalities. In Nonlinear Functional Analysis. Proc. Sympos. Pure Math., Vol. XVIII, Part 1, Chicago, Ill., (1968) pp. 271-281.
65. Discorso del prof. Stampacchia presidente dell'U.M.I. Atti del IX congr. dell'Unione Matematica Italiana, Bari 1971. (1974) p. 6.
66. On the regularity of solutions of variational inequalities. Proc. Internat. Conf. on Functional Analysis and Related Topics, Tokyo (1969) pp. 285-289.
67. (con O.G. Mancino) Convex programming and variational inequalities. J. Optimization Theory Appl. 9 (1972) pp. 3-23.
68. (con H. Lewy) On the smoothness of superharmonics which solve a minimum problem. J. Analyse Math. 23 (1970) pp. 227-236.
69. (con H. Lewy) On existence and smoothness of solutions of some non-coercive variational inequalities. Arch. Rational Mech. Anal. 41 (1971) pp. 241-253.
70. (con M.K.V. Murthy) Errata corrige del lavoro Boundary value problems for some degenerate-elliptic operators'". Ann. Mat. Pura Appl. (4) 90 (1971) pp. 413-414.
71. Introducción a las ecuaciones en derivadas parciales e inecuaciones variacionales. Universidad Nacional de Rosario, Facultad de Ciencias Exactas e Ingenieria (1971).
72. (con A. Vignoli) A remark on variational inequalities for a second order nonlinear differential operator with non Lipschitz obstacles. Boll. Un. Mat. Ital. (4) 5 (1972) pp. 123-131.
73. On a problem of numerical analysis connected with the theory of variational inequalities. Symposia Mathematica, Vol. X (1972) pp. 281-293.
74. (con H. Brézis) Une nouvelle méthode pour l'étude d'écoulements stationnaires. C. R. Acad. Sci. Paris Sér. 276 (1973) pp. 129-132.
75. Le disequazioni variazionali nella dinamica dei fluidi. In Metodi valutatiti della Fisica matematica, Acc. Lincei, Quaderno n. 217, Roma (1975) pp. 169-180.
76. Programmazione convessa e disequazioni variazionali. Ist. di Calcolo delle probabilità, Univ. Roma (1973).
77. On the filtration of a fluid through a porous medium with variable cross section. Russian Math. Surveys, 29 (4), (1974) pp. 89-102.
78. (con D. Kinderlehrer) A free boundary value problem in potential theory. Collection of articles dedicated to Marcel Brelot on the occasion of his 70th birthday. Ann. Inst. Fourier (Grenoble) 25 (1975), no. 3-4, xvii pp. 323-344.

79. (con H. Brézis) The hodograph method in fluid-dynamics in the light of variational inequalities. Archive for Rational Mechanics and Analysis, Volume 61 (1), (1976) pp. 1-18.
80. Hilbert's twenty-third problem: extensions of the calculus of variations. Mathematical developments arising from Hilbert problems, Proc. Sympos. Pure Math., XXVIII (1976) pp. 611-628.
81. (con H. Brézis) Remarks on some fourth order variational inequalities. Ann. Scuola Norm. Sup. Pisa Cl. Sci. (4) 4 (1977), no. 2 pp. 363-371.
82. (con H. Brézis e D. Kinderlehrer) Sur une nouvelle formulation du problème de l'écoulement à travers une digue. C. R. Acad. Sci. Paris Sér. (1978), no. 9 pp. 711-714.
83. Relazioni per Zentralblatt.

3.6 - Lavori e conferenze di Stampacchia di incerta pubblicazione non perfettamente identificabili

Conferenze di Stampacchia non perfettamente identificabili dal titolo noto

- Equazioni a derivate parziali di tipo ellittico negli spazi hilbertiani, conferenza tenuta a Genova il 17 maggio 1954.
- Les inéquations variationnelles pour un operateur différentiel non linéaire de deuxième ordre avec des obstacles non lipschitziens, conferenza tenuta dopo il 1964.
- Su alcuni sviluppi recenti dell'analisi matematica. Anche le Scienze applicate devono utilizzare la matematica moderna.
- L'analisi moderna.
- La nozione di infinità in matematica.

Conferenze di Stampacchia non perfettamente identificabili dal titolo non conosciuto

Si tratta dei testi di due conferenze, che sono state contrassegnate con le sigle A e B. Un breve cenno del contenuto è dato di seguito.

A In essa viene trattato il tema di una possibile definizione della matematica. Dal testo è possibile dedurre la data nella quale la conferenza è stata tenuta: 17 settembre 1966.

B Si tratta del testo di una conferenza espositiva sull'esistenza e la regolarità di equazioni alle derivate parziali di tipo ellittico di ordine qualsiasi in spazi di Sobolev. I riferimenti bibliografici sembrano collocare la data della conferenza nella prima metà degli anni Sessanta del Novecento.

Lavori non perfettamente identificabili e di incerta pubblicazione, dal titolo noto

Si tratta di 12 manoscritti. È possibile che i contenuti siano, almeno parzialmente, in lavori pubblicati. I titoli sono dati qui di seguito.

- Un teorema di confronto per l'esistenza della soluzione di un sistema di equazioni differenziali ordinarie, 1944.
- Sulle rappresentazioni quasi conformi di una superficie quadrabile (risale forse al 1947 circa).
- Generalizzazione delle disuguaglianze di Sobolev.
- Il principio di minimo per il problema di Dirichlet generalizzato.
- La formula di Stokes nell'Analisi Generale - Applicazioni.
- Le funzioni biassolutamente continue in due variabili ed il potenziale logaritmico.
- Problemi al contorno per equazioni del calcolo delle variazioni.
- Solutions continues de problèmes aux limites elliptiques avec données discontinues.
- Su un lemma di Caccioppoli.
- Sul potenziale logaritmico di densità in L^2.
- Sull'equilibrio delle piastre incastrate all'interno.
- Sulle funzioni hölderiane in due variabili.

Lavori o stralci di lavori attualmente non identificabili, di incerta pubblicazione, senza titolo né data

Sono presenti cinque manoscritti che sono stati individuati con le sigle A, B, C, D, E. Un breve cenno del contenuto è dato di seguito.

A Viene affrontato "lo studio di un'equazione differenziale non lineare

$$z''=f(x,z,z')$$

considerando come elemento differenziale la derivata totale pensata come limite di un rapporto incrementale superficiale.
Sia $z(x,y)$ una funzione di due variabili definita nel rettangolo R; se (x_0,y_0) è un punto del rettangolo R, si chiama incremento totale la quantità dipendente da h e k

$$\Delta z = z(x+h,y+k)-z(x+h,k)-z(x,y+k)+z(x,y)$$

Se esiste il limite del rapporto incrementale $\Delta z/h,k$ per h e k tendenti indipendentemente a 0, tale limite si chiama derivata totale e si indica con $z'(x,y)$,".

B Viene studiata sotto opportune ipotesi la regolarità di una funzione somma di un potenziale di singolo strato e di un potenziale di doppio strato in due variabili nei punti angolosi della curva su cui giacciono le distribuzioni di carica. Più esattamente si determina "l'esistenza del limite delle derivate quando il punto si avvicina alla frontiera".

C Si tratta di un manoscritto di 11 pagine all'apparenza incompleto. Vengono stabilite delle stime per le soluzioni del sistema ellittico del primo ordine nel

quale si può riformulare un'equazione ellittica del secondo ordine lineare in forma variazionale in assenza di ipotesi di regolarità sui coefficienti.
Una prima stima consiste nel controllare l'energia della soluzione sulla sfera di centro P e raggio ρ con l'integrale del quadrato dei termini noti sulla stessa sfera moltiplicato per un'opportuna potenza del raggio e l'integrale del quadrato della differenza tra la soluzione e una qualsivoglia costante sulla corona circolare di raggi ρ ed R diviso per $(R-\rho)^2$.
Segue poi l'attacco ad una seconda stima per la quale la soluzione u viene decomposta in una funzione u_0 , armonica, ed un resto u_1 . Al primo addendo viene applicata una stima del tipo precedente mentre il secondo addendo viene trattato con la teoria del potenziale.

D Si tratta di un manoscritto costituito da tre pagine indicate con numeri arabi e da due pagine indicate con le lettere A e B, che sembra incompleto.
Nelle pagine indicate con numeri arabi viene stabilita una diseguaglianza per soluzioni di equazioni ellittiche lineari del secondo ordine in forma variazionale. Il quadrato del gradiente della soluzione viene moltiplicato per una funzione del raggio $\omega(r)$. L'integrale di tale nuova funzione sulla sfera di centro P e raggio ρ viene controllato utilizzando da un lato gli integrali sulla superficie sferica della funzione stessa moltiplicato per ρ^{n-1} , del quadrato della soluzione e dei quadrati dei termini noti moltiplicati per ρ^{n-1} e $\omega(\rho)$ e dall'altro gli integrali sulla sfera ancora dei quadrati dei termini noti moltiplicati per $\omega(r)$ e del quadrato della differenza tra la soluzione e una funzione arbitraria u^- del solo raggio moltiplicato per il rapporto tra il quadrato della derivata di $\omega(r)$ e $\omega(r)$ stessa.
Nelle pagine indicate con A e B si sceglie come funzione u^- la media della soluzione sulla superficie sferica.

E Viene studiata la regolarità (continuità e derivabilità) di soluzioni di disequazioni variazionali. I riferimenti bibliografici sembrano collocare la data della nota nella seconda metà degli anni Sessanta del Novecento.

3.7 - Epistolario

	MITTENTI		
1	ABBATI MARESCOTTI	1	10.5.1977
2	AGMON	2	26.6.1960; 16.8.1973
3	ALBERTONI	2	24.7.1964; 12.12.1972
4	AMBROSETTI	1	14.4.1978
5	AMERICAN MATHEMATICAL SOCIETY	3	1.2.1974; 11.5.1975; 10.5.78

6	AMERIO	1	Vedi Tricomi
7	ANDREOTTI	6	19.10.1962; 5.11.1963; 18.1.1964; 16.5.1964; 1.6.1964; 18.10.1973
8	ANDREW	1	1.6.1964
9	ARONSSON	1	30.6.1965
10	ARUFFO	2	9.5.1964 1.5.1965
11	ATTOUCH	1	23.3.1978
12	ÁVILA	1	21.3.1973
13	BAIADA	2	19.11.1952; telegramma con data illeggibile
14	BALABAN	1	17.6.1963
15	BALL	2	12.5.1973; 23.11.1977
16	BARNER	1	22.12.1977
17	BARSOTTI	3	29.4.1964; 8.5.1964; 13.5.1964
18	BATEMAN	4	30.10.1973; 19.12.1973; ?.01.1974; 26.4.1974
19	BEIRÃO DA VEIGA	1	7.3.1973
20	BENCI	2	7.12.1977; 28.3.1978
21	BENJAMIN	2	17.8.1973; 22.10.1976
22	BERESTYCKI	1	Cartolina s.d.
23	BERNARDINI	1	14.7.1966
24	BLAIRE	2	7.5.1976; 3.1.1977
25	BLIC (DE)	1	30.11.1964
26	BOCCARDI	1	Vedi Togliatti
27	BOCCARDO	1	18.4.1978
28	BOLELLI	1	17.5.1966
29	BOLYAI JANOS MATHEMATICAL SOCIETY	1	s.d.
30	BOMPIANI	4	10.4.1964; 23.5.1964; 25.5.1965; 24.5.1966
31	BORSELLINO	1	17.5.1968

32	BRELOT	4	17.11.1961; 17.1.1974; 19.1.1974; s.d.
33	BREZIS	4	29.5.1967; 11.3.1970; 14.2.1974; 28.11.1977
34	BRITISH COUNCIL	1	15.11.1973
35	BROWDER	4	20.11.1964; 11.2.1965; 22.2.1965; 27.5.1965
36	BRUNSWICK	1	30.4.1964
37	BUCKLAND	1	1.11.1971
38	CAFIERO	2	31.7.1950; 18.5.1966
39	CALVERT	3	5.2.1973; 26.2.1973; 12.5.1973
40	CAMPANATO	2	19.6.1964; s.d.
41	CAMPEDELLI	1	14.3.1968
42	CAPRIOLI	1	Vedi Pagni
43	CAPRIZ	2	14.12.1972; vedi Tricomi
44	CARBONE A.	1	7.12.1977
45	CARBONE L.	1	9.4.1978
46	CARLESON	4	18.3.1965; 14.6.1973; 20.8.1973; 15.10.1973
47	CASEY	5	21.3.1974; 12.9.1974; 14.9.1974; 25.9.1974; 21.10.1974
48	CATTABRIGA	1	Telegramma con data illeggibile
49	CATTANEO	1	Vedi Segre
50	CAUSA	1	18.5.?
51	CECCHI-MORANDI	1	15.3.1977
52	CECCONI	2	26.5.1964; vedi Baiada
53	CESARI	4	31.12.1952; 17.2.1964; 20.3.1964; 16.5.1964
54	CHERUBINO	1	28.11.1952
55	CHOQUET	1	22.3.1974
56	CHRISTOFFERSON	1	14.1.1966

57	CILIBERTO	2	9.5.1977; 7.3.1978
58	CIME	1	11.6.1964
59	CIMMINO	6	28.5.1965; 31.12.1965; 15.1.1966; 28.1.1966; 14.2.1966; 19.2.1966
60	CINQUINI	2	20.11.1952 (cartolina); 3.9.1964
61	CNR	3	18.4.1974; 12.6.1974; 18.6.1974
62	COLLEGE DE FRANCE	1	Invito s.d.
63	COLUCCI	1	18.11.1952 (telegramma)
64	COMITATO DIRETTIVO CELLULA COMUNISTA UNIVERSITARIA	1	30.10.1946
65	CONLEY	1	6.2.1974
66	CONTI F.	2	21.10.1971; 20.3.1978
67	CONTI R.	10	12.11.1952; 15.1.1961; 26.4.1964; 9.7.1964; 22.9.1964; 6.1.1965; 2.5.1965; 15.5.1965; 26.5.1965; 26.1.1978
68	COOPER	1	7.8.1973
69	CORAZZIARI	1	15.5.1966
70	COTTLE	2	9.12.77; 3.1.1978
71	DABONI	1	20.11.1972
72	DAINELLI	4	23.1.1971; 1.2.1971; 7.2.1971; 4.1.1972
73	DANTONI	1	2.6.1964
74	DA PRATO	1	Vedi Campanato
75	DAS	1	22.3.1971
76	D'AURIA	1	15.5.1966
77	DE AGOSTINI ISTITUTO GEOGRAFICO	1	27.12.1973
78	DE FAZI	1	S.d.
79	DE FINETTI	2	28.11.1972; vedi Segre

80	DE LERMA	1	8.5.1964
81	DE MENNA	1	23.7.1976
82	DENY	3	16.5.1964; vedi Choquet; s.d.
83	D'ERASMO	1	6.11.1954
84	DE SOCIO	1	15.11.1973
85	DOU	2	10.7.1973; 22.10.1973
86	DUGAC	1	11.4.1973
87	ECKMANN	1	17.6.1977
88	EDMUNDS	8	9.8.1971; 10.9.1971; 15.3.1973; 1.5.1973; 21.5.1973; 15.1.1974; 6.1.1975; 10.10.1975
89	EINAUDI	4	2.9.1975; 25.9.1975; 2.10.1975; 2.3.1977
90	ELCI	1	8.5.1973
91	ELLIOTT	1	15.11.1971 (contiene una minuta di Stampacchia)
92	ENRIQUES	1	28.12.1972
93	EQUADIFF 78	1	gennaio 1978
94	EVERITT	2	28.6.1971 (contiene una minuta di Stampacchia); 16.8.1971
95	FADNIS	1	19.11.1977
96	FAEDO	8	19.5.1964; 22.6.1964; 21.7.1964; 20.11.1964; 9.2.1964; 6.6.1966; 10.9.1973; 6.2.1976
97	FANTAPPIÈ	1	16.11.1952
98	FANTOZZI	1	15.5.1956
99	FAVILLI	1	S.d.
100	FICHERA	8	27.12.1952; 23.12.1960; 12.1.1961; 4.7.1964; 4.11.1966; 12.10.1967; 2.12.1967; s.d. (telegramma)
101	FISHEL	2	10.7.1964; 24.6.1965
102	FONTONI	1	5.4.1977

103	FREHSE	6	19.3.1974; 17.10.1975; 27.4.1976; 26.10.1977; 26.10.1977; 14.4.1978
104	FRIDMAN	1	3.2.1978
105	FROSTMAN	1	29.11.1961
106	GAGLIARDO	3	?.?.1961 (cartolina); 3.1.1966; 22.10.1973
107	GÅRDING	1	1977 (?)
108	GARIBALDI	1	Vedi Gagliardo
109	GARZANTI	1	24.2.1978
110	GHEORGHIEV	1	12.12.1964
111	GHIZZETTI	3	21.11.1972; 16.7.1974; vedi Tricomi
112	GIACOSA	1	3.3.1970
113	GIANNESSI	1	Cartolina con data illeggibile
114	GIANNI	1	30.11.1966
115	GILBARG	1	10.6.1964
116	GIULIANO	2	21.3.1946; s.d. (biglietto)
117	GIUSTI	1	Vedi Campanato
118	GOLDBERG	2	14.10.1964; 29.4.1973
119	GÖRANSSON	1	5.2.1974
120	GRAFFI	2	16.7.1952; 26.9.1964
121	GRASSILLI	2	31.10.1967; 2.1.1968
122	GRECO	7	9.9.1953; 13.11.1953; 21.11.1953; 7.12.1953; 12.4.1954; 24.10.1954; vedi Cafiero
123	GRISVARD	4	21.4.1965; 1.6.?; 27.10.?; s.d.
124	GUGLIELMINO	3	15.11.1973; 25.11.1973; 23.4.1974
125	GUSSI	1	1.11.1959
126	HAIMOVICI	1	Vedi Gheorghiev
127	HAMENDE	1	10.5.1974
128	HAMPSHIRE	1	29.10.1971

129	HARTMAN	6	26.9.1965; 9.11.1965; 29.11.1965; 29.11.1965; 6.1.1966; 19.1.1966
130	HAY	2	19.3.1964; 20.3.1964
131	HELLWIG	1	1.12.1972
132	HEMÈ	3	15.9.1964; 14.101964; 25.12.1964
133	HERSTEIN	1	12.1.1973
134	HILDEBRANDT	1	10.10.1977
135	HOWARD	2	4.11.1971; 26.11.1971
136	IANNELLI	1	10.2.1971
137	IMBÒ	1	15.6.1966
138	INFORMAZIONE SCIENTIFICA	1	18.5.1966
139	ISTITUTO DI MATEMATICA DI PISA	1	13.5.1966 (telegramma)
140	JACQUJNOT	1	29.4.1964
141	JAROSZEWSKA	1	21.9.1978
142	JOHN SIMON GUGGHENHEIM MEMORIAL FOUNDATION	1	S.d.
143	JOSEPH	1	31.7.?
144	JUBERG	2	16.9.1964; 14.5.1965
145	KANNAI	1	S.d.
146	KAPLAN	1	S.d.
147	KAPLANSKY	1	23.3.1965
148	KATZNELSON	1	12.4.1973
149	KAUFMANN-BÜHLER	2	7.6.1974; 18.3.1975
150	KERIMOV	1	S.d.
151	KILCREASE	1	27.1.1978 (busta)
152	KINDERLEHRER	11	30.1.1974; 13.9.1976; 30.11.1976 (con foto allegata); 8.11.1977; 20.1.1978; 28.1.1978; 27.3.1978;

			31.3.1978; 2.4.?; 13.5.?; vedi Vergara Caffarelli
153	KIRWAN	1	12.7.1977
154	KLEE	1	22.6.1964
155	KLEIN	1	14.6.1965
156	KUSUNOKI	1	28.5.1964
157	LADYZHENSKAYA	1	9.5.1964
158	LAX	2	16.4.1976; ?.3.1978
159	LAZZARINO	1	19.5.1966
160	LEAVITT	1	7.8.?
161	LEDERMANN	2	4.5.1973; 17.8.1973
162	LERAY	9	?.02.1964; ?.02.1964; 15.3.1965; ?.3.1965; 7.4.1965; 4.5.1965; 22.12.1976 (biglietto); 20.12.1977; s.d.
163	LEWIS	3	16.4.1964; 1.6.1964; 18.6.1964
164	LEWY	20	15.6.1964; 14.8.1964; 17.5.1965; 17.3.1967; 10.4.1967; 14.4.1967; 19.4.1967; 2.5.1967; 25.5.1967; 5.10.1967; 25.3.1968; 13.5.1968; 20.10.1973; 3.5.1975; 26.5.1975; 19.12.1976; 19.4.1978; s.d. (3)
165	LIGUORI (EDITORE)	13	15.1.1962; 13.2.1962; 5.11.1962; 20.11.1962; 6.12.1962; 25.5.1963; 10.10.1963; 18.12.1975; 31.5.1976; 10.6.1976; 21.7.1976; 23.6.1977; 26.10.1977
166	LIONS	10	25.3.1964; 28.4.1964; 30.7.1964; 2.7.1966; 12.6.1973; 5.3.1974; s.d. (ma 2.4.1978); s.d. (3)
167	LOHWATER	1	21.2.1964
168	LOMBARDO	1	Vedi Segre
169	LORCH	1	28.12.1972
170	MAGENES	9	16.11.1952 (telegramma); 24.11.1952

			(telegramma); 12.1.1961 (cartolina); 31.5.1964; 29.1.1973; 6.4.1974; ?.4.1974; 23.6.1974; s.d.
171	MAJORANI	1	10.7.1973
172	MAMBRIANI	1	19.11.1952 (telegramma)
173	MANDILI	1	14.11.1972
174	MANGERON	4	9.2.1959; 2.11.1959; 29.10.1964; 24.9.1967
175	MARINESCU	1	S.d.
176	MARTANO	1	16.5.1966
177	MARTINELLI	2	16.11.1967; 15.5.1970 (telegramma)
178	MATHEMATISCHES INSTITUT DER UNIVERSITÄT ZÜRICH	1	S.d. (ma 1977) (invito)
179	MATTHES	1	1.2.1973
180	MAUGERI	1	Vedi Giannessi
181	MAZZONE	2	15.11.1971; vedi Vergara Caffarelli
182	MERLIN	1	2.5.1964
183	MEYER	1	Vedi Choquet
184	MILLER	1	28.9.1973
185	MINTY	1	23.12.1966
186	MIRANDA	7	28.11.1945; 29.11.1960; 20.4.1964; 7.5.1965; 27.5.1965; s.d.; vedi Cafiero
187	MOKOBODSKI	1	Vedi Choquet
188	MONASTERIO	1	26.5.1966
189	MONTEVERDI	1	29.11.1966
190	MORREY	1	7.5.1973
191	MOSCO	2	28.5.1966; 31.3.1978
192	MOSER	2	29.11.1959; 10.5.1965
193	MURAKAMI	1	24.3.1955

194	MURTHY	5	16.12.1972; 20.3.1973; 14.2.1974; 27.11.1975; 20.9.1976
195	MUSSA	2	5.5.1964; 13.5.1964 (telegramma)
196	NACHBIN	1	21.12.1964
197	NALDINI M.	1	24.11.1952
198	NANNIPIERI	1	28.12.1977
199	NARASIMHAN	2	5.3.1964; 11.8.1964
200	NEČAS	1	3.11.1977
201	NEVANLINNA	1	12.4.1978
202	NEWTON	1	18.2.1974
203	NEW YORK UNIVERSITY	1	S.d.
204	NICOLESCU	1	20.2.1965
205	NICOTRA	1	Vedi Conti F.
206	NIRENBERG	24	7.10.1964; ?.?.1964; 6.6.1966; 1.2.1974; 12.3.1975; 28.12.1976; 5.1.1977; 13.12.1977; 15.1.1978; 23.1.1978; 30.1.1978; 12.4.1978; 7.1.?; 21.1.?; 23.1.?; 24.3.?; 1.4.?; 13.4.?; 16.6.?; 21.6.?; 7.7.?; 14.8.?; 25.9.?; s.d.
207	NOOR	1	27.11.1973
208	NUNZIANTE CESARO	2	26. 11.1962; 29.5.1966
209	OLEINIK	4	17.12.1964; 11.6.1973; 9.10.1973; s.d. (cartolina)
210	ONO	2	22.5.1976; s.d.
211	ORLANDO	1	S.d.
212	ORTIZ	2	16.11.1973; 6.6.1975
213	ORTNER	1	22.3.1977
214	PAGNI	6	26.5.1967; 12.2.1971; 22.2.1971; 29.9.1971; 8.8.1971; s.d.
215	PANELLI	1	16.5.1966
216	PANNWITZ	1	20.1.1955

217	PEETRE	2	28.5.1964; 24.7.1964
218	PEREIRA	1	5.7.1978
219	PETTINEO	2	13.10.1964; 21.12.1964
220	PICONE	1	19.5.1968
221	POLVANI	1	7.9.1962
222	PROCURANTI	1	21.5.1964
223	PRODI	1	Vedi Magenes
224	PUCCI	11	17.11.1960 (contiene una lettera collettiva a Schwartz); 14.5.1964; 30.9.1964; 3.3.1965; 3.4.1965; 16.5.1966; 31.12.1970; 25.2.1971; 15.11.1977; s.d.; vedi Togliatti
225	PULVIRENTI	1	15.11.1973
226	RABINOWITZ	1	S.d. (minuta)
227	RADICATI	1	10.4.1964
228	RAMIS	1	14.3.1977
229	RICCI	2	1.6.1964; 3.11.1972
230	RINALDI	1	S.d.
231	RIVIÈRE	1	3.4.1973
232	RIVISTA DI MATEMATICA	1	9.3.1978
233	RIZZITELLI	2	31.5.1977; 24.9.1977
234	ROFMAN	1	S.d.
235	ROSATI	1	27.4.1964
236	ROSSI	1	S.d.
237	ROTA	2	20.1.1974; 15.3.1974
238	RUSSO	1	10.5.1946
239	SACERDOTI	1	23.5.?
240	SANSONE	9	20.1.1961; 10.7.1961; 20.12.1961; 26.6.1962; 7.6.1964; 20.11.1965; 7.12.1965; 7.12.1965; 17.5.1966

241	SANTAGATI	1	Vedi Pulvirenti
242	SCHWARTZ	3	17.11.1960; 7.10.1964; 16.11.1964
243	SCORZA	4	17.3.1964; 1.12.1964; 18.10.1971; vedi Fantappiè
244	SCUOLA NORMALE SUPERIORE (DIREZIONE)	4	19.6.1964; 29.11.1977; 14.12.1977; s.d.
245	SEGAL	1	4.12.1973
246	SEGNI (MINISTRO DELLA PUBBLICA ISTRUZIONE)	1	19.1.1953
247	SEGRE B.	4	14.5.1966; 14.5.1966; 16.6.1966; 30.10.1967
248	SEGRE F.	1	Vedi Lewy
249	SERRIN	2	12.12.1976; s.d.
250	SIBONY	1	2.2.1966
251	SIMS	1	27.10.1971
252	SINGH	1	25.7.1973
253	SMITH	2	18.8.1978; 22.11.?
254	SOCIETÀ NAZIONALE DI SCIENZE LETTERE E ARTI	1	1.1.1978
255	SOLOMON	1	25.7.1966
256	SPAGNOLO	1	27.2.1978
257	SPRINGER-VERLAG	1	14.2.1974
258	STAMPACCHIA L.	1	15.5.1966
259	STANLEY	2	5.12.1963; 29.7.1964
260	STEBBINS	2	12.6.1964; 25.6.1964
261	STOPPELLI	1	Vedi Cafiero
262	STRANG	1	6.4.1977
263	STREBEL	3	13.5.1977; 8.7.1977; 13.10.1977
264	SWANSON	5	Vedi Swanson a Kinderlehrer
265	TALENTI	1	Vedi Pucci

266	TARELLO	20	9.10.1971; 29.11.1971; 29.12.1971; 18.1.1972; 11.2.1972; 17.4.1972; 16.1.1973; 30.1.1973; 7.2.1973; 22.2.1973; 14.3.1973; 18.5.1973; 23.5.1973; 16.7.1973; 11.1.1974; 7.2.1975; 19.2.1975; 19.5.1975; 1.7.1975; 5.11.1975
267	TARTAGLIONE	1	20.5.1966
268	TATA INSTITUTE	1	16.12.1972
269	TAUTZ	1	30.5.1964
270	TAYLOR	1	30.3.1973
271	TEMAN	1	12.3.1977
272	TEODORESCU	2	30.9.1959; 16.11.1959
273	TOGLIATTI	2	19.8.1972; vedi Pucci
274	TOLOTTI	1	20.5.1966
275	TRAPANI	1	S.d. (cartolina)
276	TREVES	2	10.11.1964; 23.9.1967
277	TRICOMI	1	20.11.1972
278	TRUESDELL	1	14.3.1974
279	UNIVERSITÀ DI PISA	2	11.6.1964; 26.5.1972
280	UNIVERSITE' PIERRE ET MARIE CURIE	1	28.3.1978
281	UNIVERSITY OF CHICAGO	1	3.3.1978
282	VALLI	1	Vedi Carbone L.
283	VENEMA	1	13.12.1973
284	VERGARA CAFFARELLI	1	Cartolina con data illeggibile
285	VESENTINI	3	3.5.1964; 4.1.1968; 29.12.?
286	VIDAV	1	29.1.1973
287	VIDOSSICH	4	19.3.1973; 21.5.1973; 19.11.1976; 22.10.1976
288	VILLA	2	10.6.1964; 16.5.1966

289	VILLAGGIO	2	21.12.?; vedi Pucci
290	VINCIGUERRA	1	31.7.1950 (foglio allegato alla lettera di Cafiero)
291	WAELBROECK	1	19.1.1974
292	WALKER	1	21.3.1974
293	WASSERMANN	1	S.d.
294	WEINBERGER	2	13.3.1964; 22.6.1964
295	WELLAND	1	20.6.1973
296	WILEY INTERSCIENCE	2	8.2.1974; 15.3.1976
297	WILSON	1	8.7.1971
298	YOUZHONG	1	12.8.1982
299	ZACHER	2	S.d. (telegramma); s.d. (telegramma)
300	ZAINI	3	13.2.1973; 9.6.1973; 1.8.1975
301	ZICHICHI	1	4.6.1974 (telegramma)
302	ZITAROSA	1	Vedi Cafiero
303	ZITO	2	8.1.1964; 8.6.1964
304	ALD[...] N[…]	1	16.5.1966
305	DEYEN DE LA FACULTÈ DE SCIENCE DI ALGERI	1	20.10.1964
306	DICK	1	6.4.1973
307	DON A[...]	1	17.8.1964
308	FRANCOISE SCH[...]	1	26.1.?
309	HUGH L.Z.	2	12.1.1964; 17.4.1965
310	JAY	1	s.d. (ma venerdì)
311	KOSAKY	1	18.4.1964
312	MARCH[...]	1	15.12.1973 (biglietto di auguri)
313	R. F.	1	s.d.
314	R[...]	1	13.5.1965
315	SA[...]	1	s.d.
316	SE[...]	1	24.1.?

317	UGO BA[...]	1	22.11.1952
318		1	20.1.1951 da Napoli
319		1	18.5.1964 da Pisa

Si osservi che ai numeri 304-319 corrispondono mittenti al momento non identificati. Delle relative lettere sono stati forniti gli elementi identificativi reperibili.

DESTINATARI

1	ACCADEMIA DELLE SCIENZE DI TORINO	1	8.5.65
2	ALBERTONI	1	Vedi Tricomi
3	AMERIO	1	Vedi Tricomi
4	BERTOLINI	1	6.2.1976
5	BOERO	2	11.1.1973; 23.1.1973
6	BROWDER	1	19.2.1965
7	BUCKLAND	1	3.11.1971
8	CAPRIZ	1	Vedi Tricomi
9	CARLESON	2	13.5.1965; 9.6.1965
10	CASEY	2	11.10.1974; 9.11.1974
11	CHRISTOFFERSON	1	19.1.1966
12	CIMMINO	1	7.1.1966
13	DABBONI	1	Vedi Tricomi
14	DE FINETTI	1	Vedi Tricomi
15	DENTON	1	22.8.1971
16	EINAUDI	2	16.9.1975; 18.2.1977
17	FICHERA	5	10.1.1961; 25.7.1964; 14.4.1967; 1.12.1969; 23.2.1966 (minuta)
18	GARRONI	1	2.4.1978
19	GIANNARELLI	1	3.3.1968

20	GHIZZETTI	1	Vedi Tricomi
21	IMAZ	1	17.12.1962
22	KINDERLEHRER	1	7.2.1977
23	LERAY	1	19.2.1964 (minuta)
24	LEWY	4	3.4.1967; 15.4.1967; 20.4.1967; 4.4.1968
25	LIGUORI	7	4.7.1974; 23.7.1975; 6.2.1976; 18.10.1977; 3.12.1977; 5.12.1977; 5.12.1977
26	LIONS	2	16.1.1973; 28.6.1973
27	NEČAS	1	7.9.1977
28	NITSCHE	1	13.6.1977
29	ONO	1	12.6.1976
30	ONORATO	3	16.10.67; s.d. (minuta) (2)
31	PICONE	1	29.10.1949
32	POLVANI	1	19.6.1962
33	PUCCI	2	18.4.1971; 16.1.1973
34	RIVIÈRE	1	11.5.1973
35	ROSE	1	S.d. (minuta)
36	SANSONE	1	23.11.1965
37	SCHWARTZ	1	8.12.1964
38	SPRINGER-VERLAG	1	29.2.1974
39	STREBEL	1	1.6.1977
40	TARELLO	9	17.10.1971 (minuta); 2.12.1971; 1.2.1972; 5.4.1972; 19.2.1973; 12.5.1975; s.d. (ma fine '71, minuta); s.d. (minuta) (2)
41	TRICOMI	1	16.11.1972
42	UFFICIO ITALIANO CAMBI	1	14.1.1977
43	UNIVERSITÀ DI PISA	1	1.2.1965
44	VIGNOLI	1	2.6.1971 (minuta)

45	WEIZMANN SCIENCE PRESS OF ISRAEL	1	30.12.1972
46	WILEY INTERSCIENCE	1	S.d. (minuta)
47	WILSON	1	30.7.1971 (minuta)
48	ZICHICHI	1	14.2.1973
49	BERNARD	1	S.d. (forse 1964; minuta)

Nel precedente elenco, al n. 49 corrisponde un destinatario non identificato**.**

ALTRI CORRISPONDENTI

1	BELLMAN	KINDERLEHRER	1	17.3.1977
2	BOMPIANI	EVANGELISTI	1	2.2.1967
3	BOMPIANI	PAGNI	1	16.3.1968
4	CARDILLO	MONROY	1	4.1.1965
5	CECCHI	LIGUORI	1	22.2.1977
6	D'ATRI	BERNARDINI	1	18.4.1973
7	FAEDO	PUCCI	1	24.12.1963
8	FAEDO	PRODI	1	S.d.
9	FIGÀ-TALAMANCA	SBORDONE	1	18.1.1994
10	FRANCHETTA	CORONATO	1	26.11.1952
11	GEHRING	KINDERLEHRER	1	21.1.1977
12	ITALICA SOCIETÀ DI ASSICURAZIONI	NALDINI STAMPACCHIA	1	29.11.1960 (cartolina postale)
13	Jolanda, Giulio, Dionigi	DE ROSA	1	19.11.1952 (telegramma)
14	KAUFMANN-BÜHLER	KINDERLEHRER	3	8.2.1977; 10.3.1977; 11.5.1977
15	KINDERLEHRER	BELLMAN	1	23.3.1977
16	KINDERLEHRER	GEHRING	1	18.1.1977

17	KINDERLEHRER	KAUFMANN-BÜHLER	2	3.2.1977 20.5.1977
18	KINDERLEHRER	MC GRATH	1	3.9.1981
19	KINDERLEHRER	NALDINI STAMPACCHIA	2	9.2.1984; 25.5.1984
20	KINDERLEHRER	SWANSON	3	20.5.1977; 1.12.1977; 23.1.1978
21	LIGUORI	STRANG	1	15.3.1977
22	MAZZONE	NALDINI STAMPACCHIA	2	2.2.2004; 2.11.2009
23	MAZZONE	STAMPACCHIA M.	1	6.3.2003
24	MC GRATH	LIGUORI	1	7.6.1976
25	MICOL	NALDINI STAMPACCHIA	1	30.3.1983
26	MITROVICH	KINDERLEHRER	1	24.5.1977
27	MONROY	FAEDO	1	9.1.1965
28	NICOTRA	OWUSU-ANSAH	1	22.9.1978
29	NICOTRA	SMITH	1	22.9.1978
30	PAGNI	BUZANO	1	18.12.1967
31	PALLADINO	MAZZONE	1	31.3.2003
32	PRODI	GAGLIARDO	1	18.12.1957
33	PUCCI	LIONS	1	28.12.1972
34	SCHMITZ	KINDERLEHRER	1	31.1.1977
35	SHUBE	KINDERLEHRER	3	10.2.1977; 18.2.1977; 15.4.1977
36	STEBBINS	ANDREOTTI	2	4.5.1964; 11.5.1964;
37	STRANG	LIGUORI	1	9.2.1977
38	SWANSON	KINDERLEHRER	5	22.4.1977; 26.5.1977; 28.11.1977; 7.12.1977; 27.1.1978

Si fa notare che al n. 13 appaiono corrispondenti non meglio identificati**.**

3.8 - Fascicoli tematici

FALDONE 1

- Documenti ufficiali relativi a vita e carriera di Guido Stampacchia
- Raccolta di articoli di giornale eseguita da Guido Stampacchia

FALDONE 2

- Commemorazioni e biografie di Guido Stampacchia
- Articoli e necrologi su giornali relativi alla scomparsa di Guido Stampacchia
- Premi e convegni in memoria di Guido Stampacchia
- Partecipazioni al lutto in occasione della scomparsa di Stampacchia: Agmon; Albertoni; Amerio; Antonsiewicz e Lions; Are; Arias; Aruffo; Aruffo e Bottao; Augugliaro; Baiada, Boni e Cavazzuti; Baiocchi; Benci; Binni; Boccardo, Dolcetta e Marcellini; Borsellino; Brezis; Budinich (Budini); Cafiero; Calvi e Parisetti; Campanato; Carbone, Colombini, Conti F., Franzoni, Pratelli e Ricci; Carrelli; Cattaneo; Chiffi; Chipot; Ciampa; Cecconi; Ciliberto; Cimmino; Cinquini; Conti F.; D'Amato; Da Prato; Da Veiga; De Giorgi; Dolcher; Edmunds; Einaudi; Faedo; Favilli; Fichera; Foa; Focarelli; Galafassi, Serini e Andreatta; Garding; Gatteschi e Lerda; Ghiara; Giuliano; Goldberg; Gomez Paloma; Graffi; John; Kinderlehrer; La Penna; Lax; Lazzarino; Letta e Marino; Lewy Hans; Lewy Helen; Liguori; Littman e Weinberger; Luisi; Mannelli; Marchionna Tibiletti; Marianelli; Martano; Masetti e Milano; Mazzone; Mac Grath; Milani Sciry (?) Sepe; Mini; Miranda C.; Miranda M.; Morawetz; Mosco; Murthy e Narasimhan; Nirenberg; Pagni; Papi; Picasso; Picotti; Predonzan; Procesi; Prodi; Pucci; Pugliese Carratelli; Radicati; Reinhart; Remorini; Thomas Richard; Rizza; Roux; Salam; Salmon; Salvini; Santagati; Schwartz; Serrin; Skof; Torrigiani; Treves; Truesdell; Vaccaro; Vergara; Vesentini; Vidossich; Vinciguerra; Vinti; Webb; Zappa; Zichichi; Zitarosa; corrispondenti non individuati (3).
  Vi sono poi partecipazioni al lutto collettive individuate esclusivamente attraverso il nome di una istituzione; esse sono: Centro scientifico IMB di Pisa; Department of mathematics of the University of Maryland; Istituto matematico dell'Università di Bologna; Istituto matematico dell'Università di Camerino; Istituto matematico dell'Università di Ferrara (2); Istituto matematico dell'Università di Napoli; Istituto matematico dell'Università di Pavia; Istituto matematico dell'Università di Pisa; Laboratorio di analisi numerica del C.N.R. di Pavia; Mathematics faculty of the California institute of technology; studenti del terzo e quarto anno della Scuola normale superiore; personale non docente della Scuola normale superiore. Si osservi che alcuni

dei partecipanti al lutto scrivono in quanto rappresentanti di istituzioni e talora anche individualmente.
- Lavori di S. Mazzone sul fondo Stampacchia.

FALDONE 3

- Istituzioni: C.I.M.E.; Facoltà di architettura di Milano; International center Ettore Majorana; I.A.C.; U.M.I.
- Persone: R. Caccioppoli; B. Levi; M. Picone

FALDONE 4

- Partecipazione di Guido Stampacchia a commissioni di concorso a cattedra, 1958-60.
- Partecipazione al convegno "International Symposium", Gerusalemme 1960.
- Una controversia tra Guido Stampacchia e Fichera, 1961.
- Partecipazione di Guido Stampacchia alla commissione del Premio Caccioppoli, 1964.
- Conferimento a Guido Stampacchia del Premio Feltrinelli, 1966.
- Chiamata alla facoltà di scienze dell'Università di Roma di Guido Stampacchia, 1967.
- Tensione politica a Roma, 1970.
- Testi William Lowell Putnam Mathematical Competition, 1978.
- Pubblicazione del volume di Guido Stampacchia e David Kinderlehrer "An introduction…", 1977-78.
- Bibliografie e schede bibliografiche utilizzate da Guido Stampacchia.
- Recensioni tratte da Zentralblatt e American mathematical review da parte di Guido Stampacchia.
- Notizie relative a convegni.
- Miscellanea.

3.9 - Versioni preliminari e fotocopie di testi e capitoli di testi

- Analisi I. (di S. Campanato).
- Several complex variables. (di L. Bers).
- Equazioni alle differenze finite. (di autore non identificato, forse capitolo di un corso istituzionale o di un libro).
- Parte di un volume sulla meccanica dei continui. (di autore non identificato).
- Testo non identificato (forse di Istituzioni di analisi superiore).
- Capitolo di testo non identificato.

3.10 - Tesi di laurea e di dottorato

- D. Chenais, Identification d'ouverts lipschitziens et de variétés à bord lipchitziennes dans des équations aux dérivées partielles. Université de Nice 1977.
- M. Giordano, Alcuni teoremi di esistenza in analisi funzionale. Università di Pisa 1965-66.
- M.J. Gobert, Opérateurs matriciels de dérivation elliptiques et problèmes aux limites. Université de Liège 1960-61.
- R.M. Hervé, Recherches axiomatiques sur la théorie des fonctions surharmoniques et du potentiel. Université de Paris 1961.
- P.L. Lions, Problèmes de type Bellman. Université Pierre et Marie Curie 1978.
- R. Poncini, Introduzione e confronto delle diverse teorie dei numeri reali. Università di Genova 1958-59.
- L.C. Piccinini, Proprietà di inclusione e interpolazione tra spazi di Morrey e loro generalizzazioni. Scuola Normale Superiore di Pisa 1969.

3.11 – Estratti e versioni preliminari

Si tratta di circa 500 tra estratti e versioni preliminari. Sono da segnalare corpose raccolte di estratti di C. Severini, di R. Caccioppoli e di L. Tonelli. Su alcuni degli estratti di Caccioppoli vi sono delle dediche ed è inoltre presente quello che sembra essere un manoscritto originale di questo autore.

3.12 - Volumi a stampa

- Annuari di accademie.
- Fascicoli di riviste.
- Fascicoli illustrativi di istituzioni accademiche.
- Libri (una trentina circa; va segnalata la presenza di vari testi utilizzati verosimilmente da Stampacchia durante i suoi studi universitari, come ad esempio numerosi manuali Hoepli).
- Miscellanea (si tratta di pochi fascicoli di varia natura e di dimensioni ridotte).

3.13 - Materiale frammentario di natura matematica

Gli appunti manoscritti di natura matematica sono stati raccolti in un faldone ad essi dedicato. Molti di essi sono certamente collegati a lavori pubblicati di Stampacchia, ma data la natura frammentaria è difficile stabilire l'esatta connessione.

3.14 - Materiale fotografico

Si tratta di alcune fotografie di gruppo scattate in un convegno matematico. Altre poche fotografie, che ritraggono alcuni matematici, sono contenute in al-

cuni fascicoli tematici come ad esempio quelli relativi a R. Caccioppoli e M. Picone.

4 - BIBLIOGRAFIA

De Giorgi E. (1978) La scomparsa a Parigi di Guido Stampacchia. La Nazione, 4 maggio, p. 4.

De Giorgi E. (1980) Guido Stampacchia. Commemorazione tenuta nella seduta del 26 giugno 1980. Accademia nazionale dei Lincei, Rendiconti della classe di Scienze fisiche, matematiche e naturali. Ser. VIII, vol. LXVIII, fasc. 6. Ripubblicato in Moscariello, Sbordone (ds) (2018) pp. 45-51.

Garroni M.G. (2005) In Memory of Guido Stampacchia. In Giannessi, Maugeri (eds) (2005) pp. 31-32.

Giannessi F., Maugeri A. (eds) (2005) Variational Analysis and Applications. Springer US.

Kinderlehrer D. (1988) Un uomo che pensava agli altri. L'Unità, 26 aprile, p. 18.

Lions J.L. (1978) The Work of G. Stampacchia in Variational Inequalities. Conferenza tenuta al Centro "E. Majorana" di Erice a giugno 1978. Pubblicato in Boll. UMI, v. 15-A, n. 3, pp. 736-753. Ripubblicato in Cottle R.W., Giannessi F., Lions J.L., Wiley J. (eds) (1980) "Variational inequalities and complementarity problems. Theory and applications", pp. 1-24. Ripubblicato in Stampacchia (1996-97) vol. II, pp. XXXIII-L. Ripubblicato in Giannessi, Maugeri (eds) (2005) pp. 3-30. Ripubblicato in Moscariello, Sbordone (eds) (2018) pp. 27-44.

Magenes E. (1978a) Guido Stampacchia (1922-1978). Boll. UMI, v. 15-A, n. 3, pp. 715-736. Ripubblicato in Stampacchia (1996-97) vol. I, pp. XI-XXXII. Ripubblicato in Moscariello, Sbordone (eds) (2018) pp. 5-26.

Magenes E. (1978b) Pubblicazioni scientifiche di Guido Stampacchia. Boll. UMI, v. 15-A, n. 3, pp. 753-756. Ripubblicato in Stampacchia (1996-97) vol. I, pp. XXXII-XXXV. Ripubblicato in Moscariello, Sbordone (eds) (2018) pp. 52-55.

Magenes E. (2005) The Collaboration between Guido Stampacchia and Jacques-Louis Lions on Variational Inequalities. In Giannessi, Maugeri (eds) (2005) pp. 33-38.

Magenes E. (2018) Apertura dei lavori. Convegno "Recent trends in nonlinear partial differential equations" a tribute to Guido Stampacchia. In Moscariello, Sbordone (eds) (2018) pp. 57-58.

Mancino, O. G. (2005) In Memory of Guido Stampacchia. In Giannessi, Maugeri (eds) (2005) pp. 39-46.

Mazzone S. (2005) Guido Stampacchia. In Giannessi, Maugeri (eds) (2005) pp. 47-77. Ripreso in forma abreviata in Matapli Société de Mathématiques Appliquées et Industrielles. Bullettin n.72, (2003), pp. 71-88.

Mazzone S. (2019) Stampacchia Guido. Dizionario Biografico degli Italiani. Vol. 94, *ad vocem*.

Mazzone S. Stampacchia G. mathematica.sns.it/media/volumi/466/biografia-italiano.pdf

Moscariello G., Sbordone C. (2018a) Presentazione. In Moscariello, Sbordone (eds) (2018b), pp. VII-X.

Moscariello G., Sbordone C. (eds) (2018b) Guido Stampacchia. Opere scelte (1947-1965). Giannini Editore, Napoli.

Nirenberg L. (1996-97) Preface. In Stampacchia (1996-97) vol. I, pp. IX-X. Ripubblicato in Moscariello, Sbordone (eds) (2018) pp. 3-4.
Nirenberg L. (2005) Memories of Guido Stampacchia. In Giannessi, Maugeri (eds) (2005) pp. 79-80.
Sbordone C. (2005) In Memory of Guido Stampacchia. In Giannessi, Maugeri (eds) (2005) pp. 81-82.
Stampacchia Giulia (2005) Guido Stampacchia, My Father. In Giannessi, Maugeri (eds) (2005) pp. 83-86.
Stampacchia G. (1996-97) Opere scelte, a cura dell'Unione Matematica Italiana con il contributo del Consiglio Nazionale delle Ricerche, a cura di L. Boccardo, G. Da Prato, U. Mosco, V. Murthy, M.G. Platone, C. Sbordone, 2 volumi, Cremonese, Firenze.

Appendice

Rend. Acc. Sc. fis. mat. Napoli
Vol. LXXXVI, (2019) pp. 201-250

DOI 10.32092/1024

L'Osservatorio Meteorologico di *San Marcellino* Napoli Centro: i dati dell'anno 2019

Nota di Nicola Scafetta[1]*, Raffaele Di Cristo[2], Raffaele Viola[1], Adriano Mazzarella[3]

Presentata dal socio Giuseppe Marrucci
(Adunanza del 17 gennaio 2020)

Keywords: Air temperature, atmospheric pressure, rainfall, solar radiation, wind intensity-direction, UV index.

Abstract - The analysis of all meteorological parameters of the year 2019 shows that: (**a**) the monthly mean pressure ranges between 1010.5 hPa of November and 1022.2 hPa of February, with an annual mean of 1015.7 hPa, with an absolute minimum of 987.1 hPa measured on 12 December at 18:50 and with an absolute maximum of 1033.4 hPa measured on 14 February at 9:00; (**b**) the monthly mean air temperature ranges from 8.7°C of January and 28.2°C of August, with an annual mean of 18.6°C, with an absolute minimum of 1.4.°C measured on 4 January at 6:30 and with an absolute maximum of 35.7 °C measured on 31 August at 15:40; (**c**) the monthly mean relative humidity ranges from 64.4% of June and 79.6% of November, with an annual mean of 69.3%, with an absolute minimum of 21.0% measured on 29 June at 16:50 and with an absolute maximum of 95.0% measured on 22 December at 2:40; (**d**) The mean monthly global solar radiation ranges between 156.7 W/m^2 of November and 436.6. W/m^2 of August, with an annual mean of 323.5 W/m^2 and with an absolute maximum of 1304.0 W/m^2 measured on 30 May at 12:30; (**e**) the mean monthly UV Index ranges from 3.0 of August to 8.2 of September, with an annual average of 4.3 and with an absolute maximum of 11.5 measured on 6 June at 14.20; (**f**) the monthly mean wind intensity ranges between 0.8 m/s of October and 2.3 m/s of February, with an annual mean of 1.4 m/s and with most intense gust of 25.0 m/s measured on 23 February at 10:30; (**g**) the wind direction shows a mode from the North

[1] Osservatorio Meteorologico. Dipartimento di Scienza della Terra, dell'Ambiente e delle Risorse, Università degli Studi Federico II, Largo S. Marcellino 10, 80122 Napoli.
*Autore al quale va indirizzata la corrispondenza.
[2] Liceo "Don Carlo La Mura", Angri (SA).
[3] In pensione dall'1.11.2018.

in February, November, December, from North-East in January, from South in June, from South-West in March, April, May, July, August, September; (**h**) the monthly cumulative rainfall ranges from 0.0 mm of August to 376.0 mm of November, with a cumulative annual value of 1012.5 mm and with an absolute maximum of 54.0 mm measured on 19 December.

Riassunto - Dall'analisi di tutti i parametri meteo dell'anno 2019 emerge quanto segue: (**a**) la pressione atmosferica media mensile oscilla fra 1010.5 hPa di novembre e 1022.2 hPa di febbraio, con una media annua di 1015.7 hPa, con un minimo assoluto di 987.1 hPa registrato il 12 dicembre alle ore 18.50 e con un massimo assoluto di 1033.4 hPa registrato il 14 febbraio alle ore 9.00; (**b**) la temperatura media mensile dell'aria oscilla fra 8.7°C di gennaio e 28.2°C di agosto, con una media annua di 18.6°C, con un minimo assoluto di 1.4°C registrato il 4 gennaio alle ore 6:30 e con un massimo assoluto di 35.7°C registrato il 31 agosto alle ore 15:40; (**c**) l'umidità relativa media mensile oscilla fra 64.4% di giugno e 79.6% di novembre, con una media annua di 69.3%, con un minimo assoluto del 21.0% registrato il 29 giugno alle ore 16:50 e con un massimo assoluto di 95.0% registrato il 22 dicembre alle ore 2:40; (**d**) la radiazione solare globale media mensile oscilla fra 156.7 W/m^2 di novembre e 436.7 W/m^2 di agosto, con una media annua di 323.5 W/m^2 e con un massimo assoluto di 1304.0 W/m^2 registrato il 30 maggio alle ore 12.30; (**e**) l'indice UV medio mensile oscilla fra 3.0 di agosto e 8.2 di settembre, con una media annua di 4.3 e con un massimo assoluto di 11.5 registrato il 6 giugno alle ore 14:20; (**f**) l'intensità media mensile del vento oscilla tra 0.8 m/s di ottobre e 2.3 m/s di febbraio, con una media annua di 1.4 m/s e con la raffica più intensa di 25.5 m/s registrata il 29 ottobre alle ore 16:40; (**g**) la direzione del vento presenta un'orientazione da Nord in febbraio, novembre, dicembre, da Nord-Est in gennaio, da Sud in giugno , da Sud-Ovest in marzo, aprile, maggio, luglio, agosto, settembre; (**h**) la pioggia cumulata mensile oscilla tra il valore 0 mm di agosto e i 376.0 mm di novembre, con un valore annuale cumulato di 1012.5 mm e con un massimo giornaliero assoluto di 54.0 mm registrato il 19 dicembre.

1 - INTRODUZIONE

I dati meteo sono attualmente rilevati da una centralina automatica sita sulla torretta dell'edificio di San Marcellino (lat. 40°50'50" N; long. 14°15'29" E; quota 50 m slm), sede attuale del Dipartimento di Scienze della Terra, dell'Ambiente e delle Risorse a meno di 50 m dall'Accademia di Scienze Fisiche e Matematiche della Società Nazionale di Scienze, Lettere ed Arti in Napoli.

La stazione gestisce i seguenti sensori: temperatura dell'aria (°C), pressione atmosferica (hPa) (normalizzata a livello del mare), umidità relativa (%), velocità del vento (m/s), direzione del vento (Nord), precipitazione (mm), radiazione solare globale (W/m^2), indice UV (scala da 0 a 16).

Per ogni mese i valori estremi giornalieri sono evidenziati in grassetto.

I dati sono acquisiti con cadenza di 10 minuti ed i valori, fatta eccezione per la pioggia che viene registrata come cumulata, sono quelli istantanei; i dati gior-

nalieri di radiazione globale ed indice UV sono mediati sulla loro effettiva durata.

La direzione del vento è calcolata come moda sia a scala di 10 minuti per i grafici orari che a scala giornaliera per i grafici mensili. È considerata variabile (--) quando la direzione non è stata registrata su uno stesso quadrante per più di 8 ore.

L'assenza del dato indica sensore fuori uso.

2- MATERIALI E METODI

Il bollettino meteorologico dell'anno 2019 è così organizzato:

- un breve rapporto meteorologico per ogni mese;
- una catalogazione delle medie orarie mensili (00 -23 h) e dei relativi grafici per ogni mese;
- una catalogazione dei valori medi giornalieri e dei relativi grafici, per ogni mese, con l'indicazione dei valori estremi registrati;
- un riepilogo mensile di tutti i parametri meteo relativo all'anno in corso;
- un riepilogo mensile delle frequenze di precipitazione, temperature minime e massime distinte per soglia.

È possibile accedere via web alla consultazione dei dati rilevati in tempo reale all'indirizzo: http ://www.meteo.unina.it.

3 – RAPPORTI METEO MENSILI

GENNAIO 2019

Gennaio 2019 si pone al 15 posto nella speciale classifica delle temperature massime più basse registrate a Napoli centro dal 1872. Il motivo è da cercarsi nell'anomalo riscaldamento della stratosfera (80°C a 40 chilometri di altezza) che ha causato la scissione del vortice polare in due lobi gelidi, uno dei quali ha raggiunto l'Appennino centro-meridionale attraverso la porta della Bora. La neve è stata presente sul cono del Vesuvio per ben 20 giorni dal 3 al 13 e dal 23 al 31. La media della temperatura minima è stata di 6.3°C (mezzo grado in meno della media secolare) e la media della massima è stata di 11.3°C (un grado e mezzo in meno) e con punte di freddo di 1.4°C e 2.0°C nei giorni 3 e 4. Venti di 50 chilometri orari, più volte, hanno messo a dura prova la navigazione nel golfo e accentuato la sensazione del freddo. La pioggia è caduta in 17 giorni (ininterrottamente per 14 giorni dal 18 al 31) con una quantità di 113 mm, 20 mm in più di quella che cade normalmente a gennaio.

FEBBRAIO 2019

Un potente anticiclone delle Azzorre si è posizionato sul Mediterraneo ininterrottamente per i primi 22 giorni e gli ultimi due di febbraio ed ha determinato

il blocco della circolazione atmosferica con assenza di vento e di nuvole, elevate escursioni termiche fra il giorno e la notte e problemi di inquinamento da polveri sottili nelle aree metropolitane. Solo nei giorni 23, 24 e 25, l'anticiclone si è allungato verso il Nord Europa e la presenza simultanea di un potente anticiclone sui Balcani di 1040 hPa e di una profonda area ciclonica sullo Ionio di 1000 hPa ha permesso l'ingresso in Italia di aria gelida siberiana. Questo episodio ha determinato in Campania una netta diminuzione della temperatura, neve sulle zone interne, fiocchi di neve sulle colline di Napoli e venti forti da Nord Est che a Napoli centro, il giorno 23, hanno raggiunto i 100 chilometri orari e a Castel Sant'Elmo i 150. La notevole ventilazione ha causato intense mareggiate, valori percepiti di temperatura al di sotto dello zero (per effetto del cosiddetto Wind Chill) e la caduta di alberi secolari costringendo diverse amministrazioni comunali a chiudere scuole, parchi e cimiteri. Un vento di 100 chilometri orari, infatti, è in grado di determinare, su ogni metro quadrato di oggetto investito, una spinta di 40 chili che, se sufficientemente prolungata nel tempo, può determinarne la caduta improvvisa. Le medie delle temperature minime e massime dell'intero mese a Napoli centro sono state, perciò, rispettivamente, di 8.7°C e 14.6°C, due gradi e un grado in più delle medie stagionali. Il giorno più freddo è stato il 23 febbraio, con una temperatura minima di 3.6°C e con neve sul Vesuvio nei giorni 11, 25 e 26. La quantità di pioggia di 15 mm rappresenta l'80% in meno di quella che cade normalmente a febbraio.

MARZO 2019

Marzo 2019 è stato caratterizzato da una notevole variabilità atmosferica legata al passaggio dall'inverno alla primavera quando masse d'aria calda meridionali si scontrano con masse d'aria fredda preesistenti. Questo comportamento non deve sorprendere come ben recita la poesia *Marzo* di Salvatore Di Giacomo: "*Mo nu cielo celeste, mo n'aria cupa e nera: mo d' 'o vierno 'e tempeste, mo n'aria 'e primmaver*a". I giorni più freddi si sono concentrati intorno a metà mese (il cono del Vesuvio è stato ricoperto di neve dal 12 al 14) e a fine mese quando forti venti di libeccio e maestrale hanno messo a dura prova la navigazione nel golfo. La media delle temperature massime è stata di 17.0°C, un grado più alta della media del periodo mentre la media delle minime è stata di 11.3°C, due gradi e mezzo in più. La pioggia, caduta è stata di 20 mm, un terzo di quella che cade normalmente a marzo.

APRILE 2019

Il meteo di aprile 2019 può essere sostanzialmente diviso in due parti. Nella prima metà del mese, ripetute aree di bassa pressione hanno agevolato l'ingresso sul Mediterraneo di perturbazioni atlantiche con temperature 1-2°C al di sotto della media. Nella seconda metà, un'estesa area anticiclonica tropicale ha determinato temperature 2-3°C al di sopra della media. La media delle temperature

minime è stata così di 13.1°C, due gradi in più della media stagionale mentre quella delle temperature massime è stata di 19.0°C, in linea con la media. La pioggia caduta nell'intero mese è stata di 23 mm, il 60% in meno di quanto piove normalmente ad aprile. Il giorno più caldo è stato il 25, alle 16.50, con 29.8°C, lontano dai record di temperatura massima giornaliera dell'8 aprile 1886 (32.3°C) e del 18 aprile 1940 (32.5°C). Questo ad indicarci che siamo ancora in primavera con i suoi continui e classici alti e bassi, capace di proporci, da un giorno all'altro, periodi di freddo e di caldo. La temperatura del mare nel golfo nell'intero mese è schizzata da 14.6°C a 17.0°C.

MAGGIO 2019

L'analisi dell'archivio storico meteorologico dell'Università Federico II ha assegnato a maggio 2019 la palma di mese di maggio più freddo in assoluto a partire dal 1872 anche se in perfetto pareggio con maggio 1991. È da sottolineare, infatti, che il record di maggio 2019 è più significativo in quanto, nel corso degli ultimi 28 anni, l'isola di calore urbana si è sempre più estesa ai confini del centro storico verso la periferia rendendo sempre più alte le temperature minime notturne. La media delle massime è stata di 19.2°C, quattro gradi al di sotto della media, mentre quella delle minime è stata di 14.3°C, mezzo grado in meno. La pioggia caduta in 12 giorni è stata pari a 119 mm, il 160% in più di quella che cade di norma a maggio. La temperatura del mare nel golfo è di 19°C, tre gradi in meno della media. Con l'arrivo della primavera si ritiene che sia passato l'inverno e arrivata finalmente l'estate che a Napoli è chiamata *'a stagiòn*. Ma quest'anno maggio non ha seguito questa regola in ossequio al detto antico: "*A vecchia a 'e trenta maggio iettaie 'o laganaturo a 'o fuoco*" vale a dire: a fine maggio, la vecchia non avendo più legna da ardere, fu costretta a bruciare il matterello, arnese indispensabile per lavorare la pasta. Masse d'aria gelida provenienti dalla frantumazione del Vortice Polare hanno costretto la circolazione atmosferica a non seguire i soliti movimenti da ovest ad est ma quelli lungo i meridiani, con scambi di masse d'aria fredda da nord a sud. Attraverso questo meccanismo la Natura ha così provveduto a recuperare il deficit di pioggia e le temperature sopra media di febbraio, marzo e aprile scorsi. L'atmosfera non segue ritmi precisi come un'equazione ma ha sempre la capacità di recuperare i suoi fisiologici squilibri.

GIUGNO 2019

Dal punto di vista termico, i primi sei giorni di giugno 2019 sono stati al di sotto della media stagionale di circa 3°C per i ripetuti arrivi di flussi atlantici sul Mediterraneo. A seguire, i giorni sono stati al di sopra della media di circa 5°C per la presenza di un potente e bollente anticiclone di matrice nord-africana. Questo scenario barico molto disomogeneo ha determinato una media delle temperature massime di 29.9°C, due gradi e mezzo in più di quella stagionale, e una media

delle temperature minime di 22.7°C, quattro gradi in più. Il giorno più caldo è stato il 27 giugno con 35.2°C. La pioggia è caduta solo nel primo giorno ed è stata pari a 11 mm, un terzo di quella che cade normalmente a giugno. La temperatura del mare nel golfo è schizzata nell'intero mese da 19°C a 25°C. È da sottolineare, però, che il caldo di questo giugno non è da record. L'analisi dell'archivio ultrasecolare dell'Osservatorio Meteorologico dell'Università di Napoli Federico II mostra che il 1945 è stato il mese di giugno più caldo con 30.7°C e che il 27 giugno del 1947 è stato il giorno di giugno più caldo con ben 40.2°C.

LUGLIO 2019

Luglio 2019 ha sorpreso i climatologi per la sua intensa variabilità dovuta all'alternanza di masse d'aria bollente ed umida africana e masse d'aria atlantica più mite. Questo è il bilancio termico dettagliato: nei primi 6 giorni, la temperatura dell'aria è stata di 2°C al di sopra della media; fino al giorno 19, la temperatura è diminuita di 2°C; fino al 25, la temperatura è aumentata di 3°C e finalmente la temperatura è diminuita di nuovo di 2°C. Tali differenti scenari barici hanno determinato, a Napoli centro, una media delle temperature massime di 30.7 °C, un grado in più della media stagionale, e una media delle temperature minime di 24.6°C, tre gradi più elevata. Il giorno più caldo è stato il 23 luglio con 35.3°C e 37.2° percepiti. Il catalogo meteorologico dell'Osservatorio di San Marcellino a Napoli centro mostra, comunque, valori di temperatura massima del mese di luglio ben più elevati: il 21 e il 22 del 1939 con 38.8°C e 38.0°C, il 30 del 1901 e il 18 del 2015 con 36.7°C e tanti altri. Le precipitazioni sono state pari a 18 mm, in linea con la pioggia che cade normalmente a luglio, e concentrati nei rovesci dei giorni 9 e 10 e soprattutto del 28 che ha fatto molto bene ai campi in onore al detto "*Si chiove a Sant'Anna, l'acqua addeventa manna*". La temperatura del mare nel golfo è schizzata nella prima decade da 24.5°C a 28.5°C per poi stabilizzarsi intorno a 27°C.

AGOSTO 2019

Bollenti ed umidi anticicloni subtropicali di origine africana in successione hanno invaso il Mediterraneo al posto del più mite anticiclone delle Azzorre per l'intero mese di agosto. Tale scenario barico ha determinato per tutto il mese valori di temperatura dell'aria ed umidità al di sopra delle medie con notevole disagio notturno nella popolazione. La media delle temperature minime è stata di 25.4°C, quattro gradi in più della media, quella delle temperature massime di 32.0°C, un grado e mezzo in più. Il giorno più caldo è stato l'11 agosto con una temperatura massima di 35.8°C. Ma questi valori non sono da record: il 6 agosto del 1885 con 39.2°C, il 19 agosto del 1946 con 39.0, il 9 agosto del 1956 con 39.1°C e tanti altri. Anche la media dell'intero mese non è da record: agosto del 1947 con 32.7°C, del 1952 con 32.5°C, del 1943 con 32.4°C, del 1971 con 32.4°C, e tanti altri. La pioggia è stata assente in tutto il mese che normalmente

è uno dei mesi più asciutti dell'anno. È interessante ancora una volta osservare che la media della temperatura massima di agosto del lontano 1956, ricordato per la rigidità del suo inverno alla pari di questo 2019, ha superato i 32°C con più giorni che hanno superato i 39°C, a conferma della validità del principio di "autosomiglianza" secondo il quale un'estate bollente segue quasi sempre un inverno rigido. La temperatura del mare nel golfo in tutto il mese è aumentata progressivamente fino a metà agosto da 25.6°C a 28.4°C per poi stabilizzarsi sui 27°C.

SETTEMBRE 2019

Settembre 2019 è stato un mese dai due volti: nella prima metà del mese la temperatura dell'aria è stata di 2-3°C al di sopra della media stagionale, nella seconda metà di 1-2°C al di sotto. A livello mensile, la media delle temperature minime è stata così di 21.4°C, due gradi e mezzo in più della media stagionale, mentre quella delle temperature massime è stata di 27.7°C, mezzo grado in più. Scenari così diversi sono stati determinati dalla presenza sul Mediterraneo dell'anticiclone africano nella prima metà del mese e poi di aree cicloniche che hanno attratto masse d'aria fredda direttamente dal Nord Europa. Il giorno più caldo è stato il 13 settembre con 31.1°C mentre la temperatura del mare nel golfo, vero termometro ambientale, ha raggiunto i 27 °C nella prima decade e i 25 °C a fine mese che è una temperatura ancora buona per un bagno a mare. La pioggia è stata pari a 82 mm, 12 mm in più di quella che cade normalmente a settembre e quasi tutta concentrata negli eventi del 23 e 26 che hanno messo a dura prova la viabilità in città e la navigazione nel golfo.

OTTOBRE 2019

La temperatura dell'aria di ottobre a Napoli centro ha superato sistematicamente di circa 1-2°C la media stagionale con l'eccezione del giorno 7 e degli ultimi quattro giorni. La media delle temperature minime dell'intero ottobre 2019 è stata, perciò, di 17.4°C, due gradi in più della media stagionale, mentre quella delle temperature massime è stata di 24.1°C, un grado e mezzo in più. Le precipitazioni sono state pari a 109 mm, in linea con quanto piove normalmente ad ottobre e questo grazie all'energia termica immagazzinata dalla troposfera ad agosto e settembre. Notevoli sono stati i rovesci del 2 e del 3 che hanno messo a dura prova il traffico in città e la navigazione nel golfo. Il giorno più caldo è stato il 23 ottobre con 27.2°C. La mitezza di questo mese, tipica delle cosiddette ottobrate napoletane, è stata determinata dalla presenza quasi costante sul Mediterraneo di un'area di alta pressione di origine tropicale. Solo negli ultimi giorni del mese, una profonda depressione sul mar Ligure ha risucchiato aria umida e più fredda dal Polo con una diminuzione della temperatura ed una maggiore instabilità atmosferica. La temperatura del mare nel golfo è passata dal valore quasi estivo di 25°C degli inizi del mese al valore finalmente autunnale di 22°C.

NOVEMBRE 2019

La pioggia è caduta a Napoli per tutto novembre con l'eccezione dei giorni 26 e 30. Questo mese rimarrà negli annali dell'Osservatorio Meteorologico Fediciano, operativo dal 1872, come record sia come numero di giorni consecutivi di pioggia, pari a 26, sia come quantità di pioggia caduta, pari a 376 mm. È stato superato il record di 21 giorni consecutivi di novembre 1901 e quello della quantità di pioggia di novembre 1893, pari a 325 mm. Notevoli i danni all'agricoltura lungo il litorale domizio, ridotto a una palude come negli anni 30, per l'effetto congiunto della pioggia e dell'esondazione dei Regi Lagni e del Lago Patria. La ventilazione, per lo più proveniente da sud-est (il cosiddetto Scirocco), è stata sempre sostenuta con punte di 90 km/ora nei giorni 11, 16 e 17 che hanno causato la caduta di alberi, il blocco della navigazione nel golfo e la chiusura delle scuole. A causa dello Scirocco, le temperature medie minime e massime sono state pari a 14.0°C, due gradi e mezzo in più della media stagionale, e a 19.0°C, un grado e mezzo in più. La temperatura del mare nel golfo è passata da 22°C degli inizi di novembre a 19°C per fine mese. La causa della piovosità di questo novembre è da ricercarsi nella presenza costante dell'anticiclone delle Azzorre a sud-ovest del golfo di Biscaglia e dell'anticiclone Russo-Siberiano sull'Europa orientale. Questa configurazione barica ha causato un blocco della circolazione normale da ovest verso est e creato un corridoio preferenziale lungo il quale masse d'aria atlantica, fresca ed instabile hanno raggiunto a ripetizione la nostra penisola con tutte le drammaticità che ben abbiamo conosciuto. L'orografia del territorio e il surplus di caldo dei mari hanno poi agito congiuntamente per conferire alle precipitazioni di novembre le peculiarità tipiche dei cosiddetti "*flood alert*", mettendo a nudo la fragilità di alcune aree il più delle volte imputabile all'uomo.

DICEMBRE 2019

La temperatura dell'aria di dicembre 2019 è stata costantemente al di sopra della media con l'eccezione dei giorni dal 10 al 12 e dal 28 al 31. Le medie mensili sono state così di 10.7°C per la temperatura minima e di 16.1°C per la massima, due gradi in più delle rispettive medie secolari. Questo a causa di una ventilazione quasi sempre proveniente dai quadranti meridionali e con punte di 90 km/ora nei giorni 13 (con vento di libeccio) e 30 (con vento di grecale) che hanno determinato caduta di alberi, blocchi della navigazione e chiusure delle scuole. La pioggia è stata pari a 127 mm, circa 10 mm in più di quella che cade normalmente a dicembre. La temperatura del mare nel golfo è passata da 20°C degli inizi di dicembre a 16°C per fine mese. Solo negli ultimi giorni, l'espansione verso Nord dell'anticiclone delle Azzorre ha favorito l'irruzione di aria fredda direttamente dai Balcani con una notevole diminuzione della temperatura. A chiusura d'anno risulta utile riportarne il bilancio termo-pluviometrico. Le medie delle temperature massime e minime del 2019 sono state, rispettivamente, di 21.7°C e

di 15.8, entrambe tre decimi di grado in meno di quelle del 2018. In particolare, gennaio e maggio sono state sotto media di 2-3°C e i rimanenti mesi sopra media di 1-2°C. La pioggia caduta è stata di 1013 mm, 150 mm in più di quella che cade normalmente a Napoli centro, con surplus nei mesi di maggio, novembre e con deficit a febbraio, marzo.

TABELLE E GRAFICI

GENNAIO 2019 **(medie orarie)**

Ore	Temperatura °C	Umidità %	Pressione hPa	Vento velocità m/s	Vento direzione	Radiazione Solare W/m²	Radiazione Solare Indice UV
0	7.9	72.8	1013.0	1.3	N	0.0	0.0
1	7.6	73.7	1013.1	1.5	N	0.0	0.0
2	7.5	74.0	1013.1	1.3	N	0.0	0.0
3	7.3	74.2	1012.8	1.3	N	0.0	0.0
4	7.3	74.1	1012.5	1.2	N	0.0	0.0
5	7.3	73.9	1012.4	1.0	N	0.0	0.0
6	7.3	74.1	1012.5	1.0	N	0.0	0.0
7	7.3	74.2	1012.7	1.3	N	4.6	0.0
8	7.7	73.4	1012.9	1.1	N	61.9	1.5
9	8.6	71.2	1013.2	1.2	N	165.0	3.1
10	9.4	68.4	1013.4	1.5	N	235.7	3.5
11	9.9	65.9	1013.1	1.6	N	290.7	3.7
12	10.3	64.9	1012.7	1.7	N	281.5	3.8
13	10.5	64.9	1012.4	1.8	N	255.9	3.7
14	10.5	65.3	1012.2	1.7	N	199.2	3.3
15	10.4	65.9	1012.2	1.6	N	122.9	2.7
16	9.9	67.7	1012.3	1.6	N	37.9	0.8
17	9.5	69.2	1012.4	1.5	N	1.6	0.0
18	9.1	70.4	1012.6	1.4	N	0.0	0.0
19	8.9	71.4	1012.8	1.2	N	0.0	0.0
20	8.7	71.9	1012.9	1.3	N	0.0	0.0
21	8.5	71.7	1012.9	1.6	N	0.0	0.0
22	8.4	71.8	1012.9	1.8	N	0.0	0.0
23	8.2	72.2	1012.9	1.7	N	0.0	0.0

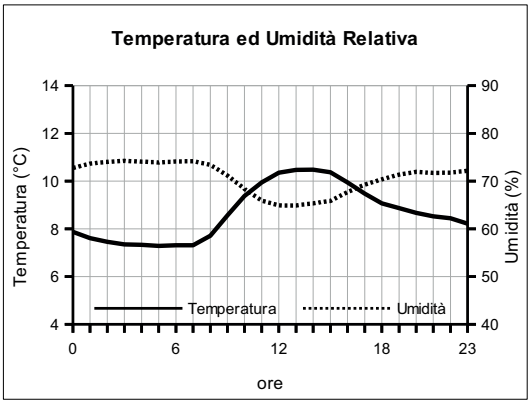

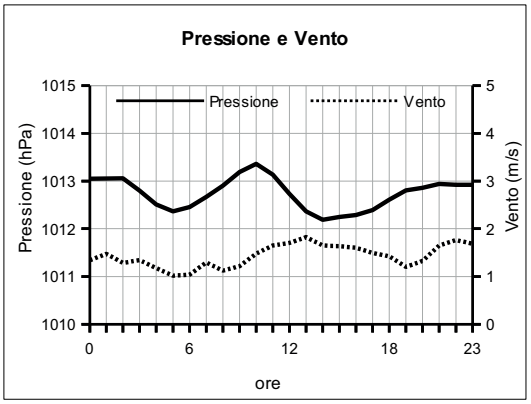

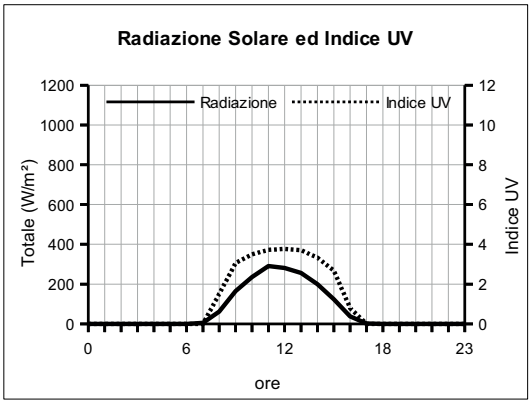

FEBBRAIO 2019 **(medie orarie)**

Ore	Temperatura °C	Umidità %	Pressione hPa	Vento velocità m/s	Vento direzione	Radiazione Solare W/m²	Radiazione Solare Indice UV
0	10.4	69.1	1022.6	1.6	N	0.0	0.0
1	10.3	69.2	1022.4	1.9	N	0.0	0.0
2	10.3	68.4	1022.3	2.1	N	0.0	0.0
3	10.2	67.7	1021.9	2.1	N	0.0	0.0
4	10.0	68.1	1021.8	2.1	N	0.0	0.0
5	9.9	68.6	1021.9	2.1	N	0.0	0.0
6	9.8	68.5	1022.0	1.8	N	0.2	0.0
7	9.8	68.6	1022.3	1.8	N	28.5	0.6
8	10.6	66.4	1022.7	1.7	N	151.4	2.7
9	11.6	62.5	1022.8	2.0	N	286.9	3.6
10	12.4	59.6	1022.9	2.5	N	385.6	4.1
11	12.8	59.4	1022.7	3.0	N	463.6	4.5
12	13.3	58.5	1022.3	3.3	N	493.2	4.8
13	13.6	58.0	1021.7	3.2	N	452.0	4.5
14	13.5	58.7	1021.5	3.2	N	364.9	4.1
15	13.5	58.9	1021.4	3.1	NW	270.6	3.7
16	13.1	59.7	1021.5	2.9	N	131.1	2.7
17	12.4	62.4	1021.7	2.6	N	21.5	0.4
18	11.9	64.3	1022.0	2.2	N	0.0	0.0
19	11.6	65.4	1022.3	2.1	N	0.0	0.0
20	11.3	66.4	1022.5	1.8	N	0.0	0.0
21	11.0	67.6	1022.7	2.0	N	0.0	0.0
22	10.8	68.2	1022.7	2.1	N	0.0	0.0
23	10.6	68.2	1022.8	2.0	N	0.0	0.0

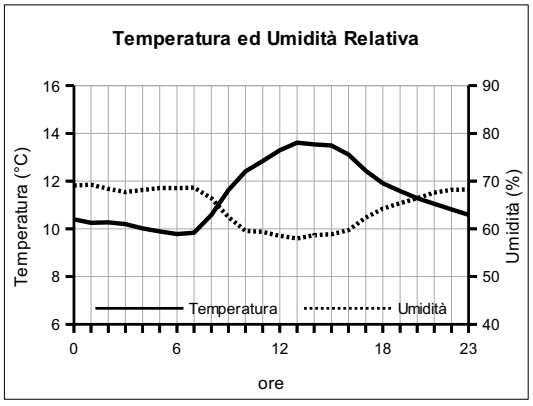

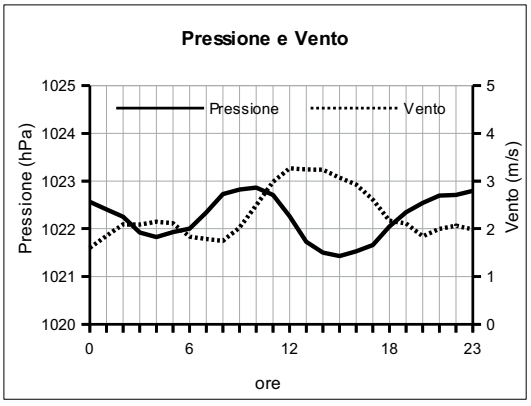

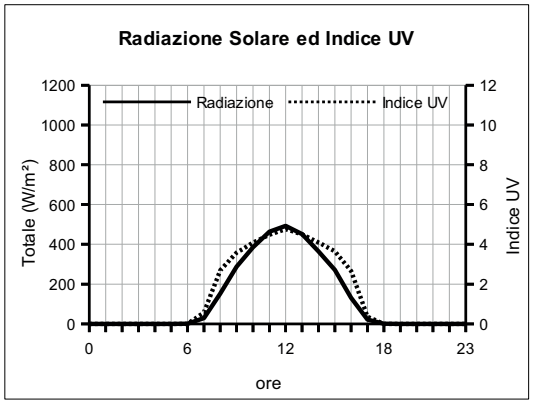

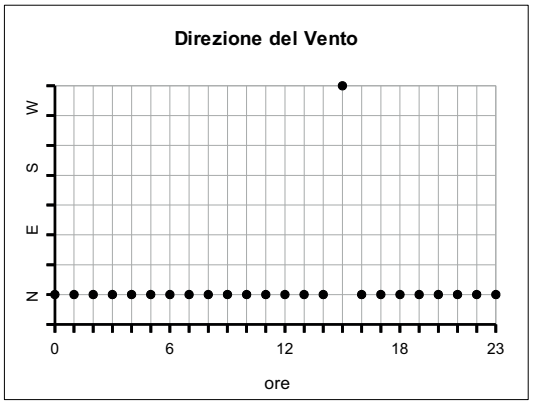

MARZO 2019 **(medie orarie)**

Ore	Temperatura °C	Umidità %	Pressione hPa	Vento velocità m/s	Vento direzione	Radiazione Solare W/m²	Radiazione Solare Indice UV
0	12.7	72.5	1019.9	1.7	W	0.0	0.0
1	12.4	72.6	1019.9	1.4	SW	0.0	0.0
2	12.2	73.1	1019.6	1.4	N	0.0	0.0
3	12.1	73.4	1019.3	1.3	N	0.0	0.0
4	12.0	73.7	1019.3	1.2	N	0.0	0.0
5	12.0	73.6	1019.4	1.3	N	0.0	0.0
6	11.8	73.6	1019.5	1.3	N	11.8	0.1
7	12.3	72.3	1019.8	1.3	N	99.2	1.9
8	13.5	68.8	1020.2	1.2	N	251.1	3.1
9	14.6	64.8	1020.4	1.7	N	414.5	4.0
10	15.2	62.3	1020.4	2.2	SE	558.3	4.8
11	15.7	61.2	1020.3	2.6	S	600.1	5.4
12	16.1	60.9	1020.1	2.7	S	572.8	5.4
13	16.3	60.8	1019.6	2.6	S	545.9	5.2
14	16.3	60.4	1019.2	2.8	S	486.4	4.7
15	16.3	60.5	1019.0	2.7	S	368.0	4.0
16	15.7	63.1	1019.0	2.5	S	207.9	3.1
17	15.2	64.2	1019.1	2.1	SW	77.3	1.5
18	14.5	66.0	1019.3	1.6	SW	8.2	0.1
19	14.1	68.2	1019.6	1.3	SW	0.4	0.0
20	13.8	69.7	1019.8	1.4	SW	0.0	0.0
21	13.5	71.0	1019.9	1.5	SW	0.0	0.0
22	13.2	72.2	1020.0	1.4	SW	0.0	0.0
23	13.0	72.7	1019.9	1.8	SW	0.0	0.0

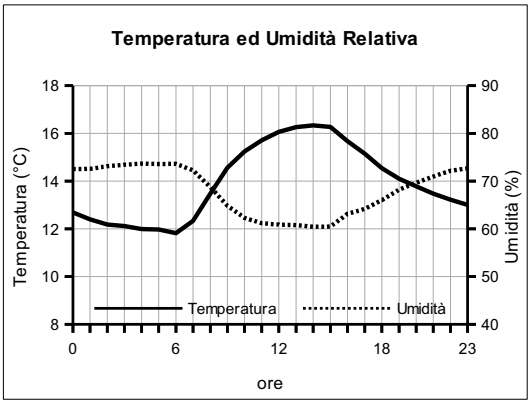

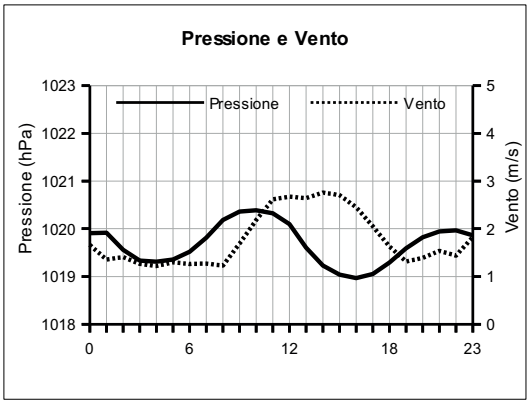

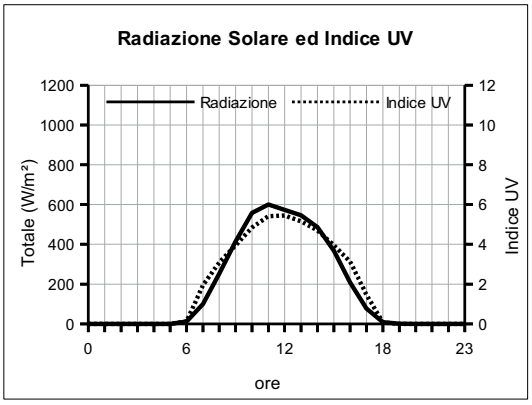

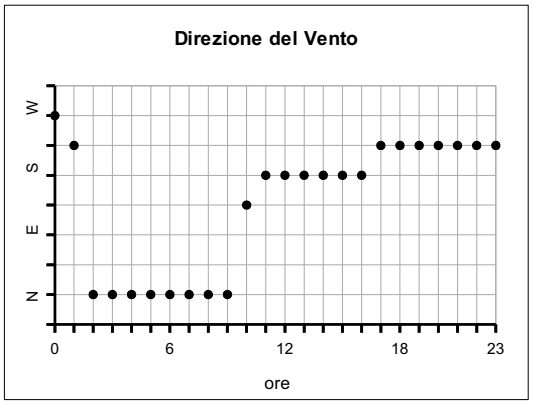

APRILE 2019 **(medie orarie)**

Ore	Temperatura °C	Umidità %	Pressione hPa	Vento velocità m/s	Vento direzione	Radiazione Solare W/m²	Radiazione Solare Indice UV
0	14.9	72.6	1014.6	0.9	N	0.0	0.0
1	14.6	72.5	1014.5	1.1	N	0.0	0.0
2	14.3	72.6	1014.2	1.3	W	0.0	0.0
3	14.1	72.5	1014.1	1.0	N	0.0	0.0
4	13.9	72.7	1013.8	0.9	N	0.0	0.0
5	13.7	72.9	1013.7	0.9	N	0.0	0.0
6	13.6	73.1	1013.7	0.9	N	6.7	0.0
7	14.0	72.0	1014.0	0.9	N	82.9	1.9
8	15.1	69.1	1014.2	0.9	N	229.1	3.3
9	16.1	66.0	1014.3	1.1	NW	355.4	4.1
10	16.8	64.0	1014.5	1.5	S	506.9	5.0
11	17.2	63.4	1014.5	2.1	S	587.2	5.6
12	17.5	62.8	1014.3	2.3	S	608.6	6.1
13	17.9	61.6	1014.1	2.5	S	687.4	6.4
14	18.0	60.9	1014.0	2.5	S	638.0	5.9
15	18.1	60.0	1013.6	2.5	S	537.6	5.2
16	17.9	60.3	1013.5	2.5	W	410.9	4.2
17	17.5	62.6	1013.5	2.2	W	260.4	3.2
18	16.9	66.5	1013.6	1.7	S	122.9	2.3
19	16.2	68.4	1013.8	1.7	SW	21.4	0.3
20	15.7	69.8	1014.1	1.4	W	0.1	0.0
21	15.5	70.0	1014.5	1.1	SW	0.0	0.0
22	15.3	71.4	1014.7	1.0	SW	0.0	0.0
23	15.1	71.5	1014.6	1.0	SW	0.0	0.0

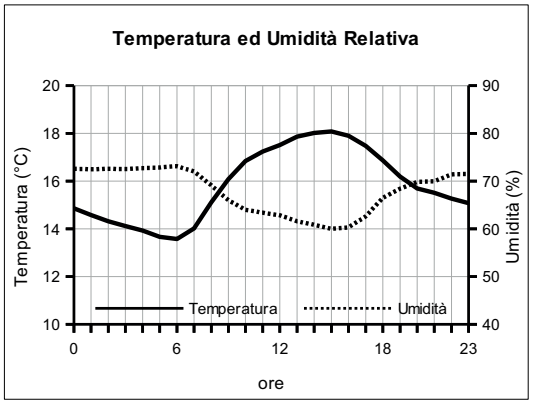

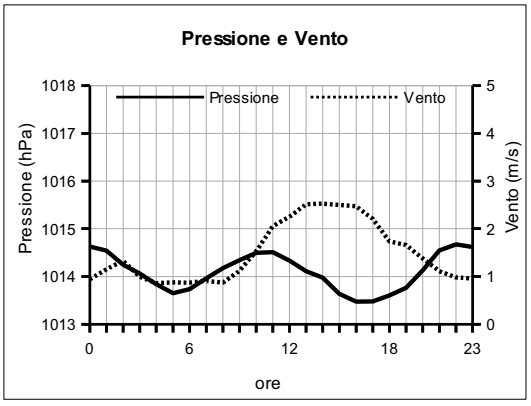

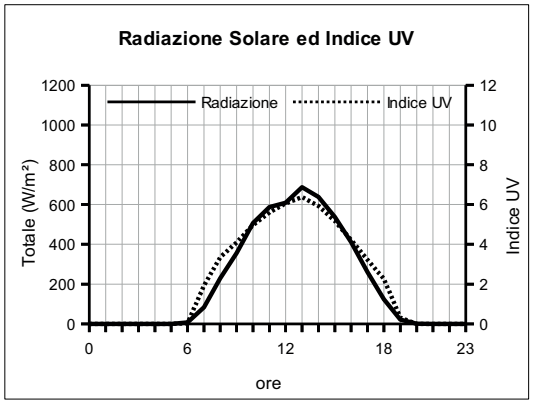

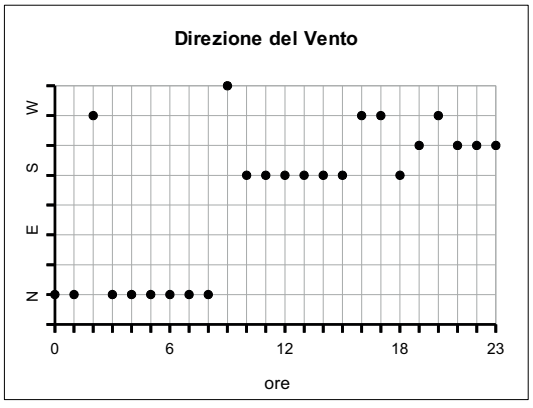

MAGGIO 2019 **(medie orarie)**

	Temperatura	Umidità	Pressione	Vento		Radiazione Solare	
Ore	°C	%	hPa	velocità m/s	direzione	W/m²	Indice UV
0	15.8	79.1	1013.4	0.7	W	0.0	0.0
1	15.6	79.5	1013.2	0.6	SW	0.0	0.0
2	15.4	80.0	1012.8	0.6	SW	0.0	0.0
3	15.2	81.3	1012.5	0.6	W	0.0	0.0
4	15.0	81.8	1012.4	0.8	W	0.0	0.0
5	14.9	82.5	1012.2	1.0	SW	0.3	0.0
6	14.9	82.5	1012.4	0.8	N	26.9	0.4
7	15.4	81.2	1012.6	0.8	SW	121.7	2.2
8	16.0	78.5	1012.8	1.1	SW	251.4	3.2
9	16.5	76.5	1013.1	1.7	S	379.3	4.1
10	17.0	74.6	1013.2	2.0	S	492.2	5.0
11	17.5	73.0	1013.3	2.0	S	573.4	5.9
12	18.0	71.3	1013.4	2.2	S	678.1	6.8
13	18.4	69.8	1013.2	2.3	S	651.8	6.7
14	18.5	69.1	1013.1	2.5	S	589.0	6.2
15	18.5	69.3	1013.0	2.6	S	502.2	5.2
16	18.2	70.2	1012.9	2.5	S	416.9	4.3
17	18.0	70.5	1012.8	2.1	S	291.1	3.6
18	17.6	72.3	1012.7	1.8	S	152.0	2.7
19	17.1	74.5	1012.9	1.4	W	50.8	1.0
20	16.7	76.1	1013.2	1.0	W	3.4	0.0
21	16.4	76.9	1013.5	0.8	S	0.0	0.0
22	16.2	77.6	1013.7	0.8	SW	0.0	0.0
23	16.1	78.3	1013.6	0.7	SW	0.0	0.0

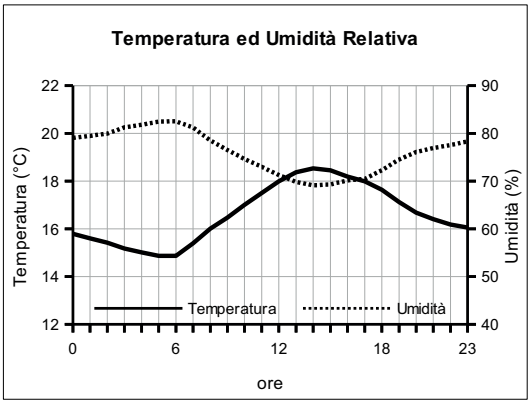

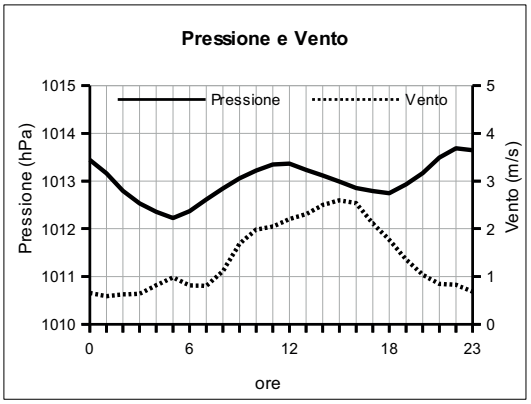

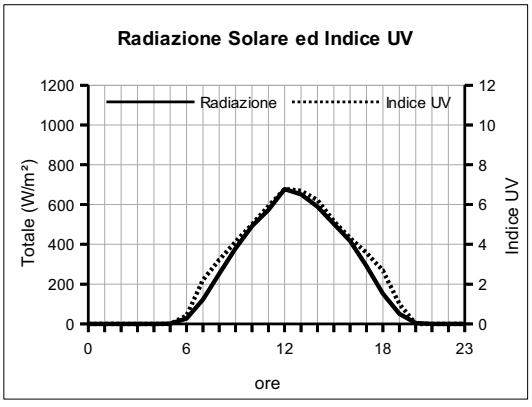

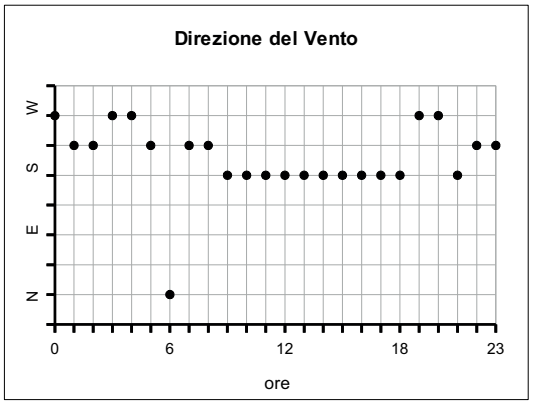

GIUGNO 2019 **(medie orarie)**

Ore	Temperatura °C	Umidità %	Pressione hPa	Vento velocità m/s	Vento direzione	Radiazione Solare W/m²	Radiazione Solare Indice UV
0	24.6	67.6	1016.0	0.4	SE	0.0	0.0
1	24.2	69.6	1015.8	0.4	SE	0.0	0.0
2	23.9	70.2	1015.6	0.4	N	0.0	0.0
3	23.5	71.1	1015.4	0.3	NW	0.0	0.0
4	23.2	72.0	1015.3	0.2	N	0.0	0.0
5	22.9	72.9	1015.4	0.3	N	1.8	0.0
6	23.1	71.9	1015.6	0.4	NW	48.1	0.8
7	24.0	70.1	1015.8	0.4	N	171.9	2.4
8	25.1	68.0	1016.1	0.5	SE	332.8	3.1
9	25.7	65.8	1016.1	1.1	SE	493.1	4.3
10	26.5	63.0	1016.0	1.6	S	626.0	5.4
11	27.4	59.4	1016.0	1.9	S	739.3	6.7
12	28.0	57.3	1016.0	2.2	S	792.3	7.5
13	28.4	57.0	1015.9	2.4	S	796.7	7.6
14	28.4	58.0	1015.6	2.6	S	738.7	7.0
15	28.6	56.2	1015.4	2.3	S	646.7	5.9
16	28.3	58.8	1015.2	2.2	S	539.6	4.7
17	28.3	57.7	1014.9	2.0	S	413.2	3.7
18	28.1	56.7	1014.9	1.8	S	256.2	3.0
19	27.1	61.1	1015.1	1.5	SW	98.8	2.0
20	26.3	63.3	1015.2	0.9	SW	13.9	0.0
21	25.8	65.3	1015.5	0.4	SE	0.0	0.0
22	25.5	66.5	1015.8	0.3	SE	0.0	0.0
23	25.2	66.0	1015.9	0.4	SE	0.0	0.0

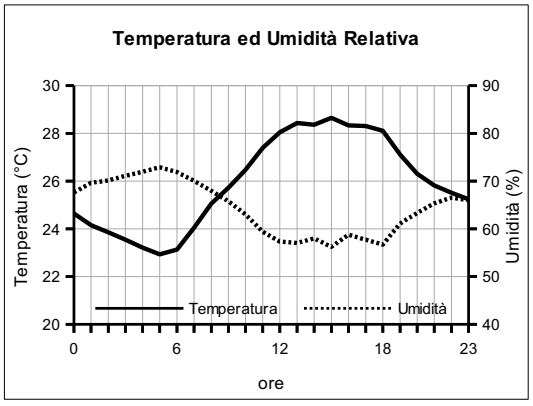

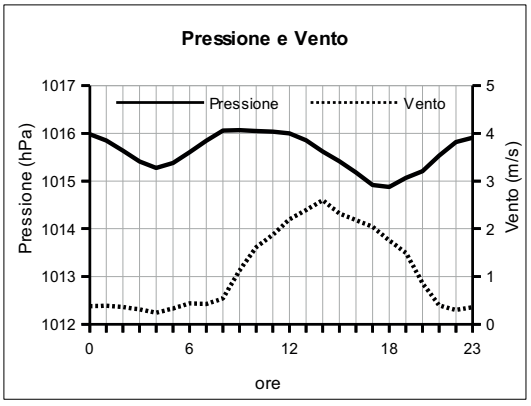

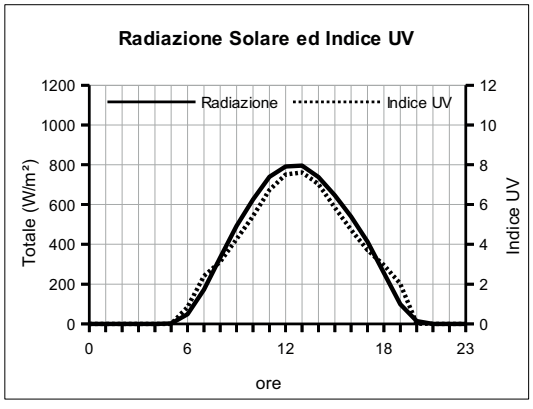

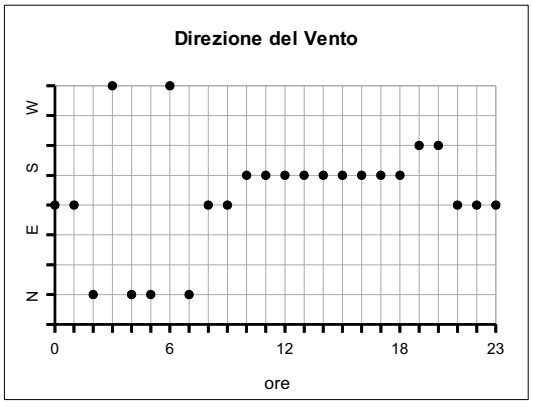

LUGLIO 2019 **(medie orarie)**

Ore	Temperatura °C	Umidità %	Pressione hPa	Vento velocità m/s	Vento direzione	Radiazione Solare W/m²	Radiazione Solare Indice UV
0	26.4	70.1	1013.2	0.5	N	0.0	0.0
1	26.1	70.5	1013.1	0.5	NW	0.0	0.0
2	25.8	70.9	1012.8	0.5	N	0.0	0.0
3	25.5	71.0	1012.6	0.4	N	0.0	0.0
4	25.3	71.2	1012.5	0.4	N	0.0	0.0
5	25.1	71.7	1012.6	0.5	SW	0.4	0.0
6	25.2	71.9	1012.7	0.5	SW	33.9	0.5
7	25.8	70.7	1012.9	0.6	SW	150.4	2.6
8	26.6	68.5	1013.0	0.9	E	311.1	3.3
9	27.1	66.8	1013.1	1.4	E	456.2	4.2
10	27.6	65.8	1013.2	1.8	S	594.1	5.3
11	28.3	64.3	1013.3	2.2	S	710.3	6.5
12	28.8	63.4	1013.2	2.4	S	782.9	7.3
13	29.1	62.9	1013.1	2.7	S	773.4	7.5
14	29.4	61.6	1012.8	2.7	S	736.7	7.0
15	29.6	60.1	1012.5	2.7	S	660.4	6.0
16	29.8	59.2	1012.3	2.6	S	517.7	4.8
17	29.7	59.2	1012.2	2.2	W	386.7	3.7
18	29.2	60.0	1012.0	1.8	W	249.1	3.0
19	28.7	61.7	1012.1	1.4	SW	96.2	2.1
20	27.9	64.9	1012.3	1.0	SW	12.7	0.0
21	27.3	67.3	1012.7	0.5	SW	0.0	0.0
22	26.9	69.4	1013.0	0.5	SW	0.0	0.0
23	26.6	70.7	1013.1	0.5	SW	0.0	0.0

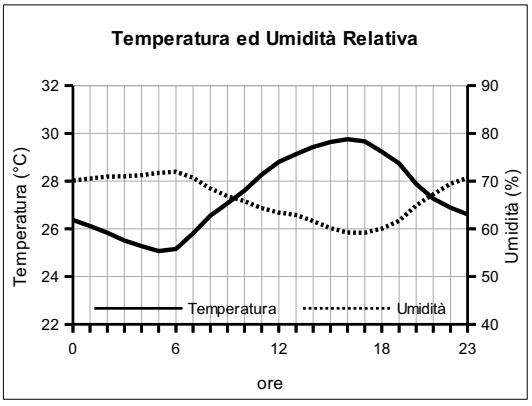

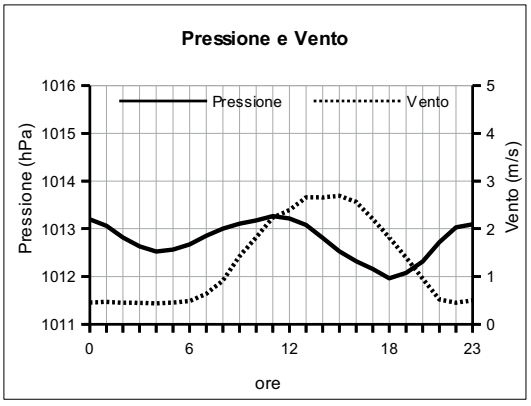

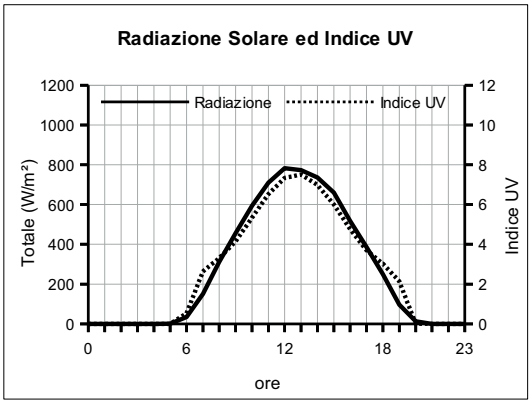

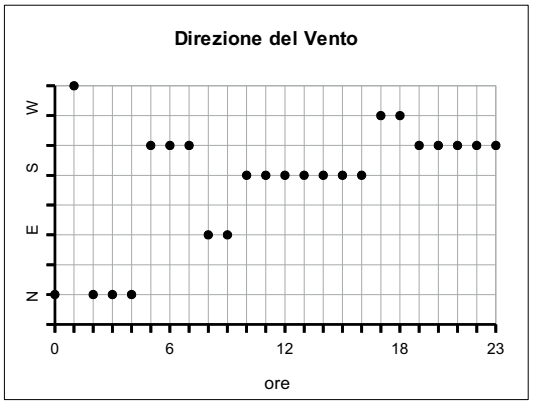

AGOSTO 2019 **(medie orarie)**

Ore	Temperatura °C	Umidità %	Pressione hPa	Vento velocità m/s	Vento direzione	Radiazione Solare W/m²	Radiazione Solare Indice UV
0	26.9	67.5	1014.6	0.0	N	0.0	0.0
1	26.6	69.7	1014.4	0.0	SW	0.0	0.0
2	26.4	71.3	1014.3	0.1	SW	0.0	0.0
3	26.1	72.0	1014.1	0.1	SW	0.0	0.0
4	25.8	71.4	1014.1	0.1	N	0.0	0.0
5	25.6	71.7	1014.1	0.0	N	0.0	0.0
6	25.5	72.0	1014.3	0.0	N	10.7	0.0
7	26.3	69.5	1014.6	0.0	N	93.2	0.1
8	27.6	65.1	1014.8	0.2	E	245.4	1.0
9	28.5	62.9	1014.9	0.6	S	412.4	1.9
10	29.1	61.1	1015.1	1.2	W	559.9	3.1
11	29.5	60.5	1015.0	1.7	W	685.5	4.2
12	29.9	59.8	1014.9	2.1	W	752.8	4.9
13	30.2	59.2	1014.6	2.2	W	774.2	5.1
14	30.8	56.7	1014.3	2.2	W	745.3	4.7
15	30.9	56.9	1014.0	2.1	W	644.2	3.6
16	30.9	55.8	1013.7	1.9	W	527.0	2.5
17	30.7	55.3	1013.6	1.6	W	368.6	1.5
18	30.1	56.2	1013.6	1.1	W	197.0	0.5
19	29.2	58.5	1013.7	0.6	W	47.0	0.0
20	28.4	60.9	1014.0	0.2	W	1.8	0.0
21	27.9	62.4	1014.4	0.1	N	0.0	0.0
22	27.6	63.8	1014.5	0.0	N	0.0	0.0
23	27.3	65.2	1014.6	0.0	N	0.0	0.0

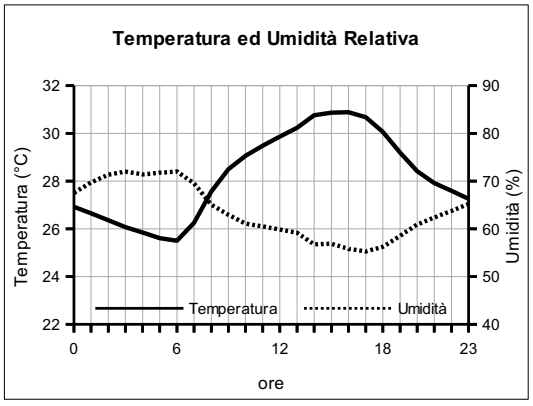

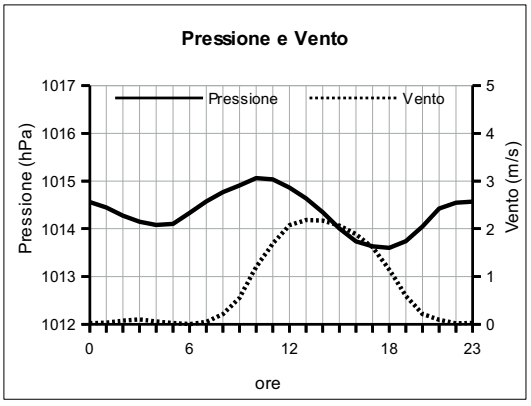

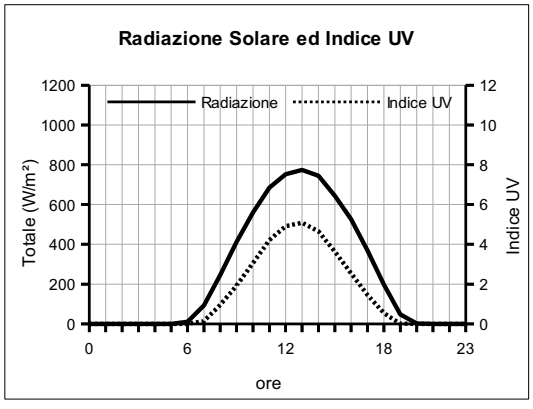

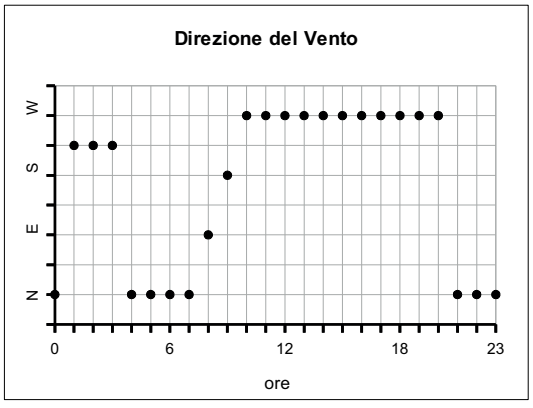

SETTEMBRE 2019 **(medie orarie)**

	Temperatura	Umidità	Pressione	Vento		Radiazione Solare	
Ore	°C	%	hPa	velocità m/s	direzione	W/m²	Indice UV
0	23.4	69.8	1018.1	0.7	N	1.7	0.0
1	23.2	70.4	1018.0	0.7	N	1.7	0.0
2	23.1	70.6	1017.8	0.9	N	1.7	0.0
3	22.8	71.4	1017.6	1.1	N	1.7	0.0
4	22.3	72.3	1017.5	0.9	N	1.7	0.0
5	22.0	73.7	1017.4	0.8	N	0.9	0.0
6	21.8	74.6	1017.5	0.7	N	0.9	0.0
7	22.0	74.3	1017.7	0.7	N	43.1	0.9
8	22.9	71.9	1017.9	0.6	N	177.6	3.1
9	24.0	68.2	1018.3	0.8	N	334.9	3.9
10	24.9	65.0	1018.4	1.4	E	478.1	4.8
11	25.6	62.4	1018.4	1.7	SE	574.1	5.7
12	26.2	60.7	1018.2	1.9	S	623.1	6.3
13	26.5	59.7	1017.9	2.1	S	608.8	6.2
14	26.9	58.3	1017.6	2.2	S	565.7	5.8
15	27.1	57.8	1017.3	2.0	S	494.9	5.0
16	27.0	58.6	1017.1	2.1	W	358.7	4.3
17	26.6	59.8	1017.0	2.0	W	233.1	3.6
18	26.0	61.4	1017.1	1.6	W	80.6	1.9
19	25.1	64.2	1017.3	1.2	W	7.9	0.0
20	24.6	65.3	1017.7	0.9	W	1.7	0.0
21	24.3	67.2	1018.1	0.7	N	1.7	0.0
22	23.9	68.6	1018.2	0.7	N	1.7	0.0
23	23.6	69.7	1018.2	0.7	N	1.7	0.0

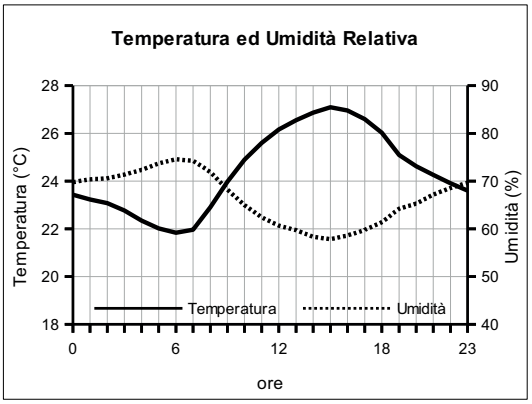

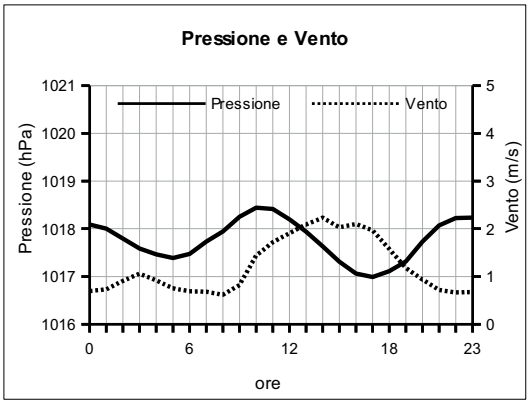

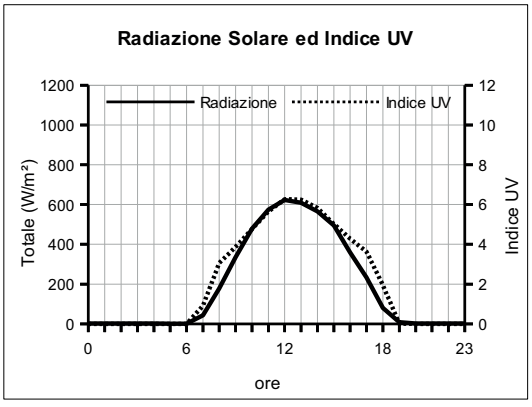

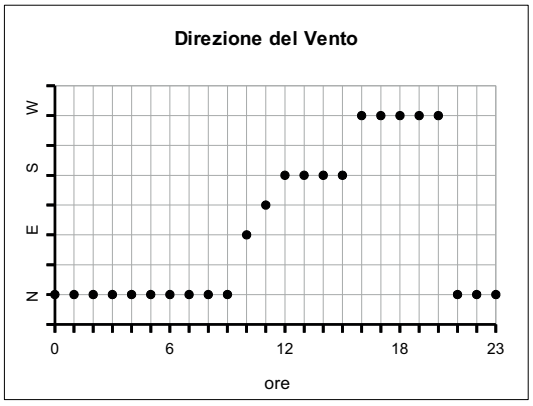

OTTOBRE 2019 **(medie orarie)**

Ore	Temperatura °C	Umidità %	Pressione hPa	Vento velocità m/s	Vento direzione	Radiazione Solare W/m²	Radiazione Solare Indice UV
0	19.3	78.2	1018.5	0.4	N	0.0	0.0
1	19.1	78.2	1018.4	0.4	N	0.0	0.0
2	18.9	78.1	1018.2	0.3	N	0.0	0.0
3	18.8	78.2	1017.9	0.4	N	0.0	0.0
4	18.5	78.8	1017.8	0.4	N	0.0	0.0
5	18.3	78.9	1017.8	0.3	W	0.0	0.0
6	18.2	78.5	1017.8	0.4	N	0.6	0.0
7	18.1	78.6	1018.0	0.4	N	23.3	0.4
8	18.9	76.9	1018.4	0.6	N	131.1	2.6
9	20.0	73.4	1018.7	0.8	N	272.7	3.4
10	21.3	70.0	1018.9	0.9	E	403.4	4.3
11	22.2	67.2	1018.8	1.3	SE	502.8	4.8
12	22.7	65.5	1018.5	1.8	S	547.0	5.5
13	23.1	63.7	1018.0	2.0	S	532.6	5.5
14	23.5	62.3	1017.6	1.9	S	468.5	5.1
15	23.6	62.4	1017.4	1.8	S	373.9	4.5
16	23.4	62.9	1017.3	1.6	W	231.5	3.6
17	22.7	65.8	1017.4	1.4	W	89.9	2.3
18	21.7	70.1	1017.7	1.0	W	10.5	0.1
19	21.1	72.4	1018.0	0.5	N	0.0	0.0
20	20.7	73.5	1018.2	0.4	W	0.0	0.0
21	20.4	74.7	1018.4	0.5	N	0.0	0.0
22	19.9	76.8	1018.6	0.5	N	0.0	0.0
23	19.5	77.8	1018.6	0.5	N	0.0	0.0

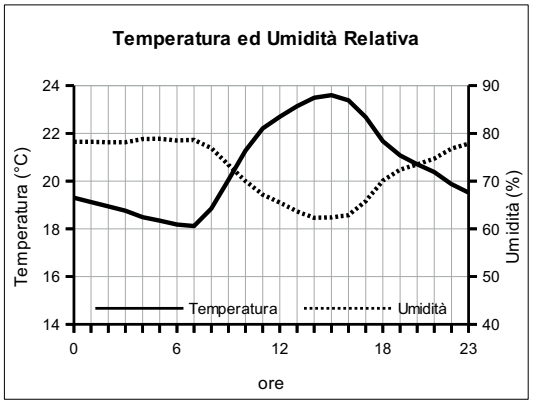

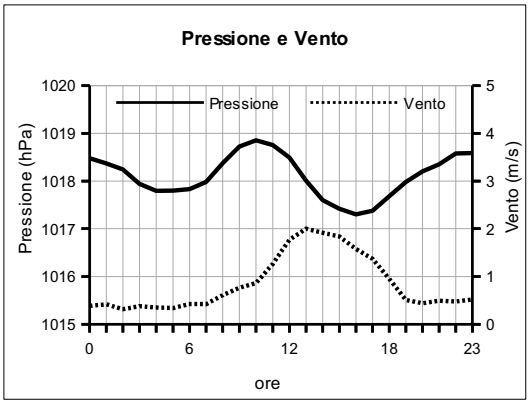

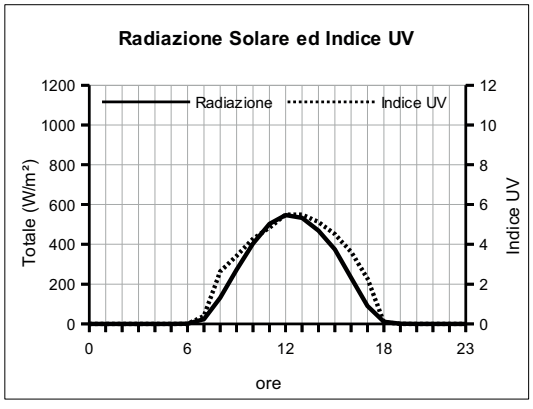

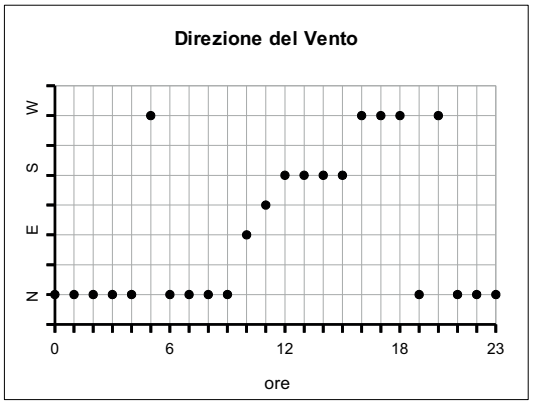

NOVEMBRE 2019 **(medie orarie)**

	Temperatura	Umidità	Pressione	Vento		Radiazione Solare	
Ore	°C	%	hPa	velocità m/s	direzione	W/m²	Indice UV
0	16.2	80.6	1010.5	1.8	S	0.0	0.0
1	16.3	80.0	1010.3	1.9	S	0.0	0.0
2	16.1	80.5	1010.2	1.9	S	0.0	0.0
3	15.8	82.1	1010.1	1.8	S	0.0	0.0
4	15.8	82.7	1010.0	1.6	S	0.0	0.0
5	15.6	83.5	1010.0	1.6	SW	0.0	0.0
6	15.5	83.8	1010.1	1.4	S	0.2	0.0
7	15.6	83.4	1010.4	1.5	W	19.5	0.2
8	15.9	83.4	1010.8	1.3	SW	77.7	2.0
9	16.3	82.6	1011.1	1.4	S	152.7	3.4
10	17.0	81.0	1011.3	1.7	S	248.3	3.8
11	17.5	78.2	1011.0	2.4	S	251.1	3.8
12	17.7	76.7	1010.6	2.6	S	264.6	3.9
13	17.7	76.1	1010.2	2.7	S	218.1	3.6
14	17.9	74.7	1010.1	2.9	S	194.6	3.7
15	17.8	74.8	1010.1	2.7	S	100.6	2.7
16	17.5	75.2	1010.2	2.5	S	20.5	0.3
17	17.3	76.1	1010.4	2.5	S	0.2	0.0
18	17.0	77.7	1010.6	2.5	S	0.0	0.0
19	16.7	78.9	1010.7	2.4	S	0.0	0.0
20	16.6	78.9	1010.8	2.3	S	0.0	0.0
21	16.6	79.1	1010.9	2.4	S	0.0	0.0
22	16.4	79.2	1010.8	2.2	S	0.0	0.0
23	16.2	80.4	1010.8	2.0	S	0.0	0.0

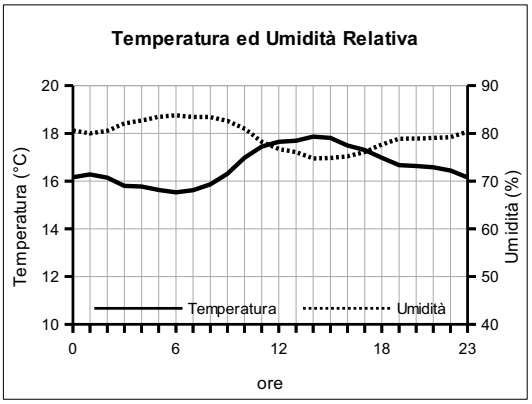

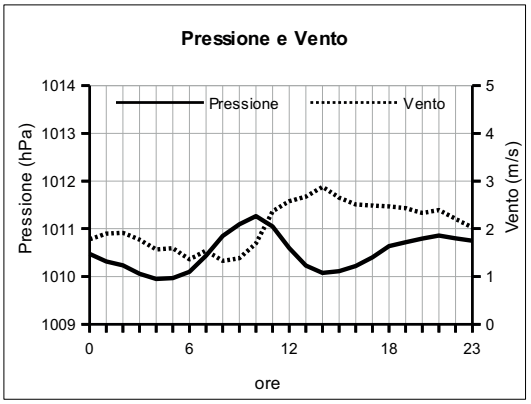

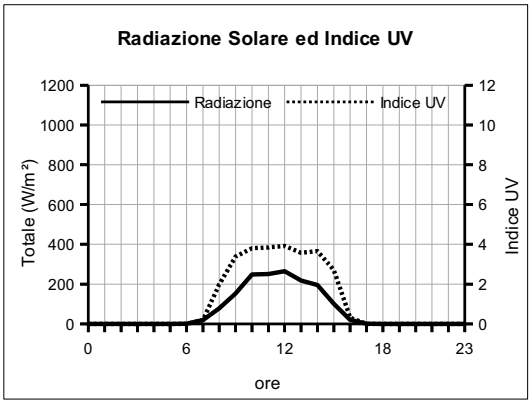

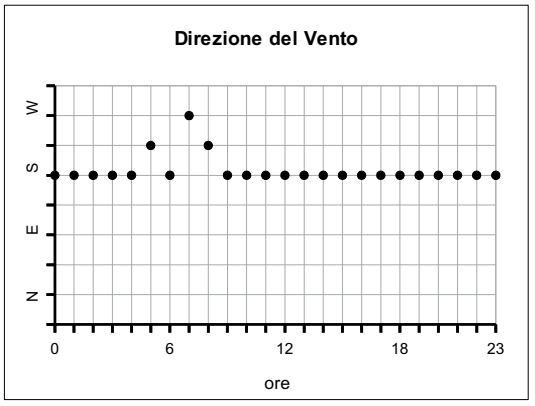

DICEMBRE 2019 **(medie orarie)**

Ore	Temperatura °C	Umidità %	Pressione hPa	Vento velocità m/s	Vento direzione	Radiazione Solare W/m²	Radiazione Solare Indice UV
0	12.7	73.8	1017.6	1.4	N	0.0	0.0
1	12.6	74.0	1017.4	1.2	N	0.0	0.0
2	12.5	74.3	1017.4	1.3	N	0.0	0.0
3	12.3	74.9	1017.2	1.2	N	0.0	0.0
4	12.0	75.3	1017.0	1.2	N	0.0	0.0
5	11.9	75.7	1017.0	1.1	N	0.0	0.0
6	11.7	76.2	1017.2	1.2	N	0.0	0.0
7	11.6	75.7	1017.6	1.2	N	7.0	0.0
8	12.0	74.7	1017.9	1.3	N	72.4	2.3
9	13.0	72.6	1018.2	1.4	N	185.7	4.0
10	14.0	69.6	1018.3	1.6	E	277.5	4.3
11	14.6	66.8	1018.1	2.0	E	297.2	4.3
12	14.9	66.1	1017.5	2.0	SE	309.1	4.4
13	15.3	65.1	1017.0	2.0	SE	297.0	4.4
14	15.4	65.3	1016.8	2.0	SE	209.1	4.0
15	15.1	66.1	1016.8	2.1	NW	106.6	3.3
16	14.6	68.1	1016.9	1.7	N	17.1	0.2
17	14.0	69.9	1017.1	1.5	N	0.0	0.0
18	13.7	70.5	1017.4	1.4	N	0.0	0.0
19	13.2	71.8	1017.6	1.5	N	0.0	0.0
20	13.1	72.7	1017.8	1.4	N	0.0	0.0
21	13.0	72.9	1017.9	1.4	N	0.0	0.0
22	12.8	73.3	1017.9	1.5	N	0.0	0.0
23	12.7	73.5	1018.0	1.5	N	0.0	0.0

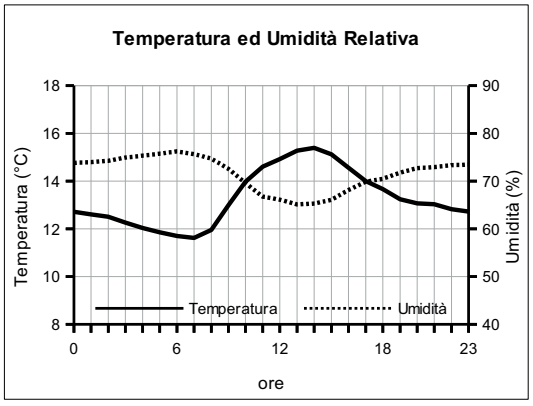

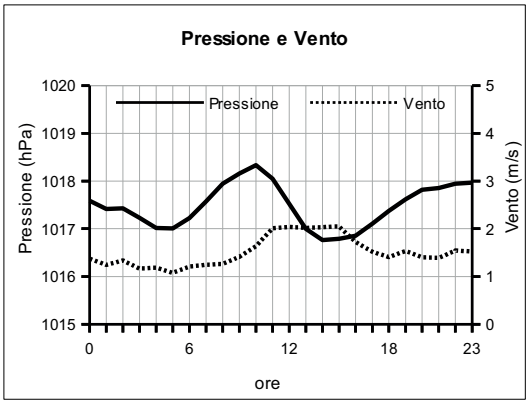

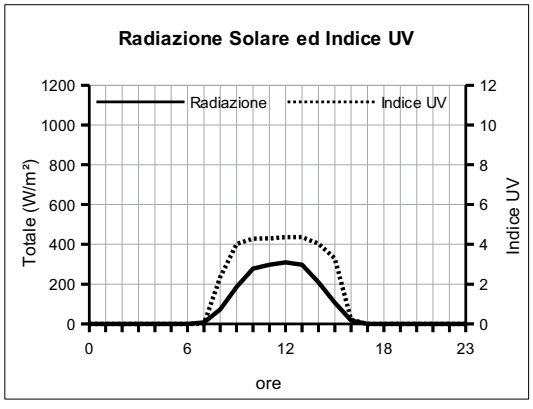

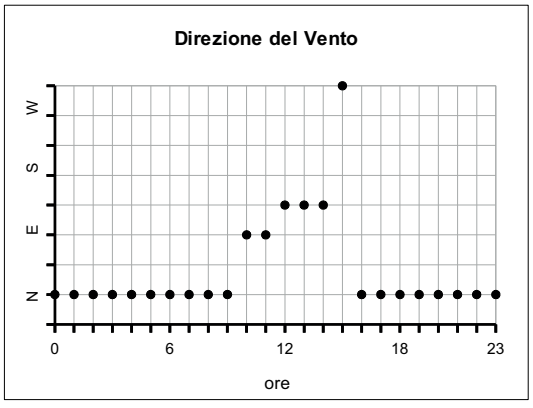

GENNAIO 2019 **(medie giornaliere)**

	Temperatura	Umidità	Pressione	Vento		Rad. Solare		Pioggia	Indice UV		
Data	°C	%	hPa	m/s	direzione	W/m²	durata	mm	medio	max	(ore)
01/01/19	9.7	49.7	1024.4	2.4	N	256.0	9:30	0.0	3.6	5.3	(12:30)
02/01/19	8.9	60.2	1016.3	1.7	NE	152.2	9:30	0.0	3.4	4.3	(13:00)
03/01/19	4.9	61.3	1022.0	3.9	N	245.3	9:30	0.0	3.8	6.4	(12:20)
04/01/19	2.9	63.6	1026.8	2.9	N	210.8	9:30	0.0	3.5	5.3	(13:40)
05/01/19	6.0	55.0	1023.2	1.4	NW	218.6	9:30	0.0	3.7	4.9	(11:50)
06/01/19	8.5	59.3	1020.6	1.0	NW	225.3	9:40	0.0	3.9	5.3	(13:20)
07/01/19	8.2	62.6	1025.9	1.8	NE	216.2	9:30	0.0	3.8	6.8	(10:50)
08/01/19	8.3	78.3	1021.4	0.4	SE	66.5	9:20	2.3	3.7	4.7	(12:10)
09/01/19	8.7	79.6	1003.7	1.1	N	52.5	9:10	1.5	3.6	5.6	(13:10)
10/01/19	7.9	59.6	1006.3	1.2	NE	161.2	9:20	0.0	3.3	4.3	(14:30)
11/01/19	6.8	62.3	1015.8	1.7	NE	227.8	9:40	0.0	3.4	5.4	(14:40)
12/01/19	7.4	54.5	1018.4	2.3	NW	266.6	9:50	0.0	3.6	4.8	(12:50)
13/01/19	8.2	68.4	1014.3	0.1	--	105.2	9:50	0.0	3.6	4.0	(09:30)
14/01/19	9.6	86.7	1005.8	0.4	N	81.8	9:00	7.6	3.9	6.7	(14:20)
15/01/19	8.9	59.5	1018.2	1.7	N	266.9	9:50	0.0	3.6	6.5	(13:20)
16/01/19	9.9	60.2	1025.4	0.4	SW	195.7	9:40	0.0	3.6	4.7	(12:40)
17/01/19	11.3	73.9	1021.0	1.9	S	230.0	9:20	0.0	3.6	5.4	(11:50)
18/01/19	12.5	79.5	1015.8	1.4	S	216.1	9:40	6.1	4.0	6.0	(14:50)
19/01/19	10.0	86.6	1015.4	0.3	NE	144.5	9:50	4.8	3.7	6.5	(12:50)
20/01/19	10.1	78.4	1014.6	0.6	E	118.7	9:50	0.8	4.0	5.4	(09:40)
21/01/19	10.6	83.4	1012.8	1.1	NE	60.7	9:00	10.6	3.2	4.8	(15:10)
22/01/19	10.0	86.2	1005.8	0.9	SW	79.8	9:30	**24.3**	3.8	8.6	(12:20)
23/01/19	7.9	81.7	999.8	0.5	SE	213.5	9:40	5.1	4.0	6.0	(10:00)
24/01/19	8.4	79.1	991.5	1.8	NE	33.0	9:00	7.6	4.1	5.7	(11:30)
25/01/19	8.6	66.1	997.4	2.8	NE	208.8	10:10	2.0	3.8	6.0	(13:20)
26/01/19	8.0	62.9	1007.9	1.1	NE	285.3	9:50	0.0	3.6	5.4	(11:40)
27/01/19	10.0	75.0	1009.5	1.7	SE	153.5	10:00	2.3	3.4	4.6	(11:10)
28/01/19	10.7	75.6	1001.1	2.1	SW	163.9	9:50	11.9	3.7	**8.8**	**(09:00)**
29/01/19	8.3	85.7	1003.8	0.6	NW	135.6	9:50	8.1	3.6	5.7	(13:40)
30/01/19	8.0	80.7	1003.0	0.9	SW	152.1	9:20	12.4	3.9	4.6	(13:50)
31/01/19	9.6	75.5	1007.2	2.2	SW	177.8	10:10	5.8	3.7	6.1	(15:30)

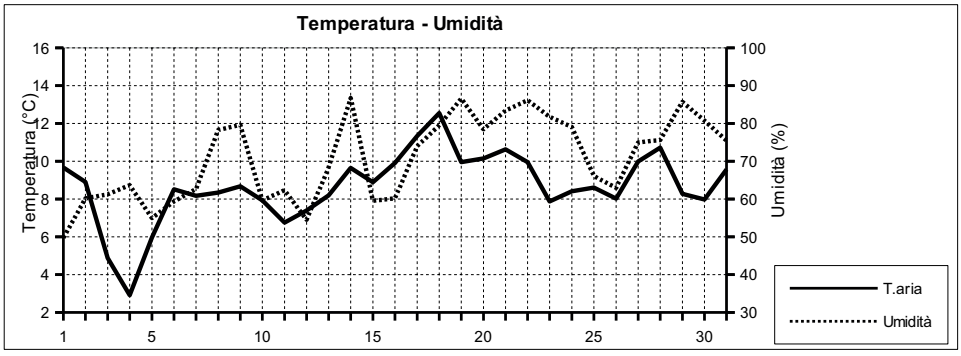

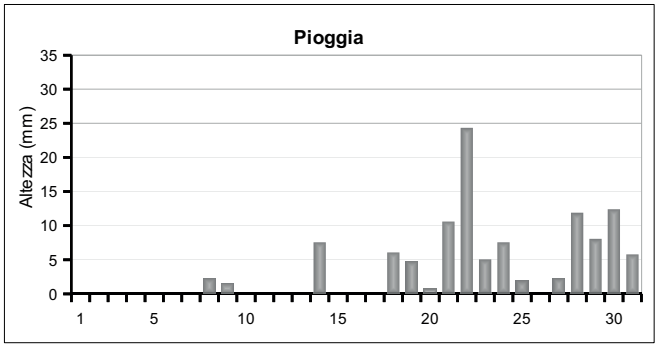

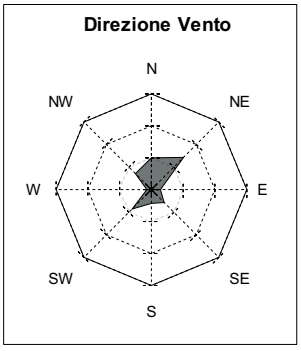

GENNAIO 2019 **(estremi giornalieri)**

	Temperatura (°C)				Umidità (%)				Pressione (hPa)				Vento (m/s)		Radiazione (W/m²)	
Data	min	(ore)	max	(ore)	min	(ore)	max	(ore)	min	(ore)	max	(ore)	max	(ore)	max	(ore)
01/01/19	7.8	(23:50)	12.1	(13:30)	42.0	(13:30)	56.0	(20:20)	1022.0	(23:50)	1026.2	(08:40)	11.6	(12:00)	443.0	(12:10)
02/01/19	6.7	(03:30)	13.3	(15:10)	46.0	(22:40)	72.0	(09:00)	1012.6	(15:20)	1021.8	(00:00)	**15.2**	**(23:40)**	425.0	(12:50)
03/01/19	2.7	(21:50)	7.8	(00:00)	49.0	(00:00)	71.0	(14:10)	1016.8	(00:00)	1025.3	(23:10)	12.5	(00:10)	570.0	(12:50)
04/01/19	**1.4**	**(06:30)**	5.4	(14:50)	45.0	(14:50)	82.0	(04:50)	1025.5	(00:00)	1027.8	(10:00)	11.2	(08:20)	566.0	(11:40)
05/01/19	2.0	(00:00)	9.9	(14:20)	**41.0**	**(14:30)**	71.0	(00:00)	1020.2	(22:50)	1025.9	(00:00)	10.3	(01:50)	591.0	(12:20)
06/01/19	4.2	(07:30)	13.2	(15:00)	44.0	(11:20)	69.0	(07:50)	1019.6	(05:20)	1023.0	(23:40)	7.6	(12:30)	645.0	(13:10)
07/01/19	6.6	(05:40)	10.6	(14:20)	55.0	(12:40)	70.0	(01:30)	1023.1	(00:00)	**1028.1**	**(22:20)**	9.4	(10:50)	526.0	(11:40)
08/01/19	6.0	(06:20)	10.3	(17:40)	68.0	(00:00)	89.0	(23:50)	1011.5	(23:50)	1027.8	(00:00)	4.9	(16:20)	425.0	(10:00)
09/01/19	7.3	(19:40)	9.9	(00:00)	68.0	(22:30)	89.0	(00:00)	1000.7	(20:20)	1011.3	(00:00)	8.0	(16:00)	197.0	(13:50)
10/01/19	5.4	(23:50)	10.3	(13:00)	46.0	(13:10)	69.0	(00:10)	1001.1	(01:40)	1013.2	(23:50)	6.7	(17:00)	526.0	(11:40)
11/01/19	5.0	(04:20)	9.7	(14:50)	52.0	(14:10)	69.0	(23:20)	1013.0	(00:00)	1018.4	(21:00)	9.8	(16:10)	522.0	(12:10)
12/01/19	4.7	(06:10)	10.6	(15:00)	43.0	(13:40)	67.0	(00:00)	1017.6	(16:10)	1019.5	(09:10)	8.0	(11:20)	464.0	(12:00)
13/01/19	4.8	(03:20)	11.3	(15:30)	51.0	(00:00)	86.0	(23:30)	1010.8	(23:30)	1017.8	(00:00)	3.6	(00:00)	348.0	(15:00)
14/01/19	7.8	(02:40)	11.8	(15:40)	72.0	(23:40)	**94.0**	**(11:50)**	1001.1	(12:10)	1010.9	(00:00)	5.8	(12:10)	385.0	(14:10)
15/01/19	6.7	(06:50)	11.8	(13:50)	41.0	(15:10)	77.0	(03:40)	1009.1	(00:00)	1025.6	(23:30)	8.9	(14:00)	545.0	(12:00)
16/01/19	5.7	(02:20)	13.3	(14:50)	51.0	(00:00)	69.0	(13:00)	1024.4	(17:50)	1026.8	(10:40)	5.8	(16:10)	621.0	(13:10)
17/01/19	8.2	(02:20)	13.3	(12:10)	63.0	(00:00)	79.0	(06:30)	1017.2	(23:40)	1024.8	(00:00)	11.2	(23:40)	606.0	(11:30)
18/01/19	9.9	(23:30)	**14.8**	**(13:10)**	67.0	(13:10)	89.0	(23:40)	1015.0	(17:40)	1017.2	(00:00)	11.2	(00:40)	638.0	(12:40)
19/01/19	8.4	(23:30)	12.7	(14:40)	73.0	(14:50)	91.0	(01:00)	1014.6	(16:10)	1016.7	(00:00)	4.9	(14:10)	524.0	(13:50)
20/01/19	8.3	(01:10)	12.1	(12:10)	68.0	(12:00)	85.0	(00:40)	1013.7	(16:00)	1015.8	(00:00)	8.0	(22:30)	454.0	(11:30)
21/01/19	9.3	(18:50)	12.0	(01:20)	76.0	(01:10)	91.0	(22:40)	1009.8	(22:40)	1014.5	(00:00)	7.2	(01:50)	197.0	(12:00)
22/01/19	7.3	(20:40)	11.8	(11:20)	75.0	(16:20)	93.0	(03:10)	1004.4	(08:50)	1009.5	(00:00)	13.4	(20:30)	649.0	(11:10)
23/01/19	5.7	(07:50)	10.4	(16:00)	69.0	(12:30)	90.0	(04:30)	994.3	(23:20)	1005.6	(00:20)	8.5	(07:30)	624.0	(12:20)
24/01/19	6.7	(02:10)	10.1	(21:50)	71.0	(11:30)	86.0	(16:00)	**989.5**	**(08:30)**	994.1	(00:00)	12.5	(22:30)	81.0	(10:40)
25/01/19	6.8	(23:50)	11.3	(13:20)	50.0	(12:20)	87.0	(01:20)	993.4	(06:00)	1003.2	(23:50)	13.4	(06:00)	670.0	(13:10)
26/01/19	5.7	(05:00)	10.9	(15:10)	51.0	(14:50)	72.0	(05:10)	1003.3	(00:00)	1011.9	(21:40)	8.9	(11:00)	512.0	(11:10)
27/01/19	6.0	(03:40)	13.3	(23:50)	69.0	(00:40)	90.0	(22:10)	1003.6	(23:50)	1012.1	(00:00)	14.3	(23:40)	422.0	(10:00)
28/01/19	8.2	(21:30)	13.4	(00:20)	56.0	(11:40)	89.0	(01:40)	999.3	(06:30)	1003.7	(00:00)	14.3	(00:50)	**724.0**	**(12:00)**
29/01/19	7.2	(07:20)	10.6	(12:20)	75.0	(12:10)	91.0	(08:20)	1002.0	(04:00)	1005.2	(21:50)	5.4	(10:00)	587.0	(11:20)
30/01/19	5.8	(06:30)	10.6	(13:00)	60.0	(22:40)	89.0	(08:00)	1001.5	(16:50)	1005.0	(00:00)	13.9	(23:20)	561.0	(13:50)
31/01/19	6.2	(00:00)	11.9	(22:50)	51.0	(11:30)	92.0	(23:50)	1002.8	(01:30)	1010.2	(21:20)	11.6	(01:10)	721.0	(11:20)

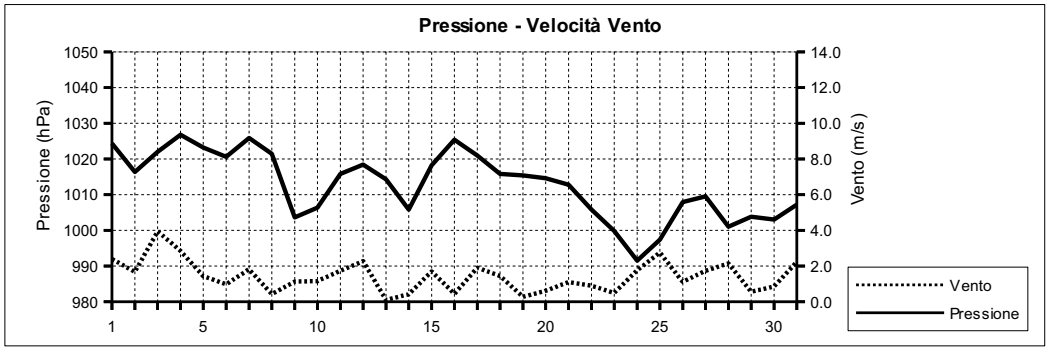

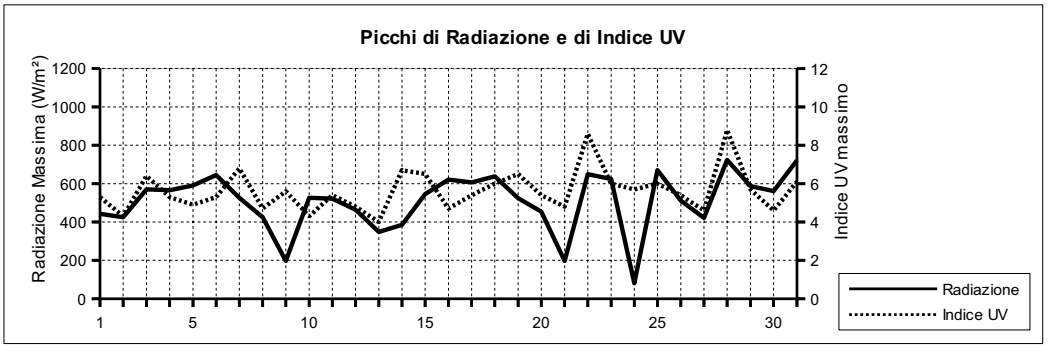

FEBBRAIO 2019 **(medie giornaliere)**

	Temperatura	Umidità	Pressione	Vento		Rad. Solare		Pioggia	Indice UV		
Data	°C	%	hPa	m/s	direzione	W/m²	durata	mm	medio	max	(ore)
01/02/19	14.2	85.3	1008.7	3.6	S	32.8	9:40	**9.6**	1.5	4.0	(11:00)
02/02/19	15.1	80.2	1003.7	4.2	SE	165.3	9:40	0.5	3.1	4.3	(12:20)
03/02/19	12.9	73.9	1007.5	2.3	S	312.3	10:20	0.5	4.0	5.6	(12:40)
04/02/19	11.4	72.3	1015.5	2.8	NE	149.3	9:50	1.3	4.3	6.0	(12:10)
05/02/19	12.0	60.9	1016.8	3.7	N	279.8	10:20	0.0	4.3	6.1	(11:10)
06/02/19	11.8	57.6	1017.2	3.4	NE	320.6	10:20	0.0	4.7	6.6	(11:40)
07/02/19	12.2	59.5	1019.7	1.3	NW	330.0	10:30	0.0	4.9	7.4	(11:20)
08/02/19	11.9	78.2	1019.8	0.5	SW	207.9	10:40	0.0	4.1	5.2	(11:50)
09/02/19	11.3	75.8	1023.4	0.7	NW	307.6	10:30	0.0	4.3	5.6	(12:20)
10/02/19	12.9	82.0	1023.3	1.9	S	255.2	10:20	0.0	4.3	6.0	(11:40)
11/02/19	11.8	76.3	1013.3	2.5	SW	152.0	10:20	2.0	3.8	7.5	(14:30)
12/02/19	9.7	56.1	1022.7	2.5	NE	302.7	10:40	0.0	3.2	4.6	(12:50)
13/02/19	9.4	43.5	1030.8	4.5	NE	363.0	10:40	0.0	3.7	6.5	(12:00)
14/02/19	11.8	54.0	1031.7	2.2	N	335.4	11:00	0.0	3.5	5.5	(12:20)
15/02/19	12.6	48.8	1028.0	2.4	NE	347.2	10:50	0.0	3.7	5.7	(11:40)
16/02/19	11.8	58.3	1030.2	1.9	NE	354.1	10:50	0.0	3.5	5.2	(13:00)
17/02/19	11.2	66.9	1029.8	0.4	NW	349.7	11:00	0.0	3.7	5.7	(13:50)
18/02/19	11.5	76.9	1027.2	0.6	NW	112.0	11:00	0.0	3.0	3.9	(13:20)
19/02/19	11.2	70.2	1025.1	0.5	NW	109.2	10:40	0.0	3.2	4.2	(12:50)
20/02/19	11.0	69.5	1025.5	0.7	W	322.0	11:00	0.0	4.2	6.3	(12:00)
21/02/19	11.3	76.8	1027.9	0.7	NW	326.8	11:00	0.0	4.1	5.8	(12:30)
22/02/19	11.9	78.8	1024.1	1.0	NW	303.3	11:00	0.0	5.1	6.5	(12:10)
23/02/19	7.0	47.2	1022.1	6.7	NE	382.4	11:10	0.3	4.6	8.5	(09:50)
24/02/19	7.4	48.0	1026.9	6.2	NE	362.0	11:10	0.0	4.8	8.7	(16:10)
25/02/19	8.2	53.4	1027.7	3.1	NE	271.7	11:00	0.5	4.0	8.5	(11:30)
26/02/19	10.9	54.7	1027.1	1.1	NW	375.1	11:10	0.0	4.5	6.5	(12:50)
27/02/19	13.4	52.4	1022.8	2.5	NE	392.1	11:20	0.0	4.7	**8.7**	**(12:20)**
28/02/19	12.7	54.1	1023.9	0.7	SW	383.9	11:30	0.0	4.7	8.3	(12:30)

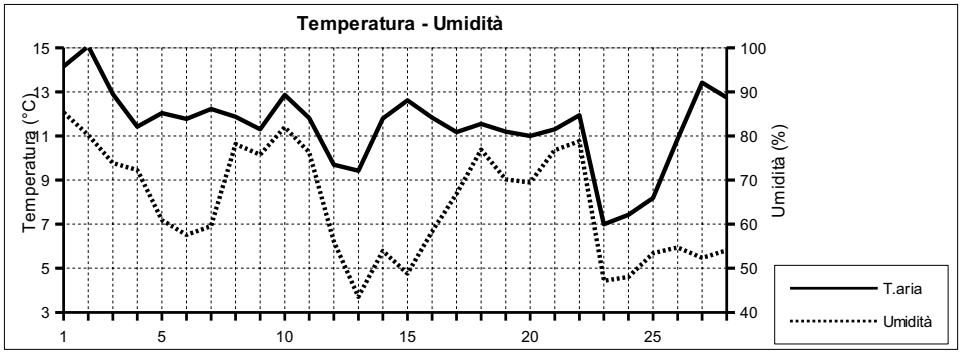

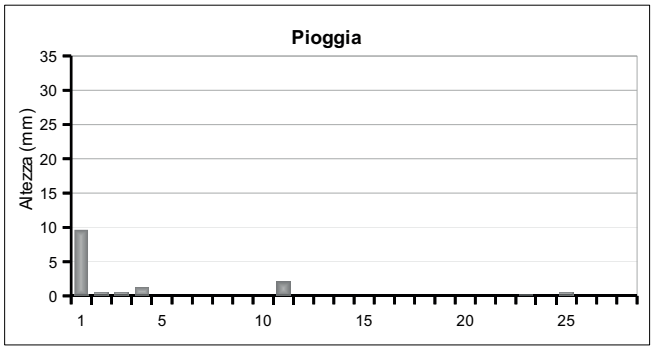

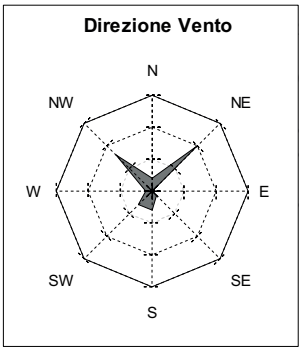

FEBBRAIO 2019 **(estremi giornalieri)**

	Temperatura (°C)				Umidità (%)				Pressione (hPa)				Vento (m/s)		Radiazione (W/m²)	
Data	min	(ore)	max	(ore)	min	(ore)	max	(ore)	min	(ore)	max	(ore)	max	(ore)	max	(ore)
01/02/19	11.8	(00:00)	15.4	(23:10)	77.0	(18:10)	**93.0**	**(01:40)**	1006.3	(22:50)	1010.6	(11:20)	12.5	(03:00)	81.0	(12:40)
02/02/19	12.8	(22:50)	16.1	(03:00)	72.0	(03:00)	87.0	(19:00)	**1000.3**	**(17:20)**	1006.5	(00:00)	13.4	(13:10)	694.0	(13:00)
03/02/19	11.3	(04:50)	14.3	(12:40)	65.0	(15:20)	83.0	(00:00)	1003.5	(04:10)	1013.9	(23:50)	9.4	(01:50)	789.0	(13:10)
04/02/19	9.2	(05:10)	13.7	(12:00)	60.0	(11:50)	82.0	(20:20)	1013.7	(00:40)	1017.6	(19:50)	13.4	(12:10)	403.0	(11:40)
05/02/19	9.7	(23:30)	15.5	(13:20)	52.0	(14:00)	71.0	(00:00)	1015.8	(03:50)	1017.8	(09:20)	11.2	(14:20)	563.0	(12:30)
06/02/19	9.4	(01:00)	14.8	(14:50)	49.0	(15:30)	63.0	(02:10)	1014.8	(05:00)	1020.1	(23:40)	13.9	(12:50)	547.0	(12:40)
07/02/19	9.5	(05:30)	16.2	(14:10)	41.0	(14:00)	79.0	(23:00)	1018.4	(14:10)	1020.7	(07:40)	6.3	(04:00)	559.0	(12:10)
08/02/19	10.1	(23:50)	14.6	(15:40)	63.0	(17:00)	85.0	(05:20)	1019.0	(04:20)	1021.6	(23:30)	4.0	(14:40)	722.0	(13:00)
09/02/19	7.9	(07:10)	14.4	(14:40)	66.0	(10:50)	83.0	(22:30)	1021.7	(00:00)	1025.4	(23:10)	5.4	(13:30)	677.0	(12:10)
10/02/19	11	(00:40)	14.5	(12:10)	72.0	(14:50)	88.0	(06:50)	1017.9	(23:40)	1025.4	(08:30)	8.9	(20:40)	733.0	(13:10)
11/02/19	7.9	(23:40)	14.2	(08:50)	51.0	(12:40)	90.0	(05:40)	1010.5	(13:00)	1017.7	(00:00)	20.6	(15:20)	724.0	(11:10)
12/02/19	7	(07:10)	14.1	(13:20)	34.0	(15:30)	76.0	(00:00)	1016.9	(00:00)	1029.2	(23:50)	11.6	(13:40)	694.0	(13:30)
13/02/19	7.7	(06:20)	11.4	(13:50)	35.0	(13:40)	53.0	(23:50)	1029.2	(00:00)	1032.1	(11:20)	17.9	(23:10)	613.0	(12:10)
14/02/19	8.4	(06:50)	16.1	(14:10)	41.0	(12:40)	67.0	(19:30)	1030.0	(22:40)	**1033.4**	**(09:00)**	14.3	(01:30)	738.0	(11:10)
15/02/19	9.8	(05:30)	16.7	(14:10)	40.0	(11:50)	61.0	(22:00)	1025.4	(15:40)	1030.4	(00:00)	14.8	(15:50)	626.0	(12:10)
16/02/19	9.4	(06:40)	15.3	(15:40)	42.0	(14:20)	78.0	(21:30)	1028.7	(00:40)	1031.3	(10:40)	10.7	(02:40)	610.0	(12:20)
17/02/19	7.3	(07:00)	15.2	(13:50)	51.0	(14:00)	83.0	(23:20)	1028.4	(16:20)	1031.0	(00:20)	4.0	(14:00)	591.0	(12:50)
18/02/19	10.3	(23:00)	13.2	(15:50)	66.0	(16:50)	83.0	(00:00)	1025.5	(17:40)	1029.2	(00:00)	4.5	(17:50)	469.0	(09:50)
19/02/19	9.2	(23:00)	12.9	(13:30)	62.0	(13:30)	78.0	(00:00)	1024.1	(17:10)	1026.1	(10:50)	4.5	(14:50)	308.0	(12:50)
20/02/19	9.3	(00:00)	13.8	(15:10)	61.0	(10:40)	78.0	(23:10)	1024.6	(03:30)	1027.1	(23:50)	5.8	(14:50)	599.0	(12:20)
21/02/19	8.2	(06:30)	15.0	(15:30)	66.0	(16:30)	84.0	(23:50)	1027.1	(00:00)	1029.1	(10:20)	5.8	(14:10)	575.0	(12:20)
22/02/19	9.1	(05:50)	14.7	(15:30)	52.0	(23:10)	89.0	(06:30)	1021.2	(15:50)	1028.0	(00:10)	9.4	(22:10)	684.0	(12:30)
23/02/19	**3.6**	**(12:20)**	13.1	(00:00)	33.0	(06:10)	68.0	(00:50)	1019.3	(13:20)	1024.4	(23:10)	**25.0**	**(10:30)**	789.0	(12:00)
24/02/19	5.3	(05:50)	9.7	(13:50)	39.0	(15:30)	54.0	(01:00)	1023.8	(00:30)	1029.3	(19:50)	20.6	(12:20)	700.0	(12:10)
25/02/19	5.1	(17:00)	12.9	(13:20)	40.0	(12:10)	79.0	(15:20)	1024.7	(13:40)	1029.7	(00:40)	15.2	(21:40)	**865.0**	**(13:30)**
26/02/19	6.2	(01:10)	15.6	(14:50)	37.0	(10:50)	79.0	(23:40)	1024.4	(23:10)	1028.9	(01:00)	7.2	(16:00)	802.0	(12:20)
27/02/19	8.8	(04:40)	**17.8**	**(11:00)**	**32.0**	**(10:30)**	82.0	(04:40)	1021.5	(13:50)	1024.8	(23:50)	13.9	(13:50)	679.0	(12:20)
28/02/19	9.4	(07:00)	16.2	(14:00)	42.0	(09:40)	81.0	(23:40)	1021.4	(23:50)	1025.4	(10:00)	6.3	(15:30)	664.0	(12:20)

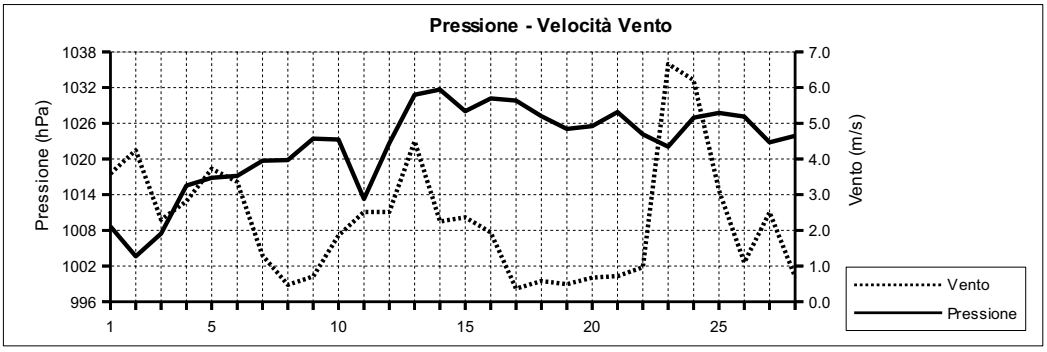

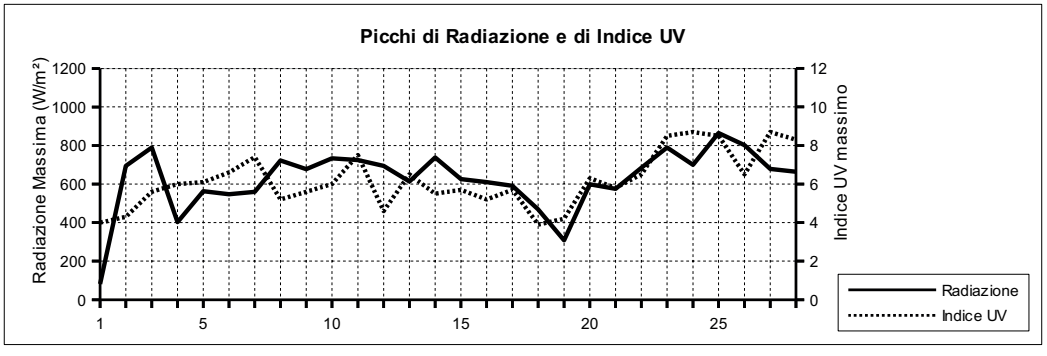

MARZO 2019 **(medie giornaliere)**

	Temperatura	Umidità	Pressione	Vento		Rad. Solare		Pioggia	Indice UV		
Data	°C	%	hPa	m/s	direzione	W/m²	durata	mm	medio	max	(ore)
01/03/19	13.0	78.3	1016.3	1.3	S	333.7	11:20	0.0	4.8	7.6	(10:50)
02/03/19	14.0	68.8	1014.8	1.0	NE	350.6	11:20	0.0	3.9	7.1	(11:50)
03/03/19	14.1	68.2	1019.7	0.9	NE	382.5	11:30	0.0	4.9	8.1	(14:10)
04/03/19	13.3	82.3	1020.0	2.0	S	369.4	11:20	0.0	5.5	**9.8**	**(12:50)**
05/03/19	14.1	84.3	1017.9	2.1	S	241.4	11:10	0.0	3.8	5.9	(11:40)
06/03/19	13.6	81.8	1021.3	0.8	SW	390.4	11:40	0.0	4.5	6.5	(12:30)
07/03/19	15.7	67.9	1018.7	1.3	SW	355.8	11:30	0.0	4.4	6.7	(11:50)
08/03/19	15.7	81.4	1021.1	1.1	SW	355.4	11:30	0.0	4.1	6.1	(11:40)
09/03/19	14.5	80.7	1026.2	1.2	SW	412.5	11:50	0.0	4.3	6.1	(12:40)
10/03/19	13.9	84.0	1025.7	1.3	SW	209.4	11:50	0.0	3.6	6.1	(10:40)
11/03/19	14.4	83.5	1016.1	1.8	SW	172.9	11:40	0.0	3.7	5.7	(11:30)
12/03/19	10.5	49.3	1017.3	3.3	N	252.0	11:50	**6.6**	3.6	6.4	(10:30)
13/03/19	11.0	61.1	1018.2	1.4	SW	404.2	11:40	5.8	4.7	7.7	(11:10)
14/03/19	12.2	74.6	1012.8	1.3	NW	328.3	11:50	3.8	3.6	5.8	(12:00)
15/03/19	13.3	74.1	1015.6	1.0	SW	433.5	12:00	0.0	4.1	6.8	(11:20)
16/03/19	13.9	86.6	1020.9	1.0	SW	194.3	12:00	0.0	3.6	5.1	(11:50)
17/03/19	13.9	82.3	1018.8	0.7	S	415.3	12:00	0.3	4.6	7.0	(12:00)
18/03/19	13.9	79.9	1016.2	1.2	SW	376.1	12:00	0.0	4.5	7.2	(12:10)
19/03/19	13.6	63.4	1017.5	1.5	NW	300.2	12:10	0.0	4.4	7.2	(11:40)
20/03/19	12.4	65.5	1022.1	3.2	NE	131.1	12:00	1.3	3.5	4.8	(13:30)
21/03/19	14.8	51.7	1024.2	4.2	NE	436.7	12:20	0.0	4.4	6.8	(11:40)
22/03/19	16.4	45.9	1024.9	3.3	N	443.4	12:20	0.0	4.4	6.7	(12:20)
23/03/19	17.5	40.1	1022.2	1.5	NE	455.3	12:20	0.0	4.4	7.0	(12:00)
24/03/19	16.1	57.0	1021.9	1.0	SW	467.1	12:20	0.0	4.8	7.5	(12:00)
25/03/19	14.5	83.9	1016.8	1.2	SW	441.7	12:20	0.0	4.5	8.1	(11:50)
26/03/19	13.4	69.8	1012.8	2.7	NE	239.8	12:20	0.0	3.9	7.1	(14:30)
27/03/19	11.9	62.8	1019.4	3.7	NE	267.0	12:20	2.0	3.5	7.2	(12:30)
28/03/19	13.1	43.5	1022.1	3.8	NE	278.2	12:40	0.0	3.8	7.8	(15:30)
29/03/19	14.1	39.0	1025.8	2.9	NE	472.3	12:40	0.0	4.4	8.2	(11:10)
30/03/19	14.9	42.6	1023.9	1.2	NW	470.0	12:40	0.0	4.3	6.7	(11:30)
31/03/19	14.1	72.6	1018.9	0.8	S	464.6	12:40	0.0	4.3	7.0	(12:50)

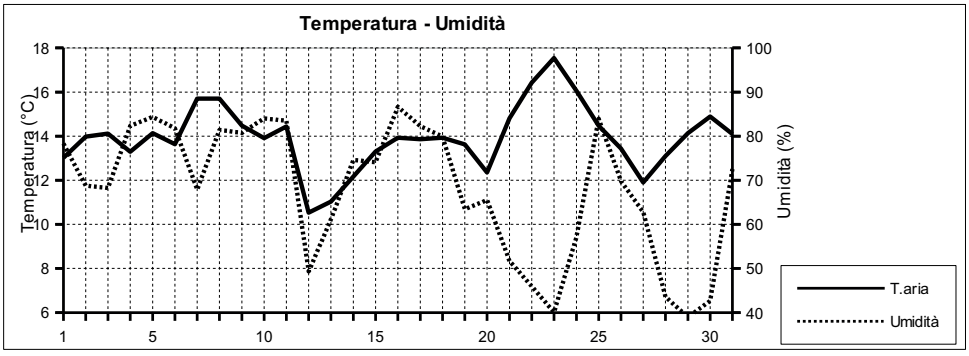

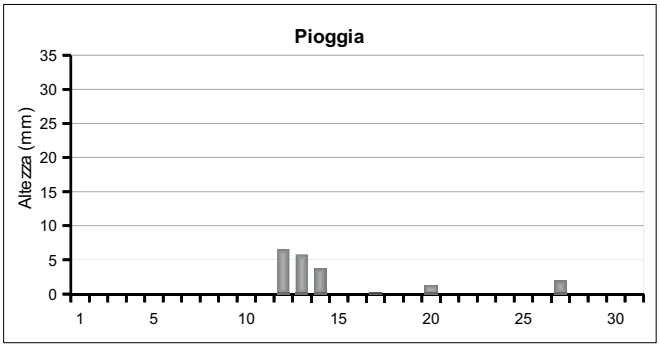

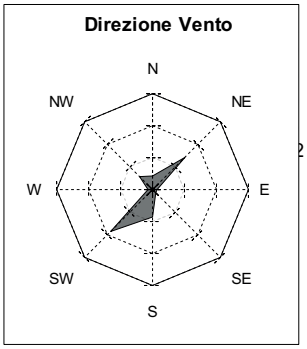

MARZO 2019 **(estremi giornalieri)**

	Temperatura (°C)				Umidità (%)				Pressione (hPa)				Vento (m/s)		Radiazione (W/m²)	
Data	min	(ore)	max	(ore)	min	(ore)	max	(ore)	min	(ore)	max	(ore)	max	(ore)	max	(ore)
01/03/19	11.4	(02:20)	15.2	(14:20)	69.0	(14:00)	83.0	(00:20)	1012.0	(23:40)	1021.3	(00:00)	6.3	(12:30)	830.0	(11:40)
02/03/19	10.9	(07:20)	18.1	(14:00)	49.0	(14:00)	84.0	(04:10)	1011.0	(03:40)	1018.4	(23:10)	8.0	(10:20)	684.0	(11:50)
03/03/19	11.3	(04:40)	18.7	(14:00)	48.0	(14:30)	83.0	(23:50)	1018.2	(05:40)	1021.5	(21:40)	6.7	(15:20)	657.0	(12:40)
04/03/19	11.3	(01:40)	15.3	(12:10)	73.0	(15:30)	89.0	(06:50)	1017.8	(23:40)	1021.7	(08:50)	11.2	(23:40)	807.0	(11:40)
05/03/19	13.1	(23:20)	15.7	(13:20)	72.0	(17:30)	90.0	(07:30)	1016.4	(04:10)	1020.6	(23:10)	9.8	(04:00)	900.0	(12:30)
06/03/19	10.9	(06:20)	16.3	(13:00)	68.0	(11:00)	89.0	(20:10)	1020.2	(23:20)	1022.7	(11:00)	6.7	(13:40)	687.0	(12:20)
07/03/19	11.9	(03:30)	20.3	(13:00)	42.0	(13:10)	90.0	(23:10)	1017.3	(17:40)	1020.1	(00:00)	8.5	(11:40)	724.0	(12:10)
08/03/19	13.7	(07:00)	18.7	(12:30)	68.0	(15:00)	90.0	(00:00)	1019.4	(03:40)	1024.0	(23:40)	7.2	(02:30)	795.0	(12:50)
09/03/19	13.4	(01:50)	16.7	(12:50)	66.0	(14:20)	91.0	(05:50)	1023.9	(00:00)	**1027.8**	**(20:50)**	7.6	(14:20)	756.0	(10:30)
10/03/19	12.6	(05:50)	15.3	(10:50)	75.0	(09:50)	91.0	(20:50)	1022.1	(23:50)	1027.8	(08:50)	7.2	(10:40)	879.0	(10:40)
11/03/19	10.9	(23:50)	15.8	(10:30)	74.0	(23:50)	90.0	(00:00)	**1008.8**	**(23:30)**	1022.0	(00:00)	17.4	(23:50)	592.0	(11:30)
12/03/19	**6.2**	**(02:00)**	13.8	(14:50)	**25.0**	**(16:10)**	86.0	(01:30)	1009.2	(00:00)	1022.1	(21:30)	**19.7**	**(00:00)**	921.0	(13:00)
13/03/19	6.7	(06:10)	14.5	(13:20)	39.0	(09:00)	90.0	(23:50)	1014.1	(23:50)	1021.6	(00:00)	9.4	(21:00)	809.0	(12:30)
14/03/19	9.2	(06:20)	15.2	(14:40)	54.0	(14:30)	91.0	(00:10)	1010.3	(05:30)	1014.4	(23:00)	11.6	(21:20)	1030.0	(12:00)
15/03/19	10.4	(05:40)	16.3	(15:10)	49.0	(17:10)	86.0	(23:50)	1012.5	(03:30)	1019.5	(23:40)	9.4	(00:00)	744.0	(12:20)
16/03/19	12.9	(06:50)	15.3	(16:40)	81.0	(11:40)	90.0	(04:50)	1019.6	(00:00)	1022.3	(11:00)	5.8	(13:50)	445.0	(12:00)
17/03/19	11.4	(06:10)	16.7	(14:20)	70.0	(14:10)	**92.0**	**(03:00)**	1016.4	(23:50)	1021.2	(00:00)	6.3	(16:00)	765.0	(12:10)
18/03/19	12.5	(23:50)	15.7	(14:10)	71.0	(14:00)	87.0	(22:30)	1014.9	(03:20)	1017.4	(23:40)	6.7	(14:20)	819.0	(11:00)
19/03/19	10.4	(06:00)	17.5	(12:00)	39.0	(11:40)	79.0	(05:30)	1016.4	(15:20)	1020.1	(23:50)	6.7	(16:30)	953.0	(11:30)
20/03/19	10.9	(09:40)	14.3	(15:30)	54.0	(21:40)	81.0	(09:40)	1019.9	(04:20)	1024.0	(22:20)	10.3	(08:30)	464.0	(14:20)
21/03/19	10.6	(03:50)	19.8	(13:20)	45.0	(14:30)	58.0	(03:50)	1023.0	(15:40)	1026.5	(22:50)	11.6	(22:30)	756.0	(12:20)
22/03/19	12.3	(02:50)	21.6	(15:00)	36.0	(15:00)	52.0	(02:40)	1023.1	(16:50)	1026.3	(00:30)	10.7	(01:30)	766.0	(12:10)
23/03/19	13.0	(05:00)	**22.8**	**(16:00)**	27.0	(14:20)	57.0	(16:50)	1020.4	(15:30)	1023.6	(00:00)	7.6	(14:10)	928.0	(12:00)
24/03/19	13.1	(06:10)	19.9	(15:40)	30.0	(08:50)	86.0	(21:00)	1020.8	(23:50)	1023.3	(09:40)	5.8	(12:50)	789.0	(12:20)
25/03/19	13.2	(05:50)	16.7	(12:50)	74.0	(12:20)	90.0	(03:10)	1012.0	(23:30)	1020.8	(00:00)	7.6	(13:00)	868.0	(13:10)
26/03/19	11.1	(22:40)	16.0	(11:20)	58.0	(13:00)	84.0	(00:00)	1010.5	(05:30)	1017.8	(23:40)	13.9	(23:30)	954.0	(12:20)
27/03/19	9.9	(04:30)	14.4	(11:00)	48.0	(21:10)	78.0	(04:50)	1017.4	(00:10)	1021.4	(21:10)	15.6	(13:20)	**1078.0**	**(11:50)**
28/03/19	11.4	(00:00)	15.7	(15:40)	32.0	(20:40)	55.0	(04:10)	1020.6	(02:50)	1024.8	(22:40)	13.4	(15:40)	849.0	(10:20)
29/03/19	10.4	(06:10)	18.0	(15:40)	28.0	(17:10)	55.0	(06:20)	1024.6	(02:10)	1027.2	(22:30)	13.0	(12:20)	821.0	(12:20)
30/03/19	10.8	(05:00)	19.9	(13:50)	28.0	(11:00)	71.0	(22:50)	1021.2	(17:40)	1026.8	(00:10)	8.5	(15:10)	812.0	(12:10)
31/03/19	11.2	(06:20)	16.4	(13:10)	61.0	(08:30)	88.0	(23:40)	1016.4	(19:10)	1021.3	(00:00)	7.2	(14:00)	802.0	(13:00)

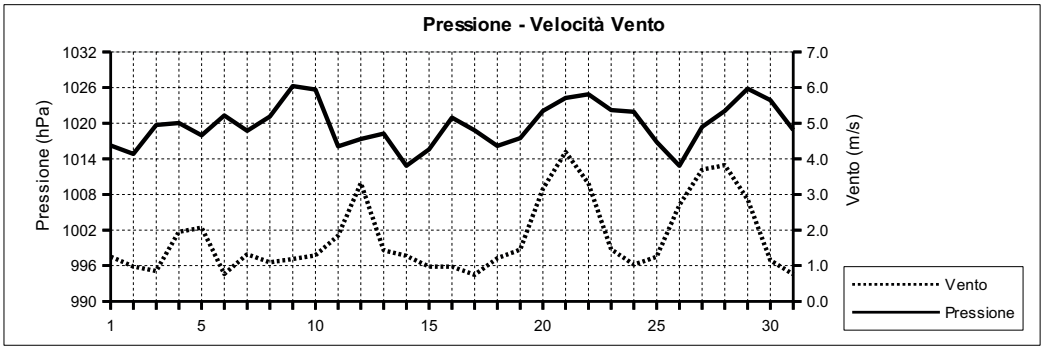

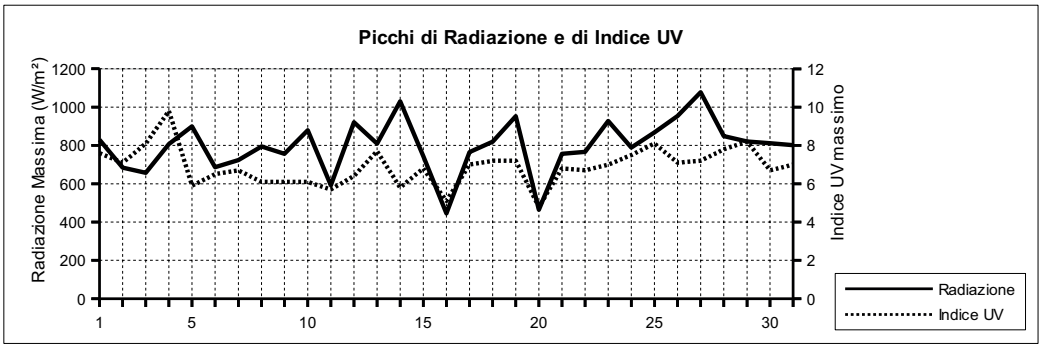

APRILE 2019 **(medie giornaliere)**

	Temperatura	Umidità	Pressione	Vento		Rad. Solare		Pioggia	Indice UV		
Data	°C	%	hPa	m/s	direzione	W/m²	durata	mm	medio	max	(ore)
01/04/19	15.1	74.4	1015.2	0.6	SE	431.7	12:50	0.0	4.3	6.6	(12:30)
02/04/19	14.7	80.2	1016.7	1.0	S	361.6	12:30	0.0	4.0	6.6	(13:50)
03/04/19	13.6	82.0	1014.2	1.0	S	145.8	12:30	1.3	3.1	5.2	(12:30)
04/04/19	14.3	77.7	1006.7	3.5	SE	114.3	12:20	2.3	3.4	7.2	(15:20)
05/04/19	13.5	66.6	1005.2	1.7	NW	492.0	13:00	**5.6**	5.2	8.1	(13:50)
06/04/19	14.2	64.2	1007.2	0.8	SW	375.0	12:50	0.0	4.9	7.7	(12:50)
07/04/19	14.4	75.2	1008.3	1.3	SW	467.7	13:00	0.0	5.0	7.3	(13:00)
08/04/19	14.1	72.5	1008.2	3.0	W	451.5	13:10	0.0	4.7	8.8	(13:40)
09/04/19	14.4	72.7	1009.1	2.3	W	451.7	13:00	0.0	4.4	7.0	(11:30)
10/04/19	13.8	76.7	1009.3	1.1	SW	337.3	13:10	0.3	4.3	9.0	(12:50)
11/04/19	13.6	78.1	1009.3	1.3	S	414.6	13:10	1.5	4.5	7.9	(13:00)
12/04/19	13.3	79.1	1010.6	1.4	--	292.1	12:50	0.3	3.9	7.0	(11:20)
13/04/19	13.8	73.6	1011.8	1.7	NW	200.1	13:20	3.3	4.0	7.5	(13:10)
14/04/19	13.7	78.7	1012.2	1.1	S	424.9	13:10	0.0	4.2	8.0	(12:30)
15/04/19	14.3	67.5	1014.0	1.7	NE	361.6	13:30	0.0	4.2	7.8	(13:40)
16/04/19	15.5	59.6	1020.0	1.0	NW	460.1	13:20	0.0	4.9	7.8	(13:10)
17/04/19	16.2	65.2	1020.4	1.1	NW	472.7	13:20	0.0	4.8	7.4	(14:00)
18/04/19	17.5	56.2	1022.2	1.0	NE	497.7	13:30	0.0	5.5	8.7	(13:20)
19/04/19	18.0	42.4	1026.1	1.7	NW	501.6	13:40	0.0	5.3	8.2	(14:00)
20/04/19	18.1	44.9	1024.4	1.2	--	492.1	13:40	0.0	5.6	8.2	(12:30)
21/04/19	18.9	42.7	1018.8	1.1	N	142.6	13:20	0.0	4.0	5.4	(11:40)
22/04/19	18.2	61.5	1010.0	1.8	NW	150.5	13:00	2.5	3.9	6.4	(15:20)
23/04/19	17.8	75.5	1008.8	3.8	SE	337.9	13:40	0.0	4.5	7.9	(13:20)
24/04/19	20.6	62.8	1015.6	0.6	--	462.0	13:50	0.0	6.2	9.0	(12:50)
25/04/19	21.6	56.2	1017.8	0.8	SW	491.5	13:40	0.0	5.8	8.4	(13:30)
26/04/19	19.7	72.1	1017.9	1.2	SW	373.4	13:40	0.0	5.3	8.0	(13:00)
27/04/19	17.5	64.9	1018.7	1.6	SW	474.9	13:50	0.0	5.3	8.3	(13:10)
28/04/19	15.8	72.1	1016.9	1.6	SW	323.6	14:00	0.3	4.7	**9.1**	**(13:20)**
29/04/19	14.8	71.4	1012.8	1.8	SW	326.8	14:00	5.6	4.5	8.9	(13:10)
30/04/19	13.8	69.9	1014.7	1.1	SE	526.8	14:00	0.0	5.5	8.6	(13:10)

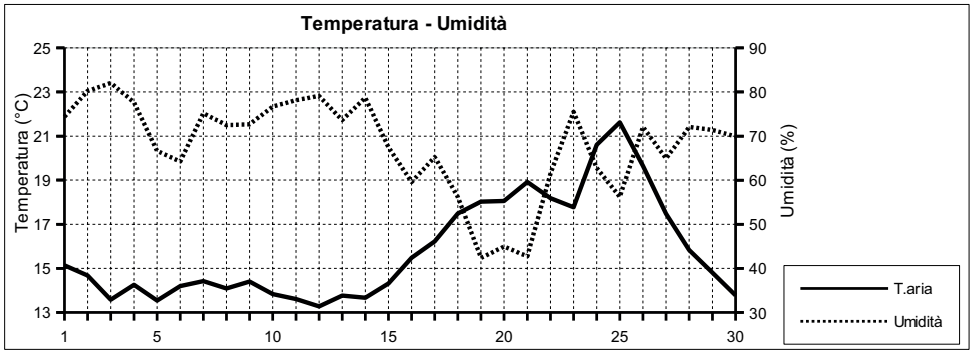

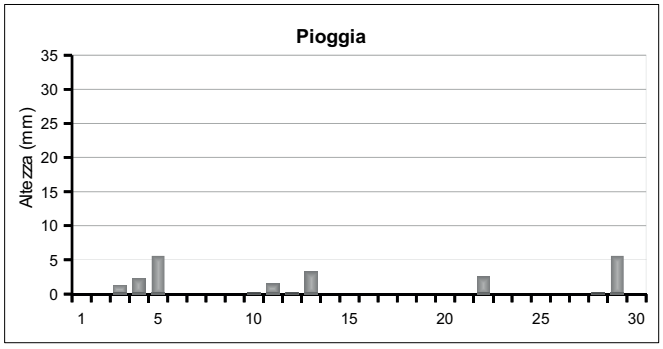

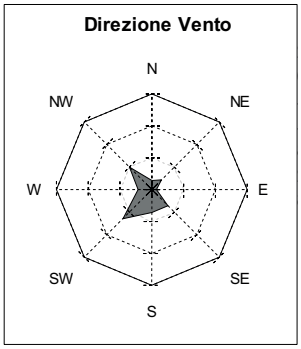

APRILE 2019 **(estremi giornalieri)**

Data	Temperatura (°C)				Umidità (%)				Pressione (hPa)				Vento (m/s)		Radiazione (W/m²)	
	min	(ore)	max	(ore)	min	(ore)	max	(ore)	min	(ore)	max	(ore)	max	(ore)	max	(ore)
01/04/19	11.0	(06:00)	20.8	(16:10)	48.0	(16:20)	89.0	(00:20)	1013.2	(16:10)	1017.4	(00:00)	4.9	(13:30)	810.0	(13:50)
02/04/19	12.7	(05:30)	17.1	(12:40)	67.0	(00:00)	86.0	(23:10)	1015.1	(04:30)	1018.0	(21:50)	8.5	(14:10)	851.0	(13:50)
03/04/19	12.6	(14:20)	14.9	(10:40)	73.0	(10:40)	88.0	(02:00)	1011.6	(22:30)	1017.5	(00:00)	8.0	(13:30)	591.0	(12:10)
04/04/19	12.3	(05:30)	16.3	(10:00)	61.0	(08:40)	92.0	(23:50)	1002.5	(23:50)	1011.5	(00:00)	15.6	(20:20)	689.0	(15:20)
05/04/19	**10.3**	**(02:00)**	17.2	(14:20)	34.0	(16:30)	**93.0**	**(00:30)**	1002.0	(00:20)	1007.1	(11:20)	**16.1**	**(00:40)**	863.0	(13:20)
06/04/19	10.3	(05:10)	18.8	(14:20)	36.0	(15:00)	78.0	(02:50)	1005.9	(04:50)	1009.1	(23:20)	8.5	(14:40)	904.0	(14:20)
07/04/19	13.0	(23:40)	16.4	(16:10)	68.0	(15:30)	81.0	(01:50)	1007.6	(17:10)	1009.1	(00:20)	7.6	(14:30)	1056.0	(13:10)
08/04/19	11.8	(06:50)	17.3	(13:00)	54.0	(13:10)	82.0	(06:50)	1007.6	(04:40)	1008.9	(01:00)	16.1	(20:50)	1020.0	(12:40)
09/04/19	12.4	(05:00)	16.8	(12:40)	60.0	(12:00)	83.0	(23:50)	1008.1	(04:00)	1010.9	(21:30)	12.5	(00:00)	932.0	(11:50)
10/04/19	11.7	(06:00)	15.7	(15:50)	65.0	(10:50)	84.0	(00:20)	1008.1	(15:50)	1010.6	(01:10)	7.6	(17:00)	1176.0	(12:50)
11/04/19	11.4	(02:50)	15.8	(14:40)	68.0	(14:30)	87.0	(03:50)	1008.5	(05:50)	1010.9	(23:20)	8.5	(02:00)	1157.0	(13:00)
12/04/19	11.5	(06:50)	15.3	(15:50)	69.0	(12:30)	87.0	(02:20)	1009.7	(16:30)	1011.5	(22:50)	7.2	(20:40)	993.0	(11:20)
13/04/19	12.4	(06:20)	17.1	(11:30)	56.0	(11:30)	83.0	(19:00)	1010.6	(05:30)	1013.3	(21:20)	8.0	(17:20)	1130.0	(13:10)
14/04/19	11.2	(05:30)	16.1	(14:10)	72.0	(14:30)	84.0	(02:30)	1011.2	(18:30)	1013.3	(00:00)	8.0	(14:00)	1165.0	(12:30)
15/04/19	10.6	(04:20)	18.2	(14:30)	53.0	(13:40)	84.0	(04:10)	1010.3	(02:40)	1019.4	(23:50)	14.3	(15:10)	**1179.0**	**(13:50)**
16/04/19	11.3	(06:00)	19.7	(15:40)	43.0	(15:50)	72.0	(23:30)	1018.9	(02:40)	1021.2	(22:00)	6.7	(13:00)	888.0	(13:50)
17/04/19	12.6	(07:20)	19.8	(14:30)	44.0	(15:30)	79.0	(05:40)	1019.5	(15:40)	1021.6	(21:40)	7.6	(15:00)	962.0	(14:00)
18/04/19	13.1	(06:30)	21.3	(13:50)	34.0	(13:10)	75.0	(01:40)	1021.3	(04:30)	1024.9	(23:40)	8.5	(20:00)	889.0	(13:10)
19/04/19	14.2	(06:20)	21.7	(13:10)	32.0	(11:40)	52.0	(06:10)	1025.0	(00:00)	**1027.2**	**(22:40)**	7.6	(15:30)	867.0	(13:20)
20/04/19	14.4	(05:00)	21.7	(13:30)	**30.0**	**(10:30)**	73.0	(19:40)	1022.2	(19:50)	1026.7	(00:00)	6.7	(13:00)	893.0	(12:50)
21/04/19	17.3	(06:50)	20.7	(13:50)	34.0	(13:10)	62.0	(11:10)	1015.1	(23:30)	1022.3	(00:10)	6.3	(13:10)	394.0	(11:40)
22/04/19	15.5	(19:50)	22.0	(11:20)	42.0	(11:20)	83.0	(19:50)	1006.1	(23:30)	1015.3	(00:20)	15.6	(18:20)	559.0	(15:20)
23/04/19	16.8	(00:00)	19.4	(16:50)	61.0	(02:10)	84.0	(12:30)	**1005.7**	**(05:10)**	1014.0	(23:40)	14.8	(03:10)	823.0	(13:10)
24/04/19	16.3	(04:50)	26.3	(17:20)	34.0	(17:30)	80.0	(00:00)	1014.0	(03:00)	1018.3	(23:00)	4.9	(13:40)	870.0	(12:50)
25/04/19	17.4	(05:20)	**29.7**	**(16:50)**	31.0	(16:40)	79.0	(22:00)	1016.2	(16:50)	1018.6	(22:00)	5.8	(18:10)	860.0	(12:00)
26/04/19	17.4	(20:00)	22.8	(13:40)	61.0	(03:50)	88.0	(17:00)	1017.0	(19:10)	1018.6	(21:50)	7.6	(13:50)	846.0	(13:00)
27/04/19	15.2	(23:40)	19.9	(15:40)	51.0	(02:00)	80.0	(23:00)	1017.9	(04:20)	1020.0	(22:00)	10.7	(16:50)	974.0	(11:50)
28/04/19	14.6	(06:00)	18.1	(13:30)	56.0	(17:30)	82.0	(00:30)	1014.4	(18:40)	1019.7	(00:10)	11.2	(12:50)	1127.0	(12:50)
29/04/19	11.7	(23:40)	17.2	(14:20)	59.0	(14:20)	78.0	(18:00)	1011.1	(16:50)	1014.9	(00:00)	12.1	(13:10)	1125.0	(13:00)
30/04/19	10.7	(04:20)	16.7	(15:00)	56.0	(14:50)	78.0	(04:30)	1013.2	(03:40)	1016.1	(22:20)	6.7	(13:00)	909.0	(12:50)

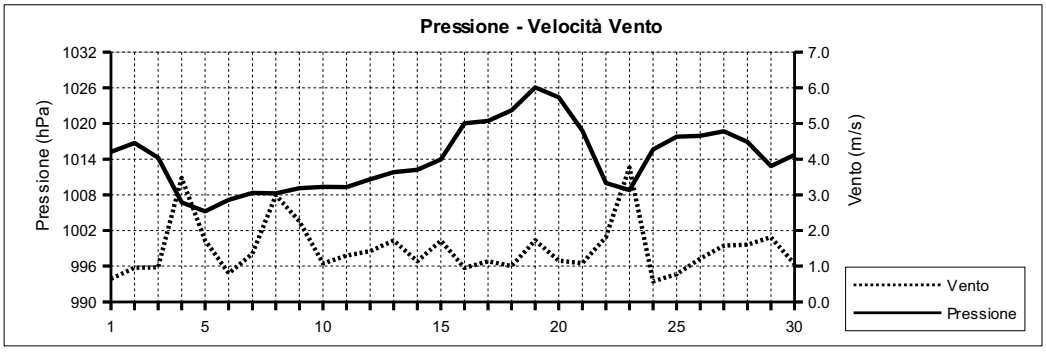

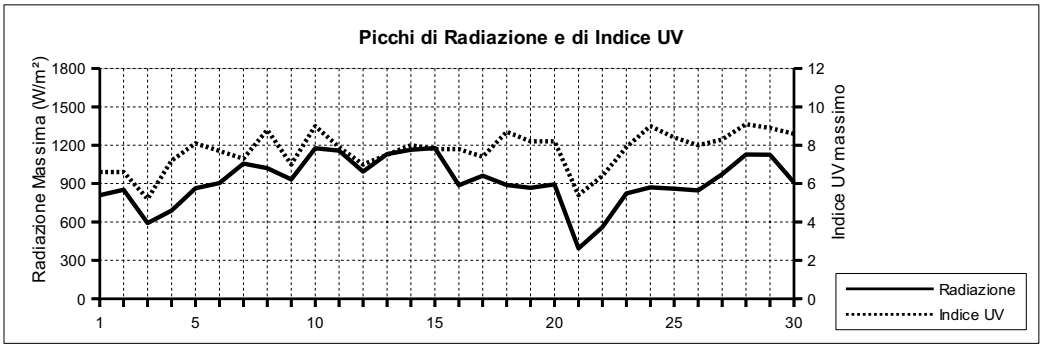

MAGGIO 2019 **(medie giornaliere)**

	Temperatura	Umidità	Pressione	Vento		Rad. Solare		Pioggia	Indice UV		
Data	°C	%	hPa	m/s	direzione	W/m²	durata	mm	medio	max	(ore)
01/05/19	15.5	70.8	1015.3	1.2	SW	468.7	14:00	0.0	5.1	8.2	(14:10)
02/05/19	16.2	77.6	1016.6	1.2	SW	514.7	14:00	0.0	5.5	8.6	(12:40)
03/05/19	16.1	79.3	1014.1	1.5	S	305.8	13:50	0.0	4.7	8.3	(12:20)
04/05/19	14.9	86.0	1005.5	0.5	NE	154.4	13:40	11.4	3.8	8.6	(15:00)
05/05/19	14.7	74.6	1004.6	1.9	W	260.5	14:10	4.1	4.4	8.5	(12:30)
06/05/19	12.4	73.8	1009.5	1.2	NW	328.0	14:10	8.1	4.7	8.7	(13:10)
07/05/19	14.2	60.3	1019.5	0.9	NW	439.5	14:20	0.0	5.1	**12.0**	**(12:20)**
08/05/19	15.3	70.6	1019.5	1.1	S	501.8	14:20	0.0	5.3	10.6	(13:30)
09/05/19	16.1	78.8	1011.1	1.5	S	122.9	14:10	0.0	3.8	8.1	(09:10)
10/05/19	17.9	77.4	1013.4	0.8	S	500.7	14:10	0.0	5.2	8.8	(13:30)
11/05/19	17.5	78.1	1017.1	1.0	SW	460.1	14:20	0.0	5.3	9.1	(13:10)
12/05/19	16.7	79.8	1010.9	1.3	SW	385.9	14:10	13.2	4.7	8.8	(13:20)
13/05/19	16.0	68.8	1009.9	1.5	NE	389.7	14:20	7.6	4.5	8.5	(12:20)
14/05/19	15.7	66.5	1011.8	2.3	NE	441.3	14:30	0.0	4.8	8.8	(13:00)
15/05/19	13.9	73.6	1011.1	1.4	NE	237.3	12:50	**19.8**	3.5	5.6	(14:30)
16/05/19	15.9	69.1	1010.1	2.1	NE	437.0	14:30	0.0	4.6	9.4	(13:40)
17/05/19	16.9	70.5	1010.7	1.2	SW	518.8	14:30	0.0	5.3	10.8	(13:00)
18/05/19	17.7	80.1	1008.1	2.6	S	293.4	14:30	0.0	4.1	8.9	(13:30)
19/05/19	17.2	77.4	1007.8	1.6	SW	445.0	14:30	0.0	5.1	11.3	(12:40)
20/05/19	16.1	77.9	1011.8	1.7	SW	332.3	14:20	2.0	4.6	8.5	(13:10)
21/05/19	17.4	76.0	1016.0	1.4	SW	371.7	14:30	3.1	5.0	10.7	(12:20)
22/05/19	17.8	80.3	1017.8	1.3	S	523.4	14:40	0.0	5.7	9.6	(12:10)
23/05/19	18.3	74.7	1017.3	1.0	SW	447.5	14:40	0.0	5.4	9.1	(13:00)
24/05/19	18.0	79.3	1016.2	1.1	S	505.9	14:40	0.0	5.9	9.6	(13:10)
25/05/19	18.2	76.7	1015.6	0.7	SW	268.0	14:50	1.0	5.2	8.4	(11:40)
26/05/19	17.2	86.9	1011.3	1.4	NW	75.0	14:10	11.6	2.6	7.2	(17:30)
27/05/19	18.3	81.0	1006.8	2.1	SE	145.2	13:50	11.4	3.2	8.4	(12:40)
28/05/19	17.8	88.3	1008.6	2.0	SW	280.0	14:00	17.7	4.8	11.5	(13:00)
29/05/19	18.9	76.8	1013.8	2.2	SW	398.9	14:40	0.0	5.4	9.9	(13:10)
30/05/19	18.2	76.3	1019.8	0.8	SE	383.4	15:00	0.0	5.4	10.2	(12:40)
31/05/19	18.2	71.5	1021.4	0.8	N	255.6	14:50	8.4	4.7	10.0	(12:20)

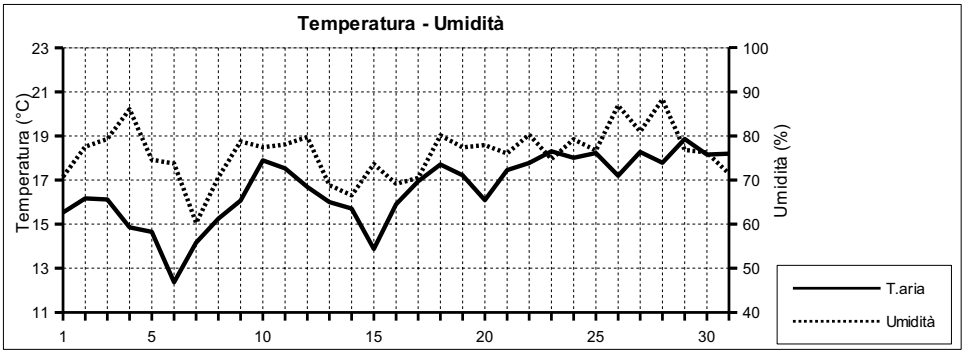

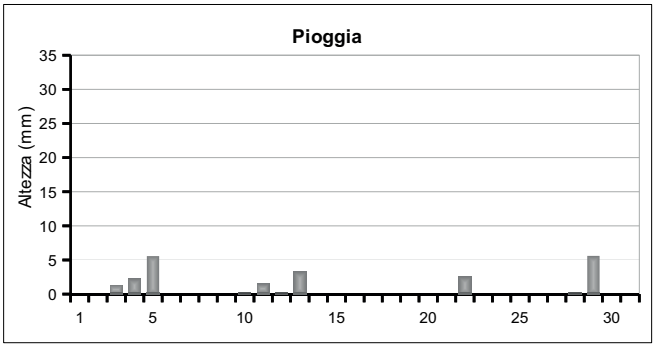

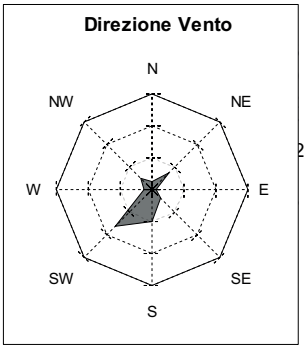

MAGGIO 2019 **(estremi giornalieri)**

Data	Temperatura (°C)				Umidità (%)				Pressione (hPa)				Vento (m/s)		Radiazione (W/m²)	
	min	(ore)	max	(ore)	min	(ore)	max	(ore)	min	(ore)	max	(ore)	max	(ore)	max	(ore)
01/05/19	12.6	(05:30)	18.8	(14:30)	57.0	(15:00)	80.0	(23:10)	1014.3	(05:40)	1016.5	(22:00)	8.9	(18:30)	1044.0	(11:30)
02/05/19	13.6	(06:20)	18.6	(14:40)	68.0	(12:50)	84.0	(05:50)	1015.7	(03:10)	1017.7	(10:50)	6.7	(13:20)	1007.0	(12:40)
03/05/19	14.8	(06:30)	17.7	(14:00)	71.0	(15:50)	84.0	(05:30)	1010.8	(23:20)	1016.7	(00:00)	7.2	(14:20)	926.0	(12:20)
04/05/19	13.1	(11:00)	16.3	(00:00)	76.0	(00:00)	93.0	(12:00)	1002.6	(18:50)	1010.8	(00:00)	4.5	(17:10)	849.0	(14:50)
05/05/19	11.7	(19:50)	17.1	(10:30)	56.0	(17:30)	87.0	(00:10)	1002.3	(04:20)	1006.9	(22:10)	12.1	(10:00)	1230.0	(14:50)
06/05/19	10.3	(00:40)	16.0	(16:30)	60.0	(12:50)	84.0	(02:30)	1005.5	(04:50)	1016.4	(23:50)	**12.1**	**(17:30)**	1206.0	(13:10)
07/05/19	10.2	(05:30)	17.8	(15:30)	**44.0**	**(15:30)**	77.0	(03:00)	1016.4	(00:00)	1021.3	(22:40)	6.7	(15:50)	1150.0	(13:40)
08/05/19	12.9	(06:20)	17.5	(16:50)	62.0	(16:40)	77.0	(06:30)	1015.8	(23:40)	1021.3	(01:20)	7.2	(14:30)	1018.0	(13:10)
09/05/19	14.0	(05:50)	17.6	(17:10)	60.0	(08:30)	93.0	(21:00)	1008.8	(16:50)	1015.8	(00:10)	9.4	(12:40)	457.0	(08:50)
10/05/19	15.5	(05:40)	20.8	(18:30)	56.0	(19:30)	**93.0**	**(00:20)**	1011.2	(02:30)	1016.7	(22:50)	6.3	(14:30)	1060.0	(14:20)
11/05/19	15.2	(06:10)	19.8	(16:00)	68.0	(19:10)	85.0	(03:20)	1015.4	(23:10)	1018.6	(11:30)	7.6	(12:10)	1116.0	(13:20)
12/05/19	14.1	(05:40)	19.4	(14:20)	58.0	(14:20)	92.0	(05:50)	1008.4	(20:40)	1015.7	(00:00)	7.2	(12:30)	1181.0	(14:00)
13/05/19	12.6	(05:10)	19.9	(13:10)	51.0	(11:00)	84.0	(00:00)	1008.2	(05:40)	1012.6	(23:20)	9.8	(16:40)	1183.0	(13:10)
14/05/19	13.6	(03:20)	19.2	(13:50)	52.0	(15:40)	82.0	(03:40)	1010.7	(04:50)	1013.1	(21:50)	10.7	(16:30)	1238.0	(12:10)
15/05/19	**11.3**	**(05:40)**	16.2	(14:30)	61.0	(00:40)	92.0	(22:20)	1009.3	(17:50)	1012.8	(00:00)	9.4	(18:40)	638.0	(14:30)
16/05/19	12.4	(00:00)	19.7	(18:30)	55.0	(16:50)	91.0	(00:00)	1008.5	(04:50)	1011.9	(22:30)	10.7	(12:50)	1211.0	(12:10)
17/05/19	13.7	(05:40)	19.3	(12:50)	62.0	(11:40)	78.0	(18:50)	1008.6	(22:10)	1012.2	(00:30)	6.7	(13:20)	914.0	(12:50)
18/05/19	16.7	(23:30)	19.2	(16:00)	67.0	(02:50)	85.0	(12:20)	1007.4	(06:20)	1009.2	(00:00)	10.3	(05:30)	1188.0	(14:50)
19/05/19	16.1	(06:00)	19.7	(13:20)	64.0	(14:20)	88.0	(05:20)	1005.9	(05:20)	1010.7	(23:20)	10.7	(14:30)	1188.0	(12:10)
20/05/19	12.0	(10:00)	18.8	(14:30)	70.0	(14:40)	88.0	(10:10)	1009.7	(05:30)	1014.3	(23:40)	9.4	(14:40)	1130.0	(14:30)
21/05/19	15.3	(07:20)	20.6	(14:30)	53.0	(14:10)	85.0	(07:20)	1013.5	(06:00)	1018.4	(23:20)	8.0	(11:40)	1136.0	(12:40)
22/05/19	16.3	(05:00)	19.8	(15:20)	72.0	(12:10)	85.0	(04:40)	1016.9	(18:00)	1018.4	(10:20)	8.5	(15:00)	1041.0	(12:40)
23/05/19	15.4	(06:00)	**21.4**	**(14:10)**	56.0	(15:00)	87.0	(06:20)	1016.7	(14:20)	1018.1	(00:30)	7.6	(12:50)	1004.0	(12:10)
24/05/19	15.3	(05:40)	20.7	(14:40)	71.0	(16:50)	86.0	(05:00)	1014.9	(19:20)	1017.1	(00:10)	7.6	(13:00)	1141.0	(12:10)
25/05/19	16.3	(05:20)	20.7	(13:20)	54.0	(17:30)	87.0	(06:20)	1014.5	(17:10)	1016.8	(11:00)	5.4	(20:30)	1034.0	(11:40)
26/05/19	15.6	(05:00)	19.1	(18:10)	77.0	(21:10)	93.0	(08:50)	1007.1	(20:50)	1015.4	(00:00)	7.6	(13:40)	311.0	(14:10)
27/05/19	16.9	(22:10)	20.1	(02:20)	73.0	(01:50)	92.0	(12:10)	1005.5	(04:40)	1007.8	(00:10)	9.4	(16:00)	810.0	(12:40)
28/05/19	15.5	(03:40)	20.4	(15:00)	76.0	(14:40)	96.0	(09:00)	**1004.9**	**(04:00)**	1012.4	(22:30)	9.8	(01:40)	1211.0	(13:00)
29/05/19	17.5	(23:40)	21.3	(13:10)	56.0	(13:20)	92.0	(02:10)	1011.7	(03:00)	1017.3	(23:50)	7.6	(11:40)	1262.0	(13:10)
30/05/19	16.1	(06:00)	20.2	(13:50)	68.0	(11:50)	85.0	(06:00)	1017.3	(00:00)	1021.9	(23:00)	6.3	(14:00)	**1304.0**	**(12:30)**
31/05/19	16.2	(02:40)	21.3	(12:20)	57.0	(12:20)	82.0	(16:20)	1020.7	(20:30)	**1022.0**	**(00:10)**	6.7	(15:10)	1229.0	(13:30)

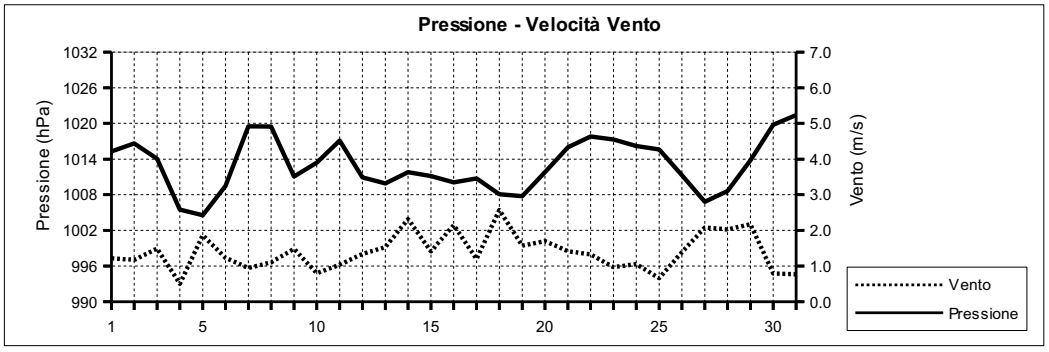

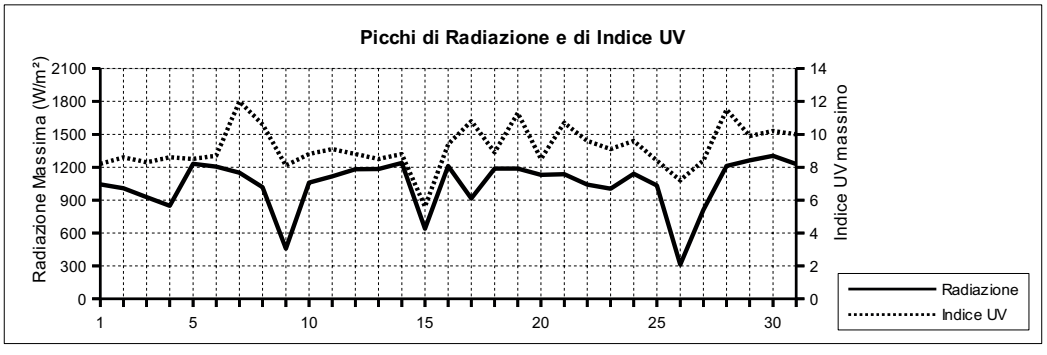

GIUGNO 2019 **(medie giornaliere)**

	Temperatura	Umidità	Pressione	Vento		Rad. Solare		Pioggia	Indice UV		
Data	°C	%	hPa	m/s	direzione	W/m²	durata	mm	medio	max	(ore)
01/06/19	19.1	64.6	1019.4	1.2	NE	372.0	14:50	0.0	4.9	9.8	(12:50)
02/06/19	18.5	81.9	1017.8	0.9	SE	401.9	14:40	**10.6**	4.9	9.6	(13:30)
03/06/19	19.4	84.7	1017.8	1.2	SW	472.8	14:50	0.0	5.5	10.2	(12:50)
04/06/19	20.1	83.4	1015.9	0.8	SW	277.7	14:50	0.0	4.8	8.5	(14:00)
05/06/19	20.8	82.2	1013.9	0.8	SW	312.5	14:50	0.0	4.6	8.4	(14:20)
06/06/19	22.2	76.9	1016.2	0.4	S	467.0	15:10	0.0	5.4	**11.5**	**(14:20)**
07/06/19	26.0	52.6	1018.9	0.4	SE	495.9	15:00	0.0	5.3	9.1	(12:50)
08/06/19	26.8	51.3	1021.0	0.9	SW	468.1	15:00	0.0	5.2	9.4	(13:10)
09/06/19	27.0	59.9	1019.5	0.6	SW	487.7	15:00	0.0	5.1	8.3	(13:30)
10/06/19	27.3	62.3	1013.3	0.8	SW	471.1	15:00	0.0	5.1	8.4	(12:50)
11/06/19	27.1	60.4	1010.4	0.8	S	433.3	15:00	0.0	4.9	8.6	(12:50)
12/06/19	27.7	55.1	1010.7	1.1	SW	472.1	15:10	0.0	5.0	8.6	(13:10)
13/06/19	25.3	78.8	1014.7	1.0	SE	479.4	15:10	0.0	5.3	10.5	(12:40)
14/06/19	28.1	69.1	1016.3	0.8	S	481.7	15:00	0.0	4.8	8.5	(13:30)
15/06/19	28.1	67.2	1014.6	1.3	SE	446.1	14:50	0.0	4.6	8.3	(12:00)
16/06/19	25.5	74.6	1014.3	1.3	SE	499.0	15:00	0.0	4.9	8.9	(13:30)
17/06/19	24.9	69.2	1013.7	1.3	NE	503.7	15:20	0.0	5.4	9.9	(14:20)
18/06/19	26.2	61.8	1013.8	1.0	NW	491.7	15:10	0.0	5.2	9.1	(13:40)
19/06/19	25.5	68.5	1014.1	0.9	SW	478.9	15:10	0.0	5.1	9.2	(12:40)
20/06/19	25.3	73.7	1014.3	1.3	SW	492.3	15:10	0.0	5.1	9.3	(13:10)
21/06/19	26.0	75.2	1015.3	0.8	S	466.6	15:00	0.0	4.8	9.3	(13:10)
22/06/19	27.4	59.9	1014.7	1.1	SW	230.8	15:10	0.0	3.8	7.6	(11:50)
23/06/19	26.4	75.8	1013.8	1.3	S	497.6	15:10	0.0	5.1	9.4	(12:50)
24/06/19	27.3	70.5	1015.9	1.2	NW	436.2	15:10	0.0	4.6	8.1	(13:00)
25/06/19	29.4	50.5	1017.9	2.0	NE	430.5	15:10	0.0	4.6	9.0	(12:30)
26/06/19	30.6	47.5	1018.7	1.9	NE	401.1	15:20	0.0	4.4	8.0	(13:40)
27/06/19	31.4	45.9	1016.5	1.7	NW	435.9	15:10	0.0	4.4	8.6	(15:00)
28/06/19	28.9	62.8	1013.2	0.9	SE	453.0	15:00	0.0	4.5	7.9	(13:10)
29/06/19	30.2	32.2	1014.3	2.9	NE	506.0	15:10	0.0	4.9	8.9	(13:20)
30/06/19	29.4	34.0	1017.3	1.0	NW	499.4	15:10	0.0	5.1	9.1	(13:00)

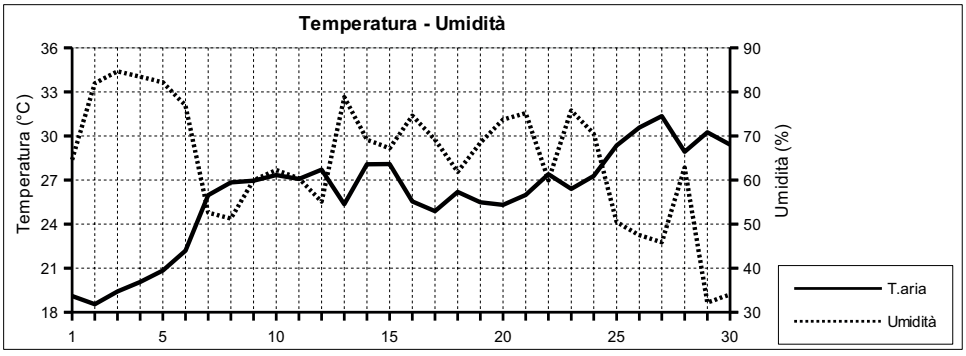

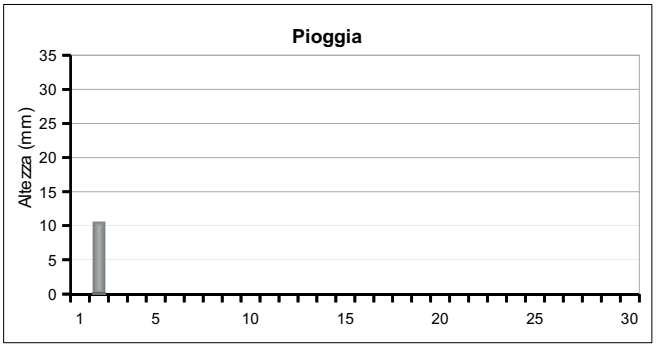

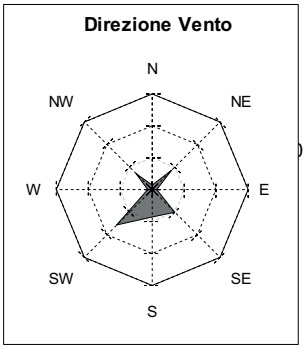

GIUGNO 2019 **(estremi giornalieri)**

Data	Temperatura (°C)				Umidità (%)				Pressione (hPa)				Vento (m/s)		Radiazione (W/m²)	
	min	(ore)	max	(ore)	min	(ore)	max	(ore)	min	(ore)	max	(ore)	max	(ore)	max	(ore)
01/06/19	15.8	(04:50)	23.9	(13:40)	46.0	(13:40)	81.0	(21:00)	1017.8	(17:30)	1021.1	(00:00)	9.8	(18:10)	1165.0	(13:30)
02/06/19	**15.3**	**(05:50)**	21.8	(13:50)	70.0	(14:10)	92.0	(06:00)	1016.9	(17:30)	1018.8	(00:00)	7.6	(14:40)	1120.0	(14:10)
03/06/19	17.2	(05:40)	21.9	(13:00)	74.0	(13:00)	**92.0**	**(06:00)**	1016.6	(20:40)	1018.7	(00:50)	7.2	(14:00)	977.0	(14:30)
04/06/19	18.7	(05:40)	22.4	(16:10)	74.0	(18:10)	89.0	(03:20)	1014.7	(18:00)	1017.4	(00:00)	6.3	(14:50)	939.0	(15:50)
05/06/19	19.1	(04:50)	23.2	(17:20)	72.0	(15:20)	89.0	(06:00)	1012.5	(18:10)	1015.2	(00:00)	5.8	(15:10)	**1167.0**	**(14:20)**
06/06/19	18.7	(04:50)	26.6	(13:10)	56.0	(13:20)	91.0	(05:00)	1014.1	(00:00)	1018.1	(23:00)	6.7	(14:00)	1111.0	(13:40)
07/06/19	20.2	(04:40)	31.0	(14:30)	28.0	(13:00)	80.0	(04:30)	1017.4	(04:00)	1020.6	(22:30)	5.8	(19:50)	891.0	(13:00)
08/06/19	24.0	(04:00)	30.1	(15:40)	36.0	(11:30)	72.0	(22:20)	1019.6	(04:50)	**1022.5**	**(21:50)**	6.3	(15:00)	965.0	(12:40)
09/06/19	22.8	(04:20)	32.8	(15:00)	39.0	(15:00)	73.0	(04:10)	1016.5	(23:20)	1022.2	(00:00)	4.5	(14:40)	881.0	(13:20)
10/06/19	24.1	(05:50)	33.2	(18:00)	37.0	(18:00)	78.0	(15:20)	1010.7	(23:20)	1016.5	(00:00)	5.8	(14:40)	860.0	(13:00)
11/06/19	23.8	(06:00)	30.8	(15:40)	36.0	(15:40)	82.0	(08:00)	1009.3	(21:00)	1011.4	(16:50)	10.7	(15:30)	884.0	(13:20)
12/06/19	24.6	(05:40)	32.2	(12:40)	33.0	(12:40)	82.0	(23:50)	**1009.2**	**(04:20)**	1012.7	(23:40)	8.9	(13:50)	854.0	(13:20)
13/06/19	22.8	(05:30)	28.0	(17:10)	63.0	(17:40)	89.0	(05:50)	1012.4	(03:10)	1016.4	(23:30)	7.6	(12:30)	875.0	(13:20)
14/06/19	23.9	(04:50)	34.2	(15:10)	45.0	(13:40)	87.0	(03:10)	1014.8	(17:30)	1017.8	(22:40)	7.6	(18:00)	909.0	(13:50)
15/06/19	25.1	(23:10)	31.1	(14:00)	48.0	(03:20)	83.0	(22:20)	1013.2	(17:20)	1016.8	(00:00)	7.2	(03:10)	889.0	(13:20)
16/06/19	23.3	(05:40)	28.7	(16:50)	46.0	(20:00)	88.0	(03:40)	1013.3	(17:30)	1015.4	(12:20)	7.2	(16:30)	888.0	(13:20)
17/06/19	21.4	(05:40)	28.8	(16:00)	44.0	(18:10)	82.0	(05:10)	1012.9	(17:30)	1014.5	(00:30)	7.2	(17:40)	907.0	(13:30)
18/06/19	22.0	(05:30)	29.9	(15:50)	42.0	(17:30)	83.0	(05:40)	1012.9	(17:40)	1014.7	(23:40)	8.0	(16:00)	870.0	(13:00)
19/06/19	22.4	(06:00)	28.6	(15:40)	56.0	(18:00)	82.0	(05:30)	1013.0	(17:50)	1014.7	(00:00)	6.7	(12:00)	861.0	(13:20)
20/06/19	22.5	(05:50)	28.9	(18:20)	60.0	(18:40)	83.0	(05:20)	1013.2	(17:40)	1015.5	(23:40)	7.2	(12:30)	893.0	(12:50)
21/06/19	22.9	(06:30)	29.1	(14:50)	60.0	(14:40)	85.0	(04:00)	1013.9	(20:30)	1016.2	(06:40)	6.7	(13:10)	933.0	(14:10)
22/06/19	24.0	(09:20)	34.5	(13:00)	32.0	(13:00)	80.0	(04:40)	1012.6	(20:30)	1018.3	(07:50)	11.6	(13:50)	995.0	(14:20)
23/06/19	24.6	(05:40)	28.8	(15:10)	59.0	(00:00)	84.0	(03:40)	1012.5	(04:10)	1015.6	(23:30)	6.7	(01:00)	916.0	(13:30)
24/06/19	23.5	(05:30)	31.7	(16:00)	53.0	(19:10)	88.0	(05:40)	1014.9	(16:00)	1017.9	(22:50)	6.3	(15:00)	939.0	(13:40)
25/06/19	25.3	(05:30)	32.9	(18:10)	42.0	(18:10)	59.0	(05:20)	1016.9	(03:40)	1019.6	(22:50)	8.9	(12:40)	1013.0	(14:40)
26/06/19	26.3	(05:30)	34.7	(14:30)	39.0	(18:30)	56.0	(04:30)	1017.5	(17:50)	1019.8	(01:10)	10.3	(19:30)	930.0	(13:30)
27/06/19	27.4	(05:10)	**35.2**	**(15:00)**	38.0	(19:40)	59.0	(23:50)	1013.8	(18:30)	1018.8	(01:00)	9.4	(18:10)	940.0	(13:20)
28/06/19	26.3	(05:40)	34.2	(15:50)	41.0	(07:40)	87.0	(20:10)	1012.1	(17:20)	1014.5	(00:00)	6.3	(11:30)	912.0	(13:10)
29/06/19	27.4	(05:40)	34.0	(16:20)	**21.0**	**(16:50)**	44.0	(00:00)	1013.1	(04:10)	1016.1	(23:20)	**13.9**	**(09:00)**	900.0	(13:10)
30/06/19	25.1	(06:00)	33.3	(17:40)	27.0	(10:40)	51.0	(20:20)	1015.9	(00:50)	1018.5	(23:50)	6.3	(14:30)	886.0	(13:10)

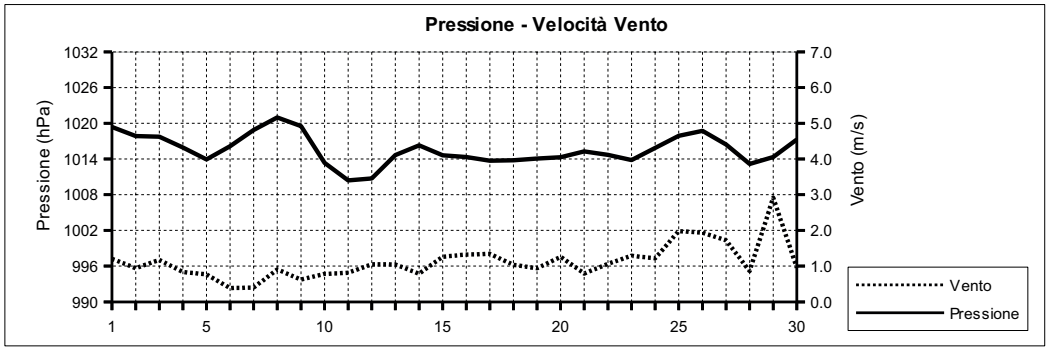

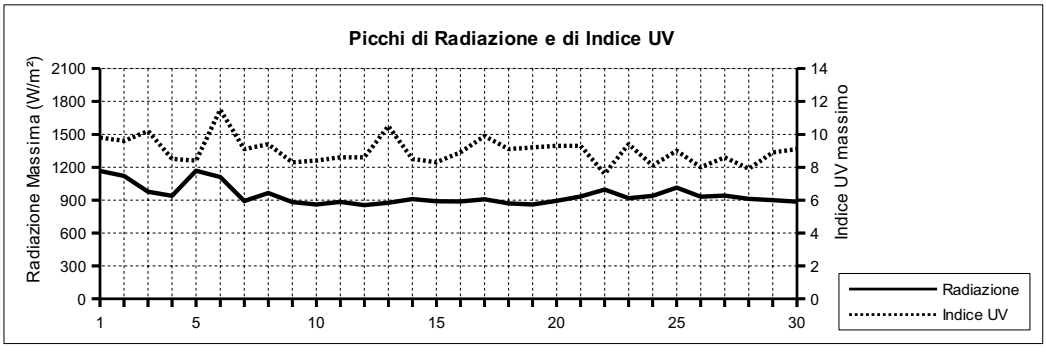

LUGLIO 2019 **(medie giornaliere)**

	Temperatura	Umidità	Pressione	Vento		Rad. Solare		Pioggia	Indice UV		
Data	°C	%	hPa	m/s	direzione	W/m²	durata	mm	medio	max	(ore)
01/07/19	28.6	53.5	1017.2	1.1	S	483.2	15:10	0.0	5.8	9.8	(13:00)
02/07/19	27.8	71.0	1014.3	0.8	SE	473.1	15:10	0.0	5.7	9.6	(13:50)
03/07/19	28.1	75.8	1013.7	0.7	SE	454.9	15:10	0.0	5.8	9.6	(13:10)
04/07/19	28.9	68.7	1015.4	1.0	SW	466.7	15:10	0.0	5.9	9.2	(13:20)
05/07/19	28.3	64.2	1015.7	1.1	--	474.3	15:10	0.0	5.7	9.8	(14:00)
06/07/19	27.9	72.9	1014.4	1.2	S	459.5	15:10	0.0	5.6	9.7	(13:10)
07/07/19	27.2	79.0	1012.9	1.5	S	430.4	15:00	0.0	5.7	10.2	(14:10)
08/07/19	28.0	76.7	1012.6	1.3	S	447.4	15:00	0.0	5.3	9.9	(12:40)
09/07/19	27.8	82.5	1013.1	1.2	SW	324.7	15:00	1.5	4.4	8.4	(12:30)
10/07/19	27.5	73.4	1008.0	1.8	SW	365.3	15:00	3.6	4.5	8.1	(13:10)
11/07/19	26.2	52.3	1011.8	1.4	N	489.7	15:00	0.0	5.0	10.2	(11:20)
12/07/19	26.1	72.7	1012.5	1.5	S	370.1	15:00	0.0	4.7	9.8	(13:30)
13/07/19	26.6	75.5	1009.9	1.4	SW	414.8	15:00	0.0	4.7	9.1	(13:40)
14/07/19	26.6	51.0	1009.4	1.5	NE	505.9	14:50	0.0	5.1	8.6	(13:40)
15/07/19	26.5	45.6	1006.8	1.6	NE	443.1	14:40	0.0	5.2	8.5	(13:40)
16/07/19	25.6	52.4	1008.1	2.6	NE	360.5	14:50	0.0	4.3	8.3	(13:20)
17/07/19	25.8	49.0	1012.3	1.0	NE	480.5	14:50	0.0	4.3	7.7	(13:20)
18/07/19	25.2	68.5	1012.6	1.0	--	451.6	14:50	0.0	4.4	7.7	(14:00)
19/07/19	26.0	71.5	1015.7	1.1	NW	405.0	14:50	0.0	4.4	7.7	(12:50)
20/07/19	26.8	69.8	1018.2	0.8	--	462.8	14:40	0.0	4.4	7.6	(13:00)
21/07/19	27.9	61.9	1019.7	0.9	SW	462.9	14:40	0.0	4.5	7.6	(13:10)
22/07/19	28.3	68.3	1019.4	0.8	SE	449.6	14:40	0.0	4.4	7.6	(13:10)
23/07/19	30.0	59.7	1016.8	0.7	SW	444.9	14:40	0.0	4.7	7.8	(12:40)
24/07/19	31.1	41.1	1015.1	0.9	NW	457.0	14:40	0.0	4.7	8.0	(12:30)
25/07/19	30.0	56.0	1015.4	1.1	S	451.5	14:40	0.0	4.3	7.9	(12:40)
26/07/19	28.1	76.7	1012.6	1.4	S	433.0	14:40	0.0	4.7	8.1	(13:30)
27/07/19	27.3	80.5	1007.2	1.6	S	352.5	14:30	0.0	4.4	8.4	(13:40)
28/07/19	26.3	73.4	1002.3	3.4	SW	345.0	14:20	**13.2**	4.3	**11.3**	**(12:30)**
29/07/19	25.7	70.7	1007.4	1.4	SW	420.2	14:30	0.0	4.9	10.0	(12:10)
30/07/19	26.2	72.7	1011.3	1.1	SW	463.9	14:30	0.0	5.8	9.5	(13:10)
31/07/19	27.3	71.9	1013.5	1.3	SW	483.0	14:20	0.0	5.1	8.3	(13:30)

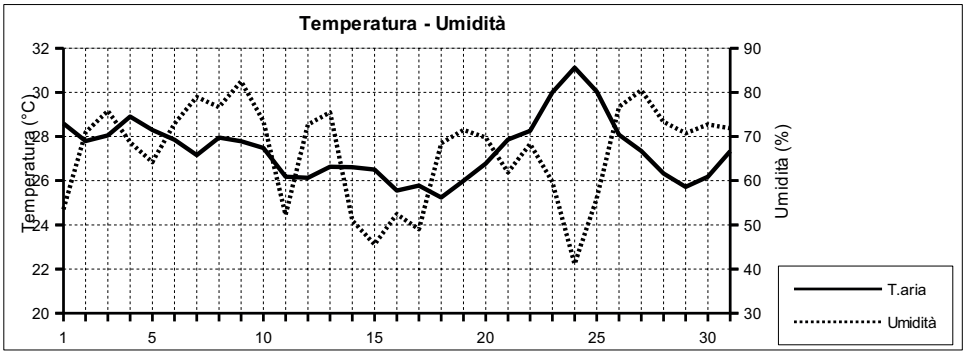

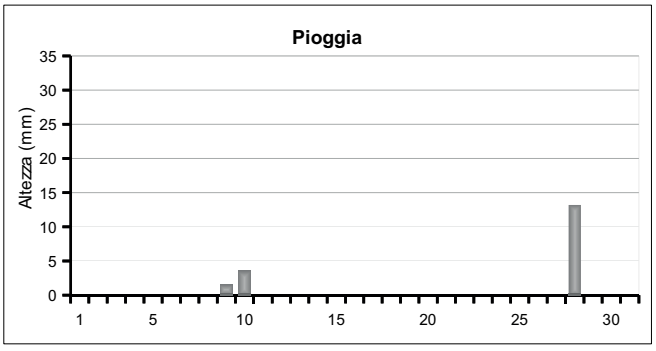

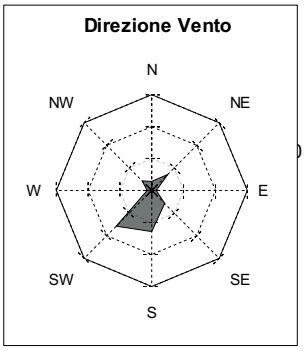

LUGLIO 2019 **(estremi giornalieri)**

	Temperatura (°C)				Umidità (%)				Pressione (hPa)				Vento (m/s)		Radiazione (W/m²)	
Data	min	(ore)	max	(ore)	min	(ore)	max	(ore)	min	(ore)	max	(ore)	max	(ore)	max	(ore)
01/07/19	25.4	(05:50)	31.4	(13:50)	43.0	(10:20)	78.0	(23:20)	1015.5	(18:10)	1018.6	(00:10)	6.3	(11:50)	867.0	(13:10)
02/07/19	24.8	(04:30)	32.1	(18:50)	53.0	(18:40)	84.0	(02:10)	1012.4	(18:40)	1016.6	(00:00)	5.8	(11:10)	846.0	(12:50)
03/07/19	25.4	(06:10)	33.2	(16:30)	56.0	(16:30)	85.0	(22:00)	1013.0	(17:40)	1014.7	(12:20)	6.7	(11:30)	842.0	(13:10)
04/07/19	25.8	(05:40)	33.3	(17:20)	35.0	(18:40)	87.0	(05:40)	1014.4	(04:20)	1016.5	(12:10)	6.3	(16:40)	826.0	(13:00)
05/07/19	24.7	(05:20)	32.1	(18:30)	42.0	(21:40)	81.0	(08:00)	1014.2	(18:50)	1016.6	(01:30)	6.7	(15:10)	861.0	(13:10)
06/07/19	26.1	(05:50)	31.3	(15:30)	52.0	(15:30)	86.0	(07:50)	1013.1	(19:00)	1015.3	(00:00)	7.6	(13:20)	858.0	(13:00)
07/07/19	25.2	(05:50)	29.0	(13:10)	73.0	(12:10)	84.0	(01:10)	1010.7	(18:50)	1014.1	(03:10)	7.2	(13:40)	874.0	(13:20)
08/07/19	25.3	(05:50)	29.6	(13:30)	68.0	(10:00)	85.0	(20:10)	1011.0	(03:30)	1014.2	(22:40)	8.0	(12:50)	819.0	(13:00)
09/07/19	26.2	(14:20)	29.7	(13:00)	69.0	(15:30)	89.0	(05:00)	1010.8	(19:10)	1016.0	(14:00)	13.0	(14:10)	954.0	(12:50)
10/07/19	23.3	(18:10)	30.2	(14:00)	61.0	(16:00)	87.0	(03:10)	1006.0	(13:50)	1012.2	(00:10)	14.8	(17:50)	967.0	(13:30)
11/07/19	22.8	(05:20)	30.1	(16:40)	**31.0**	**(13:00)**	70.0	(23:40)	1010.1	(00:00)	1013.2	(23:20)	7.2	(09:40)	912.0	(13:10)
12/07/19	24.6	(05:30)	27.8	(14:50)	66.0	(11:50)	79.0	(22:00)	1011.4	(18:40)	1013.3	(08:40)	8.5	(15:10)	**1169.0**	**(14:30)**
13/07/19	24.8	(05:20)	28.9	(17:10)	62.0	(17:10)	84.0	(04:50)	1007.8	(20:00)	1012.4	(00:00)	8.0	(13:50)	1037.0	(12:20)
14/07/19	23.4	(06:00)	29.6	(15:10)	40.0	(12:00)	71.0	(00:00)	1008.7	(18:50)	1010.6	(11:20)	7.6	(01:30)	918.0	(13:50)
15/07/19	24.0	(06:40)	29.9	(14:30)	34.0	(12:00)	59.0	(18:50)	1005.6	(17:50)	1009.5	(00:00)	7.6	(19:50)	926.0	(11:10)
16/07/19	22.3	(07:00)	29.0	(14:40)	39.0	(20:30)	67.0	(03:40)	1005.2	(02:10)	1012.4	(23:50)	11.6	(05:10)	1123.0	(13:40)
17/07/19	21.9	(05:10)	29.2	(14:10)	38.0	(13:20)	71.0	(23:00)	1011.6	(18:20)	1012.8	(08:40)	7.2	(18:00)	874.0	(13:00)
18/07/19	22.8	(06:30)	27.5	(19:10)	55.0	(19:10)	75.0	(03:50)	1011.6	(04:30)	1014.6	(23:50)	8.5	(14:10)	863.0	(13:40)
19/07/19	23.3	(05:50)	29.6	(15:10)	57.0	(15:10)	79.0	(06:30)	1014.7	(00:30)	1017.1	(23:50)	7.6	(13:40)	868.0	(13:40)
20/07/19	23.5	(05:50)	30.9	(17:30)	53.0	(16:00)	80.0	(02:00)	1016.7	(03:10)	1019.8	(23:20)	6.3	(14:40)	919.0	(14:10)
21/07/19	24.2	(06:00)	32.3	(15:10)	36.0	(19:20)	75.0	(06:40)	1018.8	(18:10)	**1020.5**	**(23:00)**	8.5	(16:00)	826.0	(13:10)
22/07/19	25.3	(06:10)	34.0	(17:10)	38.0	(16:50)	84.0	(23:50)	1018.0	(17:40)	1020.4	(00:10)	6.3	(13:30)	805.0	(13:00)
23/07/19	25.6	(01:50)	34.3	(14:20)	40.0	(14:50)	84.0	(00:00)	1015.0	(18:20)	1018.8	(00:00)	6.7	(14:30)	853.0	(12:40)
24/07/19	26.9	(06:00)	**35.2**	**(15:40)**	35.0	(15:10)	53.0	(23:30)	1013.8	(18:20)	1016.0	(00:20)	8.9	(17:50)	810.0	(13:20)
25/07/19	**27.4**	**(23:20)**	33.7	(17:50)	39.0	(10:50)	83.0	(20:30)	1014.5	(17:30)	1016.3	(11:10)	7.6	(12:50)	807.0	(13:20)
26/07/19	26.6	(03:10)	30.2	(14:50)	64.0	(01:30)	87.0	(21:40)	1010.2	(20:50)	1014.6	(00:00)	7.2	(14:00)	795.0	(13:10)
27/07/19	25.8	(05:30)	29.3	(13:40)	63.0	(11:10)	**90.0**	**(01:30)**	1004.0	(23:50)	1010.4	(00:00)	9.8	(15:10)	896.0	(13:40)
28/07/19	22.6	(10:20)	28.5	(14:30)	53.0	(14:20)	87.0	(10:50)	**1000.5**	**(06:10)**	1004.8	(23:50)	**15.2**	**(13:50)**	1058.0	(13:00)
29/07/19	23.6	(05:40)	28.3	(13:50)	61.0	(14:50)	81.0	(05:40)	1004.8	(00:00)	1010.2	(23:50)	8.5	(00:30)	972.0	(14:30)
30/07/19	24.1	(04:40)	28.9	(18:30)	64.0	(18:30)	80.0	(02:20)	1010.2	(00:00)	1012.8	(23:20)	7.2	(18:00)	986.0	(13:00)
31/07/19	24.6	(05:10)	31.1	(18:30)	50.0	(18:30)	88.0	(05:20)	1012.4	(03:30)	1014.8	(22:40)	8.0	(15:30)	837.0	(13:40)

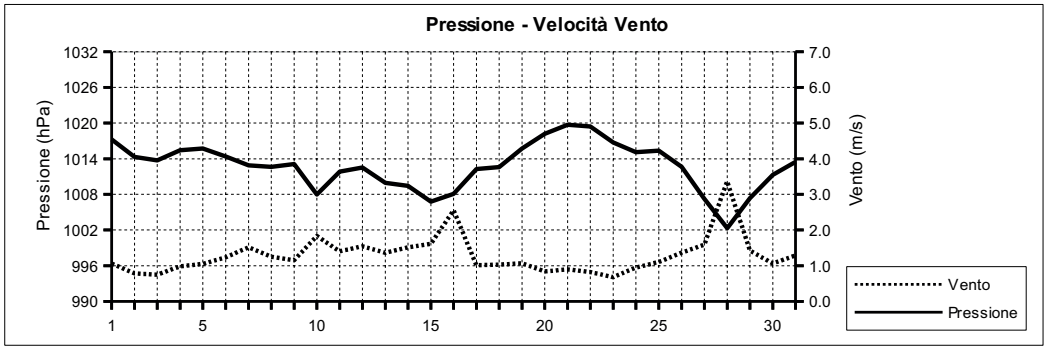

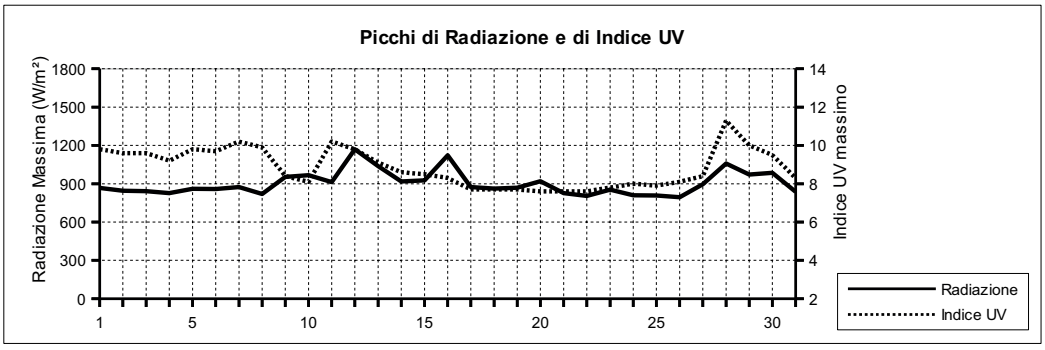

AGOSTO 2019 **(medie giornaliere)**

	Temperatura	Umidità	Pressione	Vento		Rad. Solare		Pioggia	Indice UV		
Data	°C	%	hPa	m/s	direzione	W/m²	durata	mm	medio	max	(ore)
01/08/19	27.0	72.3	1014.6	1.0	SW	496.5	14:20	0.0	3.5	6.0	(12:40)
02/08/19	27.7	60.0	1012.6	0.8	SW	368.9	14:20	0.0	2.7	6.4	(14:00)
03/08/19	28.4	63.7	1009.2	1.0	SW	488.8	14:20	0.0	3.4	**5.9**	**(13:00)**
04/08/19	28.6	53.4	1012.6	0.7	NW	484.9	14:20	0.0	3.3	5.6	(12:50)
05/08/19	28.4	53.9	1015.1	0.8	SW	476.0	14:20	0.0	3.2	5.4	(13:00)
06/08/19	27.7	61.0	1015.8	1.0	SW	473.7	14:20	0.0	3.3	5.6	(12:50)
07/08/19	28.5	54.9	1013.4	0.7	SW	478.7	14:10	0.0	3.2	5.8	(13:40)
08/08/19	29.3	51.8	1010.7	0.7	SW	433.4	14:20	0.0	3.1	6.5	(13:00)
09/08/19	29.8	64.2	1012.4	0.7	SW	448.3	14:10	0.0	3.0	5.1	(12:40)
10/08/19	29.5	70.6	1014.8	0.6	SW	447.1	14:10	0.0	3.0	5.3	(13:30)
11/08/19	29.7	74.7	1013.9	0.6	SE	455.1	14:00	0.0	3.2	5.6	(12:30)
12/08/19	30.0	75.4	1011.3	0.7	SW	457.4	14:00	0.0	3.3	5.7	(13:00)
13/08/19	29.2	74.1	1010.0	1.0	SW	444.5	14:00	0.0	3.1	5.5	(13:00)
14/08/19	27.2	68.4	1010.8	1.0	NW	447.5	14:00	0.0	3.3	5.5	(12:50)
15/08/19	27.2	58.2	1012.8	0.8	NW	446.3	14:00	0.0	3.0	5.8	(12:50)
16/08/19	26.4	68.5	1013.9	0.9	SW	469.0	13:50	0.0	3.3	5.6	(12:40)
17/08/19	27.0	68.0	1015.7	0.8	NW	456.1	13:50	0.0	3.1	5.6	(12:50)
18/08/19	27.7	64.5	1015.5	0.7	NW	455.1	13:50	0.0	3.1	5.5	(13:10)
19/08/19	28.3	55.8	1015.8	0.8	SW	450.8	13:50	0.0	3.1	5.3	(13:10)
20/08/19	28.1	63.2	1016.5	0.8	SW	453.3	13:50	0.0	3.1	5.4	(12:40)
21/08/19	27.9	66.5	1016.7	0.8	SW	436.8	13:50	0.0	3.0	5.2	(12:40)
22/08/19	28.7	62.9	1016.9	0.7	SW	429.2	13:40	0.0	3.0	5.0	(12:50)
23/08/19	29.6	55.0	1016.9	0.6	NW	417.4	13:40	0.0	3.1	5.1	(13:00)
24/08/19	28.6	52.9	1015.9	0.6	NW	410.5	13:30	0.0	2.9	4.9	(13:30)
25/08/19	27.8	63.2	1015.4	0.8	SW	436.8	13:30	0.0	2.9	5.0	(12:50)
26/08/19	27.7	61.9	1015.8	0.7	SW	437.5	13:30	0.0	3.0	5.0	(12:50)
27/08/19	27.8	68.9	1016.3	0.7	SW	434.8	13:20	0.0	2.9	4.9	(12:40)
28/08/19	27.7	69.3	1016.3	0.6	SW	422.5	13:20	0.0	3.1	5.1	(12:30)
29/08/19	27.7	65.3	1016.4	0.5	NW	292.3	13:20	0.0	2.2	4.7	(13:40)
30/08/19	28.0	66.9	1016.7	0.4	NW	271.4	13:00	0.0	2.1	4.5	(11:50)
31/08/19	28.2	61.2	1014.2	0.6	SW	413.2	13:10	0.0	2.9	4.9	(12:40)

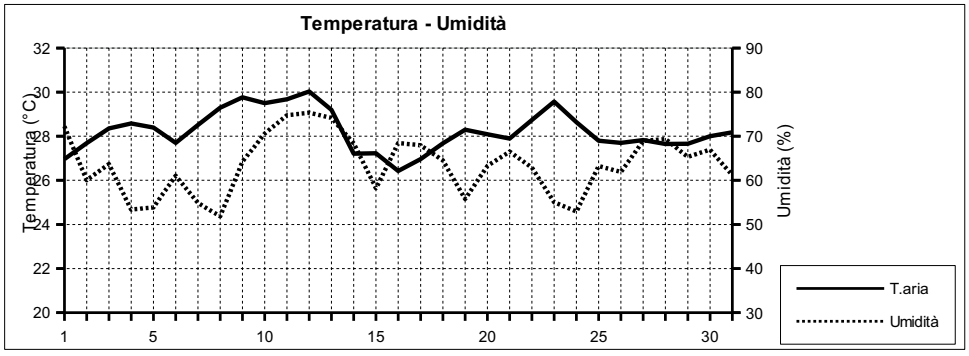

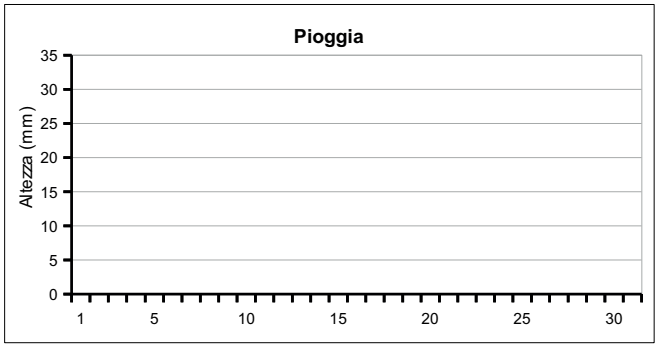

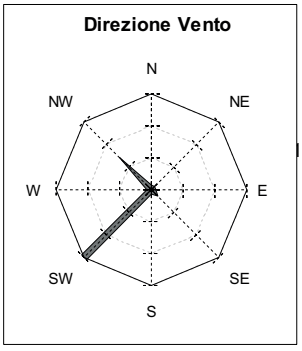

AGOSTO 2019 **(estremi giornalieri)**

	Temperatura (°C)				Umidità (%)				Pressione (hPa)				Vento (m/s)		Radiazione (W/m²)	
Data	min	(ore)	max	(ore)	min	(ore)	max	(ore)	min	(ore)	max	(ore)	max	(ore)	max	(ore)
01/08/19	24.8	(06:10)	30.4	(18:00)	49.0	(17:40)	85.0	(06:10)	1013.8	(04:30)	1015.4	(10:20)	6.7	(13:20)	874.0	(13:50)
02/08/19	24.2	(05:50)	31.9	(17:30)	37.0	(17:20)	75.0	(13:00)	1009.9	(18:20)	1014.6	(09:40)	**9.4**	**(12:30)**	1000.0	(12:30)
03/08/19	25.2	(05:40)	32.7	(15:20)	42.0	(15:10)	81.0	(02:50)	**1008.3**	**(04:40)**	1011.0	(23:50)	9.4	(17:10)	905.0	(13:30)
04/08/19	24.9	(06:00)	32.3	(14:00)	33.0	(10:40)	77.0	(03:30)	1011.1	(00:00)	1014.7	(23:50)	7.6	(17:40)	858.0	(13:30)
05/08/19	25.3	(06:00)	32.3	(17:00)	34.0	(17:40)	67.0	(02:20)	1014.4	(18:20)	1016.2	(11:00)	6.3	(12:50)	840.0	(13:40)
06/08/19	24.8	(06:00)	31.2	(17:20)	42.0	(21:00)	75.0	(05:40)	1014.4	(18:50)	1017.0	(11:30)	6.3	(11:50)	842.0	(13:10)
07/08/19	24.7	(05:10)	32.6	(15:10)	34.0	(13:30)	74.0	(04:10)	1011.2	(20:10)	1015.3	(00:00)	5.4	(13:20)	960.0	(13:40)
08/08/19	25.7	(06:20)	33.4	(14:40)	**28.0**	**(11:20)**	76.0	(23:20)	1009.6	(18:50)	1012.0	(00:00)	6.3	(16:00)	**1074.0**	**(13:00)**
09/08/19	25.3	(06:20)	34.4	(15:30)	43.0	(18:20)	82.0	(03:50)	1011.3	(00:00)	1013.9	(22:10)	6.7	(16:00)	810.0	(12:40)
10/08/19	26.7	(06:10)	33.9	(17:30)	45.0	(18:20)	80.0	(04:10)	1013.7	(00:00)	1016.0	(09:30)	6.3	(14:10)	807.0	(13:30)
11/08/19	26.4	(06:20)	**35.7**	**(15:40)**	53.0	(15:30)	85.0	(02:50)	1012.4	(18:00)	1015.2	(00:20)	6.3	(15:00)	812.0	(13:00)
12/08/19	27.9	(06:20)	33.1	(16:30)	65.0	(22:50)	84.0	(01:50)	1009.3	(18:30)	1013.0	(00:00)	7.2	(13:50)	809.0	(13:00)
13/08/19	27.2	(06:10)	31.4	(18:00)	61.0	(18:00)	**86.0**	**(05:20)**	1008.9	(19:20)	1011.1	(10:40)	6.7	(14:10)	793.0	(13:10)
14/08/19	25.2	(06:10)	30.3	(16:30)	53.0	(16:10)	80.0	(00:00)	1009.7	(01:30)	1012.4	(23:30)	6.7	(03:40)	856.0	(11:20)
15/08/19	24.1	(06:40)	30.8	(15:30)	42.0	(11:10)	77.0	(00:00)	1012.0	(04:10)	1014.1	(22:30)	7.6	(17:10)	979.0	(13:00)
16/08/19	24.2	(05:30)	28.5	(15:20)	56.0	(11:00)	74.0	(06:30)	1012.8	(04:50)	1015.7	(23:50)	6.7	(14:00)	831.0	(13:00)
17/08/19	**24.0**	**(06:10)**	30.4	(15:40)	53.0	(17:10)	81.0	(06:30)	1015.0	(19:40)	1016.8	(10:30)	7.6	(14:30)	898.0	(14:30)
18/08/19	24.3	(05:50)	31.8	(16:20)	47.0	(22:20)	80.0	(06:30)	1014.4	(19:40)	1016.3	(10:10)	7.6	(17:00)	810.0	(13:10)
19/08/19	25.1	(06:40)	32.6	(15:30)	38.0	(17:10)	68.0	(05:30)	1015.1	(05:30)	1016.6	(22:10)	8.0	(16:00)	800.0	(13:10)
20/08/19	25.4	(05:50)	30.9	(13:50)	49.0	(08:20)	81.0	(23:30)	1016.0	(04:30)	1017.1	(11:20)	6.7	(13:20)	803.0	(13:20)
21/08/19	25.4	(06:30)	31.4	(17:30)	52.0	(15:00)	81.0	(00:00)	1015.5	(18:30)	1017.8	(10:30)	6.3	(18:00)	788.0	(13:10)
22/08/19	25.2	(05:20)	33.0	(15:20)	40.0	(22:20)	78.0	(04:30)	1015.7	(17:10)	1017.9	(11:00)	6.3	(16:40)	763.0	(13:00)
23/08/19	27.1	(06:20)	33.4	(13:50)	44.0	(11:50)	70.0	(15:50)	1015.7	(16:30)	1017.7	(20:20)	6.7	(14:30)	788.0	(13:20)
24/08/19	26.1	(04:30)	32.5	(14:50)	41.0	(14:10)	75.0	(19:40)	1014.8	(17:00)	1017.0	(11:00)	5.8	(15:20)	823.0	(13:40)
25/08/19	25.5	(06:20)	30.7	(13:10)	54.0	(17:30)	74.0	(21:50)	1014.2	(17:20)	1016.6	(11:30)	5.8	(16:50)	795.0	(13:20)
26/08/19	24.7	(06:20)	30.9	(16:20)	50.0	(17:10)	70.0	(05:30)	1014.9	(17:30)	1016.7	(11:20)	6.3	(12:20)	775.0	(13:20)
27/08/19	24.9	(06:30)	30.6	(14:00)	55.0	(17:30)	81.0	(05:50)	1015.3	(18:40)	1017.4	(11:30)	5.8	(14:50)	770.0	(13:30)
28/08/19	24.9	(04:40)	31.6	(14:30)	40.0	(16:10)	82.0	(02:40)	1015.4	(19:20)	1017.0	(00:00)	6.7	(15:20)	784.0	(13:10)
29/08/19	24.9	(04:30)	32.2	(13:40)	39.0	(13:40)	80.0	(03:30)	1015.5	(03:40)	1017.3	(21:20)	5.8	(12:10)	812.0	(13:50)
30/08/19	26.1	(07:10)	32.2	(16:20)	50.0	(16:30)	78.0	(03:10)	1015.5	(16:10)	**1017.7**	**(10:10)**	5.4	(15:40)	937.0	(11:50)
31/08/19	25.8	(06:50)	31.5	(16:10)	48.0	(11:20)	71.0	(00:00)	1012.3	(17:00)	1016.1	(00:00)	5.8	(14:20)	849.0	(12:30)

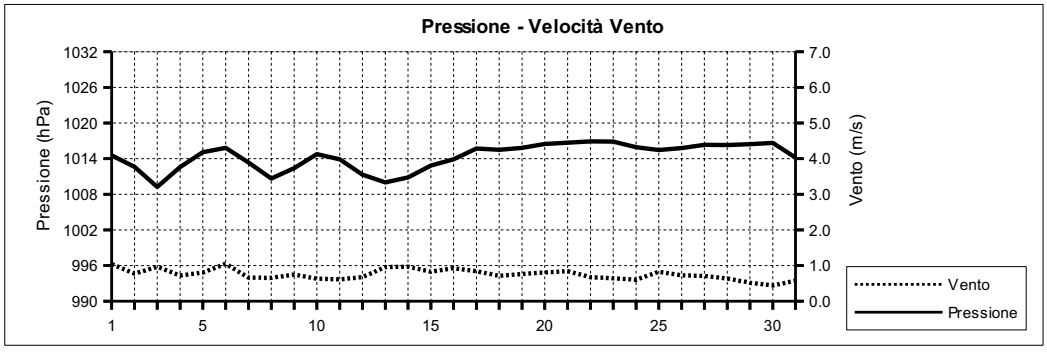

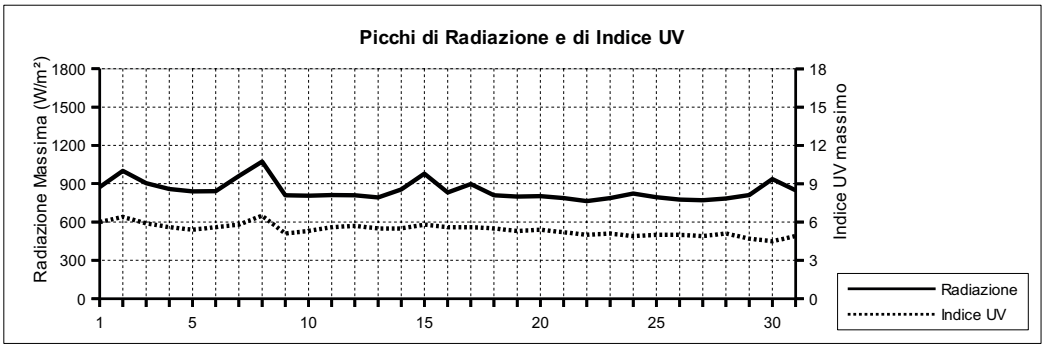

SETTEMBRE 2019 **(medie giornaliere)**

	Temperatura	Umidità	Pressione	Vento		Rad. Solare		Pioggia	Indice UV		
Data	aria (°C)	%	hPa	m/s	direzione	W/m²	durata	mm	medio	max	(ore)
01/09/19	26.6	67.4	1012.8	0.8	NE	206.0	13:00	0.0	3.6	5.8	(14:40)
02/09/19	25.1	75.6	1013.7	0.7	--	243.1	12:50	0.5	3.7	6.5	(12:00)
03/09/19	25.8	68.3	1015.1	1.3	NE	315.9	13:20	0.0	4.2	7.3	(12:20)
04/09/19	25.8	54.0	1014.9	2.0	NE	401.6	13:10	0.0	4.6	7.4	(12:20)
05/09/19	25.7	59.6	1012.7	1.4	NW	418.5	13:10	0.0	4.6	6.9	(13:10)
06/09/19	25.7	73.5	1014.4	1.1	SW	399.3	13:00	0.0	4.5	7.3	(12:20)
07/09/19	24.9	69.0	1015.5	1.1	SW	423.0	13:00	2.5	5.0	7.8	(12:30)
08/09/19	24.5	64.2	1016.3	1.3	SW	431.3	13:00	0.0	5.0	8.3	(13:50)
09/09/19	23.2	63.6	1016.1	1.2	W	367.0	12:50	6.6	4.8	**9.3**	**(13:00)**
10/09/19	23.4	56.6	1015.7	0.7	--	387.3	13:00	0.0	5.1	8.3	(12:50)
11/09/19	25.7	53.4	1018.2	1.8	NW	435.7	12:40	0.0	4.8	7.6	(11:40)
12/09/19	25.9	55.1	1024.6	1.5	NW	427.2	12:40	0.0	5.4	7.8	(13:10)
13/09/19	26.6	50.7	1026.6	2.2	NE	425.8	12:40	0.0	4.8	7.4	(11:50)
14/09/19	26.0	45.8	1025.4	1.8	N	332.3	17:10	0.0	4.9	7.5	(13:30)
15/09/19	25.6	48.2	1023.7	2.0	--	309.4	18:10	0.0	5.0	7.8	(13:10)
16/09/19	25.0	65.4	1020.3	0.8	S	408.5	12:40	0.0	4.7	7.4	(12:10)
17/09/19	24.4	76.0	1018.1	0.8	S	406.7	12:30	0.0	4.8	7.4	(12:50)
18/09/19	24.4	76.9	1017.1	0.9	S	391.9	12:30	0.0	4.5	7.3	(13:50)
19/09/19	23.8	75.2	1016.7	0.9	SW	213.4	12:30	3.3	3.6	5.8	(11:10)
20/09/19	23.0	52.2	1020.6	2.7	NE	404.4	12:20	0.0	4.5	6.8	(13:00)
21/09/19	21.8	52.9	1022.6	1.4	--	403.9	12:20	0.0	4.5	6.8	(13:30)
22/09/19	22.0	66.7	1019.8	0.6	NW	118.7	12:20	0.5	3.2	5.7	(09:40)
23/09/19	23.8	83.3	1014.9	1.6	SW	362.2	11:50	**37.3**	4.9	8.2	(13:20)
24/09/19	23.4	73.3	1013.2	1.3	W	423.1	12:10	0.0	5.5	7.9	(13:00)
25/09/19	23.0	78.8	1014.0	0.9	SW	258.5	12:10	0.0	5.0	8.3	(11:50)
26/09/19	23.1	79.5	1015.4	0.6	SW	266.4	11:40	30.2	5.1	7.4	(13:00)
27/09/19	23.7	72.3	1018.7	0.6	NW	404.8	12:10	0.0	5.1	8.1	(13:10)
28/09/19	23.2	80.9	1020.3	0.7	S	394.4	12:10	0.0	5.4	7.8	(13:10)
29/09/19	23.7	80.3	1018.8	0.8	SW	392.4	12:00	1.3	5.6	8.4	(13:10)
30/09/19	23.5	75.9	1016.4	0.8	W	337.9	12:00	0.0	5.2	7.7	(12:50)

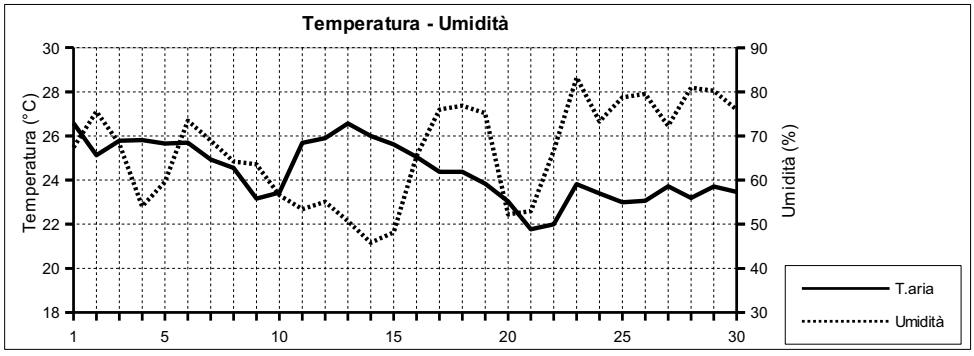

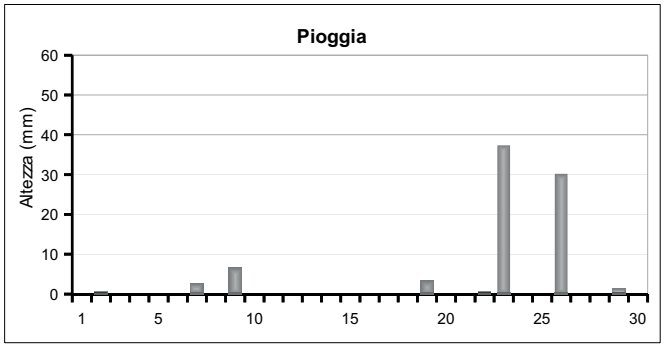

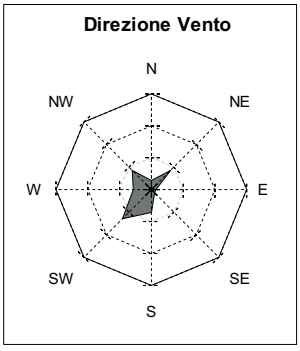

SETTEMBRE 2019 **(estremi giornalieri)**

	Temperatura (°C)				Umidità (%)				Pressione (hPa)				Vento (m/s)		Radiazione (W/m²)	
Data	min	(ore)	max	(ore)	min	(ore)	max	(ore)	min	(ore)	max	(ore)	max	(ore)	max	(ore)
01/09/19	24.9	(19:30)	28.8	(15:50)	62.0	(19:00)	74.0	(18:00)	1011.8	(16:00)	1014.3	(00:10)	9.4	(19:10)	707.0	(11:10)
02/09/19	23.3	(06:50)	27.3	(16:20)	67.0	(12:50)	86.0	(07:00)	1012.6	(04:50)	1015.2	(22:20)	5.8	(17:00)	828.0	(12:00)
03/09/19	22.9	(05:40)	30.9	(16:10)	46.0	(16:10)	85.0	(05:30)	1013.9	(16:00)	1016.6	(21:10)	11.6	(16:40)	807.0	(13:10)
04/09/19	22.8	(06:30)	29.6	(15:50)	45.0	(13:40)	63.0	(05:00)	1013.3	(17:40)	1016.5	(00:00)	8.5	(05:30)	796.0	(15:00)
05/09/19	21.9	(06:20)	30.0	(16:00)	48.0	(15:20)	75.0	(23:30)	**1011.5**	**(17:00)**	1014.0	(00:00)	6.3	(15:30)	751.0	(13:30)
06/09/19	23.6	(06:10)	28.1	(14:10)	61.0	(16:40)	81.0	(06:00)	1012.9	(00:00)	1015.8	(22:40)	6.7	(14:00)	**1034.0**	**(13:40)**
07/09/19	21.8	(08:40)	28.2	(14:50)	49.0	(16:20)	86.0	(08:30)	1014.6	(03:30)	1017.0	(23:40)	7.2	(14:20)	798.0	(13:10)
08/09/19	22.1	(07:00)	27.2	(15:30)	53.0	(11:10)	73.0	(06:30)	1015.6	(17:50)	1017.2	(00:40)	7.6	(12:20)	835.0	(13:10)
09/09/19	20.1	(05:00)	25.4	(14:30)	49.0	(12:20)	88.0	(06:40)	1014.5	(04:10)	1018.0	(21:50)	9.4	(15:40)	967.0	(13:50)
10/09/19	19.2	(07:00)	27.6	(17:50)	39.0	(18:40)	71.0	(05:50)	1013.1	(18:00)	1017.8	(00:00)	4.9	(13:20)	953.0	(12:40)
11/09/19	21.7	(07:00)	29.8	(14:40)	40.0	(13:20)	70.0	(23:40)	1015.1	(00:00)	1022.3	(22:50)	8.0	(18:40)	745.0	(13:10)
12/09/19	22.2	(05:50)	30.4	(15:30)	37.0	(20:20)	71.0	(00:00)	1022.2	(00:00)	1026.9	(23:20)	7.2	(22:10)	745.0	(13:20)
13/09/19	22.7	(05:20)	**31.1**	**(15:50)**	37.0	(16:40)	62.0	(04:40)	1025.3	(17:00)	**1028.0**	**(09:30)**	9.4	(10:20)	747.0	(12:40)
14/09/19	22.4	(06:40)	30.8	(15:30)	**33.0**	**(13:50)**	56.0	(07:10)	1023.6	(16:50)	1027.0	(00:00)	8.5	(22:00)	752.0	(13:20)
15/09/19	20.7	(05:10)	29.6	(13:40)	37.0	(18:20)	59.0	(20:40)	1022.1	(18:40)	1025.4	(08:50)	9.4	(02:00)	747.0	(12:50)
16/09/19	22.6	(07:10)	28.4	(14:30)	50.0	(13:50)	80.0	(22:30)	1018.5	(19:10)	1022.3	(00:30)	6.3	(15:20)	821.0	(13:30)
17/09/19	22.1	(06:50)	26.9	(15:40)	66.0	(15:10)	83.0	(05:40)	1016.7	(19:20)	1019.4	(00:00)	7.2	(16:10)	717.0	(13:00)
18/09/19	22.3	(05:20)	26.7	(17:30)	69.0	(17:20)	83.0	(02:40)	1016.3	(17:30)	1017.7	(21:30)	6.7	(16:10)	689.0	(13:10)
19/09/19	22.2	(07:20)	26.1	(15:50)	62.0	(15:10)	84.0	(05:00)	1015.3	(14:20)	1018.8	(23:50)	8.0	(11:30)	624.0	(15:00)
20/09/19	19.7	(23:50)	26.3	(16:10)	37.0	(16:10)	72.0	(00:00)	1018.8	(00:00)	1023.0	(22:20)	9.8	(08:40)	754.0	(11:10)
21/09/19	**17.9**	**(06:50)**	25.7	(16:00)	43.0	(10:50)	63.0	(23:40)	1021.7	(17:10)	1023.6	(10:40)	7.2	(00:00)	772.0	(13:00)
22/09/19	19.8	(04:10)	24.8	(13:20)	54.0	(13:20)	78.0	(16:00)	1016.9	(19:50)	1022.6	(02:10)	9.4	(10:10)	520.0	(12:20)
23/09/19	18.9	(04:30)	27.1	(16:10)	71.0	(00:10)	93.0	(05:20)	1013.3	(16:20)	1017.4	(03:50)	**12.1**	**(03:50)**	914.0	(12:20)
24/09/19	21.2	(07:00)	25.9	(13:40)	52.0	(13:40)	87.0	(00:00)	1012.1	(04:30)	1014.3	(21:30)	7.2	(11:00)	752.0	(13:00)
25/09/19	20.9	(05:20)	25.1	(14:00)	71.0	(15:30)	86.0	(06:50)	1013.3	(03:10)	1014.9	(23:00)	8.0	(15:00)	997.0	(13:50)
26/09/19	19.6	(07:20)	26.7	(15:00)	61.0	(15:00)	**94.0**	**(07:30)**	1013.3	(04:40)	1018.3	(23:40)	10.3	(05:20)	729.0	(14:40)
27/09/19	20.6	(06:00)	27.9	(16:20)	55.0	(11:20)	84.0	(01:00)	1017.5	(03:10)	1020.4	(23:50)	5.8	(15:50)	701.0	(13:10)
28/09/19	20.7	(07:30)	25.7	(14:40)	71.0	(15:00)	89.0	(06:50)	1019.7	(04:40)	1021.3	(10:30)	6.7	(15:40)	700.0	(12:50)
29/09/19	21.6	(07:10)	26.9	(15:40)	63.0	(15:10)	90.0	(07:30)	1017.5	(18:10)	1020.3	(00:00)	7.2	(16:00)	821.0	(12:50)
30/09/19	21.0	(06:00)	25.9	(15:20)	62.0	(12:30)	84.0	(00:30)	1015.1	(17:30)	1017.7	(00:00)	6.7	(11:30)	856.0	(13:40)

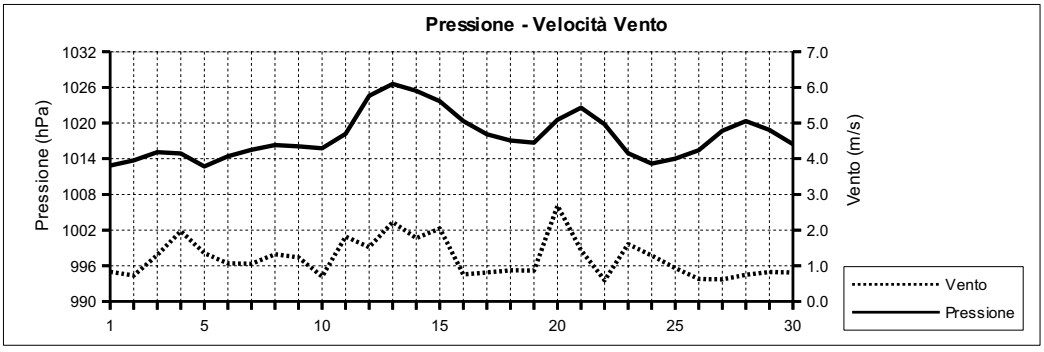

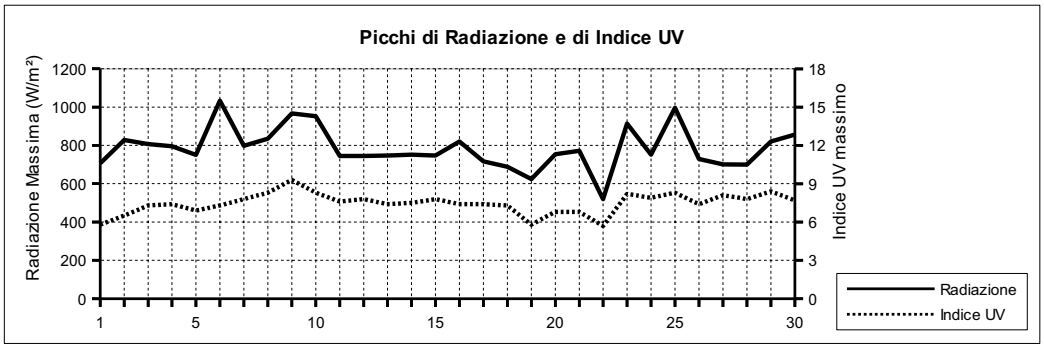

OTTOBRE 2019 **(medie giornaliere)**

	Temperatura	Umidità	Pressione	Vento		Rad. Solare		Pioggia	Indice UV		
Data	°C	%	hPa	m/s	direzione	W/m²	durata	mm	medio	max	(ore)
01/10/19	23.4	80.7	1014.5	1.0	SW	401.8	12:00	0.0	5.9	**8.6**	**(13:30)**
02/10/19	21.8	83.1	1009.8	1.5	SE	315.6	11:10	**54.3**	5.4	8.0	(12:00)
03/10/19	19.0	81.5	1007.6	1.6	--	226.5	11:40	31.7	4.4	7.3	(12:40)
04/10/19	18.5	63.2	1012.1	1.2	N	403.5	11:50	0.0	4.6	6.7	(16:10)
05/10/19	20.1	73.1	1012.0	0.6	NW	245.2	11:30	4.1	4.5	7.9	(14:50)
06/10/19	20.8	75.2	1012.9	0.5	SW	235.2	11:40	3.0	4.6	6.7	(11:40)
07/10/19	18.0	78.1	1008.0	2.2	N	119.3	11:40	6.6	3.6	6.8	(13:20)
08/10/19	20.2	52.9	1016.6	1.8	NE	396.5	11:40	0.0	4.4	6.4	(11:40)
09/10/19	21.0	56.8	1020.1	0.7	NW	385.6	11:40	0.0	4.7	6.7	(12:50)
10/10/19	21.9	68.5	1018.4	0.8	NW	374.9	11:30	0.0	4.6	7.0	(13:40)
11/10/19	21.5	73.6	1022.4	0.6	SW	362.3	11:40	0.0	4.7	6.9	(13:10)
12/10/19	20.7	76.8	1024.8	0.8	--	377.6	11:20	0.0	4.7	6.9	(12:50)
13/10/19	20.4	77.1	1024.7	0.6	SE	360.1	11:30	0.0	4.7	7.2	(13:40)
14/10/19	20.4	79.3	1022.7	0.5	SE	358.2	11:30	0.0	4.4	6.6	(12:50)
15/10/19	21.1	75.4	1019.0	1.2	SE	333.3	11:20	0.0	4.5	6.7	(12:20)
16/10/19	20.2	74.0	1019.0	1.0	NW	288.0	11:20	7.9	4.9	8.2	(12:20)
17/10/19	19.3	70.4	1020.8	0.9	--	366.4	11:20	0.0	4.6	6.7	(13:10)
18/10/19	19.4	74.5	1020.1	0.6	--	365.0	11:20	0.0	4.3	6.3	(12:50)
19/10/19	19.7	76.8	1019.6	0.6	SE	350.7	11:10	0.0	4.4	6.5	(13:20)
20/10/19	20.7	74.3	1021.1	0.5	--	300.0	11:10	0.0	4.3	5.8	(12:10)
21/10/19	22.0	73.2	1022.7	0.4	NW	337.1	11:00	0.0	4.3	5.9	(12:30)
22/10/19	21.9	71.9	1021.8	0.5	SW	334.8	11:00	0.0	4.3	5.9	(12:50)
23/10/19	22.4	62.6	1019.9	0.7	NW	337.3	11:00	0.0	4.3	6.0	(13:30)
24/10/19	21.6	61.2	1016.6	0.9	NW	276.2	11:00	0.0	3.9	5.5	(12:30)
25/10/19	22.0	66.0	1016.7	1.1	NW	232.3	10:40	0.0	4.0	5.8	(13:00)
26/10/19	22.0	62.4	1021.5	1.1	N	298.4	10:50	0.0	4.1	6.1	(11:50)
27/10/19	20.7	65.1	1021.2	0.5	SW	326.2	10:50	0.0	4.1	5.7	(11:30)
28/10/19	19.2	79.9	1018.2	0.5	S	305.2	10:50	0.0	3.9	5.5	(12:00)
29/10/19	19.4	81.0	1018.4	0.6	SW	305.3	10:40	0.0	4.2	6.1	(12:50)
30/10/19	19.4	80.0	1019.9	0.5	SW	288.3	10:40	0.0	3.9	6.3	(14:10)
31/10/19	19.2	82.7	1018.4	0.4	SE	255.4	10:30	1.8	3.9	5.8	(11:40)

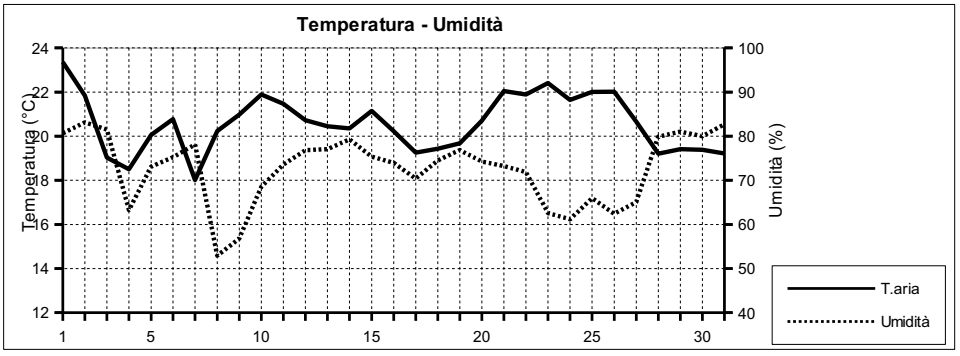

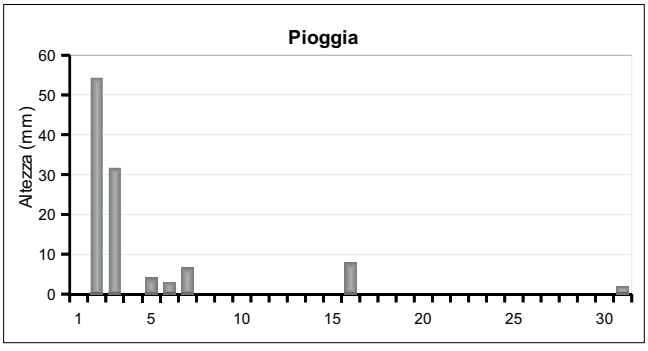

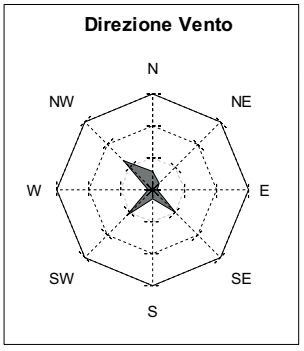

OTTOBRE 2019 **(estremi giornalieri)**

	Temperatura (°C)				Umidità (%)				Pressione (hPa)				Vento (m/s)		Radiazione (W/m²)	
Data	min	(ore)	max	(ore)	min	(ore)	max	(ore)	min	(ore)	max	(ore)	max	(ore)	max	(ore)
01/10/19	21.2	(06:50)	25.8	(14:50)	70.0	(18:00)	88.0	(06:00)	1012.5	(19:10)	1016.4	(01:20)	6.7	(13:20)	698.0	(12:30)
02/10/19	16.6	(19:40)	25.6	(13:20)	71.0	(13:20)	91.0	(20:00)	1007.8	(17:20)	1012.4	(00:00)	15.6	(18:00)	814.0	(12:50)
03/10/19	**15.1**	**(23:10)**	23.1	(15:10)	69.0	(21:20)	89.0	(00:00)	**1006.2**	**(16:40)**	1010.3	(22:40)	**19.2**	**(17:40)**	**835.0**	**(13:20)**
04/10/19	15.2	(07:00)	22.7	(15:40)	44.0	(14:50)	81.0	(00:00)	1009.7	(00:00)	1013.9	(22:40)	8.9	(00:50)	696.0	(13:00)
05/10/19	16.2	(09:40)	23.2	(16:30)	60.0	(03:20)	88.0	(10:00)	1010.8	(17:00)	1013.7	(00:00)	7.6	(14:30)	856.0	(12:10)
06/10/19	17.6	(07:30)	24.1	(12:10)	56.0	(13:40)	86.0	(05:00)	1011.8	(23:50)	1013.9	(10:50)	4.9	(18:30)	765.0	(11:00)
07/10/19	16.2	(10:10)	19.7	(00:50)	53.0	(23:00)	91.0	(08:40)	1005.5	(13:30)	1011.9	(23:50)	12.5	(21:30)	380.0	(13:20)
08/10/19	17.2	(02:20)	24.6	(16:10)	38.0	(15:20)	63.0	(23:50)	1011.8	(00:00)	1020.4	(22:50)	11.2	(08:40)	680.0	(12:40)
09/10/19	16.9	(06:10)	25.6	(14:30)	**37.0**	**(13:50)**	67.0	(22:40)	1018.7	(19:00)	1021.6	(10:30)	4.5	(15:40)	668.0	(13:00)
10/10/19	19.1	(01:40)	25.6	(14:40)	51.0	(15:50)	80.0	(23:20)	1017.2	(15:00)	1020.3	(23:40)	5.4	(14:40)	647.0	(13:00)
11/10/19	18.3	(07:50)	24.9	(13:40)	55.0	(13:10)	86.0	(08:00)	1020.3	(00:00)	1024.1	(23:20)	5.8	(14:20)	636.0	(12:50)
12/10/19	17.4	(04:50)	24.7	(14:50)	50.0	(16:50)	92.0	(04:50)	1024.1	(00:00)	**1025.8**	**(11:10)**	4.5	(14:00)	647.0	(12:50)
13/10/19	17.4	(08:00)	23.7	(15:40)	63.0	(17:00)	87.0	(05:10)	1023.4	(16:20)	1025.7	(11:00)	5.4	(14:10)	675.0	(12:20)
14/10/19	17.2	(06:30)	23.6	(15:10)	70.0	(12:50)	87.0	(02:10)	1021.0	(23:50)	1024.5	(00:20)	4.9	(14:00)	656.0	(12:30)
15/10/19	17.6	(04:40)	24.7	(15:30)	53.0	(14:00)	88.0	(01:30)	1016.9	(19:30)	1021.0	(00:00)	8.9	(23:00)	684.0	(14:50)
16/10/19	18.1	(23:40)	22.3	(00:00)	53.0	(15:20)	**92.0**	**(04:10)**	1016.8	(05:00)	1020.7	(22:20)	7.6	(11:20)	749.0	(12:00)
17/10/19	16.0	(07:50)	22.8	(14:50)	57.0	(17:00)	80.0	(23:40)	1020.3	(16:00)	1021.7	(10:40)	5.4	(13:20)	696.0	(13:00)
18/10/19	16.5	(07:40)	22.8	(15:30)	64.0	(16:40)	83.0	(02:30)	1019.0	(16:00)	1021.1	(01:00)	5.4	(15:40)	610.0	(13:00)
19/10/19	16.1	(06:50)	22.9	(16:50)	63.0	(17:00)	86.0	(06:30)	1018.9	(04:00)	1020.3	(12:00)	5.4	(14:10)	622.0	(13:20)
20/10/19	17.2	(05:20)	24.9	(15:10)	61.0	(14:30)	85.0	(03:40)	1020.3	(00:00)	1022.3	(22:40)	4.0	(14:50)	580.0	(12:50)
21/10/19	18.2	(07:30)	**26.9**	**(15:50)**	53.0	(17:00)	85.0	(06:50)	1022.0	(03:50)	1023.8	(11:20)	4.0	(15:10)	571.0	(12:40)
22/10/19	18.4	(06:10)	26.2	(11:40)	52.0	(13:30)	83.0	(23:30)	1020.9	(15:30)	1022.7	(01:00)	4.9	(13:50)	633.0	(12:50)
23/10/19	18.8	(07:30)	27.1	(15:10)	45.0	(15:00)	80.0	(00:00)	1018.2	(17:10)	1021.1	(09:30)	4.5	(16:50)	582.0	(13:10)
24/10/19	17.7	(07:40)	26.4	(16:20)	45.0	(12:50)	76.0	(22:00)	1012.9	(16:20)	1018.9	(09:40)	10.7	(22:50)	687.0	(14:00)
25/10/19	19.2	(02:00)	24.8	(12:40)	50.0	(12:40)	77.0	(02:20)	1013.2	(03:50)	1020.8	(23:40)	10.3	(18:20)	754.0	(13:50)
26/10/19	19.8	(05:40)	25.6	(13:10)	46.0	(13:10)	71.0	(00:30)	1020.2	(06:30)	1022.9	(22:40)	6.3	(07:00)	570.0	(12:50)
27/10/19	17.2	(06:20)	24.5	(15:20)	51.0	(10:30)	83.0	(22:40)	1019.7	(23:30)	1022.8	(00:10)	5.4	(13:40)	566.0	(11:40)
28/10/19	16.4	(06:10)	22.3	(14:30)	73.0	(09:30)	86.0	(23:20)	1016.4	(15:50)	1019.8	(00:00)	4.9	(13:30)	540.0	(11:30)
29/10/19	17.0	(06:10)	22.2	(12:50)	71.0	(16:00)	89.0	(05:20)	1017.3	(05:40)	1019.8	(22:40)	6.7	(13:50)	726.0	(11:50)
30/10/19	16.7	(06:40)	22.3	(14:20)	62.0	(14:20)	88.0	(06:50)	1019.2	(04:20)	1020.6	(09:20)	5.4	(14:10)	705.0	(11:20)
31/10/19	16.6	(06:20)	21.5	(12:00)	71.0	(10:40)	88.0	(04:40)	1017.1	(16:30)	1020.2	(00:00)	4.9	(12:20)	661.0	(12:10)

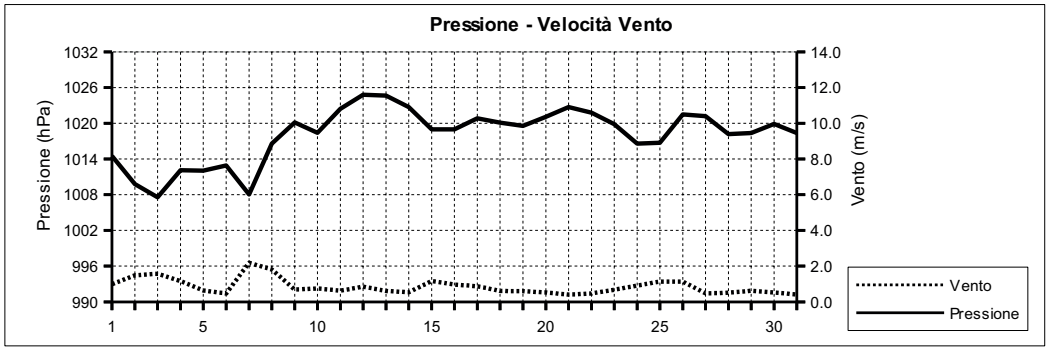

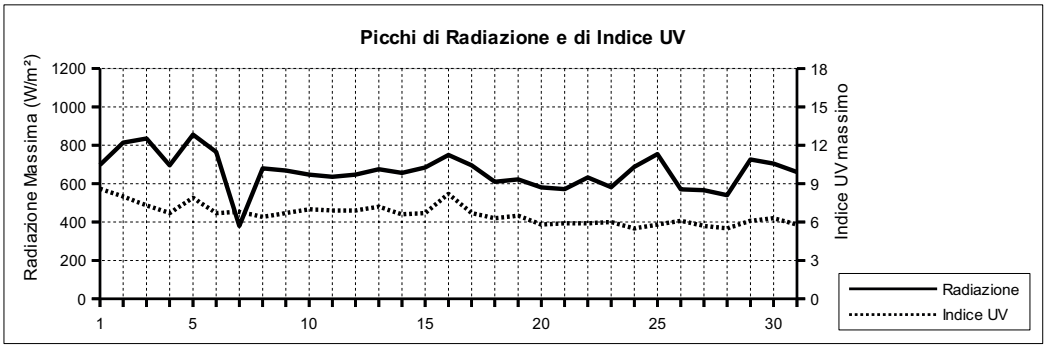

NOVEMBRE 2019 **(medie giornaliere)**

	Temperatura	Umidità	Pressione	Vento		Rad. Solare		Pioggia	Indice UV		
Data	°C	%	hPa	m/s	direzione	W/m²	durata	mm	medio	max	(ore)
01/11/19	18.7	80.1	1015.5	0.6	--	180.5	10:40	4.1	4.1	6.1	(10:20)
02/11/19	19.4	81.8	1012.3	1.4	S	241.1	10:10	13.2	4.1	5.9	(11:30)
03/11/19	20.5	85.2	1005.3	4.7	S	108.8	9:40	**37.8**	3.6	5.5	(10:40)
04/11/19	19.5	71.6	1007.1	2.1	W	204.0	10:30	7.6	3.2	7.1	(10:00)
05/11/19	20.8	83.5	1009.0	4.2	S	80.5	10:10	15.0	3.4	5.4	(11:00)
06/11/19	17.4	86.5	1008.7	1.7	S	43.7	10:00	12.4	2.9	5.1	(14:40)
07/11/19	15.8	80.3	1009.9	0.1	NW	215.1	10:30	3.0	5.4	**7.4**	**(09:20)**
08/11/19	16.6	79.0	1009.7	2.6	S	150.8	10:20	10.7	4.2	6.4	(12:20)
09/11/19	14.6	83.0	1010.7	0.7	NW	76.0	9:20	18.2	4.5	7.3	(14:30)
10/11/19	15.0	77.7	1010.8	1.0	SE	233.5	10:10	8.9	4.8	7.4	(09:20)
11/11/19	17.2	69.0	1011.2	1.3	SE	209.8	9:50	1.5	4.1	5.3	(12:00)
12/11/19	17.3	73.1	996.4	4.9	NE	106.8	9:40	8.8	4.4	6.3	(14:20)
13/11/19	15.5	77.2	1001.8	1.1	SW	171.7	10:00	33.8	3.8	4.9	(11:10)
14/11/19	15.2	80.5	1009.4	0.8	SE	141.9	9:40	27.9	3.1	4.2	(13:30)
15/11/19	18.2	74.6	1010.1	4.9	SE	217.8	10:00	3.0	4.2	5.3	(13:40)
16/11/19	19.5	74.9	1011.5	5.6	SE	122.4	9:50	1.5	3.5	4.9	(13:20)
17/11/19	17.5	72.5	1008.6	6.0	S	33.2	8:20	35.3	2.3	4.9	(11:20)
18/11/19	15.5	72.3	1016.5	2.1	SE	217.7	9:40	4.6	4.1	5.7	(10:40)
19/11/19	15.4	80.0	1016.1	2.7	SE	60.7	8:30	22.3	3.8	5.0	(09:50)
20/11/19	13.4	86.5	1015.2	0.3	SE	162.9	9:50	18.0	4.1	5.5	(10:20)
21/11/19	12.5	86.0	1015.8	0.1	NW	101.5	9:20	13.5	3.4	4.6	(13:50)
22/11/19	13.9	85.7	1015.5	0.7	--	200.3	9:40	3.5	4.4	5.9	(10:50)
23/11/19	16.7	75.5	1011.7	4.3	SE	233.1	9:50	3.3	4.5	5.7	(13:00)
24/11/19	14.9	88.0	1004.4	1.8	SE	34.2	9:10	34.7	2.9	4.6	(12:40)
25/11/19	15.1	80.9	1004.7	1.0	N	207.3	9:40	1.8	3.8	5.0	(11:50)
26/11/19	16.3	78.4	1010.8	0.7	NE	267.0	9:40	0.0	4.5	5.1	(12:10)
27/11/19	16.8	85.0	1012.4	1.6	SW	189.8	9:40	1.0	4.4	5.6	(11:30)
28/11/19	16.5	81.8	1011.0	1.2	SW	136.8	9:40	29.7	3.9	5.2	(10:20)
29/11/19	17.0	78.5	1014.7	1.7	SW	137.7	9:40	1.0	3.5	5.0	(12:00)
30/11/19	15.7	77.7	1018.0	0.4	NW	215.7	9:40	0.0	4.6	5.2	(11:30)

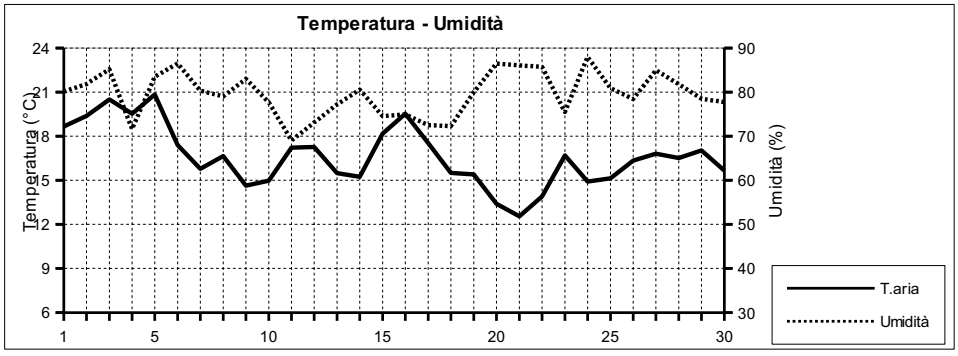

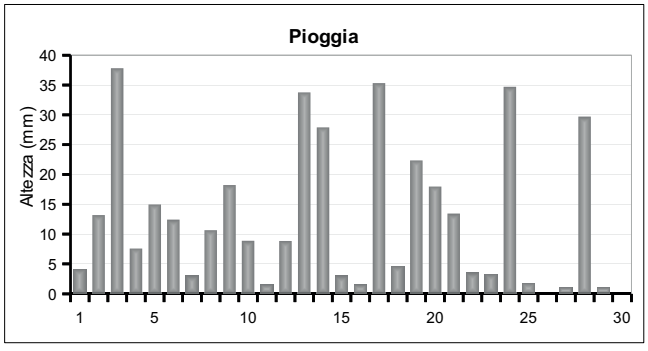

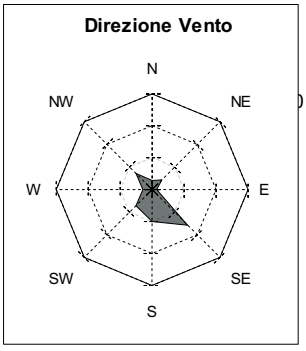

NOVEMBRE 2019 **(estremi giornalieri)**

	Temperatura (°C)				Umidità (%)				Pressione (hPa)				Vento (m/s)		Radiazione (W/m²)	
Data	min	(ore)	max	(ore)	min	(ore)	max	(ore)	min	(ore)	max	(ore)	max	(ore)	max	(ore)
01/11/19	16.6	(05:00)	21.4	(12:10)	66.0	(14:30)	92.0	(01:40)	1014.2	(23:50)	1017.1	(00:00)	6.7	(18:00)	684.0	(12:20)
02/11/19	17.1	(06:20)	21.7	(12:40)	72.0	(14:30)	**94.0**	**(08:50)**	1010.6	(23:20)	1014.3	(00:10)	11.2	(23:50)	631.0	(10:50)
03/11/19	17.0	(12:40)	**22.1**	**(11:40)**	78.0	(00:30)	91.0	(12:50)	1000.7	(23:50)	1010.6	(00:00)	20.1	(22:40)	728.0	(10:40)
04/11/19	18.1	(05:10)	21.2	(13:50)	61.0	(10:00)	90.0	(00:10)	1000.8	(00:10)	1011.5	(20:40)	15.2	(10:00)	**737.0**	**(12:00)**
05/11/19	19.6	(23:50)	21.7	(12:40)	75.0	(02:00)	89.0	(07:50)	1007.1	(14:20)	1011.3	(00:00)	15.2	(23:00)	643.0	(12:50)
06/11/19	15.2	(23:40)	20.4	(00:10)	**83.0**	**(00:30)**	91.0	(03:10)	1007.9	(00:00)	1010.0	(10:10)	12.5	(00:50)	158.0	(11:40)
07/11/19	13.8	(05:40)	18.6	(15:10)	61.0	(16:20)	91.0	(06:50)	1008.6	(00:10)	1011.0	(10:20)	8.9	(05:10)	612.0	(12:10)
08/11/19	13.2	(05:00)	20.4	(12:20)	68.0	(16:30)	90.0	(21:10)	1008.1	(14:10)	1011.5	(23:00)	13.9	(14:30)	700.0	(12:30)
09/11/19	12.2	(20:10)	17.1	(03:20)	69.0	(05:40)	92.0	(22:20)	1008.2	(23:50)	1012.6	(10:30)	13.0	(14:00)	299.0	(14:40)
10/11/19	11.5	(07:20)	17.6	(14:10)	64.0	(16:40)	90.0	(07:30)	1007.6	(02:10)	1013.7	(21:40)	8.5	(11:20)	784.0	(12:40)
11/11/19	13.9	(05:50)	19.8	(12:10)	56.0	(16:40)	85.0	(04:20)	1004.4	(23:50)	1014.2	(03:20)	11.6	(03:10)	673.0	(12:00)
12/11/19	14.2	(23:50)	18.7	(19:00)	65.0	(15:40)	88.0	(13:50)	993.6	(12:40)	1004.3	(00:00)	**24.1**	**(16:30)**	661.0	(12:00)
13/11/19	12.2	(04:20)	17.8	(13:40)	60.0	(16:00)	93.0	(04:50)	**993.1**	**(02:20)**	1008.9	(23:10)	18.3	(02:10)	714.0	(10:50)
14/11/19	12.9	(07:10)	17.4	(02:20)	59.0	(00:20)	92.0	(07:20)	1007.9	(05:00)	1010.5	(11:10)	11.6	(02:40)	564.0	(13:00)
15/11/19	13.9	(01:40)	20.6	(20:00)	63.0	(12:50)	82.0	(03:30)	1008.9	(17:20)	1012.1	(23:50)	16.5	(17:20)	506.0	(13:40)
16/11/19	15.6	(08:40)	21.4	(18:10)	58.0	(20:20)	90.0	(10:30)	1008.0	(23:20)	1014.5	(08:50)	21.5	(21:50)	425.0	(13:20)
17/11/19	13.9	(23:50)	20.8	(00:10)	59.0	(22:10)	92.0	(09:30)	1006.0	(06:40)	1013.7	(23:50)	22.8	(07:00)	107.0	(14:10)
18/11/19	12.2	(05:50)	18.1	(13:30)	59.0	(14:00)	87.0	(08:50)	1013.4	(00:10)	1018.0	(10:00)	10.7	(19:30)	647.0	(12:00)
19/11/19	12.4	(19:20)	18.5	(11:00)	67.0	(04:10)	93.0	(19:40)	1013.8	(23:00)	1017.2	(00:00)	14.3	(03:00)	216.0	(10:50)
20/11/19	11.7	(04:50)	15.2	(12:10)	74.0	(22:20)	92.0	(03:30)	1013.2	(05:40)	1017.3	(21:30)	5.8	(13:40)	647.0	(11:40)
21/11/19	**11.4**	**(02:50)**	14.4	(14:00)	78.0	(14:00)	91.0	(18:30)	1014.5	(13:50)	1017.1	(00:00)	5.8	(14:30)	608.0	(12:40)
22/11/19	11.6	(03:20)	17.1	(14:40)	76.0	(17:30)	92.0	(07:10)	1014.7	(03:10)	1016.3	(09:30)	7.2	(12:50)	529.0	(13:40)
23/11/19	12.8	(02:30)	19.3	(20:20)	66.0	(09:50)	87.0	(00:30)	1008.3	(23:00)	1015.5	(00:00)	14.8	(21:30)	557.0	(13:00)
24/11/19	13.5	(21:50)	19.0	(01:20)	76.0	(01:10)	93.0	(11:00)	1001.4	(15:20)	1008.6	(00:00)	15.6	(02:50)	81.0	(14:10)
25/11/19	12.9	(06:20)	17.4	(13:30)	70.0	(13:40)	92.0	(03:10)	1002.9	(04:30)	1008.4	(23:30)	8.0	(14:20)	642.0	(11:50)
26/11/19	13.7	(07:50)	18.8	(15:10)	69.0	(10:40)	88.0	(23:30)	1008.3	(01:10)	1013.6	(23:40)	4.5	(15:20)	454.0	(11:50)
27/11/19	14.6	(06:50)	18.4	(12:10)	77.0	(12:20)	94.0	(08:10)	1010.8	(16:40)	1013.9	(09:30)	13.0	(20:50)	642.0	(12:00)
28/11/19	13.6	(19:20)	18.7	(09:50)	66.0	(11:40)	90.0	(21:40)	1009.5	(15:30)	1012.5	(22:50)	11.6	(16:00)	577.0	(10:40)
29/11/19	15.2	(06:00)	18.7	(12:30)	72.0	(01:00)	86.0	(22:20)	1012.4	(00:00)	1016.1	(10:10)	13.0	(01:20)	626.0	(12:20)
30/11/19	13.3	(22:30)	18.1	(13:50)	60.0	(14:30)	89.0	(07:40)	1014.8	(00:00)	**1021.7**	**(23:30)**	10.3	(00:10)	512.0	(12:00)

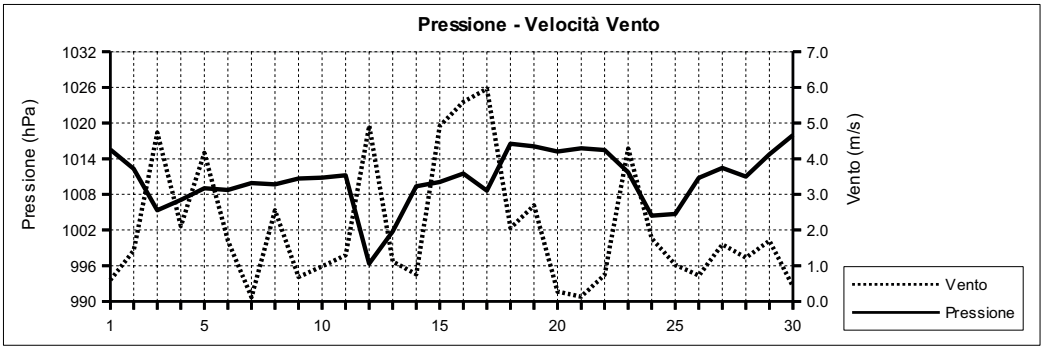

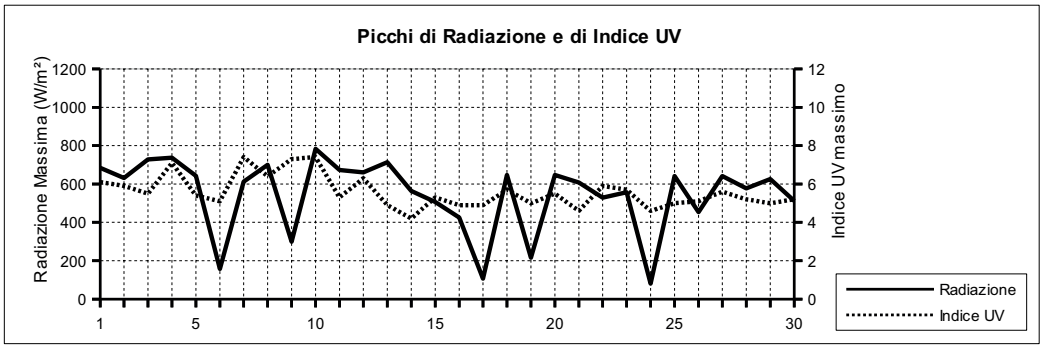

DICEMBRE 2019 **(medie giornaliere)**

	Temperatura	Umidità	Pressione	Vento		Rad. Solare		Pioggia	Indice UV		
Data	°C	%	hPa	m/s	direzione	W/m²	durata	mm	medio	max	ora
01/12/19	15.1	76.2	1021.8	1.4	--	237.5	9:40	0.0	4.5	5.4	(11:20)
02/12/19	16.8	78.8	1018.5	1.2	S	239.5	9:20	0.0	4.4	5.2	(11:00)
03/12/19	15.8	70.9	1018.0	2.4	NE	189.0	9:50	0.0	4.2	5.2	(12:50)
04/12/19	12.0	55.1	1019.1	3.6	N	253.4	9:40	0.0	4.4	5.8	(11:10)
05/12/19	13.0	64.0	1022.6	2.5	NW	201.1	9:30	0.0	4.1	4.9	(11:40)
06/12/19	14.6	79.7	1023.9	0.3	NW	112.5	9:20	0.0	4.2	4.7	(11:20)
07/12/19	15.3	83.1	1022.2	0.2	W	164.0	9:30	1.3	4.0	4.9	(13:00)
08/12/19	14.6	82.5	1021.8	0.4	--	215.1	9:30	0.0	3.9	5.1	(12:10)
09/12/19	13.8	85.5	1013.7	0.5	SW	133.3	9:10	2.8	3.7	5.3	(13:10)
10/12/19	12.7	72.3	1009.8	2.1	NE	138.5	9:30	0.3	4.2	5.3	(12:40)
11/12/19	11.3	58.5	1012.0	1.6	NE	223.0	9:20	0.0	4.8	5.6	(11:40)
12/12/19	10.6	76.6	1006.4	0.2	NW	97.0	9:30	2.8	3.3	5.0	(13:20)
13/12/19	12.1	80.0	997.3	3.1	SW	61.9	8:50	15.0	3.2	5.8	(10:00)
14/12/19	12.9	58.5	1004.3	1.4	NW	255.5	9:30	0.0	4.5	5.5	(12:00)
15/12/19	15.0	81.0	1019.9	0.8	S	191.6	9:20	0.0	4.0	4.9	(11:50)
16/12/19	15.7	80.1	1023.3	0.1	--	211.3	9:30	0.0	4.7	5.4	(12:20)
17/12/19	15.7	73.0	1022.1	1.0	--	241.9	9:20	0.0	4.7	5.3	(11:50)
18/12/19	17.4	69.6	1022.4	1.6	NE	142.3	9:10	0.0	4.4	5.4	(10:20)
19/12/19	14.2	79.9	1020.4	1.3	NE	13.0	5:50	**54.0**	1.3	4.0	(11:30)
20/12/19	14.2	85.2	1016.9	2.3	SE	170.6	9:20	2.8	4.7	5.4	(11:40)
21/12/19	16.1	89.9	1008.0	1.5	S	11.0	8:50	25.1	3.2	4.8	(11:50)
22/12/19	15.6	80.2	998.9	0.0	--	129.2	8:40	10.1	4.0	6.2	(12:40)
23/12/19	13.6	73.0	1005.3	1.4	NW	234.1	9:10	12.7	4.6	**7.4**	**(12:10)**
24/12/19	12.8	64.1	1017.3	0.4	NW	248.6	9:30	0.0	4.4	5.0	(12:40)
25/12/19	12.5	76.1	1016.8	0.2	NE	247.5	9:30	0.0	4.6	5.1	(11:20)
26/12/19	12.5	61.9	1021.3	1.1	NE	254.8	9:30	0.0	4.6	5.9	(11:50)
27/12/19	11.5	61.8	1022.9	0.3	NW	230.8	9:30	0.0	4.6	5.9	(10:00)
28/12/19	9.2	55.3	1026.3	3.9	NE	257.2	9:30	0.0	5.6	7.0	(12:00)
29/12/19	8.0	56.3	1028.7	2.7	NE	234.8	9:30	0.0	6.0	7.3	(11:40)
30/12/19	8.2	53.7	1029.4	4.7	NE	251.9	9:30	0.0	4.9	6.4	(11:00)
31/12/19	8.8	57.7	1030.9	2.6	NW	257.2	9:30	0.0	4.9	5.8	(12:30)

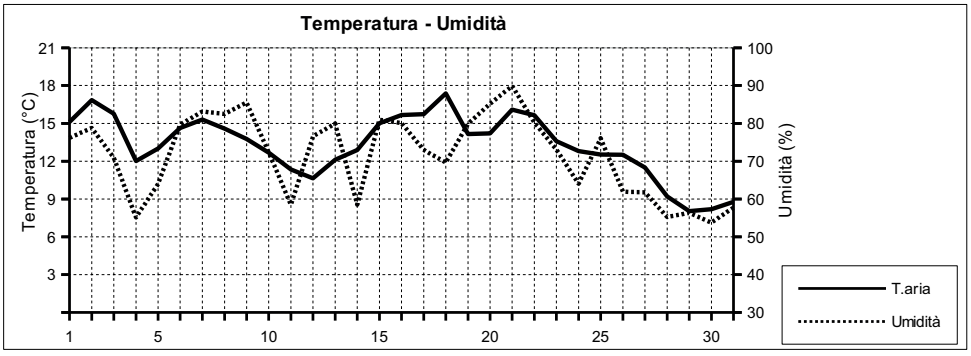

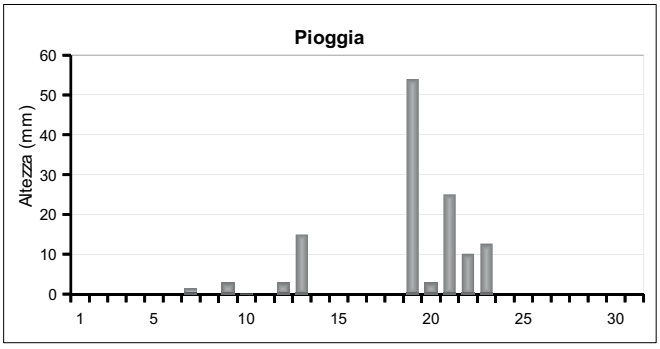

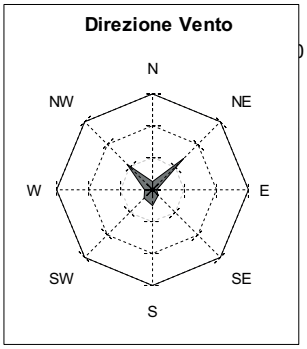

DICEMBRE 2019 **(estremi giornalieri)**

	Temperatura (°C)				Umidità (%)				Pressione (hPa)				Vento (m/s)		Radiazione (W/m²)	
Data	min	(ore)	max	(ore)	min	(ore)	max	(ore)	min	(ore)	max	(ore)	max	(ore)	max	(ore)
01/12/19	11.7	(07:40)	17.8	(13:10)	69.0	(11:10)	83.0	(00:00)	1020.8	(23:40)	1023.0	(10:20)	8.0	(14:30)	512.0	(12:50)
02/12/19	13.9	(06:00)	18.8	(13:40)	72.0	(11:00)	87.0	(06:20)	1016.7	(17:50)	1020.9	(00:00)	7.6	(11:30)	619.0	(10:50)
03/12/19	12.4	(23:50)	18.3	(12:30)	64.0	(14:20)	81.0	(00:00)	1016.9	(04:50)	1019.9	(23:00)	11.2	(17:50)	**649.0**	**(12:10)**
04/12/19	10.3	(23:30)	14.8	(13:20)	43.0	(13:10)	66.0	(00:30)	1017.1	(16:10)	1020.3	(23:50)	10.7	(13:50)	454.0	(11:50)
05/12/19	10.1	(06:30)	16.6	(15:20)	56.0	(00:30)	74.0	(22:30)	1019.7	(01:50)	1025.0	(22:30)	10.3	(02:00)	438.0	(11:10)
06/12/19	12.8	(01:40)	17.3	(15:30)	72.0	(00:20)	87.0	(23:30)	1022.7	(16:10)	1025.3	(10:20)	4.5	(02:10)	320.0	(14:30)
07/12/19	13.6	(07:00)	17.9	(14:50)	70.0	(14:50)	90.0	(06:30)	1021.1	(14:50)	1023.0	(23:00)	4.9	(20:40)	568.0	(11:00)
08/12/19	11.9	(08:10)	17.1	(15:00)	72.0	(13:20)	90.0	(08:20)	1019.7	(23:40)	1023.4	(10:00)	4.0	(12:40)	448.0	(11:40)
09/12/19	12.2	(05:50)	15.8	(15:30)	73.0	(15:20)	91.0	(06:00)	1008.9	(23:50)	1019.6	(00:00)	7.6	(11:20)	534.0	(12:50)
10/12/19	10.9	(05:40)	14.2	(13:30)	56.0	(22:00)	89.0	(01:50)	1007.5	(04:00)	1012.9	(23:30)	12.1	(22:40)	462.0	(09:50)
11/12/19	9.5	(23:50)	13.7	(13:40)	49.0	(13:40)	67.0	(20:50)	1010.3	(23:50)	1013.5	(09:30)	12.1	(01:00)	448.0	(12:00)
12/12/19	8.5	(04:40)	13.0	(14:00)	68.0	(00:00)	87.0	(23:20)	1004.3	(14:10)	1010.1	(00:00)	5.4	(12:30)	635.0	(12:10)
13/12/19	8.9	(04:30)	16.7	(18:10)	56.0	(23:20)	87.0	(00:00)	**987.1**	**(18:50)**	1005.2	(00:00)	27.3	(19:10)	383.0	(09:40)
14/12/19	9.3	(08:10)	17.0	(14:30)	41.0	(14:00)	77.0	(23:40)	990.8	(00:00)	1015.7	(23:40)	11.2	(02:30)	441.0	(12:00)
15/12/19	11.3	(03:30)	17.5	(13:20)	72.0	(11:00)	88.0	(23:20)	1015.9	(00:00)	1022.8	(23:50)	8.0	(16:20)	548.0	(13:00)
16/12/19	13.1	(08:00)	19.6	(13:50)	62.0	(14:40)	91.0	(06:20)	1022.5	(14:20)	1024.7	(10:00)	3.6	(01:30)	469.0	(12:10)
17/12/19	12.0	(06:20)	**19.6**	**(14:30)**	63.0	(14:20)	81.0	(22:10)	1021.0	(13:50)	1023.3	(20:20)	10.7	(15:50)	431.0	(11:50)
18/12/19	15.1	(00:50)	19.5	(14:20)	62.0	(14:10)	75.0	(00:00)	1021.2	(23:40)	1023.6	(10:30)	11.6	(11:00)	448.0	(10:50)
19/12/19	11.4	(16:40)	19.2	(02:20)	54.0	(01:30)	93.0	(16:20)	1018.1	(19:10)	1023.3	(09:50)	11.2	(14:40)	93.0	(11:30)
20/12/19	11.4	(00:50)	16.4	(23:50)	77.0	(10:30)	93.0	(02:30)	1013.1	(23:20)	1019.1	(08:20)	15.2	(23:50)	485.0	(11:20)
21/12/19	14.8	(10:00)	17.1	(16:40)	80.0	(00:50)	94.0	(13:30)	1004.9	(14:40)	1013.2	(00:00)	15.2	(00:00)	40.0	(15:50)
22/12/19	12.1	(07:20)	17.4	(05:50)	66.0	(14:20)	**95.0**	**(02:40)**	995.6	(14:10)	1005.5	(00:00)	0.4	(18:30)	520.0	(13:20)
23/12/19	11.2	(07:40)	16.1	(14:40)	57.0	(19:20)	87.0	(06:40)	999.6	(05:40)	1013.3	(23:40)	11.2	(13:50)	501.0	(10:20)
24/12/19	9.3	(06:20)	16.8	(12:30)	**39.0**	**(11:20)**	77.0	(23:30)	1013.4	(00:00)	1019.2	(10:20)	5.4	(16:20)	439.0	(12:40)
25/12/19	9.2	(08:10)	16.6	(14:30)	63.0	(13:20)	87.0	(07:10)	1015.6	(03:50)	1018.1	(10:20)	3.1	(09:00)	432.0	(12:00)
26/12/19	9.4	(04:20)	16.2	(14:00)	44.0	(14:20)	81.0	(04:00)	1017.7	(00:30)	1024.1	(23:40)	8.0	(11:00)	443.0	(12:10)
27/12/19	8.6	(07:20)	15.0	(13:20)	52.0	(13:10)	71.0	(23:00)	1021.4	(14:20)	1023.8	(00:10)	4.5	(12:00)	422.0	(12:20)
28/12/19	7.3	(19:20)	11.2	(12:30)	40.0	(12:30)	70.0	(00:00)	1023.4	(01:30)	1029.3	(22:50)	17.0	(12:00)	439.0	(12:00)
29/12/19	6.5	(08:00)	10.2	(14:10)	48.0	(00:10)	63.0	(08:20)	1027.1	(14:40)	1030.2	(10:20)	13.4	(21:50)	468.0	(12:20)
30/12/19	7.1	(02:50)	10.2	(14:00)	47.0	(18:00)	63.0	(14:50)	1027.5	(15:20)	1032.0	(21:30)	**20.6**	**(11:20)**	508.0	(12:00)
31/12/19	**6.2**	**(06:10)**	12.2	(14:30)	40.0	(13:40)	68.0	(22:50)	1029.7	(15:10)	**1032.4**	**(10:10)**	8.5	(08:50)	446.0	(12:30)

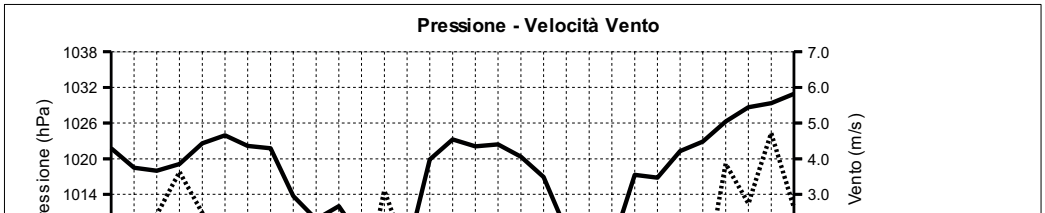

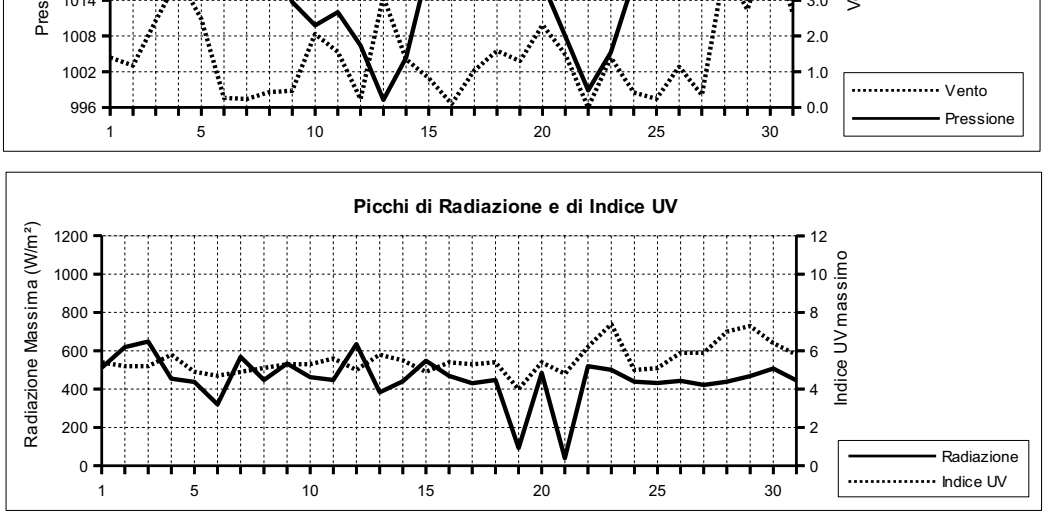

MEDIE MENSILI 2019

	Temperatura	Umidità	Pressione	Vento		Radiazione Solare		Pioggia
Mese	°C	%	hPa	m/s	direzione	W/m²	Indice UV	mm
Gennaio	8.7	70.7	1012.8	1.4	NE	171.7	3.7	112.9
Febbraio	11.4	64.7	1022.2	2.3	N	282.3	4.0	14.7
Marzo	13.9	68.0	1019.7	1.8	SW	349.8	4.2	19.7
Aprile	15.8	67.9	1014.1	1.5	SW	378.5	4.7	22.7
Maggio	16.6	76.1	1013.0	1.4	SW	361.0	4.7	119.3
Giugno	25.9	64.4	1015.6	1.1	S	445.4	4.9	10.6
Luglio	27.4	66.4	1012.8	1.3	SW	436.4	4.9	18.3
Agosto	28.2	63.6	1014.4	0.8	SW	436.6	3.0	0.0
Settembre	24.4	66.5	1017.8	1.2	SW	357.0	4.7	82.2
Ottobre	20.6	72.6	1018.1	0.8	--	318.1	4.4	109.3
Novembre	16.6	79.6	1010.5	2.1	N	156.7	3.9	376.0
Dicembre	13.3	71.6	1017.5	1.5	N	188.7	4.3	126.7
Anno	**18.6**	**69.3**	**1015.7**	**1.4**	**SW**	**323.5**	**4.3**	**1012.5**

	Temperatura (°C)		Umidità (%)		Pressione (hPa)		Raffiche	Radiazione Massima	
Mese	min	max	min	max	min	max	m/s	W/m²	Indice UV
Gennaio	6.3	11.3	57.7	81.1	1009.5	1016.1	9.6	508.7	5.6
Febbraio	8.7	14.6	51.5	77.8	1019.9	1024.5	11.1	624.9	6.2
Marzo	11.3	17.0	53.3	81.5	1017.1	1022.3	9.6	796.3	6.9
Aprile	13.1	19.0	51.7	80.9	1012.3	1016.3	9.5	916.7	7.7
Maggio	14.3	19.2	62.3	86.7	1010.9	1015.4	8.3	1,045.7	9.2
Giugno	22.7	29.9	47.2	79.0	1014.1	1017.2	7.7	942.3	9.0
Luglio	24.6	30.7	50.6	79.8	1011.2	1014.5	8.3	902.2	8.8
Agosto	25.4	32.0	45.7	77.7	1013.2	1015.6	6.7	846.6	5.4
Settembre	21.4	27.7	53.0	78.3	1016.3	1019.5	8.0	786.0	7.5
Ottobre	17.4	24.1	56.7	83.7	1016.5	1019.9	7.2	664.2	6.6
Novembre	14.0	19.0	67.6	90.2	1007.8	1013.3	12.9	545.5	5.6
Dicembre	10.7	16.1	58.9	81.7	1014.6	1020.5	9.8	453.0	5.5
Anno	**15.8**	**21.7**	**54.7**	**81.5**	**1013.6**	**1017.9**	**9.0**	**752.7**	**7.0**

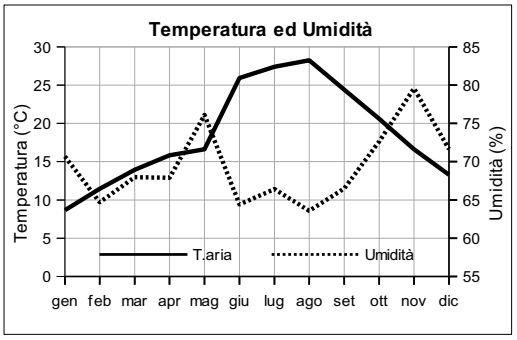

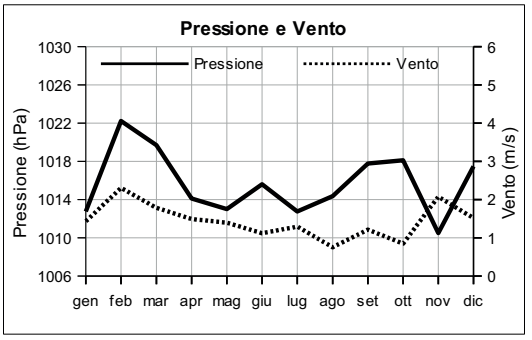

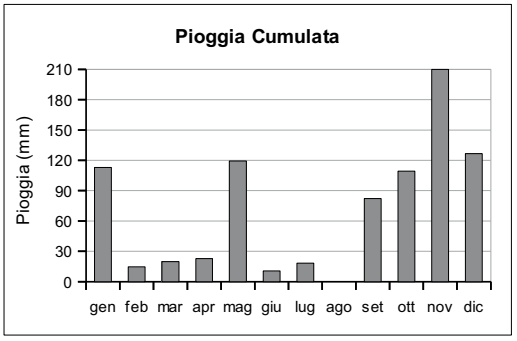

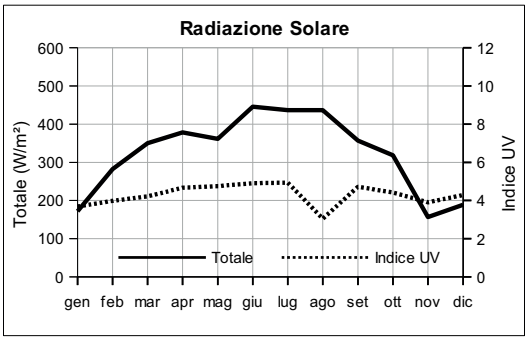

Riepilogo mensile delle precipitazioni

Mese	Pioggia Totale mm.	N. Totale giorni con pioggia	N. giorni con pioggia fino ad 1 mm	N. giorni con pioggia da 1.1 a 10 mm	N. giorni con pioggia da 10.1 a 20 mm	N. giorni con pioggia da 20.1, a 40 mm	N. giorni con pioggia da 40.1 a 60 mm	N. giorni con pioggia maggiore di 60 mm
Gennaio	**112.9**	**16**	**1**	**11**	**3**	**1**	**0**	**0**
Febbraio	**14.7**	**7**	**4**	**3**	**0**	**0**	**0**	**0**
Marzo	**19.7**	**6**	**1**	**5**	**0**	**0**	**0**	**0**
Aprile	**22.7**	**10**	**3**	**7**	**0**	**0**	**0**	**0**
Maggio	**119.3**	**13**	**1**	**6**	**6**	**0**	**0**	**0**
Giugno	**10.6**	**1**	**0**	**0**	**1**	**0**	**0**	**0**
Luglio	**18.3**	**3**	**0**	**2**	**1**	**0**	**0**	**0**
Agosto	**0.0**	**0**	**0**	**0**	**0**	**0**	**0**	**0**
Settembre	**82.2**	**8**	**2**	**4**	**0**	**2**	**0**	**0**
Ottobre	**109.3**	**7**	**0**	**5**	**0**	**1**	**1**	**0**
Novembre	**376.0**	**28**	**1**	**13**	**7**	**7**	**0**	**0**
Dicembre	**126.7**	**10**	**1**	**4**	**3**	**1**	**1**	**0**
Totali	**1012.5**	**109**	**14**	**60**	**21**	**12**	**2**	**0**

Riepilogo mensile delle Tmax					Riepilogo mensile delle Tmin				
Mese	N. giorni con Tmax > 10°C	N. giorni con Tmax > 20°C	N. giorni con Tmax > 30°C	N. giorni con Tmax > 35°C	Mese	N. giorni con Tmin ≤ 15°C	N. giorni con Tmin ≤ 10°C	N. giorni con Tmin ≤ 5°C	N. giorni con Tmin ≤ 0°C
Gennaio	**26**	**0**	**0**	**0**	Gennaio	**31**	**31**	**7**	**0**
Febbraio	**27**	**0**	**0**	**0**	Febbraio	**28**	**22**	**1**	**0**
Marzo	**31**	**3**	**0**	**0**	Marzo	**31**	**4**	**0**	**0**
Aprile	**10**	**9**	**0**	**0**	Aprile	**23**	**0**	**0**	**0**
Maggio	**31**	**10**	**0**	**0**	Maggio	**16**	**0**	**0**	**0**
Giugno	**30**	**30**	**16**	**1**	Giugno	**0**	**0**	**0**	**0**
Luglio	**31**	**31**	**16**	**1**	Luglio	**0**	**0**	**0**	**0**
Agosto	**22**	**22**	**21**	**1**	Agosto	**0**	**0**	**0**	**0**
Settembre	**30**	**30**	**4**	**0**	Settembre	**0**	**0**	**0**	**0**
Ottobre	**31**	**30**	**0**	**0**	Ottobre	**0**	**0**	**0**	**0**
Novembre	**30**	**10**	**0**	**0**	Novembre	**22**	**0**	**0**	**0**
Dicembre	**31**	**0**	**0**	**0**	Dicembre	**30**	**12**	**0**	**0**
Totali	**330**	**175**	**57**	**3**	**Totali**	**181**	**69**	**8**	**0**

Istruzioni e modello

ISTRUZIONI PER LA REALIZZAZIONE DEI DATTILOSCRITTI

Il *Rendiconto* pubblica le comunicazioni fatte dai soci in una delle adunanze ordinarie dell'Accademia. I soci possono presentare anche lavori di altri autori. In questo caso l'accettazione della *Nota* per la pubblicazione è condizionata al parere favorevole di una commissione designata dall'Accademia.

Le Note dovranno essere inviate al segretario per posta elettronica sia in formato doc che pdf. Il file pdf dovrà incorporare tutti i font utilizzati nel documento originario.

La stesura dovrà essere conforme al modello che è riportato di seguito,riprodotto sotto forma di *template* sul sito web dell'Accademia: Non sono ammesse modifiche al modello fornito.

Layout di pagina. Margine superiore: 5,8 - margine inferiore: 4,8 - margine sinistro e margine destro: 4,25.

Spaziatura prima e dopo: 0; interlinea: singola. Sillabazione automatica.

Iriferimentibibliograficisonoindicatineltestotraparentesi(cognomeprimo autore, anno di pubblicazione). Se gli autori sono due si indicheranno entrambi, se più di due si indicherà il primo autore seguito da '*et al.*' Nella sezione Bibliografia, i riferimenti bibliografici dovranno riportare quanto indicato nei seguenti esempi per periodici elibri:

Cognome A.B., Cognome C.D. […] e Cognome E.F. (anno) Titolo. Rivista (corsivo). Numero volume (grassetto), numeri pagina iniziale-finale.

Cognome G.H. and Cognome I.L. (anno) Titolo. Casa editrice, città, stato, numeri pagina iniziale-finale.

Le illustrazioni dovranno avere una risoluzione minima di 300 dpi e dimensioni non superiori a mm 125x180 comprensive dell'eventuale didascalia. Le fotografie a mezzi toni e quelle a colori, devono rispondere a criteri di riproducibilità ed essere utilizzate solo se necessarie per la completezza dell'esposizione.

Saranno forniti gratuitamente 50 estratti, senza copertina, di ciascuna *Nota*, anche nel caso in cui il numero degli autori dovesse essere superiore a uno. Ulteriori estratti e/o la richiesta di una copertina personalizzata saranno a carico degli autori, che ne dovranno fare esplicita richiesta all'atto della presentazione del dattiloscritto all'Editore, che inoltrerà agli interessati un preventivo di spesa.v

Composizione del manoscritto in Word

Prima pagina (vedi modello .doc sul sito web dell'Accademia) 7 righi vuoti

Titolo: centrato, Times New Roman (TNR) 13, grassetto. Rigo vuoto.

Autori della nota: centrato, TNR 11. Gli apici numerici per indicare indirizzi e affiliazioni di ciascun autore sono da precisare a fondo pagina. La formula da adottare è: "Nota del socio e di…" oppure "Nota dei soci…" ovvero "Nota di Nome e Cognome (1), Nome e Cognome (2)…".

Rigo vuoto.

Presentatore: centrato, TNR 10. (“Presentata dal socio…”)

Data adunanza: centrato, in parentesi, TNR 10. La data dell’adunanza va posta direttamente sotto gli autori, ovvero sotto il presentatore, senza lasciare spazi.

Due righi vuoti.

Keywords: in inglese, TNR 10. Rigovuoto.

Abstract: in inglese, TNR 10. Rigovuoto.

Riassunto: in italiano, TNR 10. Due righi vuoti.

1 - INTRODUZIONE, TNR 10, grassetto maiuscolo Rigovuoto.

Testo, TNR 11, giustificato, indentatura paragrafi 6 mm Rigovuoto.

Altri titoli (tutti numerati in sequenza), TNR 10, grassetto maiuscolo Rigovuoto.

Altro testo, TNR 11, giustificato, indentatura paragrafi 6 mm Rigovuoto.

Bibliografia (numerata in sequenza), TNR 10, grassetto maiuscolo

Testo della bibliografia, TNR 10. Primo rigo intero, secondo ed altri: indentatura 6 mm

Rigo vuoto Ringraziamenti, TNR 10.

ISTRUZIONI SPECIALI PER GLI UTILIZZATORI
DEL PROGRAMMA LaTeX

[Sono disponibili istruzioni in formato .tex (inviare richiesta a carmine.colella@unina.it)]

```
\documentclass[a4paper, 14pt, oneside, openright]{article}
\usepackage{geometry}

\usepackage[latin1]{inputenc}
\usepackage[italian,english]{babel}
\usepackage{amsmath, amsfonts, amsthm}
\usepackage{paralist, times, indentfirst}
\usepackage[T1]{fontenc}
\usepackage{amsthm}
\usepackage{mathptmx}

\geometry{a4paper}

\setcounter{secnumdepth}{0}

\newtheorem{prop}{Proposition}
\newtheorem{lem}{Lemma}
\newtheorem{thm}{Theorem}
\newtheorem{theorem}{Theorem}
\newtheorem{cor}{Corollary}
\newtheorem{obs}{Observation}
\newtheorem{exa}{Example}
\newtheorem{defn}{Definition}
\theoremstyle{remark}
\newtheorem{rem}{Notation}
\newenvironment{sistema}%
{\left\lbrace\begin{array}{@{}l@{}}}%
{\end{array}\right.}

\linespread{1.00}

\title{titolo}
\textwidth = 12.4 cm
\textheight = 19.5 cm
\topmargin = 2 cm
\oddsidemargin = 2 cm
```

```
\begin{document}

\vspace*{20 mm}

\pagestyle{empty}

\begin{center}
{\fontsize{13}{14}\selectfont \textbf
{Titolo}\\}

\bigskip

\fontsize{12}{11}\selectfont

Nota di Autore \footnote{\fontsize{10}{10}\selectfont Dipartimento di ...,
Universit\`a di ..., Via
..., cap, Citt\`a, Nazione. e-mail: ...@...}\\

\vspace{11pt}


{\fontsize{10}{10}\selectfont Presentata dal socio ... \linebreak (Adunanza
del ...)}
\end{center}

\vspace{11pt}

\fontsize{10}{10}\selectfont \noindent \emph{Key words:} Qui bisogna
mettere le parole chiave\\

\fontsize{10}{11}\selectfont \noindent
\textbf{Abstract -- }
qui bisogna mettere il riassunto in inglese\\

\fontsize{10}{11}\selectfont \noindent
\textbf{Riassunto -- }
e qui il riassunto in italiano

\vspace{11pt}

\section{\fontsize{10}{12}\selectfont \bf 1 -INTRODUCTION}
{\fontsize{11}{12} \selectfont
```

```
\section{\fontsize{10}{10}\selectfont \bf2-        }

{\fontsize{11}{12}\selectfont

\section{\fontsize{10}{10}\selectfont \bf 3 - REFERENCES}

\noindent Il primo rigo di ciascuna referenza non deve rientrare, gli altri s\`i.

{\fontsize{10}{11}\selectfont
\noindent

\noindent

\end{document}
```

SEGUE MODELLO DI TESTO
(riprodotto in word sul sito web dell'Accademia)

Un breve ricordo di Guido Barone (1937-2016) e dei suoi cinquant'anni di vita accademica

Nota del socio Lelio Mazzarella[1]
(Adunanza del 16 giugno 2017)

Keywords: Proprietà termodinamiche, macromolecole, Società Chimica, effetto idrofobico, ambiente, clima, effetto serra.

Abstract - Guido Barone graduated in Industrial Chemistry in 1961 and has carried out research activity in the field of thermodynamics of synthetic and biological macromolecules, paying particular attention to the hydrophobic effect. He has promoted new and interesting scientific initiatives and contributed to the dynamic of the university politics. In the final part of his activity, he got deeply interested in the environmental risks and in the human impact on the climate, with particular emphasis on the release of greenhouse gases.

Riassunto - Laureato in Chimica Industriale nel 1961, Guido Barone ha svolto attività di ricerca nel campo della termodinamica delle soluzioni di macromolecole sintetiche e biologiche, con particolare riferimento all'effetto idrofobico, promuovendo iniziative scientifiche di grande prestigio. Ha anche dato contributi fondamentali nella dinamica della politica universitaria e del rapporto docenti-studenti. Nella parte finale della sua attività di docente si è estesamente interessato ai rischi ambientali ed all'impatto antropico sul clima, con particolare riferimento agli effetti della potenziale liberazione di grosse masse di gas serra.

1 - INTRODUZIONE

Mi è stato affidato il compito di delineare, alla distanza di un anno dalla sua scomparsa, un breve ritratto di Guido Barone (Fig. 1), socio di questa Accademia,

[1] Dipartimento di Scienze Chimiche, Università Federico II di Napoli, Complesso Universitario di Monte S. Angelo, via Cinthia, 80129 Napoli e Accademia di Scienze Fisiche e Matematiche della Società Nazionale di Scienze, Lettere e Arti in Napoli, via Mezzocannone 8, 80134 Napoli

alla cui vita ha contribuito con la pubblicazione di diversi lavori sui Rendiconti, e con la partecipazione attiva alle riunioni mensili ed alle discussioni sui temi presentati dai vari relatori (vedi i primi 14 titoli della Bibliografia). Compito che ho assunto con tristezza, unita a nostalgia, per la lunga comunanza che mi ha legato a Guido sul piano umano e familiare e sul piano degli interessi culturali e scientifici, anche se non abbiamo mai pubblicato insieme, a parte, negli ultimi tempi, alcune ricostruzioni storiche riguardanti figure e avvenimenti che appartengono ai nostri anni giovanili.

Fig. 1 – Guido Barone nel suo studio.

Il ritratto non scorre però facile dalla mia penna, perché Guido è stato tutt'altro che una persona monocorde, ma, al contrario, è stato capace di adattarsi, interpretare, partecipare attivamente alle complesse evoluzioni del mondo scientifico e del mondo accademico, nei suoi aspetti organizzativi, politici e sociali. Questa ricostruzione della sua figura non vuole essere puramente e vanamente agiografica, ma far conoscere la persona, e, soprattutto, porre l'accento sull'importanza di un impegno a partecipare e contribuire con idee e lavoro allo sviluppo

della nostra società; impegno di cui Guido è stato un luminoso esempio. È per questo che cercherò di ripercorrere alcuni degli avvenimenti occorsi nel trascorrere della sua vita accademica che ritengo importanti per lo sviluppo della sua personalità.

2 - GLI ANNI DELLA FORMAZIONE

Guido Barone era nato ad Avellino il 14/04/1937 da una famiglia della media borghesia, che si era trasferita a Napoli, dove il padre lavorava in banca e dove Guido aveva conseguito la licenza liceale nel Liceo classico Gian Battista Vico. Si era iscritto all'Università di Napoli in Chimica Industriale nel 1955. È lì che ci siamo incontrati per la prima volta, verso il terzo anno, nelle aule dei corsi afferenti alla laurea in Chimica Industriale, che a noi pareva all'epoca quella che fornisse migliori prospettive e sbocchi professionali.

Erano anni in cui seguire un corso di laurea, di per sé non facile, era un'impresa non proprio trascurabile. Da un lato si richiedeva una frequentazione assidua, dall'altra si era quasi respinti dalle strutture universitarie. I meno motivati spesso ci rinunciavano. Il rapporto tra docenti e studenti era del tutto carente. Lo sviluppo del corso di studio era ostacolato da regolamentazioni estremamente rigide: bastava una sciocchezza, una non accorta pianificazione degli studi, un impedimento imprevisto perché si perdesse un anno; e i professori non facevano sconti. Fu quello che successe a Guido, che però ne approfittò per capire a fondo l'ambiente in cui si trovava ed acquisire un'esperienza ed una sensibilità verso la condizione studentesca che gli risulterà utile per comprendere le istanze che saranno poi sollevate dagli studenti nelle agitazioni, che avrebbero di lì a poco preso il via. Ci trovammo a seguire insieme i corsi del triennio applicativo della Chimica Industriale allora svolti insieme agli ingegneri chimici. Essi a loro volta stavano vivendo un profondo rivolgimento, catalizzato dall'arrivo di Leopoldo Massimilla prima e, poco dopo, di Gianni Astarita, due giovani e brillanti ricercatori, freschi dei loro studi all'estero. Fummo così coinvolti nella progettazione dell'impiantistica chimica: i reattori catalitici, i processi a letto fluido in fase eterogenea, un po' a disagio rispetto agli iscritti in ingegneria chimica, che venivano da una preparazione più specifica. Ci riunivamo in gruppo per affrontare le difficoltà ed è lì che incominciò ad emergere la figura di Guido, favorita anche, fisicamente, da una aspetto imponente e da un vistoso paio di baffi che lo rendevano subito riconoscibile da lontano, carico al solito di una quantità enorme di carte. Incominciò subito a stendere la sua rete socializzante, prodigo di consigli per quelli più giovani ma anche di grosso aiuto per quelli molto più anziani. Allora era facile che gli studenti impiegassero otto-dieci anni per laurearsi: si risentivano ancora gli sconquassi della guerra, i soldi erano pochi, molti venivano da sedi lontane - in quell'epoca il triennio applicativo della Chimica Industriale di Napoli era l'unico in tutto il CentroSud - e soggiornavano a Napoli in condizioni

6 – CONCLUSIONI

Guido faceva parte di numerosi gruppi di discussione, non c'era riunione in cui non intervenisse: di fronte a problemi nuovi in cui si cercava di valutare quale posizione prendere, il suo intervento, di solito lucido e ben ponderato, apriva spesso una via.

Negli ultimi anni avevamo avviato assieme un'attività di tipo storico riguardante la chimica napoletana: abbiamo così pubblicato insieme a Pietro Greco (Greco *et al*., 2014) un libro su quella irripetibile stagione scientifica che aveva caratterizzato Napoli agli inizi degli anni sessanta del secolo scorso, e di cui ho fatto un fugace cenno all'inizio di questo mio intervento. Abbiamo anche insieme preparato due note, presentate ai convegni sulla storia dell'Ingegneria, riguardanti la nascita e sviluppo dell'Elettrochimica a Napoli nel corso della prima metà del secolo scorso (Barone e Mazzarella, 2016), e la figura di Francesco Giordani (Barone e Mazzarella, 2016), un personaggio importante non solo nell'ambito delle vicende scientifiche italiane ma anche, e forse soprattutto, per il suo contributo alla rinascita economica italiana del dopoguerra. Altre iniziative erano in programma, inesorabilmente chiuse dalla sua improvvisa dipartita.

Guido è intervenuto più volte anche sul Blog di Climalteranti e quello della Chimica, un sito quest'ultimo organizzato e condotto sul web da Claudio della Volpe, un suo antico studente da tempo all'Università di Trento. Il sito è sede di dibattito politico, culturale, scientifico di grande interesse. Tempo fa tra i partecipanti nacque il vezzo di identificarsi con l'elemento chimico avente il medesimo numero atomico dell'età di chi aveva scelto di parlarne, per richiamarne succintamente storia e proprietà. Così nel 2015 Guido divenne … Platino:

Quest'anno sono.... Platino.

Visto che nessun Collega si è fatto ancora sentire, ho pensato che toccasse a me celebrare il Platino il cui numero atomico corrisponde per quest'anno alla mia età. In verità non sono riuscito a trovare una qualche mia caratteristica che possa associarsi a questo nobile metallo. La mia è solo una aspirazione al color grigio, per di più opaco; sono fragile poco malleabile e facilmente attaccabile da ogni agente chimico La mia densità media è di poco inferiore all'unità, infatti galleggio in acqua.

Ma tant'è bisogna pur parlare di questo importante elemento: il nome deriva dallo spagnolo platìna...

7 – BIBLIOGRAFIA

Barone G (2010) I fattori che regolano il clima seguono differenti scale temporali. Acc. Sc. Fis., Mat. di Napoli. Conversazione del 5 /3.

Barone G., (2011) A new hole in the stratospheric ozone on Arctic Ocean, Rend. Acc. Sc. Fis., Mat. di Napoli, LXXVII, 293-298.

Barone G. (2012) Estrazione di gas mediante fratturazione idraulica delle rocce scistose:

prospettive di sviluppo e pericoli ambientali. Rend. Acc. Sc. Fis., Mat. di Napoli, LXXIX, 5-10.
Barone G. (2012) Inquinamento atmosferico: il Progetto Regionale sulla Qualità dell'Aria in Campania; il contributo della Modellistica numerica. Rend. Acc. Sc. Fis., Mat. di Napoli, LXXIX, 11-18.
Barone G. (2012) Recente accumulo di metano in atmosfera: origini, influenza sul clima. Acc. Sc. Fis., Mat. di Napoli. Conversazione del 9/12.
Barone G. (2013) Formazione e preservazione di molecole organiche nelle condizioni estreme del Sistema Solare. Rend. Acc. Sc. Fis., Mat. di Napoli, LXXX, 41-50.
Barone G. (2014) Nuove informazioni dalle missioni spaziali sulle basi chimiche delle origini della vita. Acc. Sc. Fis., Mat. di Napoli. Conversazione del 7/2.
Barone G. (2014) L'acqua: le proprietà chimiche e fisiche e interazioni con molecole biologiche. Acc. Sc. Fis. Mat. di Napoli. e Acc. Pontaniana: XIV Giornata mondiale dell'acqua, 28/3.
Barone G. (2014) Le Conferenze delle Nazioni Unite e il V Rapporto dell'IPCC sulle Variazioni Climatiche. Rend. Acc. Sc. Fis., Mat. di Napoli, LXXXI, 167-181.
Barone G. (2016) Le Conferenze delle Nazioni Unite sul Clima: 2015, una svolta negli impegni internazionali ?. Rend. Acc. Sc. Fis., Mat. di Napoli, LXXXIII, 15-22.
Barone G.e Chianese F.(2010) Gli idrati di gas naturali. Struttura, proprietà e origini: loro utilizzo come fonti di energia. Acc. Sc. Fis., Mat. di Napoli. Conversazione del 5 /3.
Barone G., Chianese F., Duro I. e Trifuoggi M. (2010) Studies on air quality in cultural heritage: a preliminary research on Capodimonte Museum in Naples. Rend. Acc. Sc. Fis., Mat. di Napoli, LXXVI. 53-62.
Barone G.e Graziano G. (1991) Rischio chimico ambientale. Convegno su Rischi naturali ed impatto antropico nell'area metropolitana napoletana, Facoltà di Ingegneria 7-8 Giugno.
Barone G. e Mazzarella L. (2014) Il ruolo di Francesco Giordani, scienziato e manager, tra la R. Scuola Superiore Politecnica e la Facoltà di Scienze MM.FF.NN. Atti del 5° Convegno di Storia dell'Ingegneria; International Conference, Napoli 19-20 Maggio 2014.
Barone G. e Mazzarella L., (2016) La scuola di Elettrochimica a Napoli da Oscar Scarpa a Mario Maria Jacopetti: sviluppo di un importante settore della Chimica tra Ingegneria e Scienze. Atti del 6° Convegno di Storia dell'Ingegneria; International Conference, Napoli 22-23 Aprile.
Barone G. e Sassi E. (2011) The United Nation Conferences on Climate Change. Rend. Acc. Sc. Fis., Mat. di Napoli, LXXVII, 79-88.
Elia V., Rosati F., Barone G., Monroy A. e Liquori A. M., (1983) A thermodynamic study of sperm-egg interaction. The EMBO J., 2, 2053-2058.
Greco P., Mazzarella L. e Barone G. (2014) Alfonso Maria Liquori. Il risveglio scientifico negli anni '60 a Napoli. Saggi Bibliopolis, Napoli, pp 232.